

Chapter 7 Digital Transmission through Additive White Gaussian Noise Channel

Text. [1] J. G. Proakis and M. Salehi, Communication Systems Engineering, 2/e. Prentice Hall, 2002.

- 7.1 Geometric Representation of Signals
- 7.2 Pulse Amplitude Modulation
- 7.3 Two-dimensional Signals
- 7.4 Multidimensional Signals
- 7.5 Optimum Receiver for Digitally Modulated Signals in Additive White Gaussian Noise
- 7.6 Probability of Error for Signal Detection in Additive White Gaussian Noise
- 7.7 Performance Analysis for Wireline and Radio Communication Channels
- 7.8 Symbol Synchronization (partly skipped)

The **additive white Gaussian noise (AWGN)** channel is one of the simplest mathematical models for various physical communication channels, including wireless and some radio channels.

Such channels are basically analog channels for which the digital information sequence to be transmitted must be mapped into analog signals.

We consider both **baseband channels**; that is, channels having frequency passbands that usually include zero frequency ($f = 0$), and **bandpass channels**; that is, channels having frequency passbands far removed from $f = 0$. (Most of these will be dealt in a undergraduate course titled “Communication Systems.”)

When the digital information is transmitted through a baseband channel, there is no need to use a carrier frequency for transmission of digitally modulated signals.

When the digital information is transmitted through a bandpass channel such as telephone channels, radio channels, and satellite channels, the information-bearing signal is impressed on sinusoidal carrier, which shifts the frequency content of the information-bearing signal to the appropriate frequency band that is passed by the channel.

Thus, the signal is transmitted by carrier modulation.

7.1 Geometric Representation of Signals

Suppose we have a set of M signals $s_m(t)$, $m=1, 2, \dots, M$, which are to be used for transmitting information over a communication channel.

From the set of M waveforms, we first construct a set of $N \leq M$ orthonormal waveforms, where N is the dimension of the signal space.

Gram-Schmidt Orthogonalization Procedure

We begin with the first waveform $s_1(t)$, which is assumed to have energy ε_1 .

The first waveform of the orthonormal set is constructed simply as

$$\psi_1(t) = \frac{s_1(t)}{\sqrt{\varepsilon_1}} \tag{7.1.1}$$

which is $s_1(t)$ normalized to unit energy.

The second waveform is constructed from $s_2(t)$ by first computing the projection of $s_2(t)$ onto $\psi_1(t)$, which is

$$c_{21} = \int_{-\infty}^{\infty} s_2(t)\psi_1(t)dt. \quad (7.1.2)$$

Then, $c_{21}\psi_1(t)$ is subtracted from $s_2(t)$ to yield

$$d_2(t) = s_2(t) - c_{21}\psi_1(t). \quad (7.1.3)$$

Now, $d_2(t)$ is orthogonal to $\psi_1(t)$, but it does not possess unit energy.

Denoting the energy in $d_2(t)$ by ε_2 , the energy normalized waveform orthogonal to $\psi_1(t)$ is given by

$$\psi_2(t) = \frac{d_2(t)}{\sqrt{\varepsilon_2}} \quad (7.1.4)$$

where

$$\varepsilon_2 = \int_{-\infty}^{\infty} d_2^2(t)dt. \quad (7.1.5)$$

In general, the orthogonalization of the k th function leads to

$$\psi_k(t) = \frac{d_k(t)}{\sqrt{\mathcal{E}_k}} \quad (7.1.6)$$

where

$$d_k(t) = s_k(t) - \sum_{i=1}^{k-1} c_{ki} \psi_i(t) \quad (7.1.7)$$

$$\mathcal{E}_k = \int_{-\infty}^{\infty} d_k^2(t) dt \quad (7.1.8)$$

and

$$c_{ki} = \int_{-\infty}^{\infty} s_k(t) \psi_i(t) dt, \quad i = 1, 2, \dots, k-1. \quad (7.1.9)$$

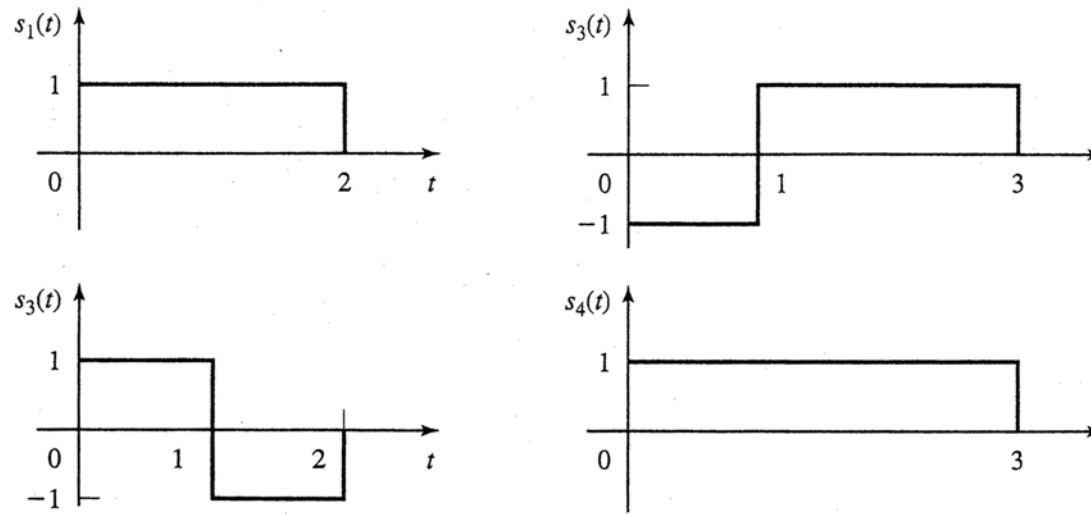
The orthogonalization process is continued until all the M signals $\{s_m(t)\}$ have been exhausted and $N \leq M$ orthonormal waveforms have been constructed.

The N orthonormal waveforms $\{\psi_n(t)\}$ form a **basis** in the N -dimensional signal space.

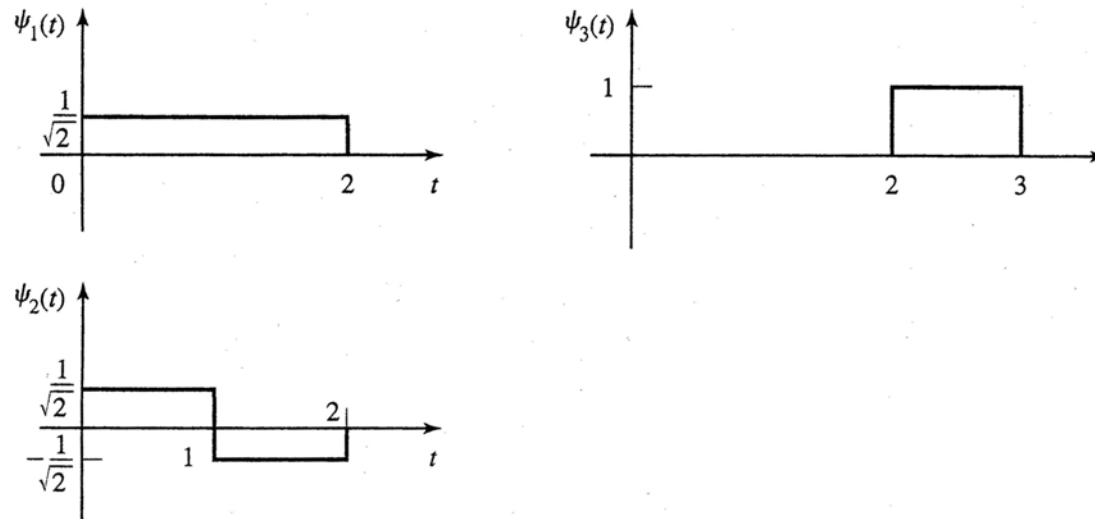
The dimensionality N of the signal space will be equal to M if all the M signals are linearly independent; that is, if none of the signals is a linear combination of the other signals.

Ex. 7.1.1

Apply the Gram-Schmidt procedure to the set of four waveforms shown in Figure 7.1(a).



(a) Original signal set



(b) Orthonormal waveforms

Figure 7.1 Application of Gram-Schmidt orthogonalization procedure to signals $\{s_i(t)\}$.

The waveform $s_1(t)$ has energy $\varepsilon_1 = 2$, so we have

$$\psi_1(t) = \frac{s_1(t)}{\sqrt{2}}.$$

Next, we observe that $c_{21} = 0$, so that $\psi_1(t)$ and $s_2(t)$ are orthogonal.

Therefore, we have

$$\begin{aligned}\psi_2(t) &= \frac{s_2(t)}{\sqrt{\varepsilon_2}} \\ &= \frac{s_2(t)}{\sqrt{2}}.\end{aligned}$$

To obtain $\psi_3(t)$, we compute c_{31} and c_{32} , which are $c_{31} = 0$ and $c_{32} = -\sqrt{2}$.

Hence,

$$d_3(t) = s_3(t) + \sqrt{2}\psi_2(t).$$

Since $d_3(t)$ has unit energy, i.e., $\varepsilon_3 = 1$, it follows that

$$\psi_3(t) = d_3(t).$$

Finally, we find that $c_{41} = \sqrt{2}$, $c_{42} = 0$, $c_{43} = 1$.

Hence,

$$\begin{aligned} d_4(t) &= s_4(t) - \sqrt{2}\psi_1(t) - \psi_3(t) \\ &= 0. \end{aligned}$$

Thus, $s_4(t)$ is a linear combination of $\psi_1(t)$ and $\psi_3(t)$ and, consequently, the dimensionality of the signal set is $N = 3$.

The function $\psi_1(t)$, $\psi_2(t)$, and $\psi_3(t)$ are shown in Figure 7.1(b).

Once we have constructed the set of orthogonal waveforms $\{\psi_n(t)\}$, we can express the M signals $\{s_m(t)\}$ as exact linear combinations of the $\{\psi_n(t)\}$.

We may write

$$s_m(t) = \sum_{i=1}^N s_{mi} \psi_i(t), \quad m = 1, 2, \dots, M, \quad (7.1.10)$$

where

$$s_{mi} = \int_{-\infty}^{\infty} s_m(t) \psi_i(t) dt$$

and

$$\begin{aligned} \mathcal{E}_m &= \int_{-\infty}^{\infty} s_m^2(t) dt \\ &= \sum_{i=1}^N s_{mi}^2. \end{aligned} \quad (7.1.11)$$

Based on the expression in (7.1.10), each signal may be represented by the vector

$$\mathbf{s}_m = (s_{m1}, s_{m2}, \dots, s_{mN}) \quad (7.1.12)$$

or equivalently, as a point in the N -dimension signal space with coordinates $\{s_{mi}, i = 1, 2, \dots, N\}$.

The energy of the m th signal is simply the square of the length of the vector or, equivalently, the square of the Euclidean distance from the origin to the point in the N -dimensional space.

We can also show that the inner product of two signals is equal to the inner product of their vector representations, that is,

$$\int_{-\infty}^{\infty} s_m(t) s_n(t) dt = \mathbf{s}_m \cdot \mathbf{s}_n. \quad (7.1.13)$$

Thus, any N -dimensional signal can be represented geometrically as a point in the signal space spanned by the N orthonormal functions $\{\psi_n(t)\}$.

Ex. 7.1.2

Determine the vector representation of the four signals shown in Figure 7.1(a) by using the orthonormal set of functions in Figure 7.1(b).

Since the dimensionality of the signal space is $N = 3$, each signal is described by three components, which are obtained by projecting each of the four signals on the three orthonormal basis functions $\psi_1(t)$, $\psi_2(t)$, $\psi_3(t)$.

Thus, we obtain $\mathbf{s}_1 = (\sqrt{2}, 0, 0)$, $\mathbf{s}_2 = (0, \sqrt{2}, 0)$, $\mathbf{s}_3 = (0, -\sqrt{2}, 1)$, $\mathbf{s}_4 = (\sqrt{2}, 0, 1)$.

These signal vectors are shown in Figure 7.2.

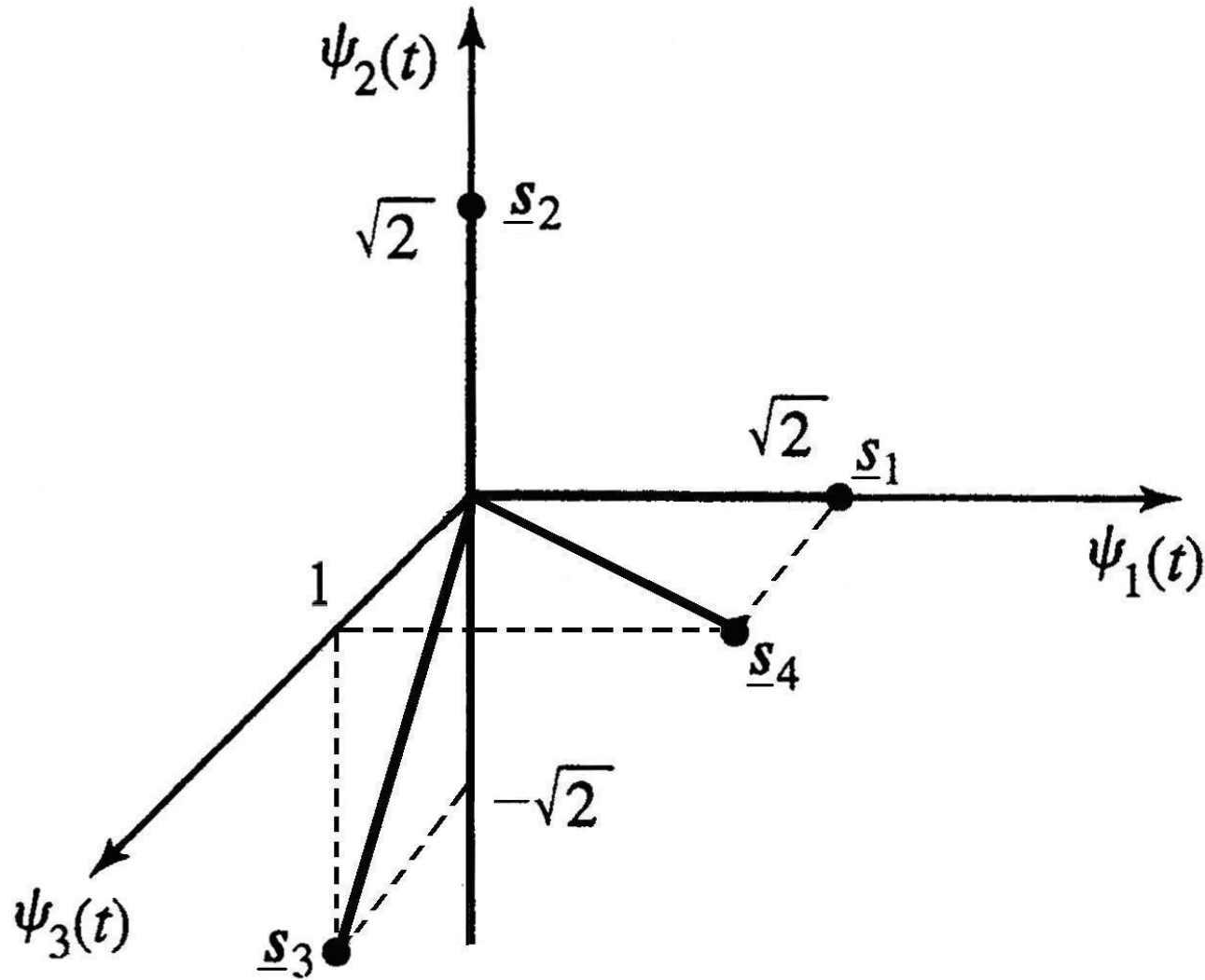


Figure 7.2 Signal vectors corresponding to the signals $s_i(t)$, $i = 1, 2, 3, 4$.

Notice that the set of basis functions $\{\psi_n(t)\}$ obtained by the Gram-Schmidt procedure is not unique.

For example, another set of basis functions that span the three-dimensional space is shown in Figure 7.3.

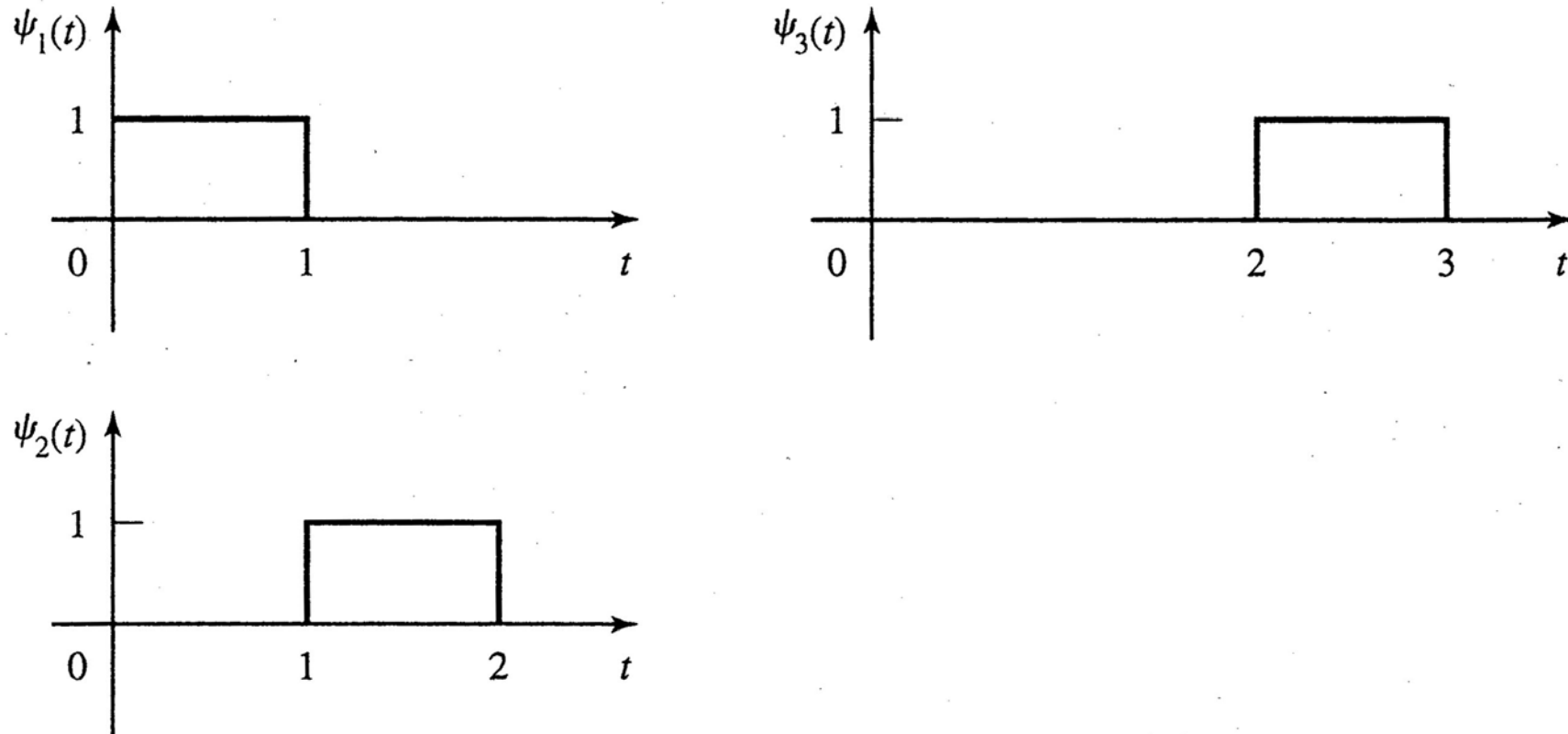


Figure 7.3 Alternate set of basis functions.

For this basis, the signal vectors are expressed as $\mathbf{s}_1 = (1, 1, 0)$, $\mathbf{s}_2 = (1, -1, 0)$, $\mathbf{s}_3 = (-1, 1, 1)$, and $\mathbf{s}_4 = (1, 1, 1)$.

Note that the change in the basis functions does not change the dimensionality of the space N , the lengths (energies) of the signal vectors, or the inner product of any two vectors.

Although the Gram-Schmidt orthogonalization procedure is guaranteed to generate an orthonormal basis for representation of the signal set, in many cases it is simpler to use a method based on inspection to generate the orthonormal basis. (This method is explored in the problems of this chapter.)

7.2 Pulse Amplitude Modulation

In **pulse amplitude modulation (PAM)**, the information is conveyed by the amplitude of the transmitted signal.

Baseband Signals

Binary PAM is the simplest digital modulation method.

In binary PAM, the information bit 1 may be represented by a pulse of amplitude A and the information bit 0 is represented by a pulse of amplitude $-A$, as shown in Figure 7.4.

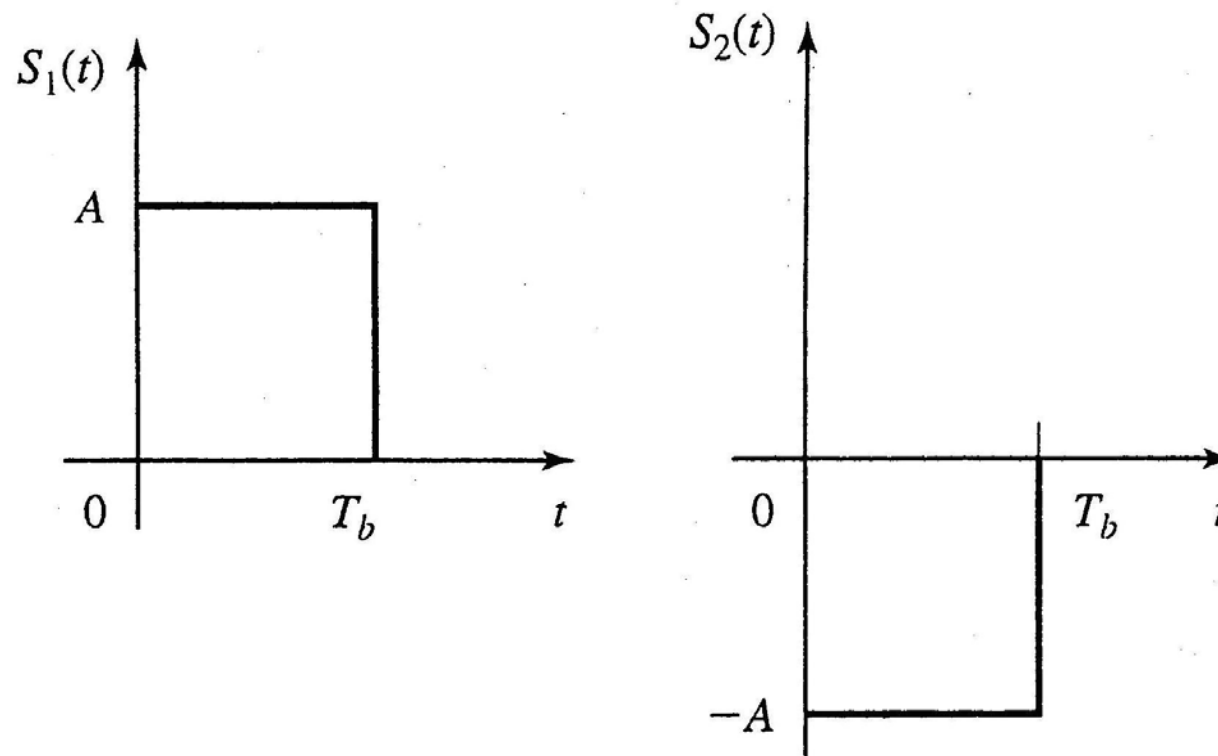


Figure 7.4 Binary PAM signals.

This type of signaling is also called **binary antipodal signaling**.

Pulses are transmitted at a bit rate $R_b = \frac{1}{T_b}$ bits/sec, where T_b is called the bit interval.

Although the pulses are shown as rectangular, in practical systems the rise time and decay time are nonzero and the pulses are generally smoother.

The pulse shape determines the spectral characteristics of the transmitted signal.

The generalization of PAM to nonbinary (M -ary) pulse transmission is relatively straightforward.

Instead of transmitting one bit at a time, the binary information sequence is subdivided into blocks of k bits, called **symbols**, and each block, or symbol, is represented by one of $M = 2^k$ pulse amplitude values.

Thus with $k = 2$, we have $M = 4$ pulse amplitude values. Figure 7.5 shows the PAM signals for $k = 2$, $M = 4$.

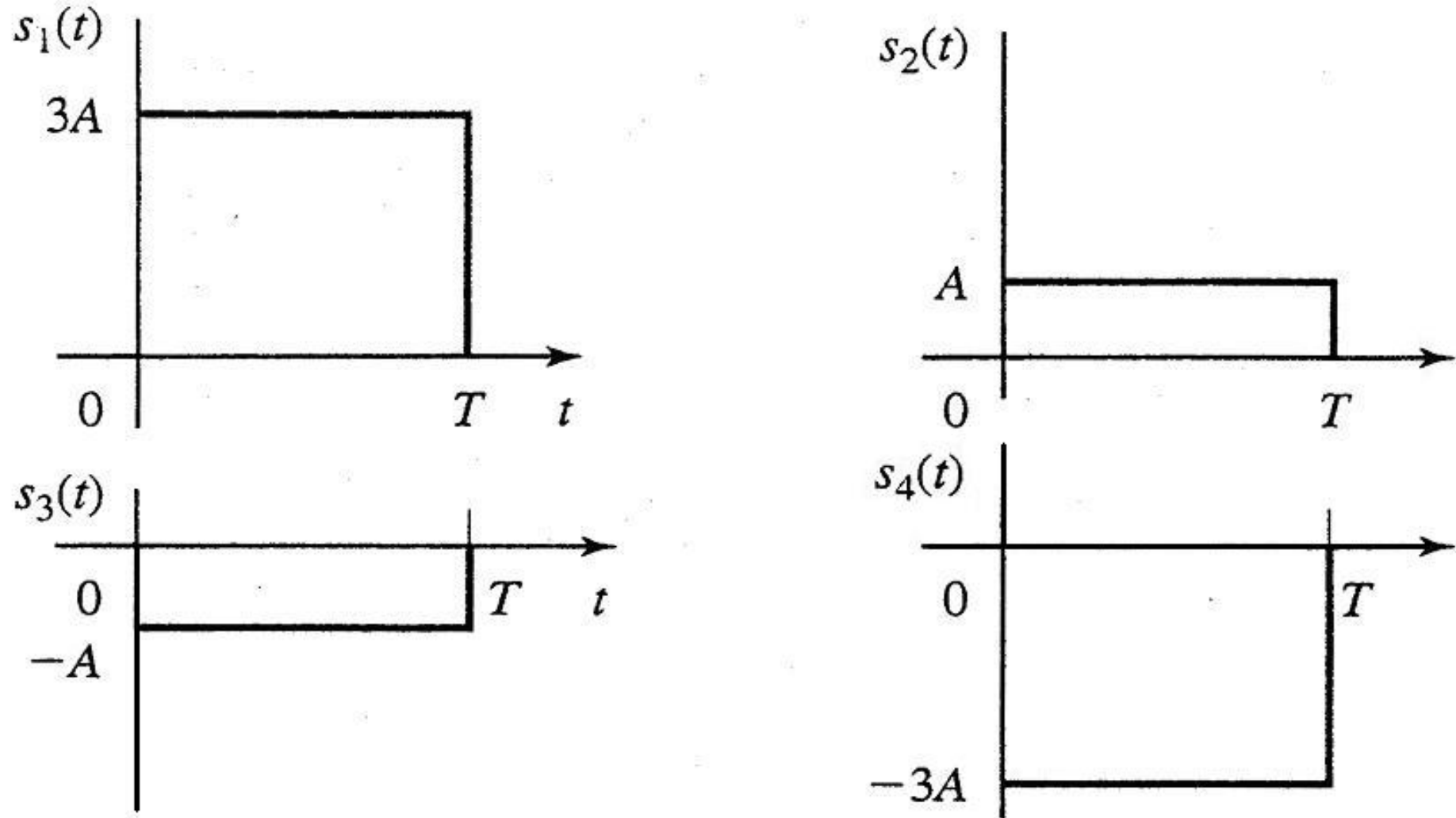
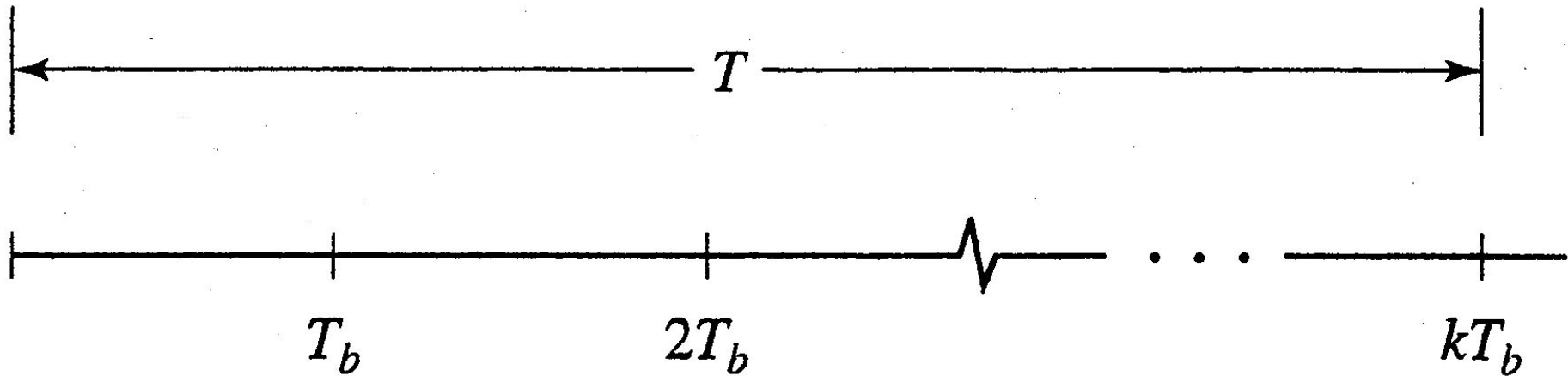


Figure 7.5 $M = 4$ PAM signals.

Note that when the bit rate R_b is fixed, the symbol interval (or “symbol duration”) is given by

$$\begin{aligned} T &= \frac{k}{R_b} \\ &= kT_b \end{aligned} \tag{7.2.1}$$

as shown in Figure 7.6. (Sometimes T_s is used to represent the symbol interval instead of T .)



T_b = bit interval
 T = symbol interval

Figure 7.6 Relationship between the symbol interval and the bit interval.

In general, the M -ary PAM signals may be expressed as

$$s_m(t) = A_m g_T(t), \quad 0 \leq t \leq T, \quad (7.2.2)$$

$m = 1, 2, \dots, M$, where $g_T(t)$ is a pulse of some arbitrary shape as shown for example in Figure 7.7.

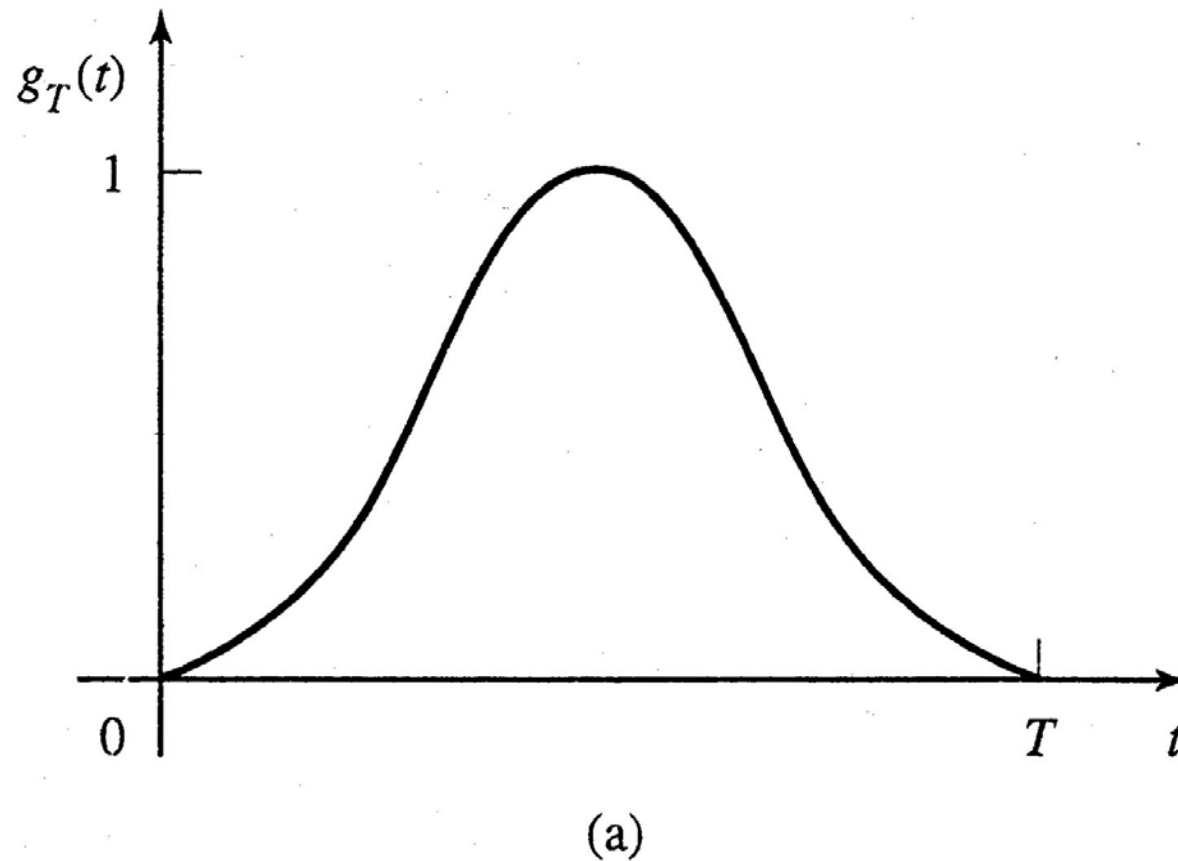


Figure 7.7 Signal pulse for PAM

The distinguishing feature among the M signals is the signal amplitude. All the M signals have the same pulse shape.

Another important feature of these signals is their energies.

Note the signals have different energies; that is,

$$\begin{aligned}\varepsilon_m &= \int_0^T s_m^2(t) dt \\ &= A_m^2 \int_0^T g_T^2(t) dt \\ &= A_m^2 \varepsilon_g,\end{aligned}\tag{7.2.3}$$

$m = 1, 2, \dots, M$, where ε_g is the energy of the signal pulse $g_T(t)$.

Bandpass Signals

To transmit the digital signals through a bandpass channel by amplitude modulation, the baseband signals $s_m(t)$, $m = 1, 2, \dots, M$, are multiplied by a sinusoidal carrier of the form $\cos 2\pi f_c t$, as shown in Figure 7.8, where f_c is the carrier frequency and corresponds to the center frequency in the passband of the channel.

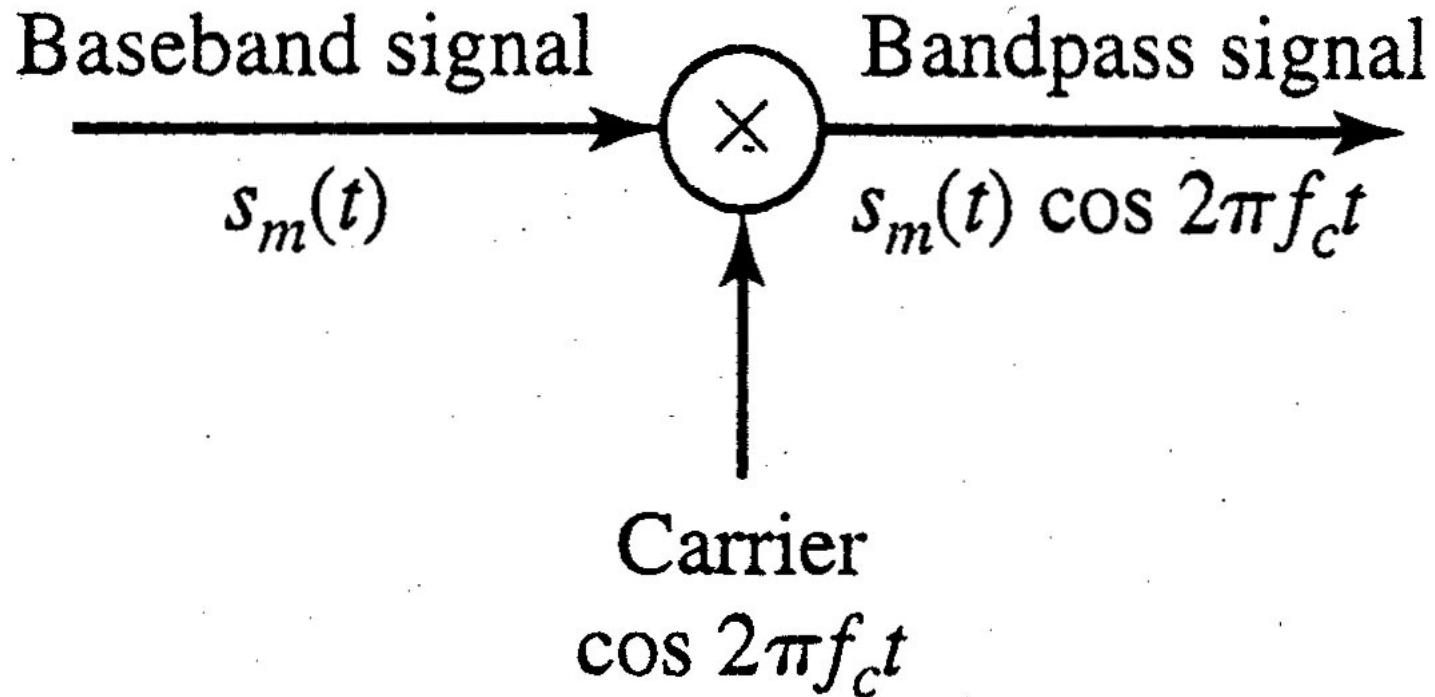


Figure 7.8 Amplitude modulates sinusoidal carrier by the baseband signal.

Thus, the transmitted signals is expressed as

$$u_m(t) = A_m g_T(t) \cos 2\pi f_c t, \quad m = 1, 2, \dots, M. \quad (7.2.4)$$

As described in Section 3.2, amplitude modulation of the carrier $\cos 2\pi f_c t$ by the baseband signals

$s_m(t) = A_m g_T(t)$, shifts the spectrum of the baseband signal by an amount f_c and, thus places the signal into the passband of the channel.

Recall that the Fourier transform of the carrier $\cos 2\pi f_c t$ is $\frac{[\delta(f - f_c) + \delta(f + f_c)]}{2}$.

The spectrum of the amplitude-modulated (that is, DSB-SC modulated) signal in (7.2.4) is given by

$$U_m(f) = \frac{A_m}{2} [G_T(f - f_c) + G_T(f + f_c)]. \quad (7.2.5)$$

Thus, the spectrum of the baseband signal $s_m(t) = A_m g_T(t)$, is shifted in frequency by an amount equal to the carrier frequency f_c .

The result is a DSB-SC AM signal, as shown in Figure 7.9.

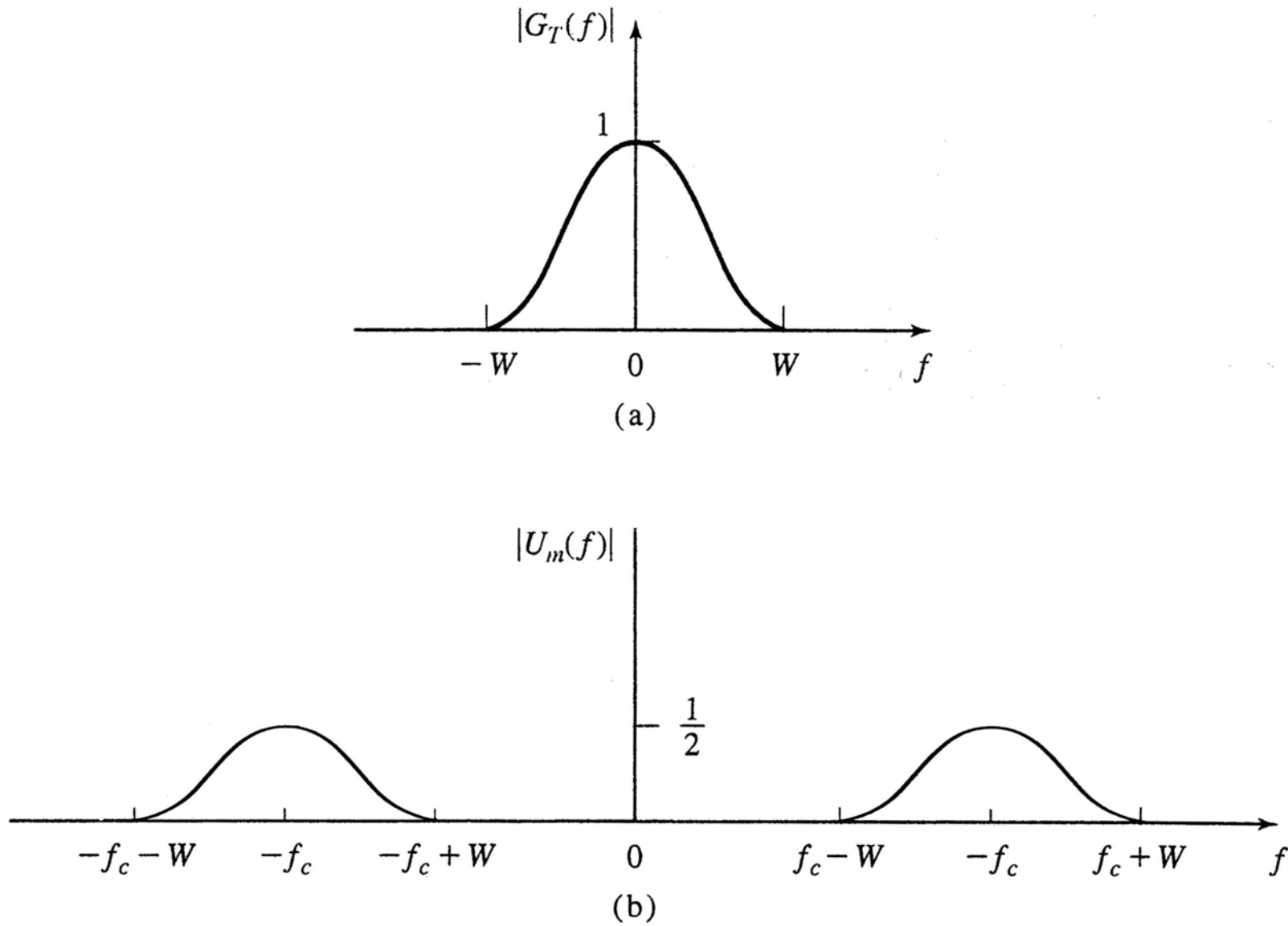


Figure 7.9 Spectra of (a) baseband and (b) amplitude-modulated signals.

The upper sideband of the carrier modulated signal is comprised of the frequency content of $u_m(t)$ for $|f| > f_c$; that is, for $f_c < |f| \leq f_c + W$.

The lower sideband of $u_m(t)$ comprises the frequency content for $|f| < f_c$; that is, for $f_c - W \leq |f| < f_c$.

Hence, the DSB-SC amplitude-modulated signal occupies a channel bandwidth of $2W$, which is twice the bandwidth required to transmit the baseband signal.

The energy of the bandpass signals $u_m(t)$, $m = 1, 2, \dots, M$, given by (7.2.4) is defined as

$$\begin{aligned}\mathcal{E}_m &= \int_{-\infty}^{\infty} u_m^2(t) dt \\ &= \int_{-\infty}^{\infty} A_m^2 g_T^2(t) \cos^2 2\pi f_c t dt \\ &= \frac{A_m^2}{2} \int_{-\infty}^{\infty} g_T^2(t) dt + \frac{A_m^2}{2} \int_{-\infty}^{\infty} g_T^2(t) \cos 4\pi f_c t dt .\end{aligned}\tag{7.2.6}$$

Note that when $f_c \gg W$, the term

$$\int_{-\infty}^{\infty} g_T^2(t) \cos 4\pi f_c t dt \quad (7.2.7)$$

involves the integration of the product of a slowly varying function, namely $g_T^2(t)$, with a rapidly varying sinusoidal term, namely $\cos 4\pi f_c t$ as shown in Figure 7.10.

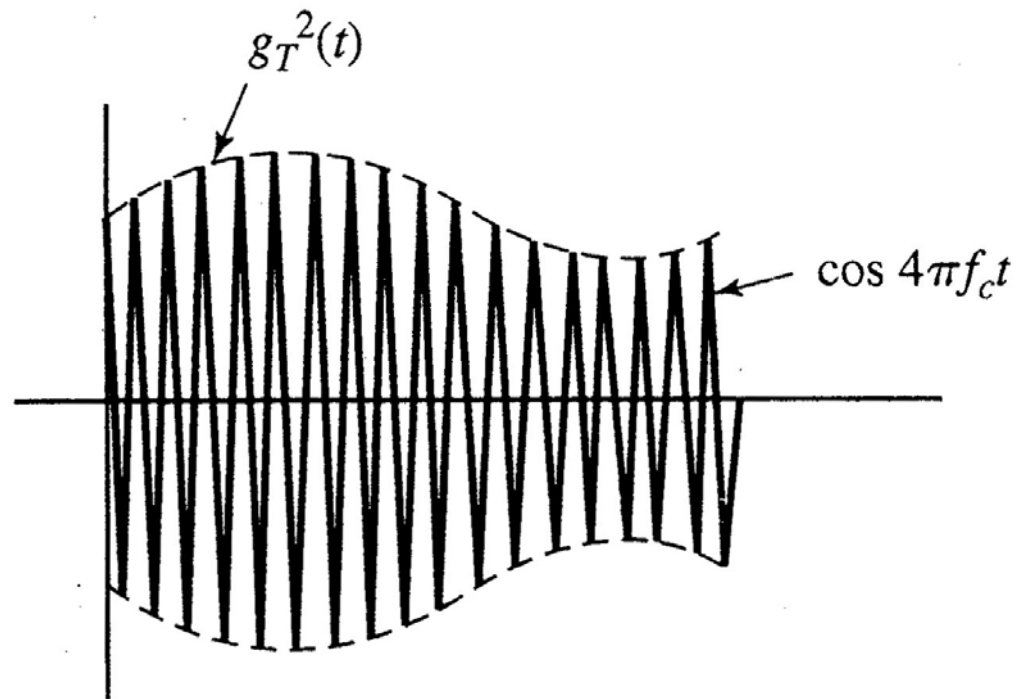


Figure 7.10 Signal $g_T^2(t) \cos 4\pi f_c t$.

Because $g_T(t)$ is slowly varying relative to $\cos 4\pi f_c t$, the integral in (7.2.7) over a single cycle of $\cos 4\pi f_c t$ is zero and, hence, the integral over an arbitrary number of cycles is also zero.

Consequently,

$$\begin{aligned}\varepsilon_m &= \frac{A_m^2}{2} \int_{-\infty}^{\infty} g_T^2(t) dt \\ &= \frac{A_m^2}{2} \varepsilon_g\end{aligned}\tag{7.2.8}$$

where ε_g is the energy in the signal pulse $g_T(t)$.

Thus, we have shown that the energy in the bandpass signal is one-half of the energy in the baseband signal.

The scale factor of $\frac{1}{2}$ is due to the carrier component $\cos 2\pi f_c t$, which has an average power of $\frac{1}{2}$.

When the transmitted pulse shape is rectangular, $g_T(t)$ is given by

$$g_T(t) = \begin{cases} \sqrt{\frac{\mathcal{E}_g}{T}}, & 0 \leq t \leq T, \\ 0, & \text{otherwise.} \end{cases} \quad (7.2.9)$$

The amplitude-modulation with a PAM signal as its message signal is usually called **amplitude-shift keying (ASK)**.

Geometric Representation of PAM Signals

The baseband signals for M -ary PAM are given in (7.2.2), where $M = 2^k$, and $g_T(t)$ is a pulse with peak amplitude normalized to unity as previously shown in Figure 7.7.

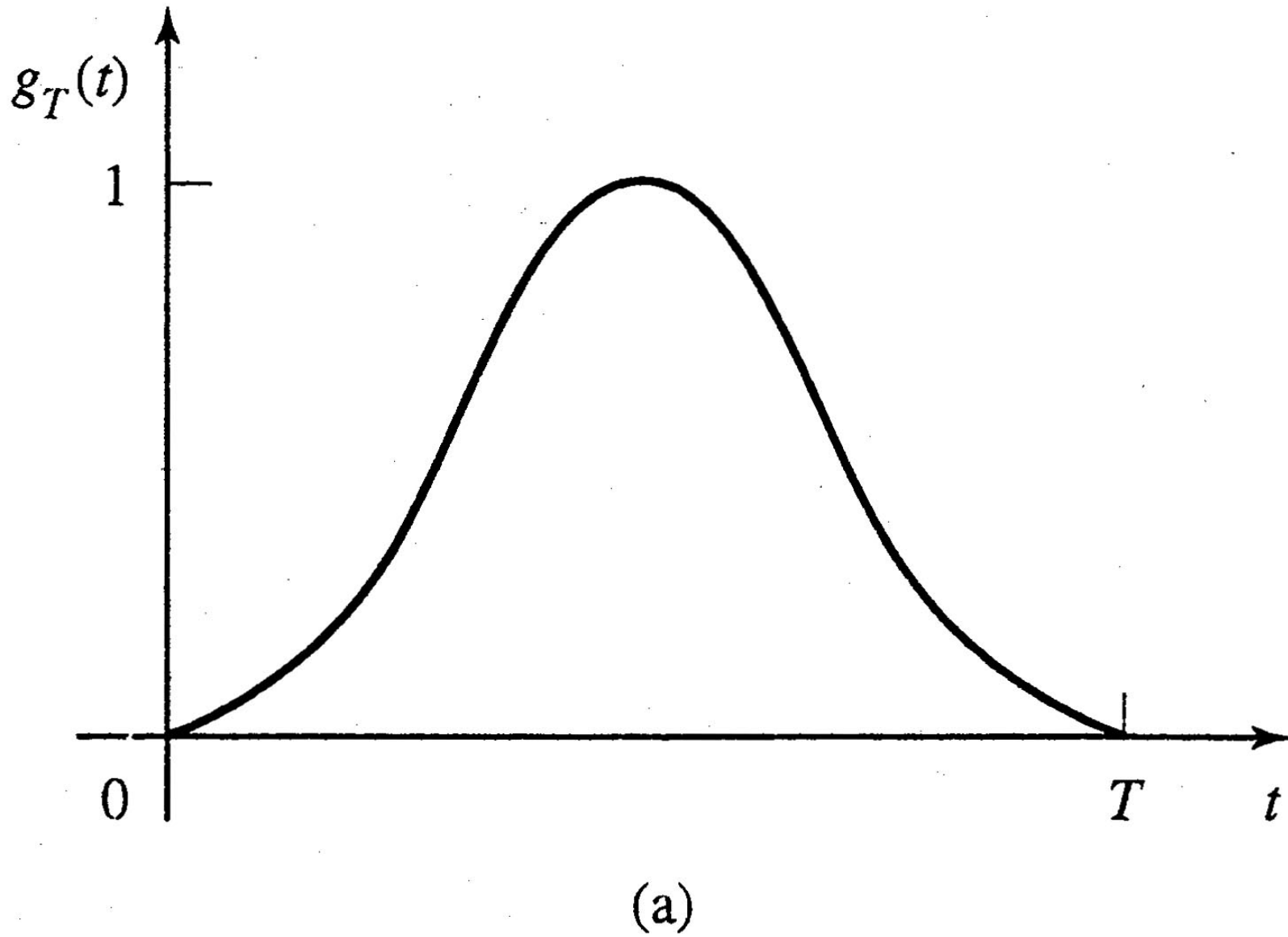


Figure 7.7 Signal pulse for PAM.

The M -ary PAM waveforms are one-dimensional signals, which may be expressed as

$$s_m(t) = s_m \psi(t), \quad m = 1, 2, \dots, M, \quad (7.2.10)$$

where $\psi(t)$ is the basis function defined as

$$\psi(t) = \frac{1}{\sqrt{\varepsilon_g}} g_T(t), \quad 0 \leq t \leq T, \quad (7.2.11)$$

where ε_g is the energy of the signal pulse $g_T(t)$, and s_m are the signal coefficients (one-dimensional vectors) given by

$$s_m = \sqrt{\varepsilon_g} A_m, \quad m = 1, 2, \dots, M. \quad (7.2.12)$$

The Euclidean distance between two signal points is defined as

$$\begin{aligned} d_{mn} &= \sqrt{|s_m - s_n|^2} \\ &= \sqrt{\varepsilon_g (A_m - A_n)^2}. \end{aligned} \quad (7.2.13)$$

If we select the signal amplitudes $\{A_m\}$ to be symmetrically spaced about zero and equally distant between adjacent signal amplitudes, we obtain the signal points for symmetric PAM, as shown in Figure 7.11.

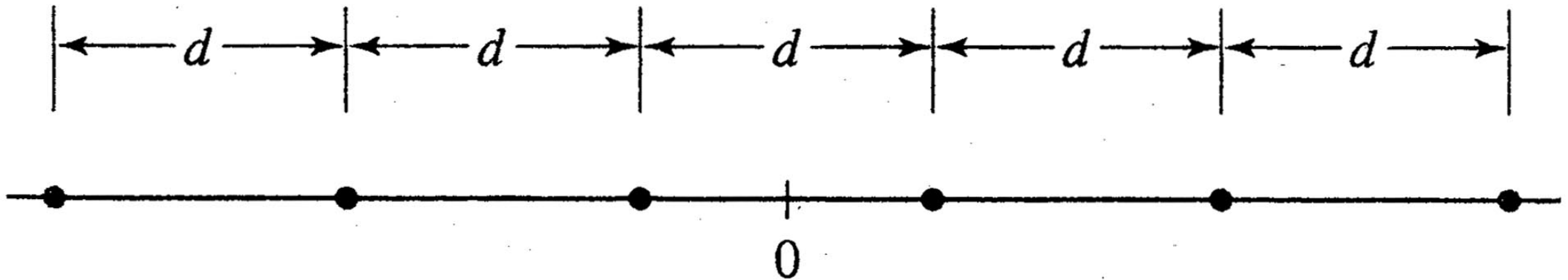


Figure 7.11 Signal points (constellation) for symmetric PAM

We observe that the PAM signals have different energies. In particular, the energy of the m th signal is given by

$$\begin{aligned} \mathcal{E}_m &= s_m^2 \\ &= \mathcal{E}_g A_m^2, \quad m=1, 2, \dots, M. \end{aligned} \tag{7.2.14}$$

For equi-probable signals, the average energy is given by

$$\mathcal{E}_{av} = \frac{1}{M} \sum_{m=1}^M \mathcal{E}_m$$

$$= \frac{\varepsilon_g}{M} \sum_{m=1}^M A_m^2. \quad (7.2.15)$$

If the signal amplitudes are symmetric about the origin, then we have

$$A_m = 2m - 1 - M, \quad m = 1, 2, \dots, M, \quad (7.2.16)$$

and, hence, the average energy is given by

$$\begin{aligned} \varepsilon_{av} &= \frac{\varepsilon_g}{M} \sum_{m=1}^M (2m - 1 - M)^2 \\ &= \frac{\varepsilon_g (M^2 - 1)}{3}. \end{aligned} \quad (7.2.17)$$

Ex.

Find A_m for a) $M = 4$, and b) $M = 5$. c) Also find ε_{av} with respect to ε_g .

Solution

a) $\{A_m\} = \{-3, -1, 1, 3\}$

b) $\{A_m\} = \{-4, -2, 0, 2, 4\}$

$$c) \quad \varepsilon_{av} = \frac{\varepsilon_g}{M} \sum_{m=1}^M (2m-1-M)^2$$

$$\varepsilon_{av} = 5 \text{ for } M = 4, \quad \varepsilon_{av} = 8 \text{ for } M = 5.$$

When the baseband PAM signals are impressed on a carrier, the basic geometric representation of the digital PAM signals remains the same.

The bandpass signals $u_m(t)$ may be expressed as

$$u_m(t) = s_m \psi(t) \tag{7.2.18}$$

where $\psi(t)$ is the basic signal defined as

$$\psi(t) = \sqrt{\frac{2}{\varepsilon_g}} g_T(t) \cos 2\pi f_c t \tag{7.2.19}$$

and

$$s_m = \sqrt{\frac{\varepsilon_g}{2}} A_m, \quad m = 1, 2, \dots, M. \tag{7.2.20}$$

Note that the only change in the geometric representation of bandpass PAM signals, compared to baseband signals, is the scale factor $\sqrt{2}$, which appears in (7.2.19) and (7.2.20).

7.3 Two-Dimensional Signals

7.3.1 Baseband Signals

Let us begin with the construction of two orthogonal signals.

Two signals $s_1(t)$ and $s_2(t)$ are said to be orthogonal over the interval $(0, T)$ if

$$\int_0^T s_1(t)s_2(t)dt = 0. \quad (7.3.1)$$

Two examples of orthogonal signals are shown in Figure 7.12.

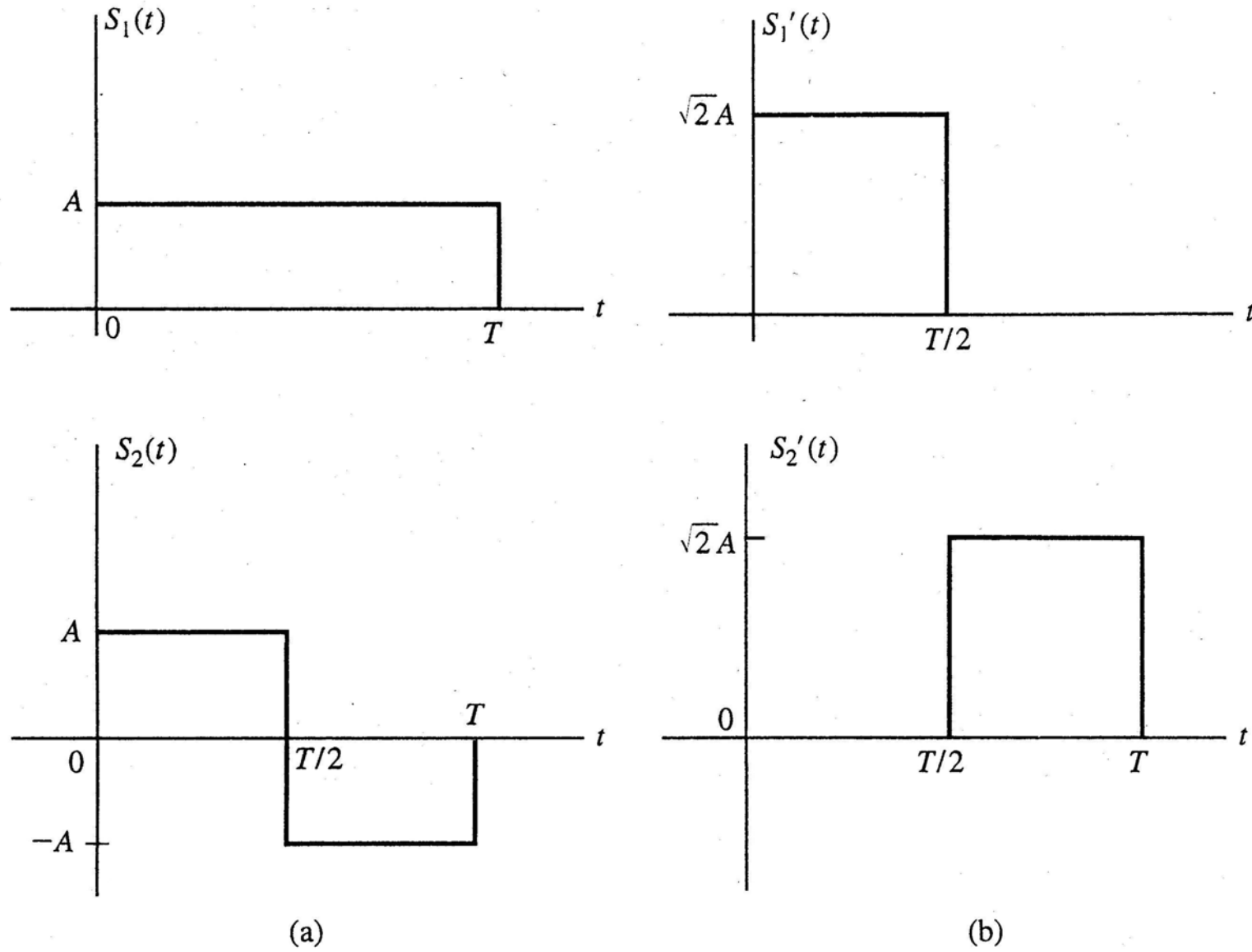


Figure 7.12 Two sets of orthogonal signals.

Note that the two signals $s_1(t)$ and $s_2(t)$ completely overlap over the interval $(0, T)$, while the signals $s'_1(t)$ and $s'_2(t)$ are nonoverlapping in time.

Both signal satisfy the orthogonality property in (7.3.1) and both signal pairs have identical energy; that is,

$$\begin{aligned}\mathcal{E} &= \int_0^T s_1^2(t) dt \\ &= \int_0^T s_2^2(t) dt \\ &= \int_0^T [s'_1(t)]^2 dt \\ &= \int_0^T [s'_2(t)]^2 dt \\ &= A^2T.\end{aligned}\tag{7.3.2}$$

Either pair of these signals may be used to transmit binary information, with one signal corresponding to a 1 and the other signal conveying the information bit 0.

Geometrically, these signals can be represented as signal vectors in two-dimensional space.

As basis functions, we may select the unit energy, rectangular functions:

$$\begin{aligned}\psi_1(t) &= \begin{cases} \sqrt{\frac{2}{T}}, & 0 \leq t \leq \frac{T}{2}, \\ 0, & \text{otherwise} \end{cases} \\ \psi_2(t) &= \begin{cases} \sqrt{\frac{2}{T}}, & \frac{T}{2} < t \leq T, \\ 0, & \text{otherwise.} \end{cases}\end{aligned}\tag{7.3.3}$$

Then, the signals $s_1(t)$ and $s_2(t)$ shown in Figure 7.12(a) can be expressed as

$$\begin{aligned}s_1(t) &= s_{11}\psi_1(t) + s_{12}\psi_2(t) \\ s_2(t) &= s_{21}\psi_1(t) + s_{22}\psi_2(t)\end{aligned}\tag{7.3.4}$$

where

$$\begin{aligned}\mathbf{s}_1 &= (s_{11}, s_{12}) \\ &= \left(A\sqrt{\frac{2}{T}}, A\sqrt{\frac{2}{T}} \right) \\ \mathbf{s}_2 &= (s_{21}, s_{22})\end{aligned}$$

$$= \left(A\sqrt{\frac{2}{T}}, -A\sqrt{\frac{2}{T}} \right). \quad (7.3.5)$$

The signal vectors \mathbf{s}_1 and \mathbf{s}_2 are shown in Figure 7.13.

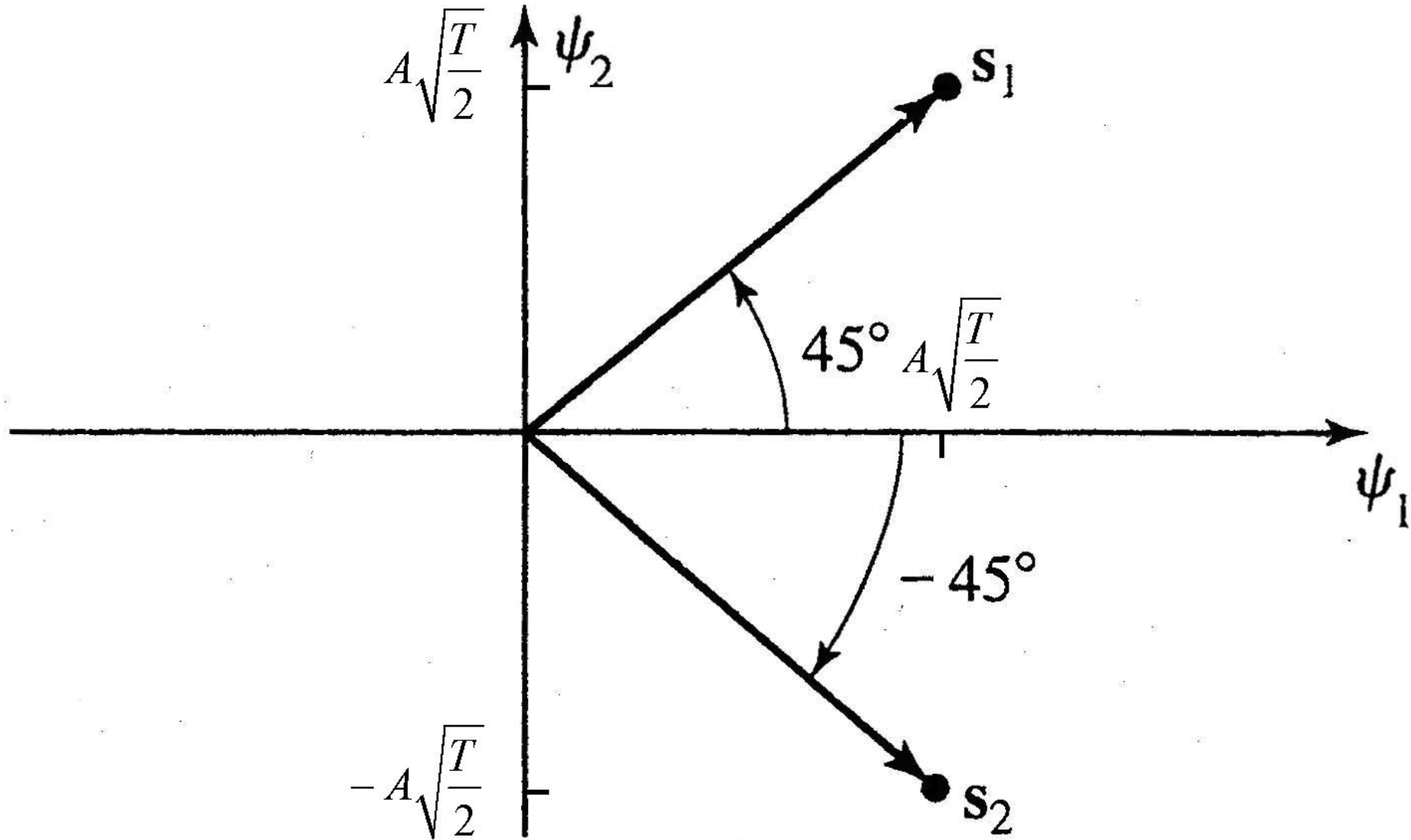


Figure 7.13 The two signal vectors corresponding to the signals $s_1(t)$ and $s_2(t)$.

Note that the signal vectors are separated by 90° , so that they are orthogonal.

Furthermore, the square of the length of each vector gives the energy in each signal; that is,

$$\begin{aligned}\varepsilon_1 &= \|\mathbf{s}_1\|^2 \\ &= A^2T\end{aligned}$$

and

$$\begin{aligned}\varepsilon_2 &= \|\mathbf{s}_2\|^2 \\ &= A^2T.\end{aligned}\tag{7.3.6}$$

The Euclidean distance between the two signals is given by

$$\begin{aligned}d_{12} &= \sqrt{\|\mathbf{s}_1 - \mathbf{s}_2\|^2} \\ &= A\sqrt{2T} \\ &= \sqrt{2A^2T} \\ &= \sqrt{2\varepsilon}\end{aligned}\tag{7.3.7}$$

where $\varepsilon = \varepsilon_1 = \varepsilon_2$ is the bit energy.

Similarly, the pair of orthogonal signals shown in Figure 7.12(b) can be expressed as in (7.3.4), where

$$\begin{aligned}\mathbf{s}'_1 &= (A\sqrt{T}, 0) \\ &= (\sqrt{\mathcal{E}}, 0)\end{aligned}$$

$$\begin{aligned}\mathbf{s}'_2 &= (0, A\sqrt{T}) \\ &= (0, \sqrt{\mathcal{E}}).\end{aligned}\tag{7.3.8}$$

These two signal vectors are shown in Figure 7.14.

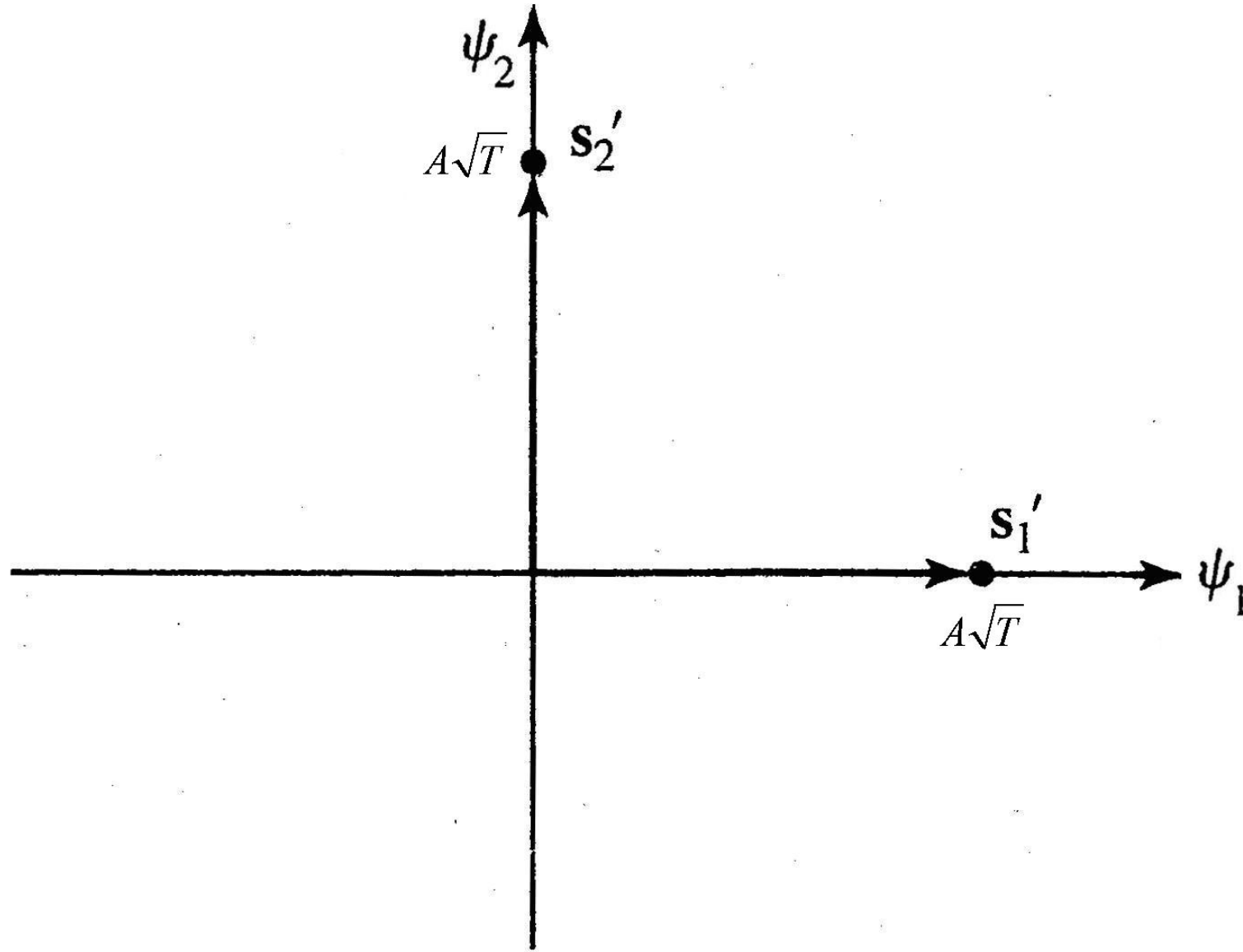


Figure 7.14 Two signal vectors corresponding to the signals $s_1'(t)$ and $s_2'(t)$.

Note that \mathbf{s}'_1 and \mathbf{s}'_2 are related to the signal vectors shown in Figure 7.13 by a simple 45° rotation.

Hence, the Euclidean distance between the signal points \mathbf{s}'_1 and \mathbf{s}'_2 is identical to that for signal points \mathbf{s}_1 and \mathbf{s}_2 .

Suppose that we wish to construct four signals in two dimensions.

With four signals, we can transmit two information bits in a signaling interval of T .

If we begin with the two orthogonal signals $s_1(t)$ and $s_2(t)$, shown in Figure 7.12(a), and their corresponding vector representation in Figure 7.13, it is easy to see that a simple construction is one that adds two additional signal vectors, namely, $-\mathbf{s}_1$ and $-\mathbf{s}_2$.

Thus, we obtain the 4-point signal-point constellation shown in Figure 7.15, which corresponds to the analog signals $s_1(t)$, $s_2(t)$, $-s_1(t)$, and $-s_2(t)$.

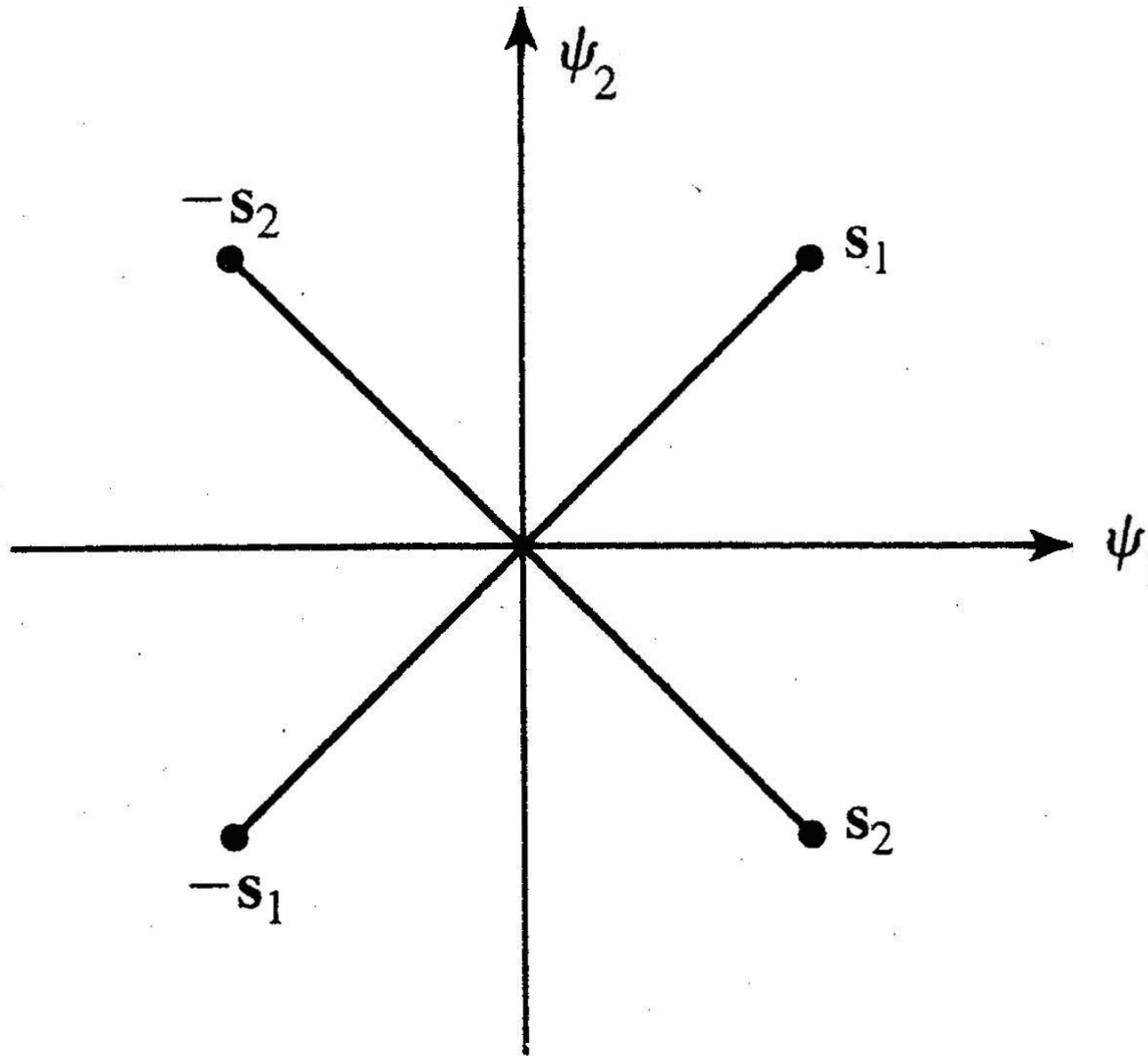


Figure 7.15 Signal constellation for $M = 4$ biorthogonal signals.

Since the pair $s_1(t)$ and $s_2(t)$ are orthogonal and the pair $-s_1(t)$ and $-s_2(t)$ are orthogonal, the signal set consisting of the four signals is called a set of **biorthogonal signals**.

The procedure for constructing a larger set of signals is relatively straightforward.

Specifically, we can add additional signal points (signal vectors) in the two-dimensional plane, and construct the corresponding signals by using the two orthonormal basis functions $\psi_1(t)$ and $\psi_2(t)$ given by (7.3.3).

For example, suppose we wish to construct $M = 8$ two-dimensional signals, all of equal energy ϵ_s .

These eight signal points are shown in Figure 7.16, and allow us to transmit three bits at a time.

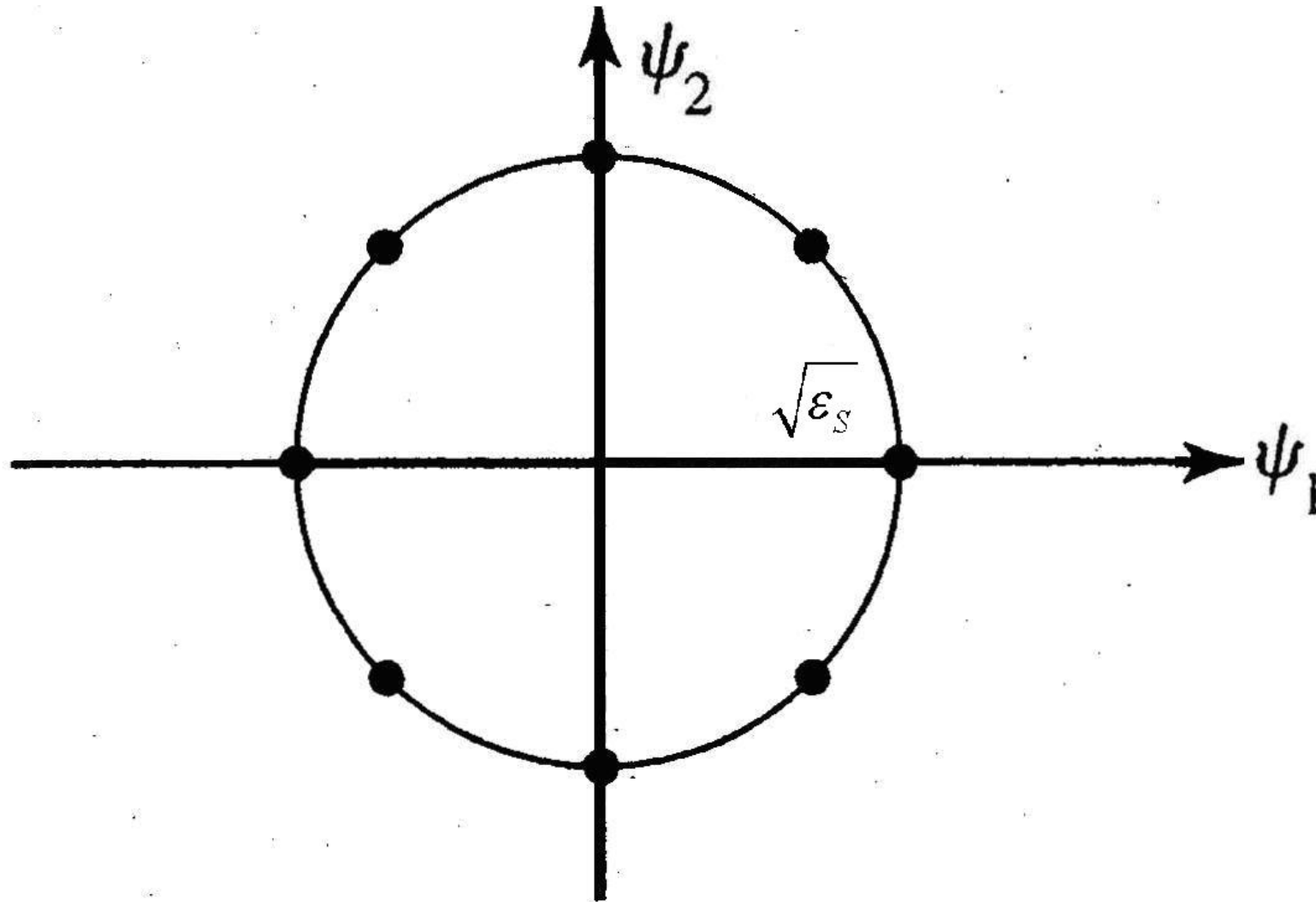


Figure 7.16 Signal-point constellation with $M = 8$ corresponding to the two points of orthogonal signals in Figure 7.12 and their negatives, that is, $s_1(t), s_2(t), s_1'(t), s_2'(t), -s_1(t), -s_2(t), -s_1'(t)$ and $-s_2'(t)$.

The corresponding eight signals are the two sets of biorthogonal signals constructed from the two pairs of orthogonal signals shown in Figure 7.12.

Alternatively, suppose that we remove the condition that all eight waveforms have equal energy.

For example, suppose that we select four biorthogonal waveforms that have energy ε_1 and another four biorthogonal waveforms that have energy ε_2 , where $\varepsilon_2 > \varepsilon_1$.

Two possible eight signal-point constellation are shown in Figure 7.17, where the signal points are located on two concentric circles of radii $\sqrt{\varepsilon_1}$ and $\sqrt{\varepsilon_2}$.

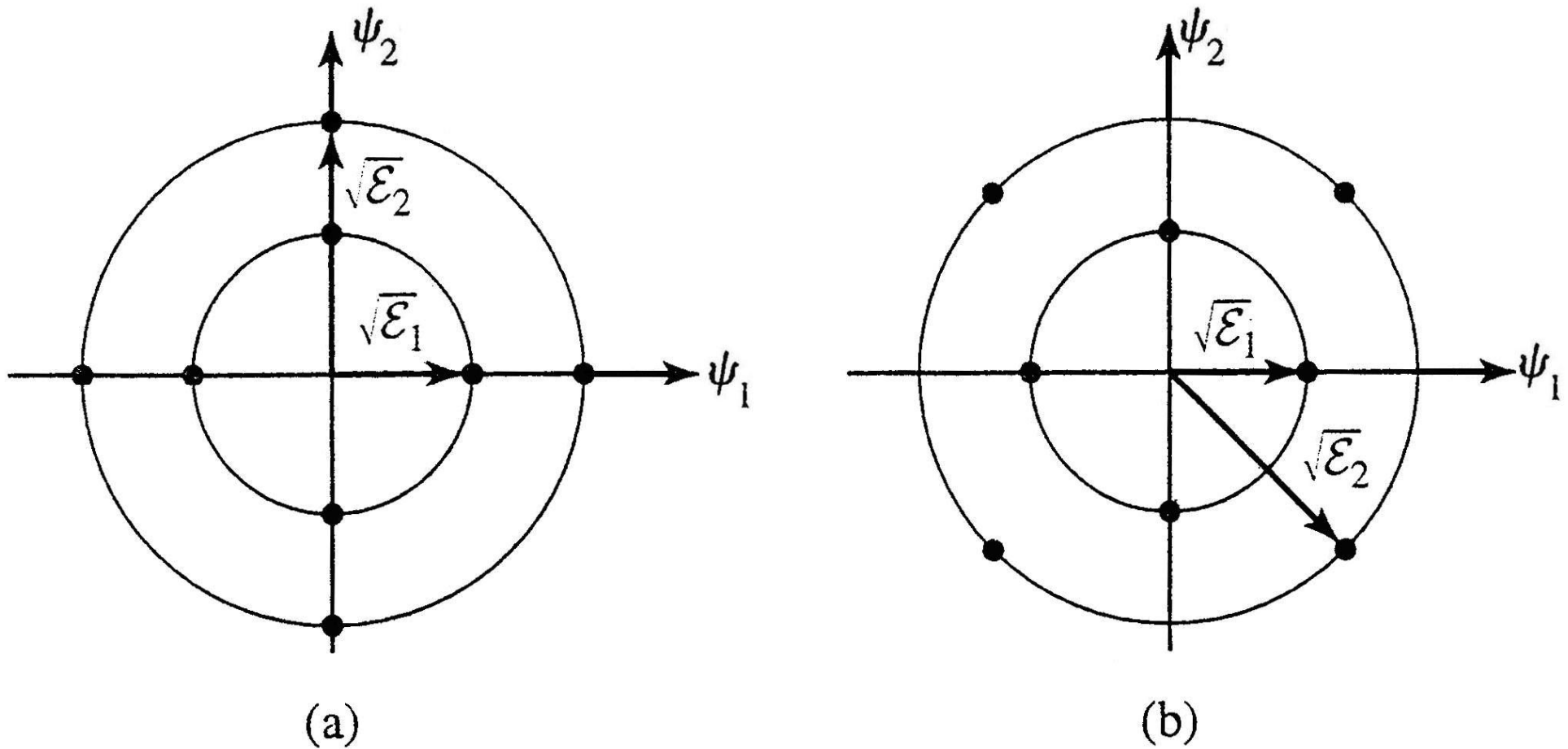


Figure 7.17 Two $M = 8$ signal-point constellation in two dimension, corresponding to a superposition waveforms with different energies.

In Section 7.6.5 we show that the signal set in Figure 7.17(b) is preferable in an AWGN channel to that shown in Figure 7.17(a).

7.3.2 Two-dimensional Bandpass Signals- Carrier-Phase

In the case of PAM, we recall that bandpass signals, appropriate for transmission on bandpass channels, were generated by taking a set of baseband signals and impressing them on a carrier.

In a similar manner, if we have a set of M two-dimensional signals, say $s_m(t)$, $m = 1, 2, \dots, M$, we can generate a set of M bandpass signals as

$$u_m(t) = s_m(t) \cos 2\pi f_c t, \quad m = 1, 2, \dots, M, \quad 0 \leq t \leq T. \quad (7.3.9)$$

We consider the special case in which the M two-dimensional bandpass signals waveforms are constrained to have the same energy; that is,

$$\begin{aligned} \mathcal{E}_m &= \int_0^T u_m^2(t) dt \\ &= \int_0^T s_m^2(t) \cos^2 2\pi f_c t dt \\ &= \frac{1}{2} \int_0^T s_m^2(t) dt + \frac{1}{2} \int_0^T s_m^2(t) \cos 4\pi f_c t dt. \end{aligned} \quad (7.3.10)$$

As indicated previously, the integral of the double-frequency component in (7.3.10) average to zero when $f_c \gg W$, where W is the bandwidth of the baseband signal $s_m(t)$.

Hence,

$$\begin{aligned}\varepsilon_m &= \frac{1}{2} \int_0^T s_m^2(t) dt \\ &= \varepsilon_s, \quad \text{for all } m,\end{aligned}\tag{7.3.11}$$

where ε_s is the energy per symbol or symbol energy.

When all the signals have the same energy, the corresponding signal points in the geometric representation of the signals fall on a circle of radius $\sqrt{\varepsilon_s}$.

In case of the four biorthogonal waveforms, the signal points are as shown in Figure 7.15 or, equivalently, any phase-rotated version of these signal points.

From this geometric representation for $M = 4$, we observe that the signal points are equivalent to a single signal whose phase is shifted by multiples of $\frac{\pi}{2}$.

That is, a bandpass signal of the form $s(t)\cos\left(2\pi f_c t + \frac{\pi m}{2}\right)$, $m = 0, 1, 2, 3$, has the same geometric representation as an $M = 4$ general biorthogonal signal set.

Therefore, a simple way to generate a set of M bandpass signals having equal energy is to impress the information on the phase of the carrier.

Thus, we have a carrier-phase modulated signal.

The general representation of a set of M phase modulated signals is given by

$$u_m(t) = g_T(t)\cos\left(2\pi f_c t + \frac{2\pi m}{M}\right), \quad m = 0, 1, \dots, M-1, \quad 0 \leq t \leq T, \quad (7.3.12)$$

where $g_T(t)$ is a baseband pulse shape, which determine the spectral characteristics of the transmitted signal.

When $g_T(t)$ is a rectangular pulse, defined as

$$g_T(t) = \sqrt{\frac{2\mathcal{E}_s}{T}}, \quad 0 \leq t \leq T, \quad (7.3.13)$$

the corresponding transmitted signals

$$u_m(t) = \sqrt{\frac{2\mathcal{E}_s}{T}} \cos\left(2\pi f_c t + \frac{2\pi m}{M}\right), \quad m = 0, 1, \dots, M-1, \quad 0 \leq t \leq T, \quad (7.3.14)$$

have a constant envelope (notice that the pulse shape $g_T(t)$ is a rectangular pulse) and the carrier phase changes abruptly at the beginning of each signal interval.

This type of digital phase modulation is called **phase-shift keying (PSK)**.

Figure 7.18 shows a four-phase ($M = 4$) PSK signals, usually called a quadrature PSK (QPSK) signal.

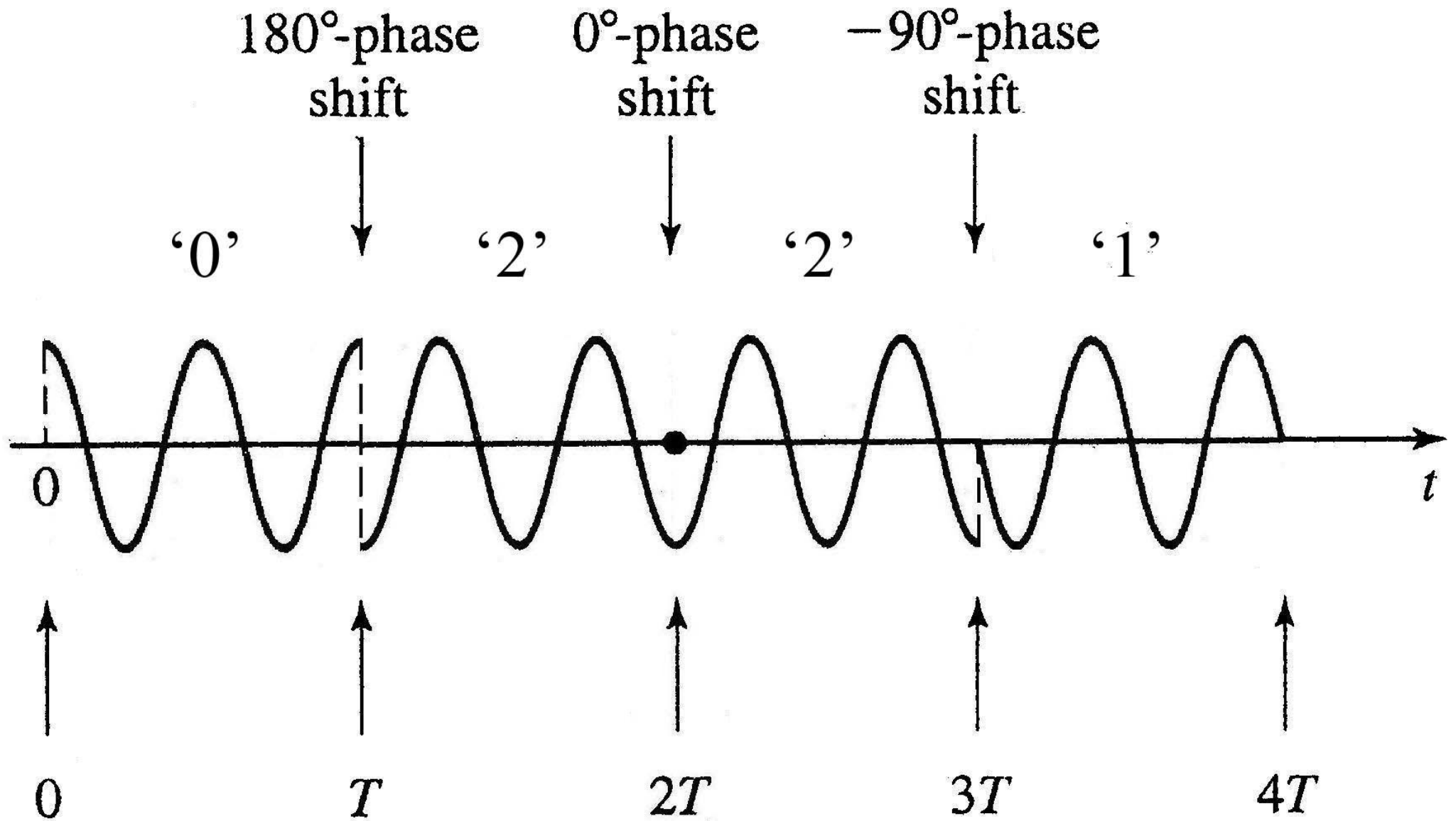


Figure 7.18 Examples of a four PSK signal.

The waveforms in (7.3.14) are written as

$$\begin{aligned}
 u_m(t) &= \sqrt{\frac{2\varepsilon_s}{T}} \cos 2\pi \frac{m}{M} \cdot \cos 2\pi f_c t - \sqrt{\frac{2\varepsilon_s}{T}} \sin 2\pi \frac{m}{M} \cdot \sin 2\pi f_c t \\
 &= \sqrt{\varepsilon_s} \cos 2\pi \frac{m}{M} \cdot \sqrt{\frac{2}{T}} \cos 2\pi f_c t + \sqrt{\varepsilon_s} \sin 2\pi \frac{m}{M} \cdot \left(-\sqrt{\frac{2}{T}} \sin 2\pi f_c t\right) \\
 &= \sqrt{\varepsilon_s} \cos 2\pi \frac{m}{M} \cdot \psi_1(t) + \sqrt{\varepsilon_s} \sin 2\pi \frac{m}{M} \cdot \psi_2(t), \tag{7.3.15}
 \end{aligned}$$

$m = 0, 1, \dots, M - 1$, where

$$\psi_1(t) = \sqrt{\frac{2}{T}} \cos 2\pi f_c t,$$

and

$$\psi_2(t) = -\sqrt{\frac{2}{T}} \sin 2\pi f_c t. \tag{7.3.16}$$

Notice that

$$\int_0^T \sqrt{\frac{2}{T}} \cos 2\pi f_c t = \int_0^T \left(-\sqrt{\frac{2}{T}} \sin 2\pi f_c t\right) = 1.$$

Hence, $\sqrt{\frac{2}{T}} \sin 2\pi f_c t$ and $-\sqrt{\frac{2}{T}} \sin 2\pi f_c t$ are the basis functions for the signal set $\{u_m(t), m = 0, 1, \dots, M - 1\}$.

Thus, a phase modulated signal $u_m(t)$ is viewed as the sum of two quadrature carriers with amplitudes $\sqrt{\mathcal{E}_s} \cos 2\pi \frac{m}{M}$ and $\sqrt{\mathcal{E}_s} \sin 2\pi \frac{m}{M}$ as shown in Figure 7.19, which depend on the phase of the transmitted signal $2\pi \frac{m}{M}$ in each interval.

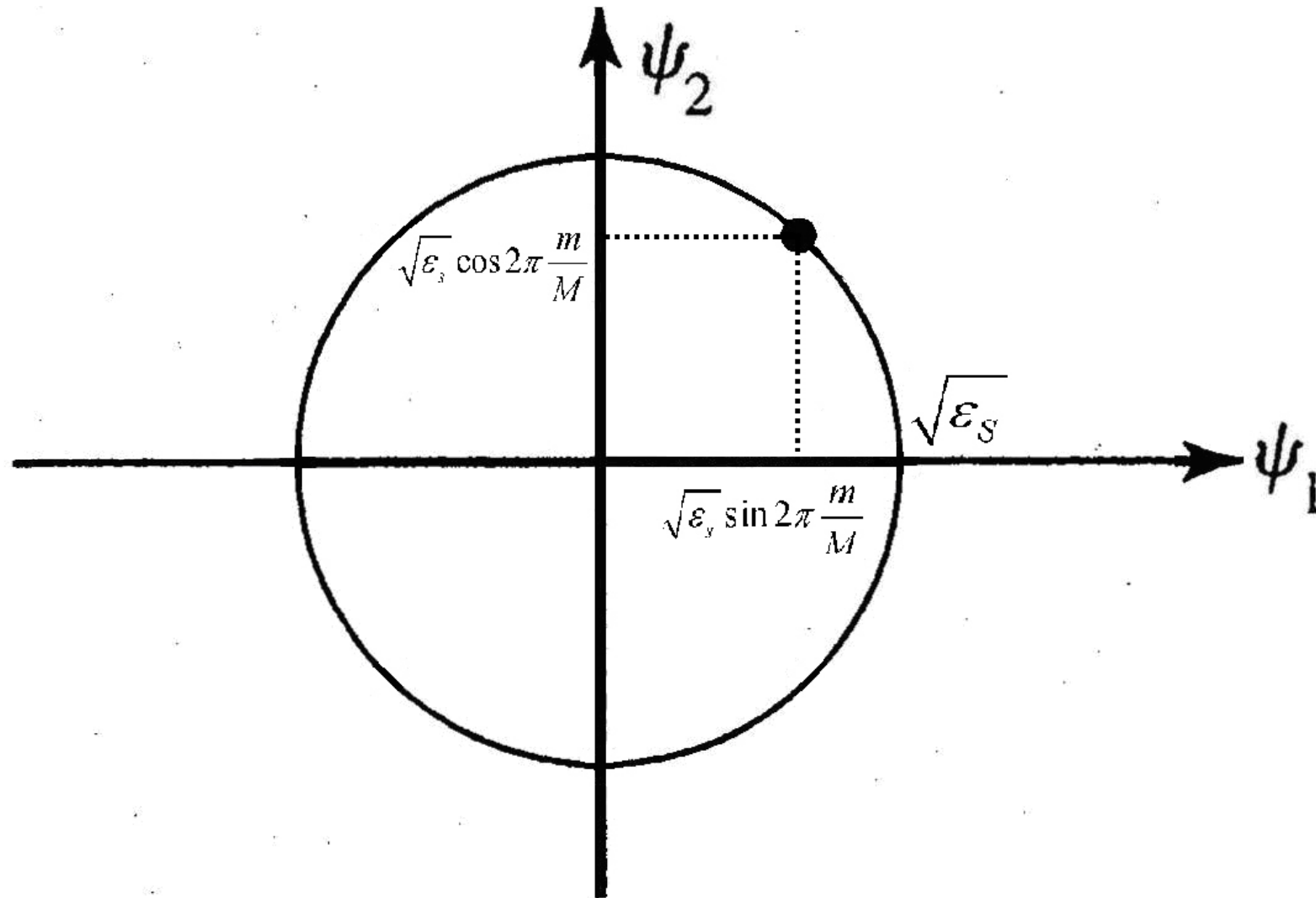


Figure 7.19 Phase modulated signal viewed as sum of two amplitude-modulated quadrature carriers.

It follows from (7.3.15) that digital phase-modulated signals can be represented geometrically as two-dimensional vectors with components $\sqrt{\varepsilon_s} \cos 2\pi \frac{m}{M}$, and $\sqrt{\varepsilon_s} \sin 2\pi \frac{m}{M}$, that is,

$$\mathbf{s}_m = \left(\sqrt{\varepsilon_s} \cos 2\pi \frac{m}{M}, \sqrt{\varepsilon_s} \sin 2\pi \frac{m}{M} \right). \quad (7.3.17)$$

Note that for a set of phase modulated signals in (7.3.12), its basis functions become

$$\psi_1(t) = \sqrt{\frac{2}{\varepsilon_g}} g_T(t) \cos 2\pi f_c t,$$

and

$$\psi_2(t) = -\sqrt{\frac{2}{\varepsilon_g}} g_T(t) \sin 2\pi f_c t.$$

Compare these basis functions and those in (7.3.16).

Signal-point constellations for $M = 2, 4, 8$ are shown in Figure 7.20.

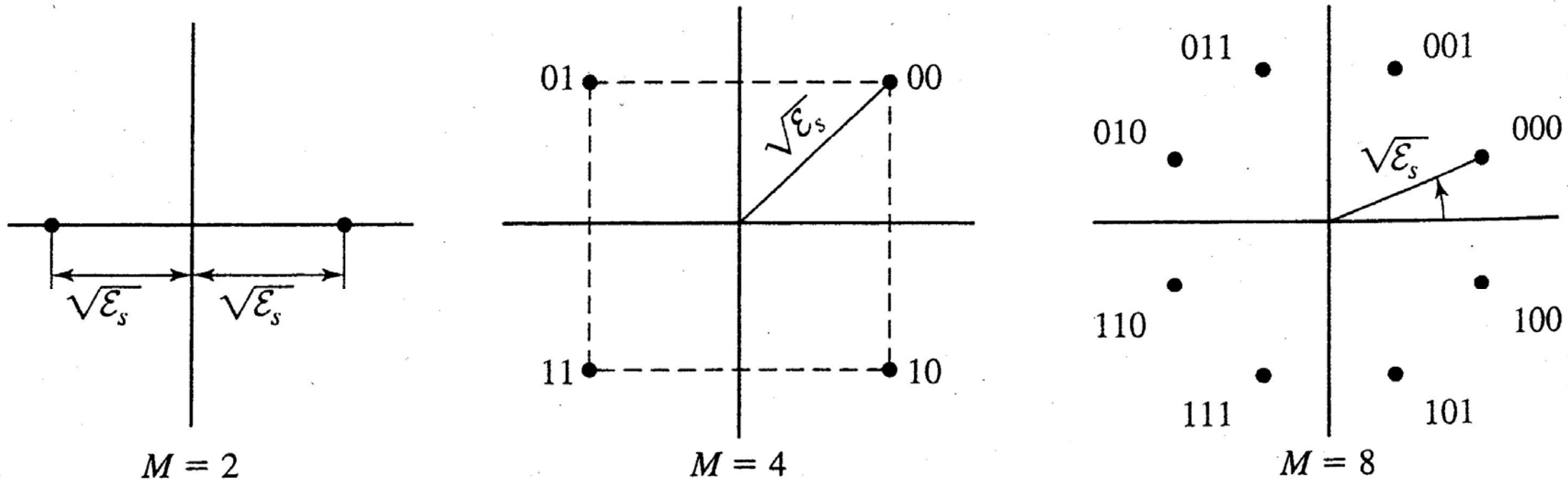


Figure 7.20 PSK signal constellations.

Note that binary phase modulation is identical to binary PAM.

The mapping or assignment of k information bits into the $M = 2^k$ possible phases can be done in various ways.

The preferred assignment is to use **Gray encoding** (or Gray coding) in which adjacent phases differ by one binary digit as shown in Figure 7.20.

Because the most likely errors caused by noise involve the erroneous selection of an adjacent phase to the transmitted phase, only a single bit error occurs in the k -bit sequence when Gray encoding is adopted.

The Euclidean distance between any two signal points in the constellation is given by

$$\begin{aligned} d_{mn} &= \sqrt{\|\mathbf{s}_m - \mathbf{s}_n\|^2} \\ &= \sqrt{2\mathcal{E}_s \left(1 - \cos \frac{2\pi(m-n)}{M} \right)} \end{aligned} \quad (7.3.18)$$

and the minimum Euclidean distance (distance between two adjacent signal points) is simply given by

$$d_{\min} = \sqrt{2\mathcal{E}_s \left(1 - \cos \frac{2\pi}{M} \right)}. \quad (7.3.19)$$

The minimum Euclidean distance d_{\min} plays an important role in determining the bit error rate (or symbol error rate) performance of the receiver which demodulates and detects the information from the received signal in the presence of an additive Gaussian noise.

7.3.3 Two-dimensional Bandpass Signals – Quadrature Amplitude Modulation

We observed that the phase two-dimensional bandpass signals can be viewed as a sum of two orthogonal carrier signals, $\cos 2\pi f_c t$ and $\sin 2\pi f_c t$, modulated by the information bits.

If we remove the constraint of equal symbol energy ε_s which is applied to a PAM signal set, we can construct signals that are not constrained to fall on a circle of radius $\sqrt{\varepsilon_s}$.

The simplest way to construct such signals to impress separate information bits on each of the quadrature carriers, $\cos 2\pi f_c t$ and $\sin 2\pi f_c t$.

This type of digital modulation is called **quadrature amplitude modulation (QAM)**.

We may view this method of information transmission as a form of quadrature-carrier multiplexing, previously described in Section 3.2.6.

The transmitted signals have the form

$$u_m(t) = A_{mc} g_T(t) \cos 2\pi f_c t + A_{ms} g_T(t) \sin 2\pi f_c t, \quad m = 1, 2, \dots, M, \quad (7.3.20)$$

where $\{A_{mc}\}$ and $\{A_{ms}\}$ are the sets of amplitude levels that are obtained by mapping k -bit sequence into signal amplitudes.

For example, Figure 7.21 shows a 16-QAM signal constellation that is obtained by amplitude modulating each quadrature carrier by $M = 4$ PAM.

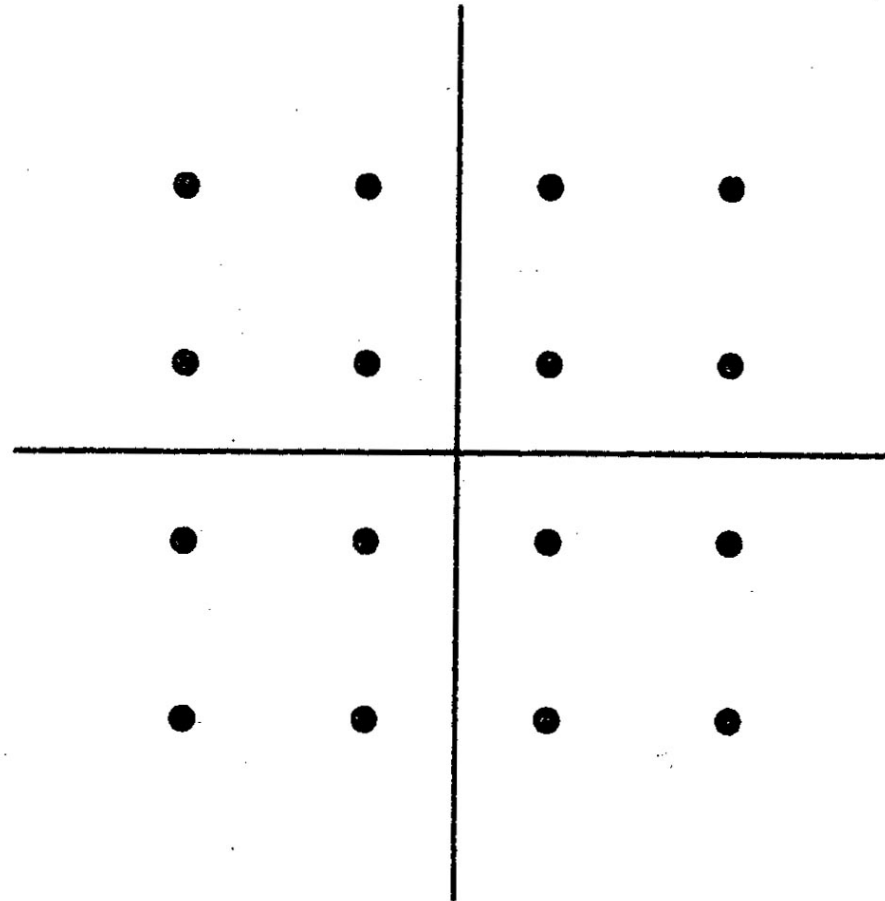


Figure 7.21 $M = 16$ -QAM signal constellation

In general, a rectangular signal constellation is obtained when two quadrature carriers are each modulated by PAM.

More generally, QAM may be viewed as a form of combined digital amplitude and digital-phase modulation.

The transmitted signal of QAM of the combined amplitude-and phase-modulation method is expressed as

$$u_{mn}(t) = A_m g_T(t) \cos(2\pi f_c t + \theta_n), \quad m = 1, 2, \dots, M_1, \quad n = 1, 2, \dots, M_2. \quad (7.3.21)$$

If $M_1 = 2^{k_1}$ and $M_2 = 2^{k_2}$, the combined amplitude-and phase-modulation method results in the simultaneous transmission of $k_1 + k_2 = \log_2 M_1 M_2$ binary digits occurring at a symbol rate $\frac{R_b}{(k_1 + k_2)}$.

Figure 7.22 shows the functional block diagram of a QAM modulator.

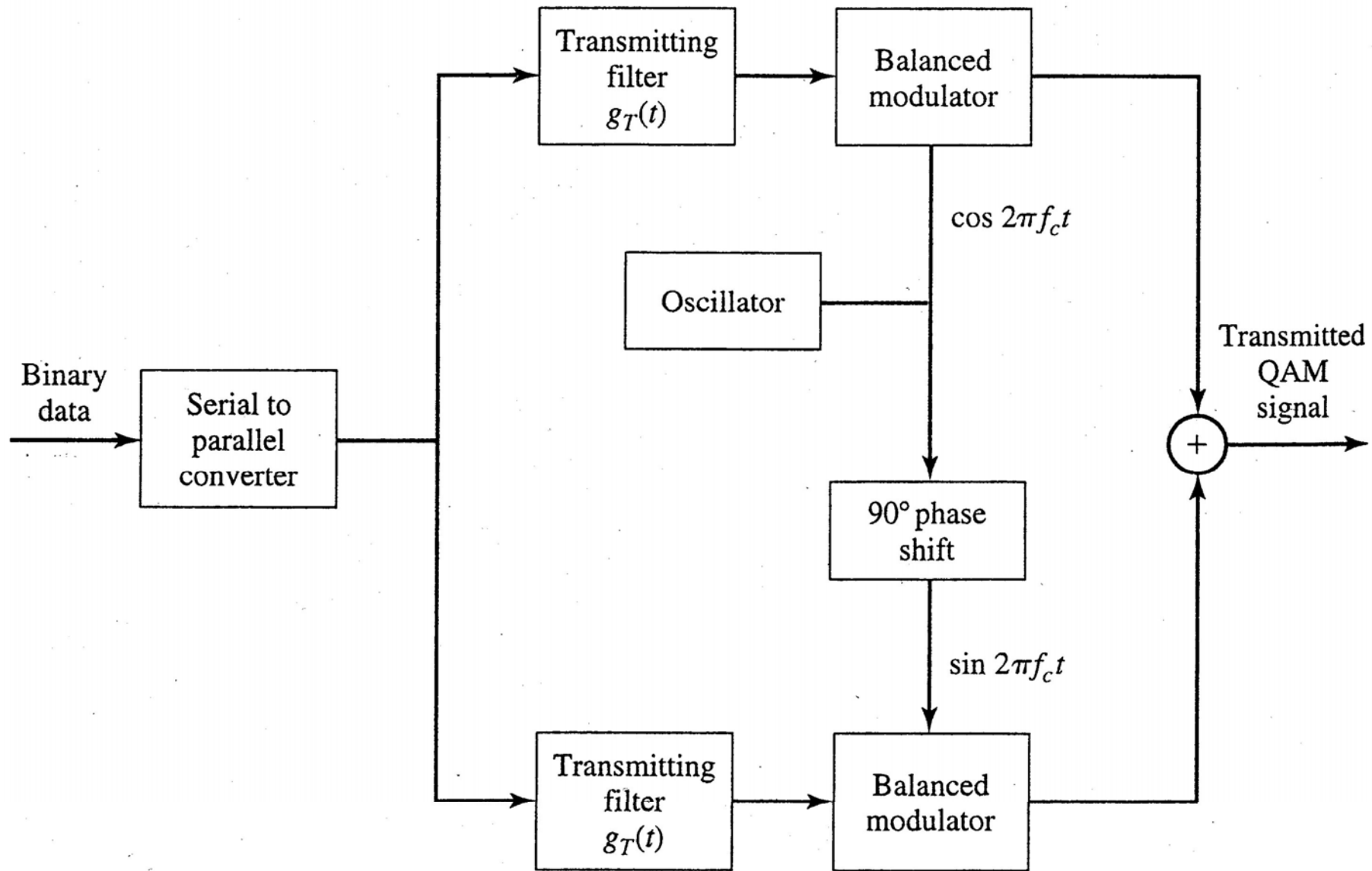


Figure 7.22 Functional block diagram of modulator for QAM.

It is clear that the geometric signal representation of the signals given by (7.3.20) and (7.3.21) is in terms of two-dimensional signal vectors of the form

$$s_m = \left(\sqrt{\varepsilon_s} A_{mc}, \sqrt{\varepsilon_s} A_{ms} \right), \quad m = 1, 2, \dots, M. \quad (7.3.22)$$

Examples of signal space constellations for QAM are shown in Figure 7.23.

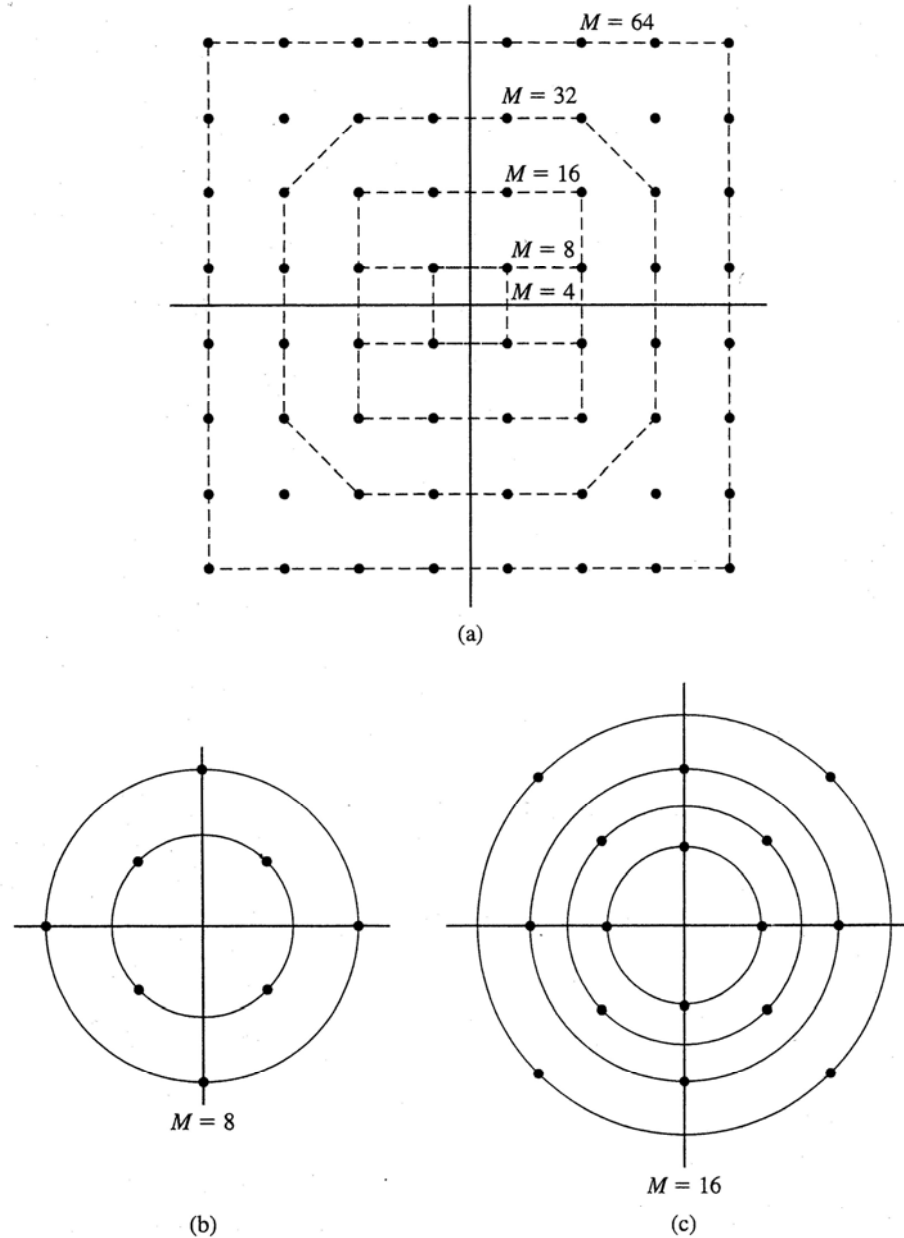


Figure 7.23 (a) Rectangular signal-space constellations for QAM. (b, c) Examples of combined PAM-PSK signal-space constellations.

The average transmitted energy for these signal constellations is simply the sum of the average energies on each of the quadrature carriers.

For rectangular signal constellations, as shown in Figure 7.23(a), the average energy/symbol is given by

$$\varepsilon_{av} = \frac{1}{M} \sum_{i=1}^M \|\mathbf{s}_i\|^2.$$

The Euclidean distance between any pair of signal points is given by

$$d_{mn} = \sqrt{\|\mathbf{s}_m - \mathbf{s}_n\|^2} \quad . \quad (7.3.23)$$

7.4 Multidimensional Signals

Consider the design of a set of $M = 2^k$ signals having more than two dimensions.

Transmission using a multidimensional signal set has advantages which will be shown in Section 7.6.6 .

7.4.1 Orthogonal Signals

Consider the construction of baseband orthogonal signals first and then discuss the design of bandpass signals.

Baseband Signals

Orthogonal signals at baseband can be constructed in various ways.

Figure 7.24 shows two sets of orthogonal signals for $M = 4$.

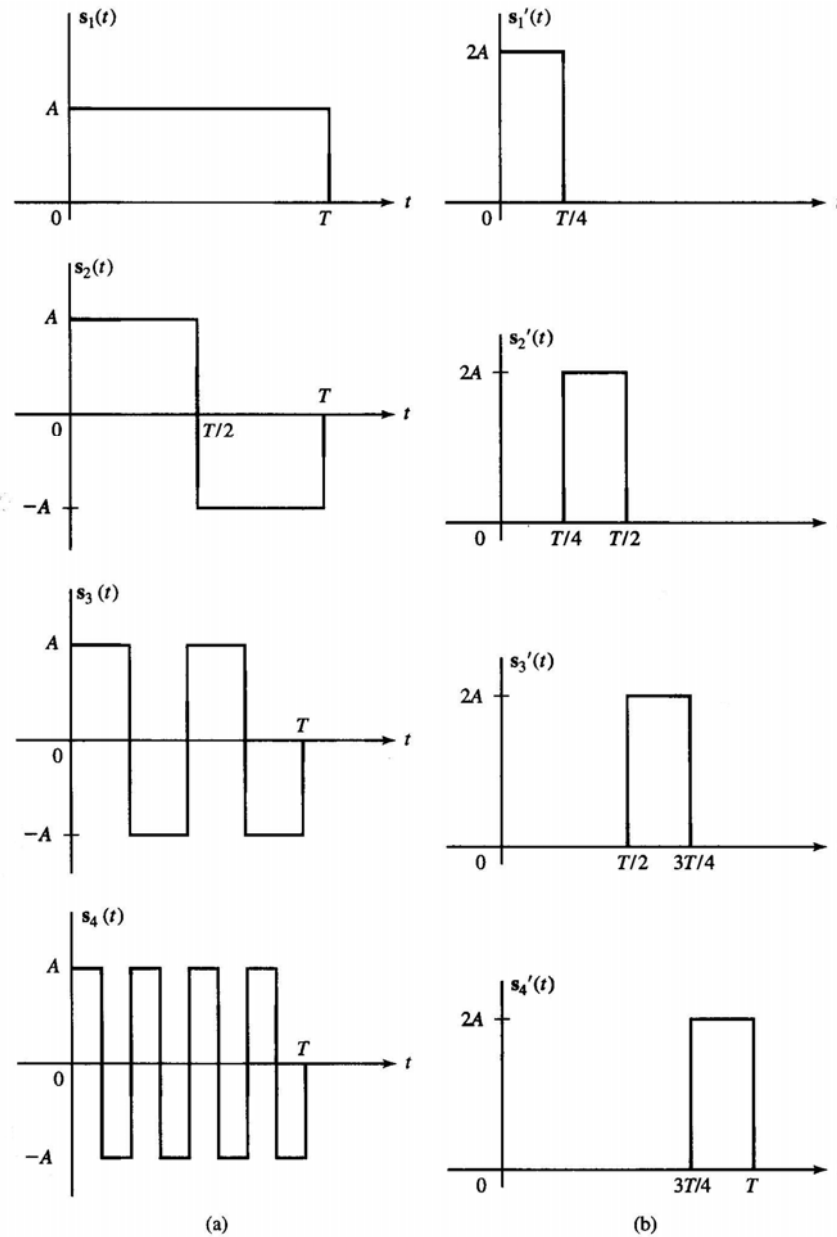


Figure 7.24 Two sets of $M = 4$ orthogonal signal waveforms.

In Figure 7.24, it is shown that the signals $s_i(t)$, $i = 1, 2, 3, 4$, completely overlap over the interval $(0, T)$, while the signals $s'_i(t)$, $i = 1, 2, 3, 4$, are non-overlapping in time, that is, they are a set of orthogonal signal with $M = 4$.

For a set of K baseband signals, we can apply the Gram-Schmidt procedure to construct $M \leq K$ mutually orthonormal waveforms $\psi_i(t)$, $i = 1, 2, \dots, M$.

Ex. (Walsh-Hadamard sequences)

A set of Hadamard sequences is a set of $M = 2^k$ overlapping orthogonal waveforms (see Problem 7.31). Walsh-Hadamard sequences (Walsh-Hadamard sequences, Walsh sequences, Walsh codes, or Hadamard codes in short) with sequence length of 64 are used in the IS-95 system which the CDMA cellular system deployed in Korea.

When the M orthogonal waveforms are non-overlapping in time, the transmitted digital information is conveyed by the time interval in which the signal pulse occupies.

This type of signaling is called pulse position modulation (PPM).

In this case, the M baseband signals are expressed as

$$s_m(t) = A g_T(t - \frac{(m-1)T}{M}), \quad \frac{(m-1)T}{M} \leq t < \frac{mT}{M}, \quad m = 1, 2, \dots, M, \quad (7.4.1)$$

where $g_T(t)$ is a signal pulse of duration $\frac{T}{M}$ having arbitrary shape.

Although each signal in a set of M orthogonal signals can have different energy, usually it is designed to have the same energy so that the signal set could achieve smaller error probability (to be dealt later).

For example, for a set of M PPM signals (non-overlapping signal pulses of duration $\frac{T}{M}$) with the same amplitude A , its symbol energy is given by

$$\begin{aligned} \int_0^T s_m^2(t) dt &= A^2 \int_{(m-1)T/M}^{mT/M} g_T^2(t - \frac{(m-1)T}{M}) dt \\ &= A^2 \int_0^{T/M} g_T^2(t) dt \\ &= \varepsilon_s, \quad \text{all } m \end{aligned} \quad (7.4.2)$$

where ε_s is symbol energy.

We define the M basis functions for a PPM signal set as

$$\psi_m(t) = \begin{cases} \frac{1}{\sqrt{\mathcal{E}_s}} g\left(t - \frac{(m-1)T}{M}\right), & \frac{(m-1)T}{M} \leq t < \frac{mT}{M}, \\ 0, & \text{otherwise,} \end{cases} \quad (7.4.3)$$

for $m = 1, 2, \dots, M$.

Hence, M -ary PPM signals are represented geometrically by the M -dimensional vectors:

$$\begin{aligned} \mathbf{s}_1 &= (\sqrt{\mathcal{E}_s}, 0, 0, \dots, 0) \\ \mathbf{s}_2 &= (0, \sqrt{\mathcal{E}_s}, 0, \dots, 0) \\ &\vdots \\ \mathbf{s}_M &= (0, 0, 0, \dots, \sqrt{\mathcal{E}_s}). \end{aligned} \quad (7.4.4)$$

which are orthogonal as $\mathbf{s}_i \cdot \mathbf{s}_j = 0$ when $i \neq j$.

Note that the M signal vectors are mutually equi-distant; that is,

$$\begin{aligned} d_{mn} &= \sqrt{\|\mathbf{s}_m - \mathbf{s}_n\|^2} \\ &= \sqrt{2\mathcal{E}_s}, \quad \text{for all } m \neq n. \end{aligned} \quad (7.4.5)$$

Hence, the minimum distance between signal points of the signal set is $\sqrt{2\varepsilon_s}$.

Figure 7.25 shows an example of an orthogonal signal set with $M = 3$.

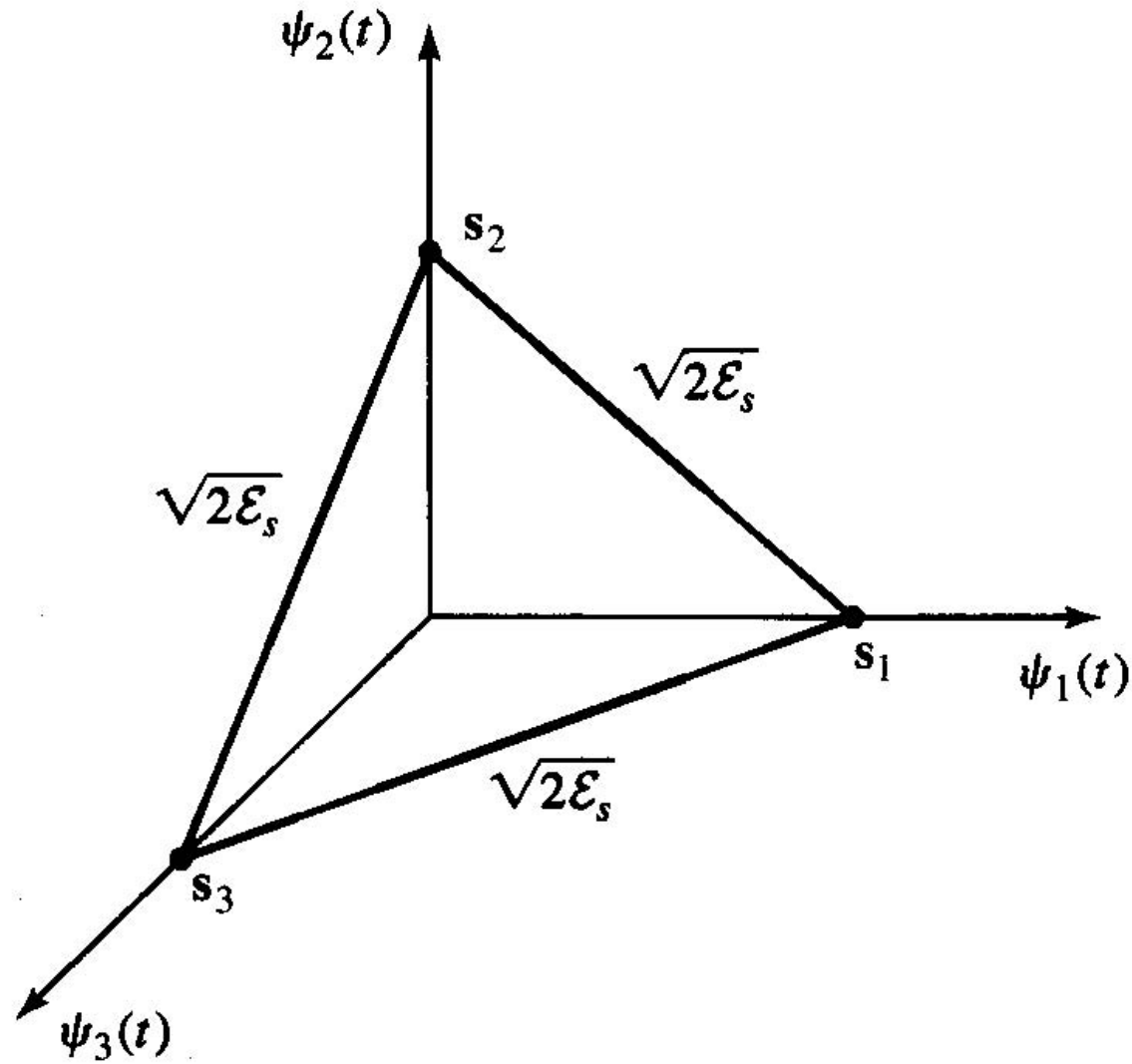


Figure 7.25 Orthogonal signals. $M = N = 3$.

Bandpass Signals

Bandpass orthogonal signals are constructed from a set of baseband orthogonal signals $s_m(t) = 1, 2, \dots, M$, by multiplying them by the carrier $\cos 2\pi f_c t$.

Then, M bandpass signals are obtained as

$$u_m(t) = s_m(t) \cos 2\pi f_c t, \quad 0 \leq t \leq T, \quad m = 1, 2, \dots, M. \quad (7.4.6)$$

each of which energy is one-half of the energy of the corresponding baseband signal $s_m(t)$.

The orthogonality of the bandpass signals as verified by

$$\begin{aligned} \int_0^T u_m(t) u_n(t) dt &= \int_0^T s_m(t) s_n(t) \cos^2 2\pi f_c t dt \\ &= \frac{1}{2} \int_0^T s_m(t) s_n(t) dt + \frac{1}{2} \int_0^T s_m(t) s_n(t) \cos 4\pi f_c t dt \\ &= 0 \end{aligned}$$

where the double frequency term becomes zero when $T \cdot 2f_c =$ integer or the carrier frequency f_c is much larger than the bandwidth of the baseband signals, that is, the symbol duration T is much larger than the duration of a cycle of the carrier.

While a set of M -ary PPM signals achieve orthogonality in time domain by means of non-overlapping pulses, alternatively a set of M modulated signals can achieve orthogonality in frequency domain.

Modulation having orthogonality in frequency domain is generally called carrier-frequency modulation.

Frequency-Shift Keying (FSK)

The simplest carrier-frequency modulation is binary frequency-shift keying.

Other types of carrier-frequency modulation are described in Chapter 10.

In binary FSK we employ two different frequencies, f_1 and $f_2 = f_1 + \Delta f$, to transmit a binary information.

The two signals are given by

$$\begin{aligned} u_1(t) &= \sqrt{\frac{2\varepsilon_b}{T_b}} \cos 2\pi f_1 t, \quad 0 \leq t \leq T_b, \\ u_2(t) &= \sqrt{\frac{2\varepsilon_b}{T_b}} \cos 2\pi f_2 t, \quad 0 \leq t \leq T_b, \end{aligned} \tag{7.4.7}$$

where ε_b is the energy/bit (or bit energy) and T_b is the duration of the bit interval.

M -ary FSK is used to transmit a block of $k = \log_2 M$ bits/signal whose signals are given by

$$u_m(t) = \sqrt{\frac{2\varepsilon_s}{T}} \cos(2\pi f_c t + 2\pi m \Delta f t), \quad 0 \leq t \leq T, \quad m = 0, 1, \dots, M-1, \quad (7.4.8)$$

where $\varepsilon_s = k\varepsilon_b$ is the energy/symbol (or symbol energy),

$T = kT_b$ is the symbol interval, and

Δf is the frequency separation between successive frequencies; i.e., $\Delta f = f_m - f_{m-1}$, where $f_m = f_c + m\Delta f$.

Note that the M FSK waveforms have equal symbol energy ε_s .

The frequency separation Δf determines the degree of discrimination among the M possible transmitted signals.

As a measure of the similarity (or dissimilarity) between a pair of signals, the crosscorrelation coefficient between $u_m(t)$ and $u_n(t)$ is defined as

$$\gamma_{mn} = \frac{1}{\varepsilon_s} \int_0^T u_m(t) u_n(t) dt. \quad (7.4.9)$$

,From (7.4.8) and (7.4.9) the crosscorrelation coefficient between signals $u_m(t)$ and $u_n(t)$ of M -ary FSK is given by

$$\begin{aligned}
 \gamma_{mn} &= \frac{1}{\mathcal{E}_s} \int_0^T \frac{2\mathcal{E}_s}{T} \cos(2\pi f_c t + 2\pi m \Delta f t) \cos(2\pi f_c t + 2\pi n \Delta f t) dt \\
 &= \frac{1}{T} \int_0^T \cos 2\pi(m-n)\Delta f t dt + \frac{1}{T} \int_0^T \cos[4\pi f_c t + 2\pi(m+n)\Delta f t] dt \\
 &= \frac{\sin 2\pi(m-n)\Delta f T}{2\pi(m-n)\Delta f T}
 \end{aligned} \tag{7.4.10}$$

where the second integral vanishes when $T \cdot 2f_c = \text{integer}$ or $f_c \gg \frac{1}{T}$.

Figure 7.26 shows crosscorrelation coefficient γ_{mn} as a function of the frequency separation Δf .

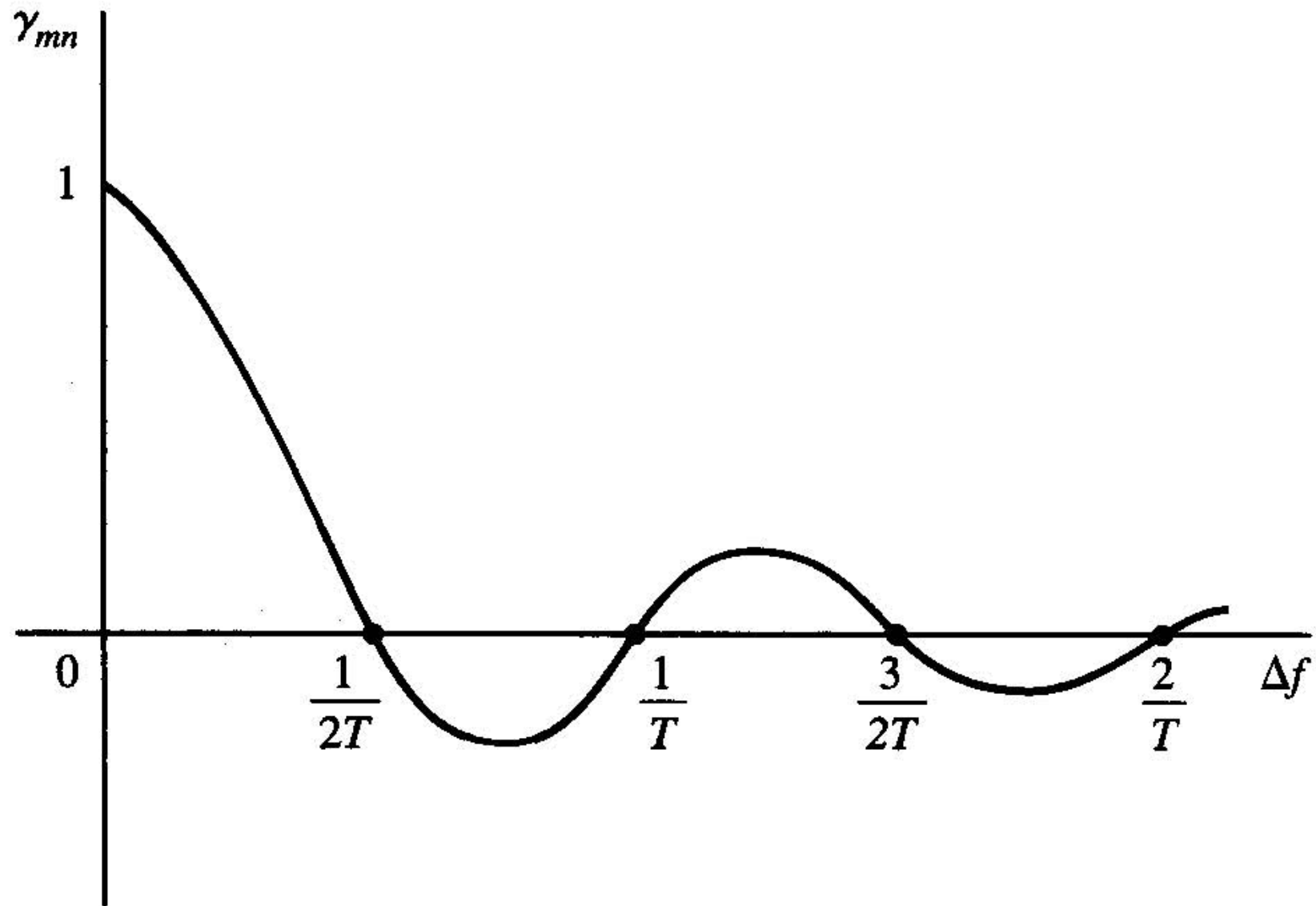


Figure 7.26 Crosscorrelation coefficient as a function of frequency separation for two FSK signals.

Observe that the signals are orthogonal when Δf is a multiple of $\frac{1}{2T}$.

Hence, the minimum frequency separation between successive frequencies to achieve orthogonality is $\frac{1}{2T}$.

Also note that the minimum value of the crosscorrelation coefficient is $\gamma_{mn} = -0.217$, which occurs at the frequency separations $\Delta f = \frac{0.715}{T}$.

M -ary orthogonal FSK waveforms have a geometric representation as M , M -dimensional orthogonal vectors, given as

$$\begin{aligned} \mathbf{s}_1 &= (\sqrt{\varepsilon_s}, 0, 0, \dots, 0) \\ \mathbf{s}_2 &= (0, \sqrt{\varepsilon_s}, 0, \dots, 0) \\ &\vdots \\ \mathbf{s}_M &= (0, 0, \dots, 0, \sqrt{\varepsilon_s}) \end{aligned} \tag{7.4.11}$$

of which basis functions are $\psi_m(t) = \sqrt{\frac{2}{T}} \cos 2\pi(f_c + m\Delta f)t$, $m = 1, 2, \dots, N$.

The distance between pairs of signal vectors is $d = \sqrt{2\varepsilon_s}$ for all m and n , which is also minimum distance among the M signals, that is, any pair of signals has minimum distance.

7.4.2 Biorthogonal Signals

Biorthogonal signals are constructed for transmission through both of baseband channels and passband channels.

Baseband Signals

Ex.

Biorthogonal signals with $M = 4$ can be constructed in two dimensions by using a signal set in Figure 7.12.

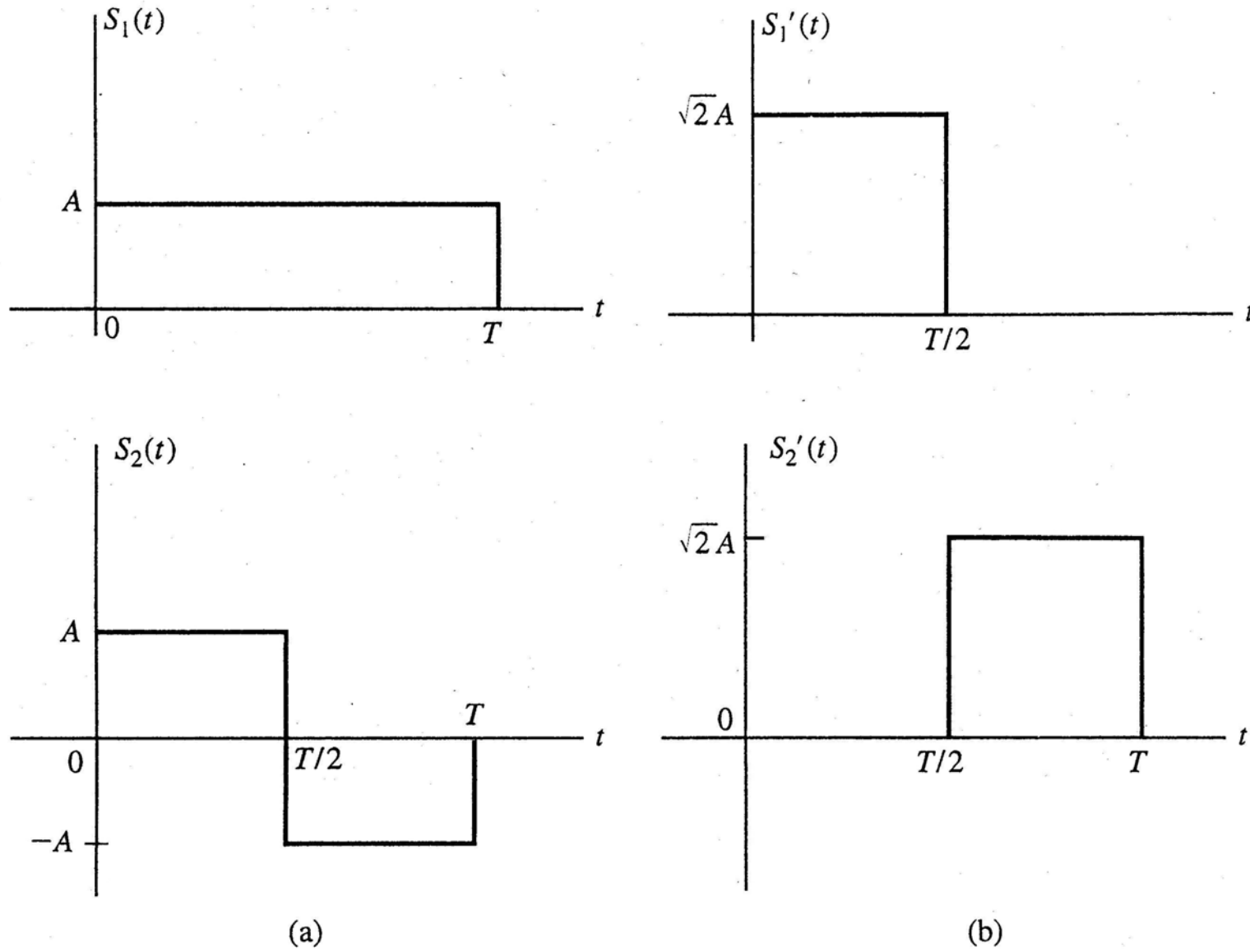


Figure 7.12 Two sets of orthogonal signals.

A set of M biorthogonal signals can be constructed from a set of $\frac{M}{2}$ orthogonal signals $s_i(t)$, $m = 1, 2, \dots, \frac{M}{2}$ and their negatives $-s_i(t)$, $m = 1, 2, \dots, \frac{M}{2}$.

The channel bandwidth required to transmit the information sequence by use of biorthogonal signals is just one-half of that required to transmit M orthogonal signals as will be shown in Section 7.6.10.

Because of their higher bandwidth efficiency, biorthogonal signals are preferred in some applications over orthogonal signals.

Find the geometric representation of M -ary biorthogonal signals:

$$\left\{ s_m(t), 1 \leq m \leq \frac{M}{2}, -s_m(t), \frac{M}{2} + 1 \leq m \leq M \right\}.$$

Begin with $\frac{M}{2}$ orthogonal vectors in $N (= \frac{M}{2})$ dimensions and then append their negatives.

For example, if the $\frac{M}{2}$ orthogonal waveforms are PPM signals, the M biorthogonal vectors are given as

$$\begin{aligned} s_1 &= (\sqrt{\mathcal{E}_s}, 0, 0, \dots, 0) \\ s_2 &= (0, \sqrt{\mathcal{E}_s}, 0, \dots, 0) \\ &\vdots \\ s_{M/2} &= (0, 0, 0, \dots, \sqrt{\mathcal{E}_s}) \\ s_{\frac{M}{2}+1} &= (-\sqrt{\mathcal{E}_s}, 0, 0, \dots, 0) \\ &\vdots \\ s_M &= (0, 0, 0, \dots, -\sqrt{\mathcal{E}_s}). \end{aligned} \tag{7.4.12}$$

Figure 7.15 shows the signal constellation of biorthogonal signals for $M = 4$.

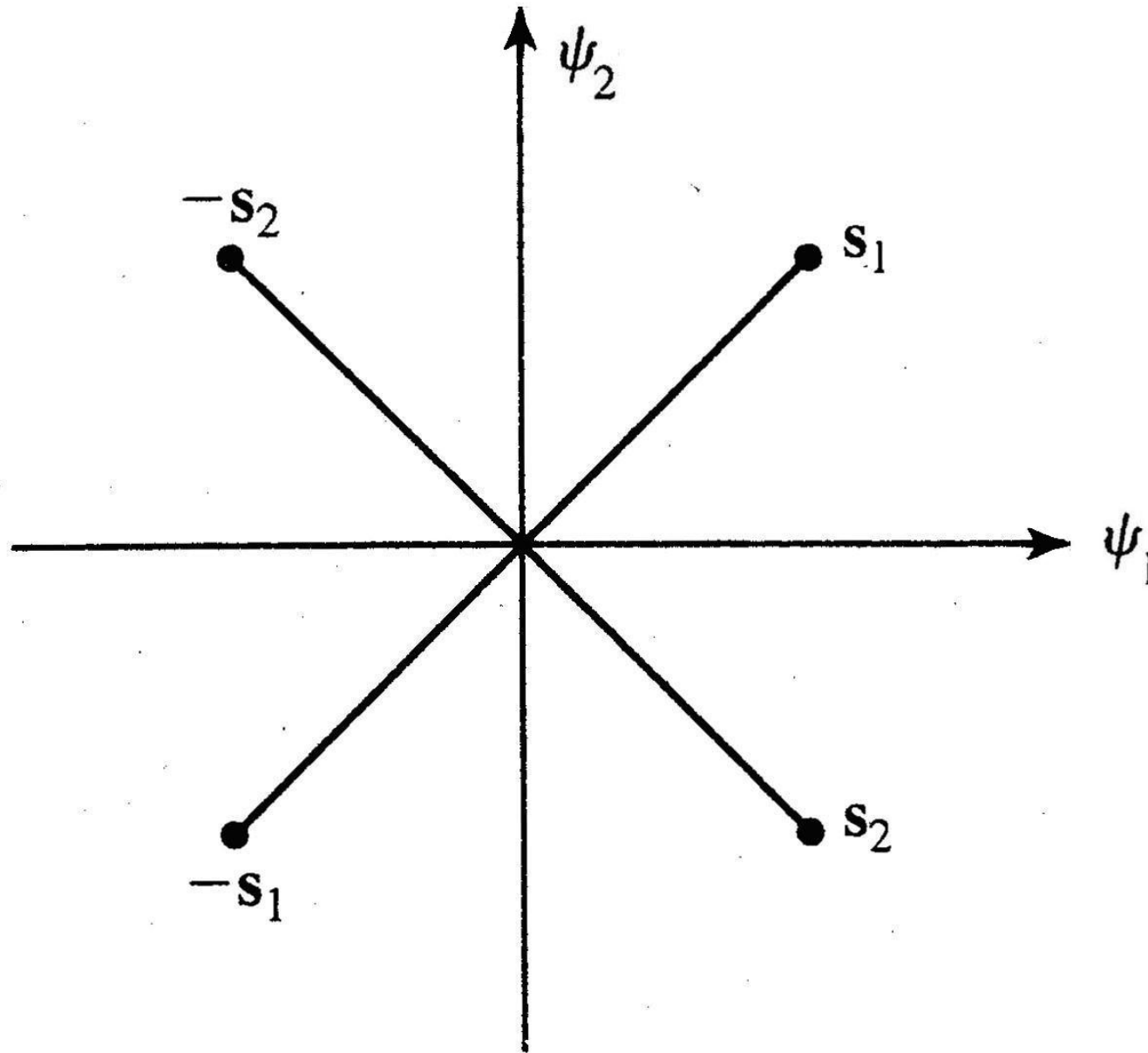


Figure 7.15 Signal constellation for $M = 4$ biorthogonal signals.

Note that the constellation of biorthogonal signals for $M = 4$ is identical to the signal constellation for quadrature (four phase) phase-shift keying.

Bandpass Signals

Given a set of M baseband biorthogonal signals $\{s_m(t)\}$, a corresponding set of M bandpass signals $\{u_m(t)\}$ is obtained by modulating the carrier $\cos 2\pi f_c t$ with the baseband signals; that is,

$$u_m(t) = s_m(t) \cos 2\pi f_c t, \quad 0 \leq t \leq T, \quad m = 1, 2, \dots, M. \quad (7.4.13)$$

The geometric representation of the bandpass signals is identical to that of the corresponding baseband signals, where the energy of the bandpass signals is one-half of that of the corresponding baseband signals.

7.4.3 Simplex Signals

A set of M signals, called **simplex signals**, is obtained by subtracting the average vector of the M orthogonal signals from each of the orthogonal signals.

If we have M orthogonal baseband signals $\{s_m(t)\}$, the simplex signals are obtained as

$$s'_m(t) = s_m(t) - \frac{1}{M} \sum_{k=1}^M s_k(t). \quad (7.4.14)$$

Then, the energy of the signal $s'_m(t)$ (or symbol energy) in the simplex signal set is given by (see Problem 7.7)

$$\begin{aligned} \varepsilon'_s &= \int_0^T [s'_m(t)]^2 dt \\ &= \left(1 - \frac{1}{M}\right) \varepsilon_s \end{aligned} \quad (7.4.15)$$

and

$$\int_0^T s'_m(t) s'_n(t) dt = -\frac{1}{M-1} \varepsilon_s, \quad m \neq n, \quad (7.4.16)$$

where ε_s is the signal energy (or symbol energy) in the orthogonal signal set.

Note that the signals in the simplex set have smaller energy than those in the orthogonal signal set.

Also note that simplex signals are not orthogonal, but they have a negative correlation, which is equal for all pairs of signals.

Later it will be shown that among all the possible sets of M -ary signals of equal symbol energy ε_s , the simplex signal set achieves the smallest error probability when used in an additive white Gaussian noise channel.

The geometric representation of a set of M simplex signals is obtained by subtracting the mean-signal vector from a set of M orthogonal vectors.

That is, we have

$$\begin{aligned}\mathbf{s}'_m &= \mathbf{s}_m - \frac{1}{M} \sum_{k=1}^M \mathbf{s}_k \\ &= \mathbf{s}_m - \bar{\mathbf{s}}, \quad m = 1, 2, \dots, M,\end{aligned}\tag{7.4.17}$$

where

$$\bar{\mathbf{s}} = \frac{1}{M} \sum_{k=1}^M \mathbf{s}_k . \quad (7.4.18)$$

By subtracting the mean signal from each orthogonal vector, the origin of the M orthogonal signals is translated to the point $\bar{\mathbf{s}}$ and the energy in the signal set $\{\mathbf{s}'_m\}$ is minimized.

If the average symbol energy of the orthogonal signal set is $\varepsilon_s = \|\mathbf{s}_m\|^2$, then the average energy of the simplex signal set is given by

$$\begin{aligned} \varepsilon'_s &= \|\mathbf{s}'_m\|^2 \\ &= \|\mathbf{s}_m - \bar{\mathbf{s}}\|^2 \\ &= \left(1 - \frac{1}{M}\right) \varepsilon_s . \end{aligned} \quad (7.4.19)$$

The distance between any two signal points is not changed by the translation of the origin; that is, the distance between signal points remains as $d = \sqrt{2\varepsilon_s}$.

The (normalized) crosscorrelation coefficient between the m th and n th signals is given by

$$\begin{aligned}\gamma_{mn} &= \frac{s'_m \cdot s'_n}{\|s'_m\| \|s'_n\|} \\ &= \frac{1}{M} \\ &= \frac{1}{(1 - \frac{1}{M})} \\ &= -\frac{1}{M - 1}.\end{aligned}\tag{7.4.20}$$

which implies that all the signals have the same pair-wise correlation.

Figure 7.27 shows a set of simplex signals for $M = 4$.

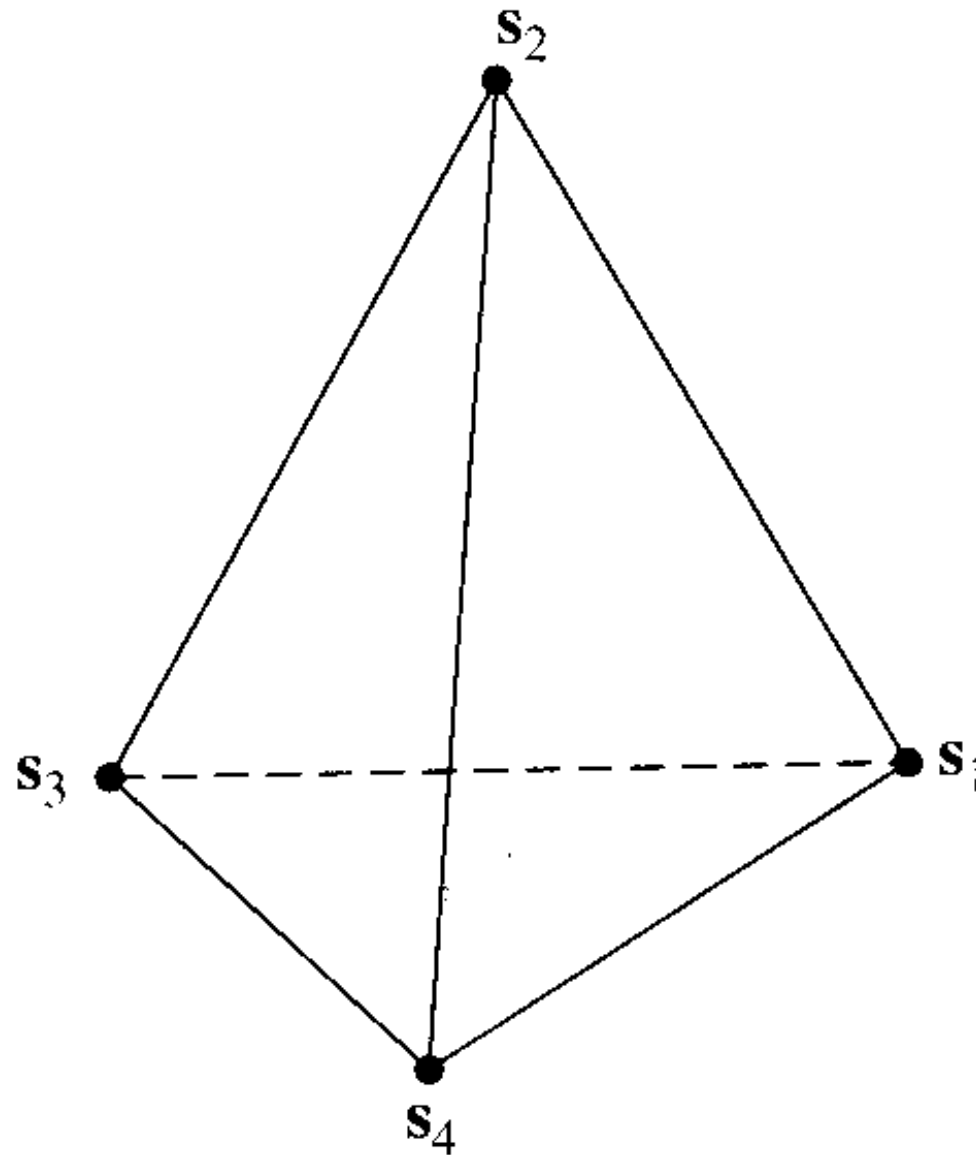


Figure 7.27 Signal constellation for M=4 simplex signals.

By modulating the carrier signal $\cos 2\pi f_c t$ by a set of M baseband simplex signals, a set of M bandpass signals is obtained which satisfy the properties of the baseband simplex signals.

7.4.4 Binary-coded signals

Transmission signals can also be constructed from a set of M binary codewords of the form

$$\mathbf{c}_m = (c_{m1}, c_{m2}, \dots, c_{mN}), \quad m = 1, 2, \dots, M,$$

where N is the blocklength (or codelength) of the codewords and c_{mj} is either 0 or 1 for all m and j .

Given M codewords, M signals are constructed by mapping a code bit $c_{mj} = 1$ into a pulse $g_T(t)$ of duration $\frac{T}{N}$ and a code bit $c_{mj} = 0$ into the negative pulse $-g_T(t)$.

Ex. 7.4.1

Given the codewords

$$\mathbf{c}_1 = [1 \ 1 \ 1 \ 1 \ 0]$$

$$\mathbf{c}_2 = [1 \ 1 \ 0 \ 0 \ 1]$$

$$\mathbf{c}_3 = [1 \ 0 \ 1 \ 0 \ 1]$$

$$\mathbf{c}_4 = [0 \ 1 \ 0 \ 1 \ 0],$$

construct a signal set for $M = 4$, using a rectangular pulse $g_T(t)$.

Solution

Map a code bit 1 into the rectangular pulse $g_T(t)$ of duration $\frac{T}{4}$ and a code bit 0 into the rectangular pulse $-g_T(t)$.

Then, the 4 signals are obtained which correspond to the 4 codewords as shown in Figure 7.28.

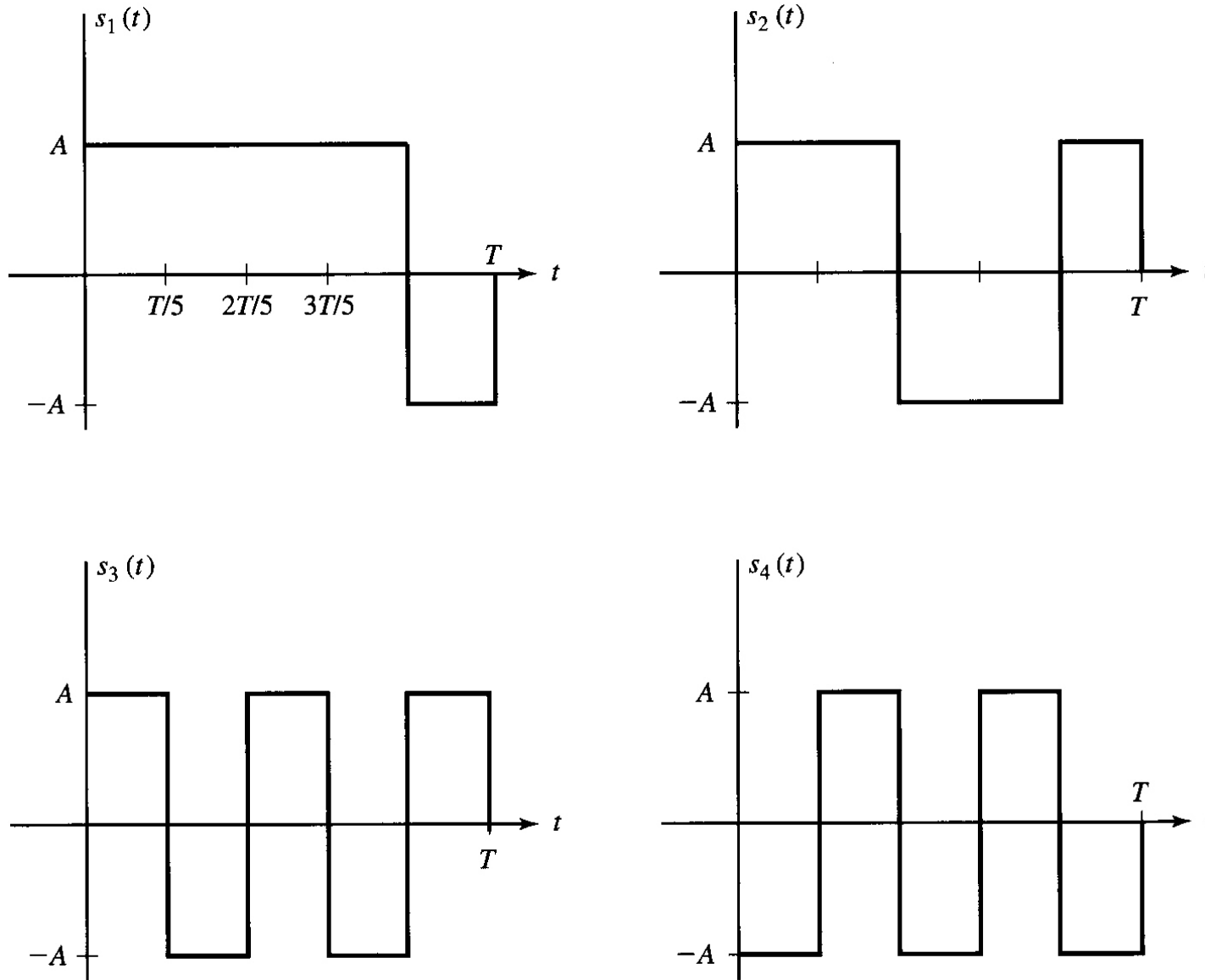


Figure 7.28 A set of $M = 4$ signal waveforms of dimension $N = 5$ constructed from the four code words in Example 7.4.1.

Now we construct the set of **signals at vertices of a hypercube**.

Consider a set of M binary codewords

$$\mathbf{c}_m = (c_{m1}, c_{m2}, \dots, c_{mN}), \quad m = 1, 2, \dots, M,$$

where c_{mj} is either 0 or 1 for all m and j .

Notice that $M = 2^N$.

Then a set of M signals of dimension N is generated from the set of M binary codewords and are represented in vector form as

$$\mathbf{s}_m = (s_{m1}, s_{m2}, \dots, s_{mN}), \quad m = 1, 2, \dots, M,$$

where s_{mj} is either $+\sqrt{\frac{\mathcal{E}_s}{N}}$ or $-\sqrt{\frac{\mathcal{E}_s}{N}}$ depending on c_{mj} for all m and j .

The M ($= 2^N$) signal points correspond to the vertices of an N -dimensional hypercube with its center at the origin.

Figure 7.29 shows the signal points at the vertices of an N -dimensional hypercube with its center at the origin for dimension $N = 2$ and $N = 3$.

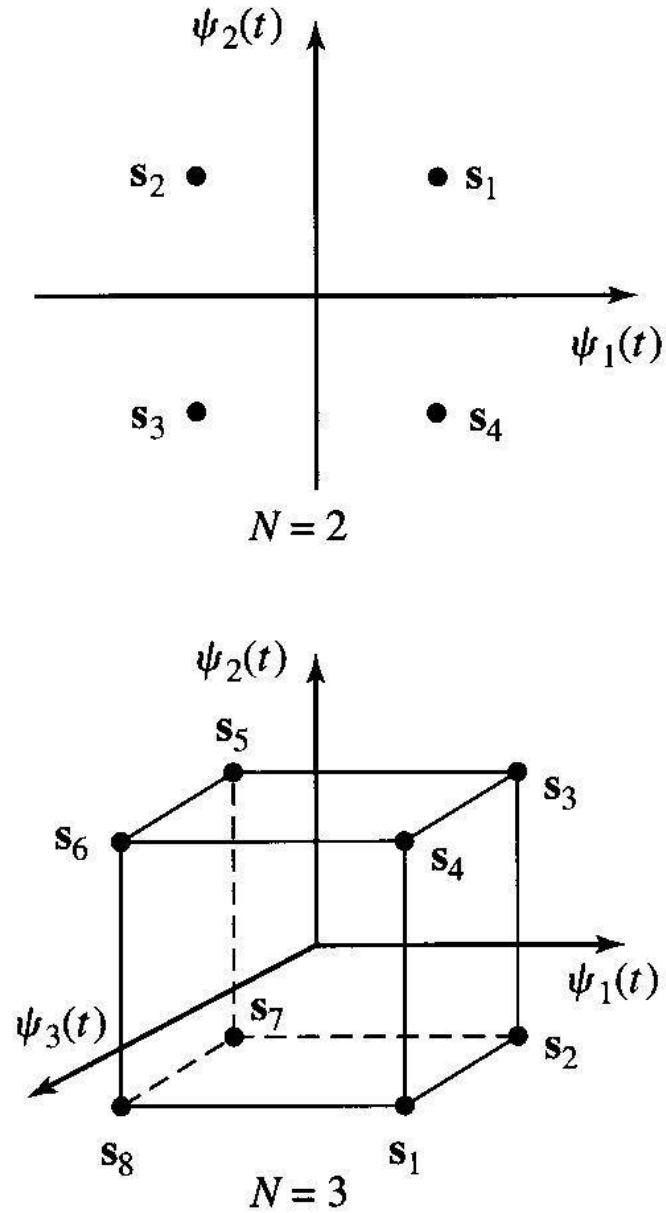


Figure 7.29 Signals at the vertices of an N -dimensional hypercube.

Note each of M signals has equal energy ε_s .

Note that any adjacent two signal points have a crosscorrelation coefficient of

$$\gamma = \frac{N-2}{N}$$

and a corresponding Euclidean distance

$$d = 2\sqrt{\frac{\varepsilon_s}{N}}$$

(see Problem 7.2).

7.5 Optimum Receiver for Digitally Modulated Signals in Additive White Gaussian Noise

Consider a digital communication system that transmits digital information using any one of the M -ary signal sets.

The input sequence to the modulator is subdivided into k -bit blocks or a symbol and each of the $M = 2^k$ symbols is associated with a corresponding baseband signal from the signal set $\{s_m(t), m = 1, 2, \dots, M\}$.

Each signal is transmitted within the symbol (signaling) interval (or time slot) of duration T .

To be specific, consider the transmission of information over the interval $0 \leq t \leq T$.

Assume that the channel corrupts the signal by the addition of white Gaussian noise (AWGN) as shown in Figure 7.30.

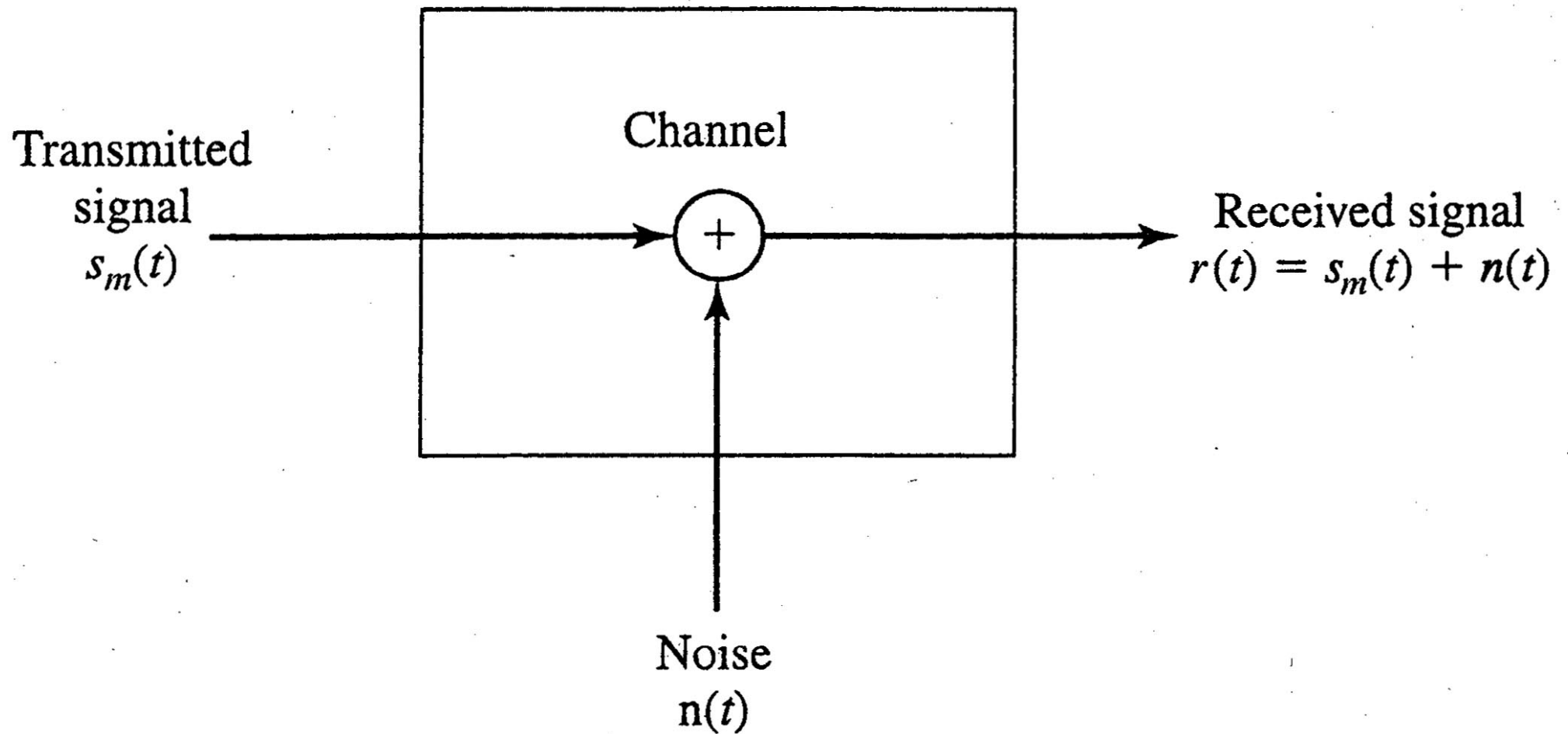


Figure 7.30 Model for received signal passed through an AWGN channel.

The received signal in the interval $0 \leq t \leq T$ is given by

$$r(t) = s_m(t) + n(t), \quad 0 \leq t \leq T, \quad (7.5.1)$$

where $n(t)$ is the sample function of the additive white Gaussian noise (AWGN) process with power-spectral

density $S_n(f) = \frac{N_0}{2}$ W/Hz.

Based on the observation of $r(t)$ over the interval $0 \leq t \leq T$, we wish to design a receiver that is optimum in the sense that it minimizes the probability of making an error.

It is convenient to subdivide the receiver into two parts: the demodulator and detector.

The demodulator converts the received waveform $r(t)$ into an N -dimensional vector $\mathbf{r} = (r_1, r_2, \dots, r_N)$, where N is the dimension of the transmitted signals.

The detector decides which of the M possible signals was transmitted based on observation of the vector \mathbf{r} .

Two realizations of the demodulator are described in Sections 7.5.1 and 7.5.2: one based on signal correlators and one based on matched filters.

The optimum detector which follows the demodulator is designed to minimize the probability of error.

7.5.1 Correlation-Type Demodulator

A correlation-type demodulator decomposes the received signal and the noise into N -dimensional vectors.

In other words, the signal and the noise are expanded into a linear combination of orthonormal basis functions of the set $\{\psi_n(t)\}$.

Assume that the N basis functions of $\{\psi_n(t)\}$ span the signal space, so that each of the possible transmitted signals of the set $\{s_m(t), m=1, 2, \dots, M\}$ can be represented as a linear combination of basis functions of the set $\{\psi_n(t)\}$.

Notice that the functions $\{\psi_n(t)\}$ do not span the noise space.

It is shown below that the noise terms that fall outside the signal space are irrelevant to the detection of the received signal.

Suppose the received signal $r(t)$ is passed through a parallel bank of N cross-correlators which compute the projection of $r(t)$ onto the N basis functions $\{\psi_n(t)\}$, as shown in Figure 7.31.

Sampling the integrator output at $t = T$ is called “**integrate-and-dump.**”

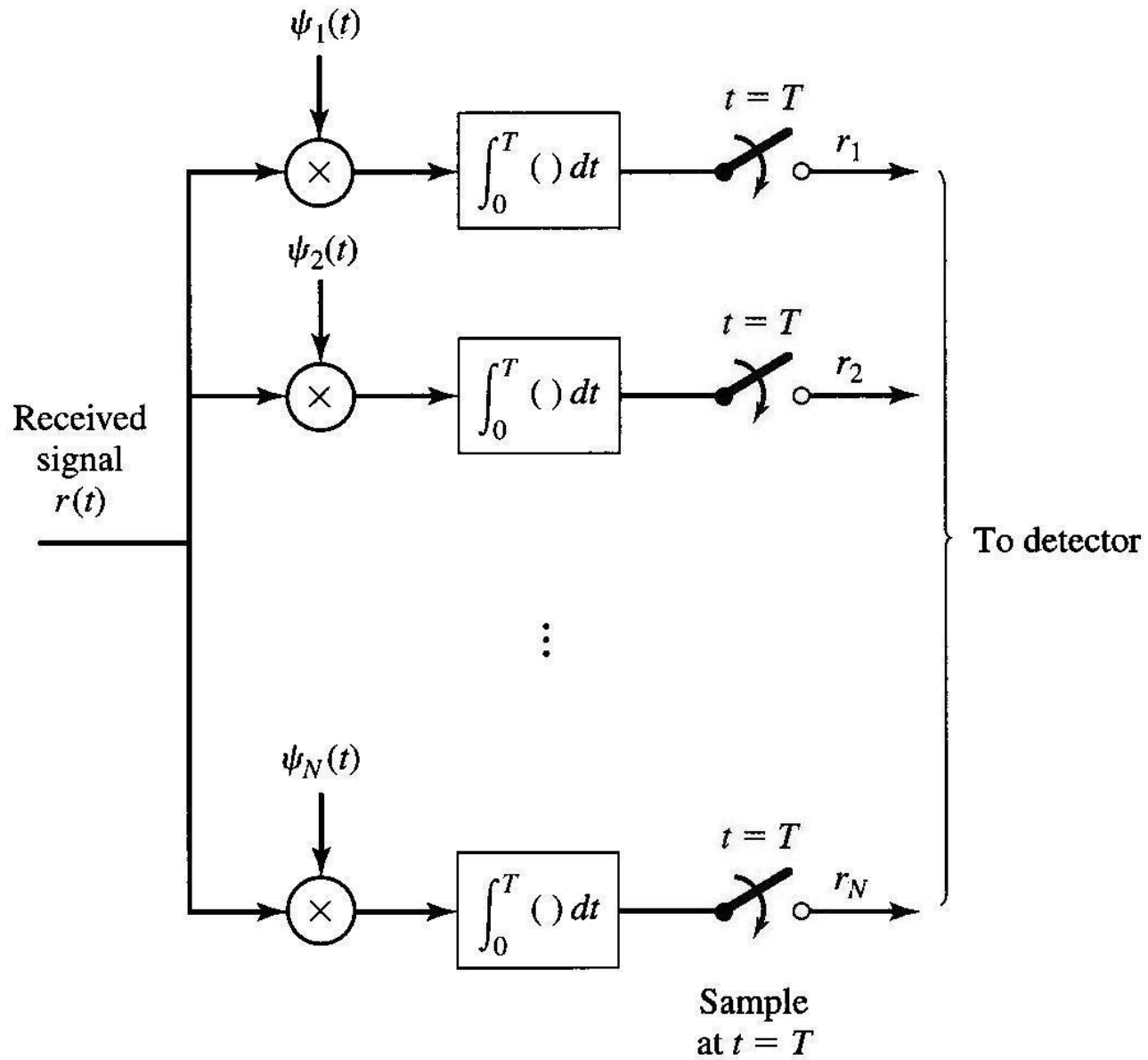


Figure 7.31 Correlation-type demodulator.

Thus, we have

$$\begin{aligned} r_k &= \int_0^T r(t) \psi_k(t) dt \\ &= \int_0^T [s_m(t) + n(t)] \psi_k(t) dt. \\ &= s_{mk} + n_k, \quad k = 1, 2, \dots, N, \end{aligned} \tag{7.5.2}$$

where

$$\begin{aligned} s_{mk} &= \int_0^T s_m(t) \psi_k(t) dt, \\ n_k &= \int_0^T n(t) \psi_k(t) dt, \end{aligned} \tag{7.5.3}$$

$$k = 1, 2, \dots, N.$$

(7.5.2) is equivalent to

$$\mathbf{r} = \mathbf{s}_m + \mathbf{n} \tag{7.5.4}$$

where

$$\mathbf{s}_m = (s_{m1}, s_{m2}, \dots, s_{mN})$$

$$\mathbf{n}_m = (n_{m1}, n_{m2}, \dots, n_{mN}).$$

The components of \mathbf{n} , that is, n_1, n_2, \dots, n_k , are random variables representing the additive noise.

From (7.5.1) and (7.5.2), the received signal $r(t)$ in the interval $0 \leq t \leq T$ is rewritten as

$$\begin{aligned} r(t) &= \sum_{k=1}^N s_{mk} \psi_k(t) + \sum_{k=1}^N n_k \psi_k(t) + n'(t) \\ &= \sum_{k=1}^N r_k \psi_k(t) + n'(t). \end{aligned} \tag{7.5.5}$$

where

$$n'(t) = n(t) - \sum_{k=1}^N n_k \psi_k(t) \tag{7.5.6}$$

is a zero-mean, Gaussian random process which represents the difference between the noise random process $n(t)$ and its part corresponds to the projection of $n(t)$ onto the basis functions $\{\psi_k(t)\}$.

It will be shown later that $n'(t)$ is irrelevant to the decision regarding which signal was transmitted so that the decision is based entirely on the correlator output signal and noise components

$$r_k = s_{mk} + n_k, \quad k = 1, 2, \dots, N.$$

Since the signals $\{s_m(t)\}$ are deterministic, the signal components are deterministic.

The noise components $\{n_k\}$ are Gaussian with mean given by

$$\begin{aligned} E[n_k] &= \int_0^T E[n(t)] \psi_k(t) dt \\ &= 0 \end{aligned} \tag{7.5.7}$$

for $k = 1, 2, \dots, N$, and covariances given by

$$\begin{aligned} E[n_k n_m] &= E \left[\int_0^T n(t) \psi_k(t) dt \int_0^T n(\tau) \psi_m(\tau) d\tau \right] \\ &= \int_0^T \int_0^T E[n(t)n(\tau)] \psi_k(t) \psi_m(\tau) dt d\tau \\ &= \int_0^T \int_0^T \frac{N_0}{2} \delta(t - \tau) \psi_k(t) \psi_m(\tau) dt d\tau \\ &= \frac{N_0}{2} \int_0^T \psi_k(t) \psi_m(t) dt \\ &= \frac{N_0}{2} \delta_{mk} \end{aligned} \tag{7.5.8}$$

where $\delta_{mk} = \begin{cases} 1, & m = k, \\ 0, & \text{otherwise.} \end{cases}$

Therefore, the N noise components $\{n_k\}$ are zero-mean, uncorrelated Gaussian random variables with a common variance $\sigma_n^2 = \frac{N_0}{2}$, and joint probability density function (PDF)

$$\begin{aligned} f(\mathbf{n}) &= \prod_{i=1}^N f(n_i) \\ &= \frac{1}{(\pi N_0)^{\frac{N}{2}}} e^{-\sum_{i=1}^N \frac{n_i^2}{N_0}} \end{aligned}$$

It follows that the correlator outputs $\{r_k\}$ conditioned on the m th signal being transmitted are Gaussian random variables with mean

$$\begin{aligned} E[r_k] &= E[s_{mk} + n_k] \\ &= s_{mk}, \end{aligned} \tag{7.5.9}$$

and equal variance

$$\begin{aligned} \sigma_{r_k}^2 &= \sigma_n^2 \\ &= \frac{N_0}{2}, \end{aligned} \tag{7.5.10}$$

$k = 1, 2, \dots, N$.

Since the noise components $\{n_k\}$ are uncorrelated Gaussian random variables, they are also statistically independent.

As a consequence, the correlator outputs $\{r_k\}$ conditioned on the m th signal being transmitted are statistically independent Gaussian variables.

Hence, the conditional probability density functions (PDFs) of the random variables $\mathbf{r} = (r_1, r_2, \dots, r_N)$ are simply given by

$$f(\mathbf{r}|\mathbf{s}_m) = \prod_{k=1}^N f(r_k|s_{mk}), \quad m = 1, 2, \dots, M, \quad (7.5.11)$$

where

$$f(r_k|s_{mk}) = \frac{1}{\sqrt{\pi N_0}} e^{-\frac{(r_k - s_{mk})^2}{N_0}}, \quad k = 1, 2, \dots, N. \quad (7.5.12)$$

From (7.5.12) and (7.5.11), the joint conditional PDFs is given by

$$f(\mathbf{r}|\mathbf{s}_m) = \frac{1}{(\pi N_0)^{\frac{N}{2}}} \exp \left[-\sum_{k=1}^N \frac{(r_k - s_{mk})^2}{N_0} \right] \quad (7.5.13)$$

$$= \frac{1}{(\pi N_0)^{\frac{N}{2}}} \exp \left[-\frac{\|\mathbf{r} - \mathbf{s}_m\|^2}{N_0} \right], \quad m = 1, 2, \dots, M. \quad (7.5.14)$$

Now we show that the correlator outputs (r_1, r_2, \dots, r_N) are **sufficient statistics** for a decision on which of the M signals was transmitted; that is, that no additional relevant information can be extracted from the remaining noise process $n'(t)$.

Notice that $n'(t)$ is uncorrelated with the N correlator outputs $\{r_k\}$; that is,

$$\begin{aligned} E[n'(t)r_k] &= E[n'(t)]s_{mk} + E[n'(t)n_k] \\ &= E[n'(t)n_k] \\ &= E \left\{ \left[n(t) - \sum_{j=1}^N n_j \psi_j(t) \right] n_k \right\} \end{aligned}$$

$$\begin{aligned}
 &= E \left[n(t) \int_0^T n(\tau) \psi_k(\tau) d\tau \right] - E \left[\sum_{j=1}^N n_j n_k \psi_j(t) \right] \\
 &= \int_0^T E[n(t)n(\tau)] \psi_k(\tau) d\tau - \sum_{j=1}^N E[n_j n_k] \psi_j(t) \\
 &= \int_0^T \frac{N_0}{2} \delta(t - \tau) \psi_k(\tau) d\tau - \sum_{j=1}^N \frac{N_0}{2} \delta(j, k) \psi_j(t) \\
 &= \frac{N_0}{2} \psi_k(t) - \frac{N_0}{2} \psi_k(t) \\
 &= 0
 \end{aligned} \tag{7.5.15}$$

Since $n'(t)$ and $\{r_k\}$ are Gaussian and uncorrelated, they are also statistically independent.

Consequently, $n'(t)$ does not contain any information that is relevant to the decision on which signal was transmitted and all the relevant information is contained in the correlator outputs $\{r_k\}$.

Hence, $n'(t)$ can be ignored.

Ex. 7.5.1

Consider an M -ary PAM signal set whose basic pulse shape $g_T(t)$ is rectangular as shown in Figure 7.32.

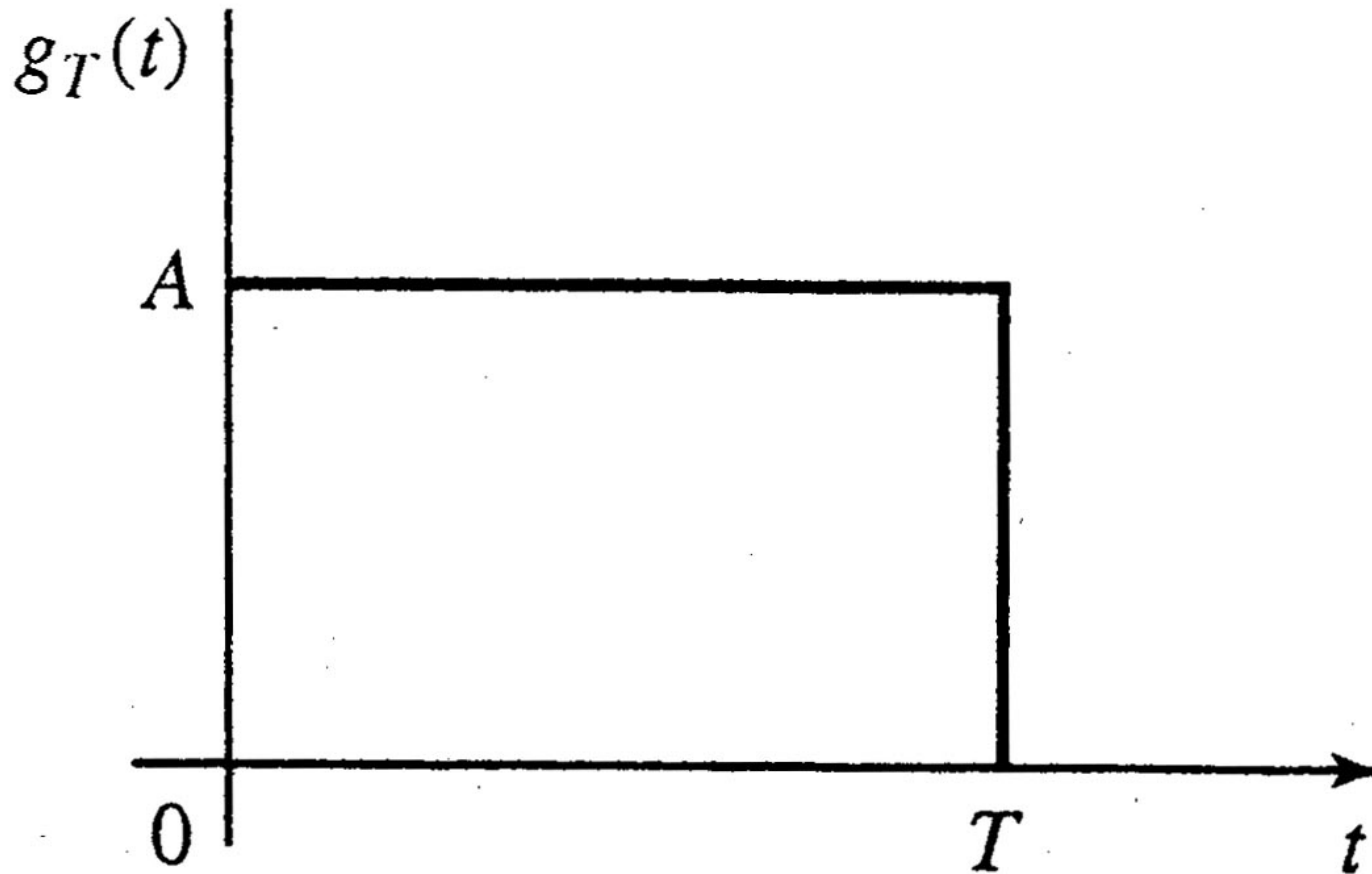


Figure 7.32 Pulse shape for Example 7.5.1

The additive noise is a zero-mean white Gaussian random process.

Determine the basic function $\psi(t)$ and the output of the correlation-type demodulator.

Solution

The energy in the rectangular pulse is given by

$$\begin{aligned}\mathcal{E}_g &= \int_0^T g_T^2(t) dt \\ &= \int_0^T A^2 dt \\ &= A^2 T.\end{aligned}$$

Since the PAM signal set has a dimension $N=1$, there is only one basic function $\psi(t)$ which is, from (7.2.11), given by

$$\begin{aligned}\psi(t) &= \frac{1}{\sqrt{A^2 T}} g_T(t) \\ &= \begin{cases} \frac{1}{\sqrt{T}}, & 0 \leq t \leq T, \\ 0, & \text{otherwise.} \end{cases}\end{aligned}$$

The output of the correlation-type demodulator is given by

$$\begin{aligned} r &= \int_0^T r(t)\psi(t)dt \\ &= \frac{1}{\sqrt{T}} \int_0^T r(t)dt. \end{aligned}$$

which implies that the correlator becomes a simple integrator when $\psi(t)$ is a rectangular pulse, i.e.,

$$\psi(t) = \begin{cases} \frac{1}{\sqrt{T}}, & 0 \leq t \leq T, \\ 0, & \text{otherwise.} \end{cases}$$

By plugging (7.5.1) into the above equation, the output of the correlation-type demodulator becomes

$$\begin{aligned} r &= \frac{1}{\sqrt{T}} \int_0^T [s_m(t) + n(t)]dt \\ &= \frac{1}{\sqrt{T}} \left[\int_0^T s_m \psi(t)dt + \int_0^T n(t)dt \right] \\ &= s_m + n \end{aligned}$$

where

$$n = \frac{1}{\sqrt{T}} \int_0^T n(t) dt .$$

Notice that the above expression for n is valid only when $\psi(t)$ is a rectangular pulse, i.e.,

$$\psi(t) = \begin{cases} \frac{1}{\sqrt{T}}, & 0 \leq t \leq T, \\ 0, & \text{otherwise.} \end{cases}$$

The mean and variance of the noise random variable n are given by

$$E[n] = 0$$

and

$$\begin{aligned} \sigma_n^2 &= E \left[\left(\frac{1}{\sqrt{T}} \int_0^T n(t) dt \right)^2 \right] \\ &= E \left[\frac{1}{T} \int_0^T \int_0^T n(t) n(\tau) dt d\tau \right] \\ &= \frac{1}{T} \int_0^T \int_0^T E[n(t) n(\tau)] dt d\tau \\ &= \frac{N_0}{2T} \int_0^T \int_0^T \delta(t - \tau) dt d\tau \end{aligned}$$

$$= \frac{N_0}{2},$$

respectively.

The conditional probability density function for the sampled output is given by

$$f(r|s_m) = \frac{1}{\sqrt{\pi N_0}} e^{-\frac{(r-s_m)^2}{N_0}}.$$

Later we will check that the output SNR is given by

$$\begin{aligned} \left(\frac{S}{N} \right)_o &= \frac{P_s}{P_n} \\ &= \frac{\varepsilon_s}{\frac{N_0}{2}} \\ &= \frac{2\varepsilon_s}{N_0} \end{aligned} \tag{7.5.32}$$

7.5.2 Matched-Filter-Type Demodulator

Instead of using a bank of N correlators to generate the variables $\{r_k\}$, we may use a bank of N linear filters.

Suppose that the impulses of the N filters are given by

$$h_k(t) = \psi_k(T - t), \quad 0 \leq t \leq T, \quad (7.5.16)$$

where $\{\psi_k(t)\}$ are the N basis functions and $h_k(t) = 0$ outside of the interval $0 \leq t \leq T$.

The outputs of these filters are given by

$$\begin{aligned} y_k(t) &= \int_0^t r(\tau) h_k(t - \tau) d\tau \\ &= \int_0^t r(\tau) \psi_k(T - t + \tau) d\tau, \quad k = 1, 2, \dots, N. \end{aligned} \quad (7.5.17)$$

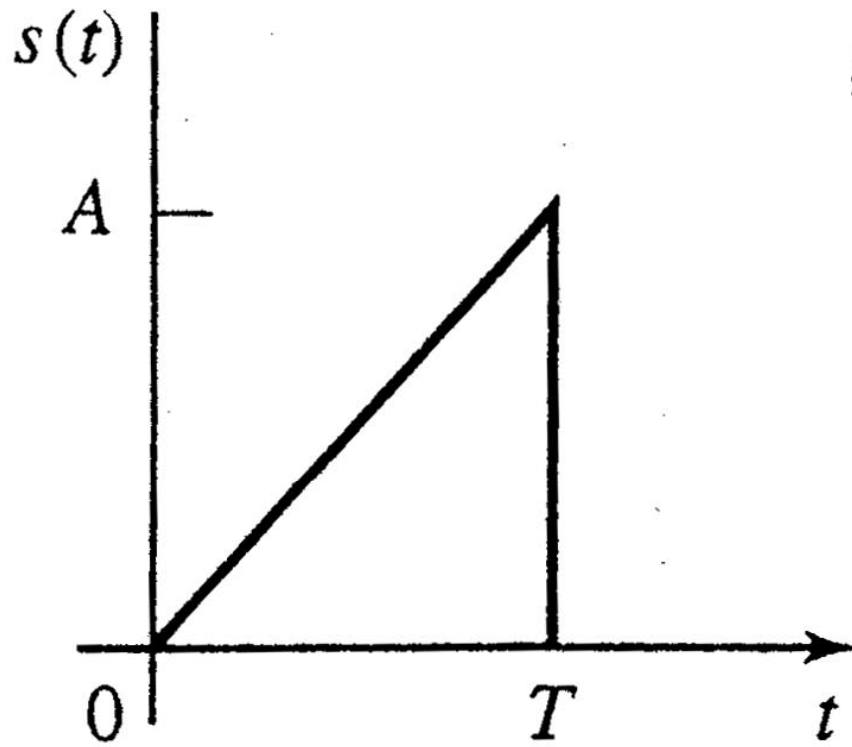
If the outputs of the filters are sampled at $t = T$, we obtain

$$y_k(T) = \int_0^T r(\tau) \psi_k(\tau) d\tau = r_k, \quad k = 1, 2, \dots, N. \quad (7.5.18)$$

Hence, the sampled outputs of the filters at time $t = T$ are exactly the same as the set of values $\{r_k\}$ obtained from the N linear correlators.

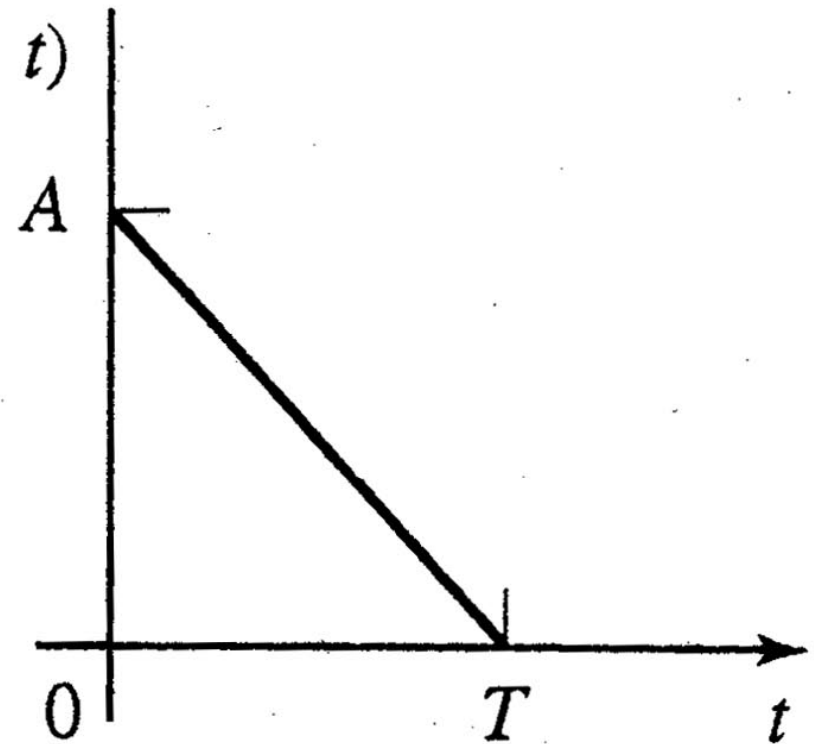
A filter whose impulse response $h(t) = s(T - t)$, where $s(t)$ is assumed to be confined to the time interval $0 \leq t \leq T$, is called the **matched filter** to the signal $s(t)$.

An example of a signal and its matched filter are shown in Figure 7.33.



(a) Signal $s(t)$

$$h(t) = s(T - t)$$



(b) Impulse response
of filter matched to $s(t)$

Figure 7.33 Signal $s(t)$ and the filter matched to $s(t)$.

The output of the matched filter $h(t)$ to the signal $s(t)$ is given by

$$\begin{aligned} y(t) &= \int_0^t s(\tau)h(t - \tau)d\tau \\ &= \int_0^t s(\tau)s(T - t + \tau)d\tau \end{aligned}$$

which is the time-autocorrelation function of the signal $s(t)$.

Figure 7.34 shows the matched filter output $y(t)$ to the input signal $s(t)$ shown in Figure 7.33.

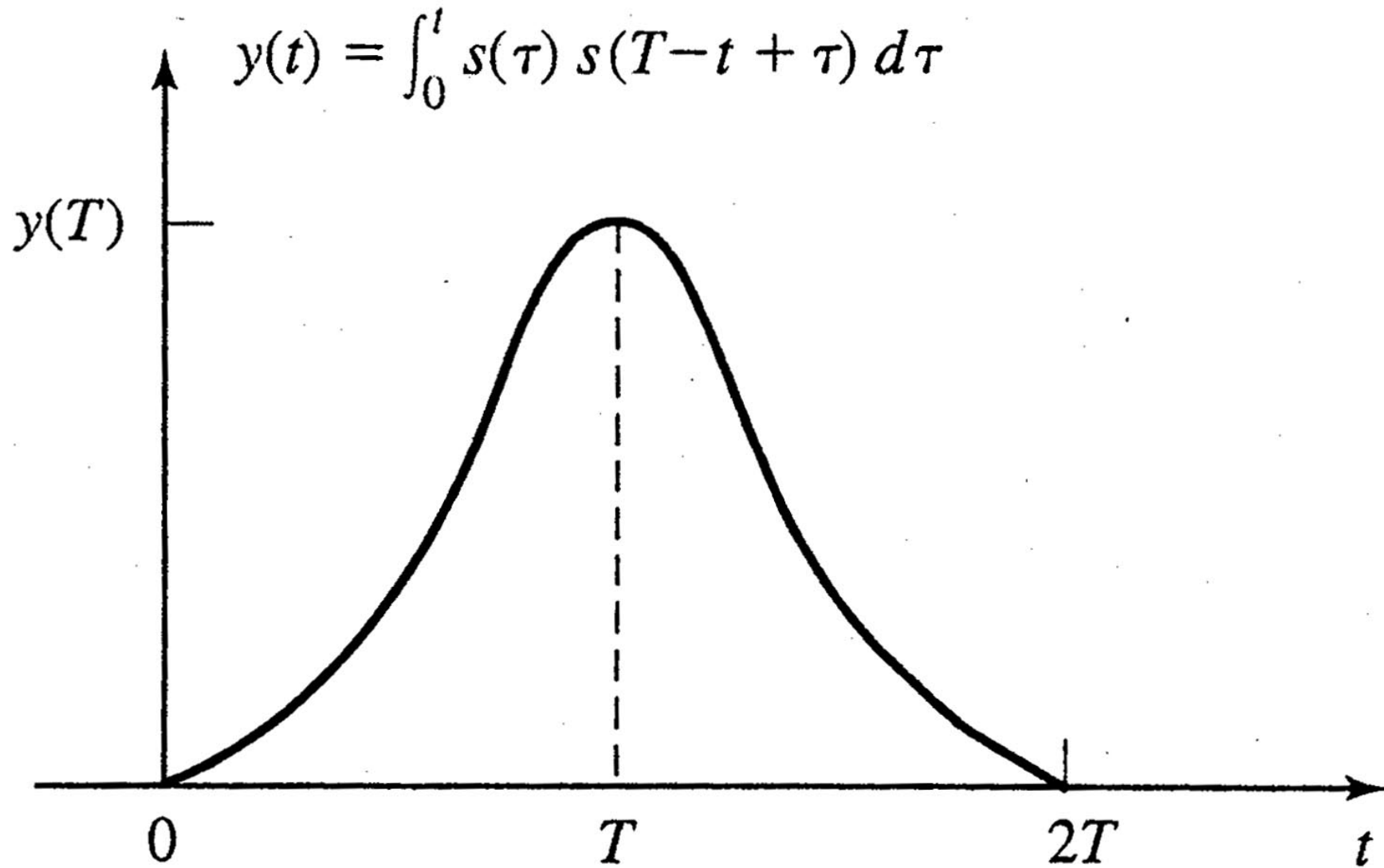


Figure 7.34 Matched filter output to the input signal $s(t)$ shown in Figure 7.33.

Note that the autocorrelation function $y(t)$ is an even function of t which attains a peak at $t = T$.

In the case of the demodulator described above, the N matched filters are matched to the basis functions $\{\psi_k(t)\}$.

Figure 7.35 shows the matched filter-type demodulator that generates the observed variables $\{r_k\}$.

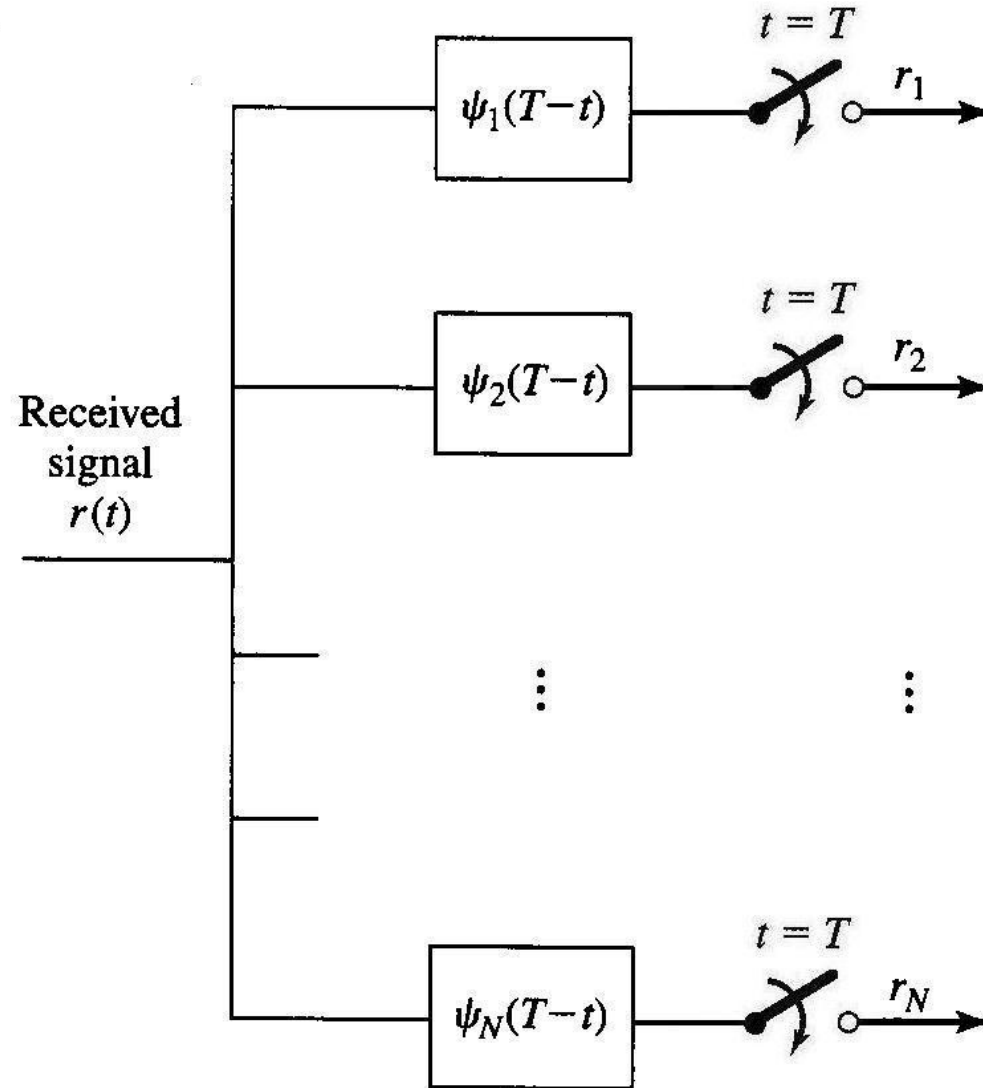


Figure 7.35 Matched filter-type demodulator.

Properties of the Matched Filter.

An important property of a matched filter is as follows:

If a signal $s(t)$ is corrupted by AWGN, the filter with impulse response matched to $s(t)$ maximizes the output SNR.

To prove this property, assume that the received signal $r(t)$ consists of the signal $s(t)$ and AWGN $n(t)$ which has zero-mean and power-spectral density $S_n(f) = \frac{N_0}{2}$ W/Hz.

Suppose the signal $r(t)$ is passed through a filter with impulse response $h(t)$, $0 \leq t \leq T$, and its output is sampled at time $t = T$.

The filter response to the received signal (which consists of the signal and noise components) is given by

$$\begin{aligned} y(t) &= \int_0^t r(\tau)h(t-\tau)d\tau \\ &= \int_0^t s(\tau)h(t-\tau)d\tau + \int_0^t n(\tau)h(t-\tau)d\tau. \end{aligned} \tag{7.5.19}$$

At the sampling instant $t = T$, the signal and noise components at the output of the filter are given by

$$\begin{aligned} y(T) &= \int_0^T s(\tau)h(T - \tau)d\tau + \int_0^T n(\tau)h(T - \tau)d\tau \\ &= y_s(T) + y_n(T) \end{aligned} \tag{7.5.20}$$

where $y_s(T)$ is the signal component and $y_n(T)$ is the noise component.

Now, the problem is to select the filter impulse response that maximizes the output SNR defined as

$$\left(\frac{S}{N} \right)_0 = \frac{y_s^2(T)}{E[y_n^2(T)]}. \tag{7.5.21}$$

The denominator in (7.5.21) is simply the variance of the noise term $y_n(T)$ at the output of the filter given by

$$\begin{aligned} E[y_n^2(T)] &= \int_0^T \int_0^T E[n(\tau)n(t)]h(T - \tau)h(T - t)dtd\tau \\ &= \frac{N_0}{2} \int_0^T \int_0^T \delta(t - \tau)h(T - \tau)h(T - t)dtd\tau \\ &= \frac{N_0}{2} \int_0^T h^2(T - t)dt \end{aligned} \tag{7.5.22}$$

which depends on the power-spectral density of the noise and the energy in the impulse response $h(t)$.

From (7.5.20), (7.5.21) and (7.5.22), the output SNR s given by

$$\begin{aligned} \left(\frac{S}{N}\right)_0 &= \frac{\left[\int_0^T s(\tau)h(T-\tau)d\tau\right]^2}{\frac{N_0}{2}\int_0^T h^2(T-t)dt} \\ &= \frac{\left[\int_0^T h(\tau)s(T-\tau)d\tau\right]^2}{\frac{N_0}{2}\int_0^T h^2(T-t)dt}. \end{aligned} \tag{7.5.23}$$

Since the denominator of $\left(\frac{S}{N}\right)_0$ depends on the energy in $h(t)$, the maximum output SNR $\left(\frac{S}{N}\right)_0$ over

$h(t)$ is obtained by maximizing the numerator of $\left(\frac{S}{N}\right)_0$ subject to the constraint that the denominator is held

constant.

The numerator is maximized by using the Cauchy-Schwarz inequality (see Problem 2.9), which states in general that if signals $g_1(t)$ and $g_2(t)$ have finite energy, then

$$\left[\int_{-\infty}^{\infty} g_1(t)g_2(t)dt \right]^2 \leq \int_{-\infty}^{\infty} g_1^2(t)dt \int_{-\infty}^{\infty} g_2^2(t)dt \quad (7.5.24)$$

where equality holds when $g_1(t) = c g_2(t)$ for any arbitrary constant c .

If we set $g_1(t) = h(t)$ and $g_2(t) = s(T - t)$, it is clear that the $\left(\frac{S}{N} \right)_0$ is maximized when $h(t) = c s(T - t)$;

i.e., $h(t)$ is matched to the signal $s(t)$.

The scale factor c^2 drops out of the expression for $\left(\frac{S}{N} \right)_0$ since it appears in both the numerator and the denominator.

Hence, the (maximum) output SNR obtained with the matched filter is given by

$$\begin{aligned}
 \left(\frac{S}{N}\right)_0 &= \frac{\left[\int_0^T h(\tau)s(T-\tau)d\tau\right]^2}{\frac{N_0}{2}\int_0^T h^2(T-t)dt} \\
 &= \frac{\int_0^T c^2 s^2(T-\tau)d\tau \int_0^T s^2(T-\tau)d\tau}{\frac{N_0}{2}\int_0^T c^2 s^2(t)dt} \\
 &= \frac{2}{N_0}\int_0^T s^2(t)dt \\
 &= \frac{2\varepsilon_s}{N_0}
 \end{aligned} \tag{7.5.25}$$

where $\varepsilon_s = \int_0^T s^2(t)dt$ and we used the relation that $\int_0^T s^2(T-\tau)d\tau = \int_0^T s^2(\tau)d\tau$.

Note that the output SNR of the matched filter depends on the energy of the waveform of $s(t)$ but not on the characteristics of $s(t)$.

Also note that the output SNR of the matched filter is the same as that of the correlator type demodulator

Frequency Domain Interpretation of Matched Filter

Suppose that $c = 1$ in $h(t) = c s(T - t)$ for a matched filter.

Then, the Fourier transform of the impulse response of the matched filter is given by

$$\begin{aligned} H(f) &= \int_0^T s(T - t) e^{-j2\pi ft} dt \\ &= \left[\int_0^T s(\tau) e^{j2\pi f\tau} d\tau \right] e^{-j2\pi fT} \\ &= S^*(f) e^{-j2\pi fT}. \end{aligned} \tag{7.5.26}$$

Hence, $|H(f)| = |S(f)|$ so that the magnitude response of the matched filter is identical to that of the transmitted signal spectrum.

Notice that the phase of $H(f)$ is the negative of the phase of $S(f)$.

Now, if the signal $s(t)$ having spectrum $S(f)$ is passed through the matched filter, the filter output has a spectrum

$$\begin{aligned} Y(f) &= H(f)S(f) \\ &= S^*(f)e^{-j2\pi fT} S(f) \\ &= |S(f)|^2 e^{-j2\pi fT}. \end{aligned}$$

Hence, the output waveform of the matched filter is given by

$$\begin{aligned} y_s(t) &= \int_{-\infty}^{\infty} Y(f)e^{j2\pi ft} df \\ &= \int_{-\infty}^{\infty} |S(f)|^2 e^{-j2\pi fT} e^{j2\pi ft} df \\ &= \int_{-\infty}^{\infty} |S(f)|^2 e^{j2\pi f(t-T)} df. \end{aligned} \tag{7.5.27}$$

By sampling the output of the matched filter at $t = T$, we obtain

$$\begin{aligned} y_s(T) &= \int_{-\infty}^{\infty} |S(f)|^2 df \\ &= \int_0^T s^2(t)dt \\ &= \mathcal{E}_s \end{aligned} \tag{7.5.28}$$

where the last step follows from Parseval's relation.

The output signal power is given by

$$\begin{aligned} P_s &= y_s^2(T) \\ &= \mathcal{E}_s^2. \end{aligned} \tag{7.5.31}$$

The noise in the output of the matched filter has a power-spectral density

$$S_{n_0}(f) = \frac{N_0}{2} |H(f)|^2 \tag{7.5.29}$$

Hence, the total noise power at the output of the matched filter is given by

$$\begin{aligned} P_n &= \int_{-\infty}^{\infty} S_{n_0}(f) df \\ &= \int_{-\infty}^{\infty} \frac{N_0}{2} |H(f)|^2 df \\ &= \frac{N_0}{2} \int_{-\infty}^{\infty} |S(f)|^2 df \\ &= \frac{\mathcal{E}_s N_0}{2}. \end{aligned} \tag{7.5.30}$$

The output SNR is given by

$$\begin{aligned}\left(\frac{S}{N}\right)_o &= \frac{P_s}{P_n} \\ &= \frac{\mathcal{E}_s^2}{\mathcal{E}_s \frac{N_0}{2}} \\ &= \frac{2\mathcal{E}_s}{N_0}\end{aligned}\tag{7.5.32}$$

which agrees with the result given by (7.5.25).

Ex. 7.5.2

Consider the $M = 4$ biorthogonal signals constructed from the binary PPM signals and their negatives in Figure 7.12(b), for transmitting information over an AWGN channel.

The noise is assumed to have zero mean and power spectral density $\frac{N_0}{2}$.

Determine the basis functions for this signal set, the impulse response of the matched-filter demodulators, and the output waveforms of the matched filter demodulators when the transmitted signal is $s_1(t)$.

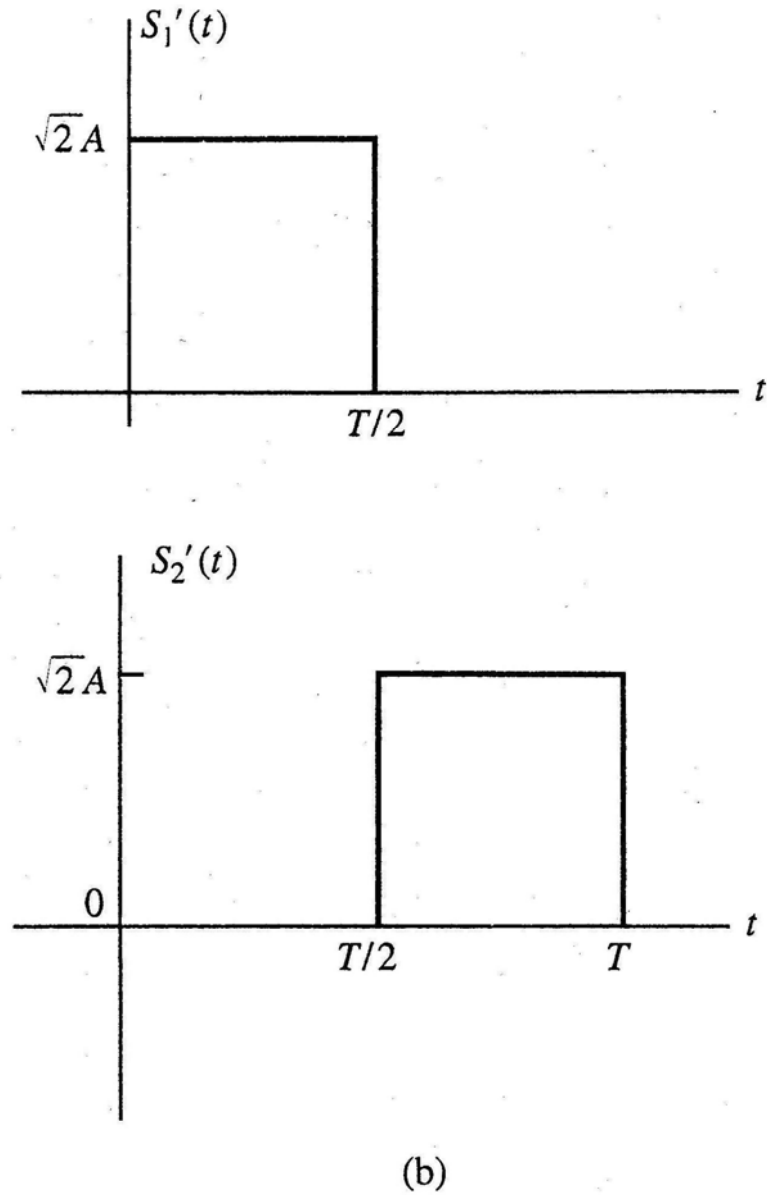


Figure 7.12 Two sets of orthogonal signals.

Solution

The biorthogonal signals for $M = 4$ have dimension $N = 2$.

Hence, two basis functions are needed to represent the signals.

From Figure 7.12(b), we choose $\psi_1(t)$ and $\psi_2(t)$ as

$$\begin{aligned}\psi_1(t) &= \begin{cases} \sqrt{\frac{2}{T}}, & 0 \leq t \leq \frac{T}{2}, \\ 0, & \text{otherwise,} \end{cases} \\ \psi_2(t) &= \begin{cases} \sqrt{\frac{2}{T}}, & \frac{T}{2} \leq t \leq T, \\ 0, & \text{otherwise.} \end{cases}\end{aligned}\tag{7.5.33}$$

which are shown in Figure 7.36(a).

The impulse responses of the two matched filters are given by

$$h_1(t) = \psi_1(T - t)$$

$$= \begin{cases} \sqrt{\frac{2}{T}}, & \frac{T}{2} \leq t \leq T, \\ 0, & \text{otherwise,} \end{cases}$$

$$h_2(t) = \psi_2(T - t)$$

$$= \begin{cases} \sqrt{\frac{2}{T}}, & 0 \leq t \leq \frac{T}{2}, \\ 0, & \text{otherwise,} \end{cases}$$

(7.5.34)

which are shown in Figure 7.36(b).

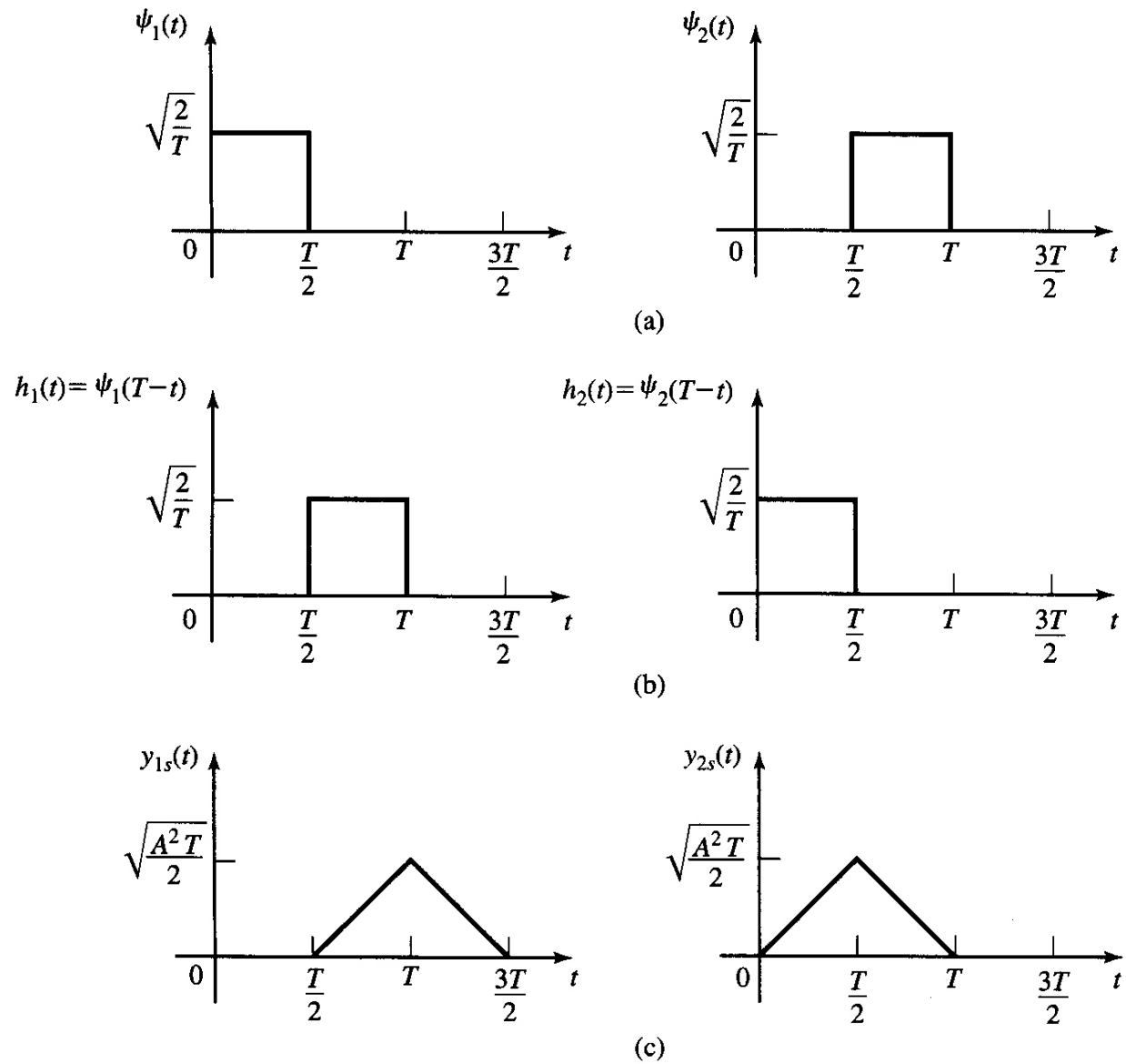


Figure 7.36 Basis functions and matched filter responses for Example 7.5.2.

If $s_1(t)$ is transmitted, the (noise-free) responses of the two matched filters are shown in Figure 7.36(c).

Since $y_1(t)$ and $y_2(t)$ are sampled at $t = T$, we observe that

$$y_{1s}(T) = \sqrt{\frac{A^2T}{2}} \quad \text{and}$$

$$y_{2s}(T) = 0.$$

Note that $\frac{A^2T}{2} = \varepsilon_s$ which is the symbol energy.

Hence, the received vector formed from the two matched filter outputs at the sampling instant $t = T$ is given by

$$\begin{aligned} \mathbf{r} &= (r_1, r_2) \\ &= (\sqrt{\varepsilon_s} + n_1, n_2) \end{aligned} \tag{7.5.35}$$

where $n_1 = y_{1n}(T)$ and $n_2 = y_{2n}(T)$ are the noise components at the outputs of the matched filters, given by

$$y_{kn}(T) = \int_0^T n(t)\psi_k(t)dt, \quad k = 1, 2. \tag{7.5.36}$$

The mean and variance of the random variable n_k are given by

$$\begin{aligned} E[n_k] &= E[y_{kn}(T)] \\ &= 0 \end{aligned}$$

and

$$\begin{aligned} \sigma_n^2 &= E[y_{kn}^2] \\ &= \int_0^T \int_0^T E[n(t)n(\tau)]\psi_k(t)\psi_k(\tau)dt d\tau \\ &= \frac{N_0}{2} \int_0^T \int_0^T \delta(t-\tau)\psi_k(\tau)\psi_k(t)dt d\tau \\ &= \frac{N_0}{2} \int_0^T \psi_k^2(t)dt \\ &= \frac{N_0}{2}, \end{aligned} \tag{7.5.37}$$

respectively.

The output SNR for the first matched filter is given by

$$\left(\frac{S}{N}\right)_o = \frac{(\sqrt{\mathcal{E}_s})^2}{\frac{N_0}{2}}$$

$$= \frac{2\mathcal{E}_s}{N_0}$$

which agrees with our previous result.

Also note that four possible outputs of the two matched filters, which correspond to the four possible transmitted signals, are $(r_1, r_2) = (\sqrt{\mathcal{E}_s} + n_1, n_2)$, $(n_1, \sqrt{\mathcal{E}_s} + n_2)$, $(-\sqrt{\mathcal{E}_s} + n_1, n_2)$, and $(n_1, -\sqrt{\mathcal{E}_s} + n_2)$.

7.5.3 Optimum Detector

The optimum decision rule is based on the observation of the received vector $\mathbf{r} = (r_1, r_2, \dots, r_N)$ obtained by both a correlation-type demodulator and a matched-filter-type demodulator.

(In this section we assume that there is no memory between signals transmitted in successive signal intervals.)

The received vector \mathbf{r} is the sum of the transmitted signal vector \mathbf{s}_m and the noise vector \mathbf{n} .

The signal vector \mathbf{s}_m is a point in the signal constellation and the noise vector \mathbf{n} is an N -dimensional random vector with i.i.d. components each being a Gaussian random variable with mean 0 and variance $\frac{N_0}{2}$.

Since the components of the noise vector are independent and have the same mean and variance, the distribution of the noise vector \mathbf{n} in the N -dimensional vector space has spherical symmetry.

When \mathbf{s}_m is transmitted, the received vector \mathbf{r} is represented by a spherical cloud centered at \mathbf{s}_m .

The density of this cloud is higher at the center since each component of the noise vector is a Gaussian random variable with mean 0.

The variance of the noise $\frac{N_0}{2}$ determines the density of the noise cloud around the center signal \mathbf{s}_m .

For low $\frac{N_0}{2}$, the cloud is quite centered around \mathbf{s}_m and its density (representing the probability) reduces sharply as the distance from the center is increased.

For high $\frac{N_0}{2}$, the cloud is spread and larger distances have a higher probability compared with the low $\frac{N_0}{2}$ case.

The signal constellation, the noise cloud, and the received vector are shown in Figure 7.37 for the case of $N = 3$ and $M = 4$.

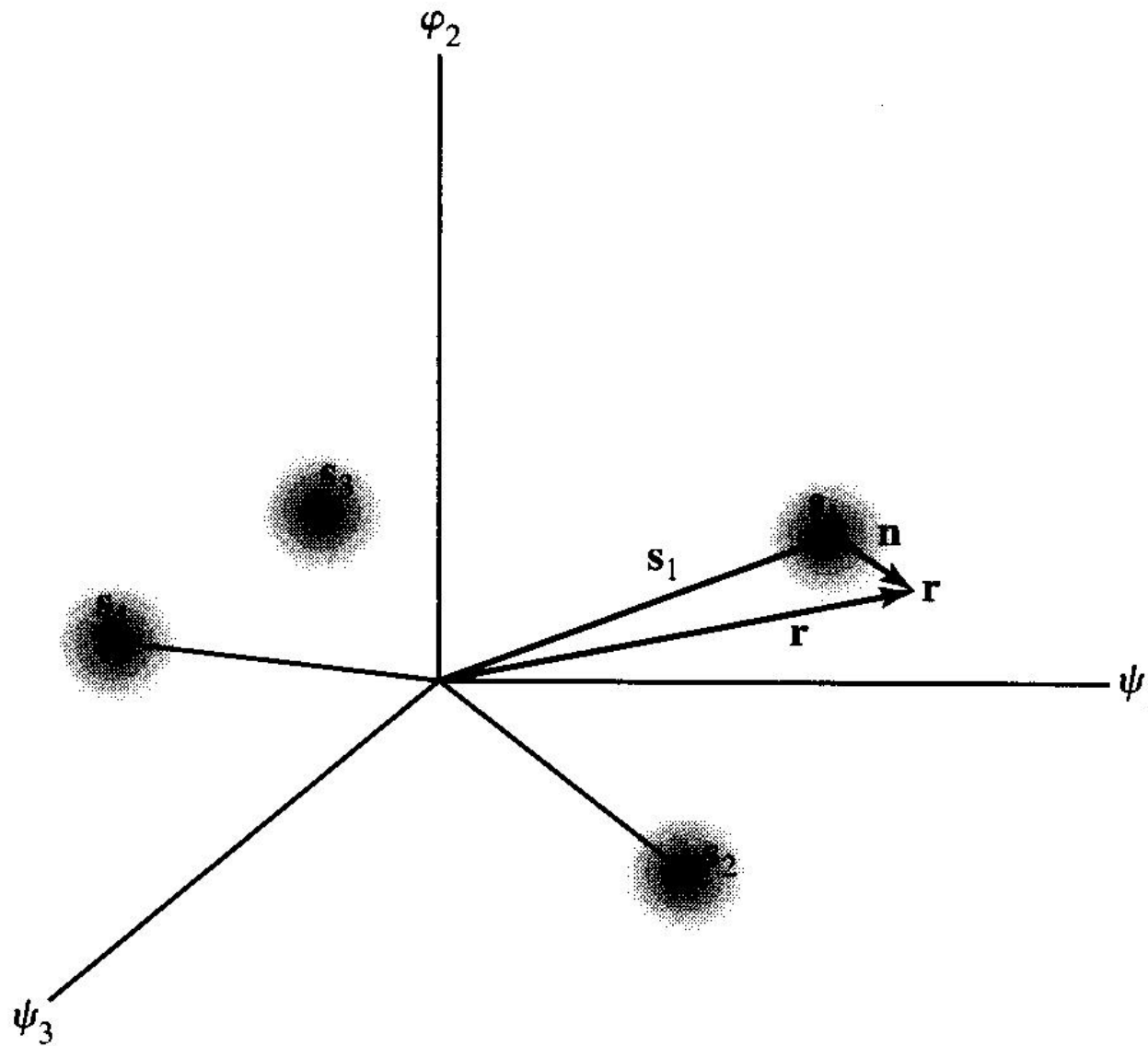


Figure 7.37 Signal constellation, noise cloud, and received vector for $N = 3$ and $M = 4$. s_1 is transmitted.

Now we design a signal detector that makes a decision on the transmitted signal in each signal interval based on the observation of the received vector \mathbf{r} in each interval such that the probability of a correct decision is maximized (the probability of wrong decision is minimized in other words) .

Consider a decision rule based on the computation of the **a posteriori probabilities** defined as

$$P(\mathbf{s}_m|\mathbf{r}) = P(\text{signal } \mathbf{s}_m \text{ was transmitted}|\mathbf{r}), \quad m = 1, 2, \dots, M .$$

The decision criterion is based on selecting the signal corresponding to the maximum of the set of a posteriori probabilities $\{ P(\mathbf{s}_m|\mathbf{r}) \}$.

In case of the absence of any received information \mathbf{r} , the best decision is to choose the signal \mathbf{s}_m that has the highest **a priori** probability $P(\mathbf{s}_m)$.

After receiving the information (i.e., the received vector) \mathbf{r} , the receiver chooses \mathbf{s}_m that maximizes **a posteriori** (conditional) **probabilities** $P(\mathbf{s}_m|\mathbf{r})$ instead of a priori probability $P(\mathbf{s}_m)$.

This decision criterion is called the **maximum a posteriori probability (MAP)** criterion.

The detector based on the MAP criterion is called the **optimum detector** (or **optimum receiver**).

Intuitively this decision is the best possible decision that minimizes the error probability.

By Bayes rule, the a posteriori probabilities is given by

$$P(\mathbf{s}_m | \mathbf{r}) = \frac{f(\mathbf{r} | \mathbf{s}_m) P(\mathbf{s}_m)}{f(\mathbf{r})} \quad (7.5.38)$$

where $f(\mathbf{r} | \mathbf{s}_m)$ is the conditional PDF of the observed vector given \mathbf{s}_m , and

$P(\mathbf{s}_m)$ is the **a priori probability** of the m th signal being transmitted.

The denominator of (7.5.38) is given by

$$f(\mathbf{r}) = \sum_{m=1}^M f(\mathbf{r} | \mathbf{s}_m) P(\mathbf{s}_m) \quad (7.5.39)$$

which is independent of which signal is transmitted.

From (7.3.38) and (7.3.39), note that the computation of the a posteriori probabilities requires knowledge of the **a priori probabilities** $P(\mathbf{s}_m)$ and the conditional PDFs $f(\mathbf{r}|\mathbf{s}_m)$, $m = 1, 2, \dots, M$.

Consider the case that the M signals have equal a priori probability, that is,

$$P(\mathbf{s}_m) = \frac{1}{M} \text{ for all } M.$$

Then, (7.5.38) becomes

$$\begin{aligned} P(\mathbf{s}_m|\mathbf{r}) &= \frac{f(\mathbf{r}|\mathbf{s}_m)P(\mathbf{s}_m)}{f(\mathbf{r})} \\ &= \frac{f(\mathbf{r}|\mathbf{s}_m)P(\mathbf{s}_m)}{\sum_{m=1}^M f(\mathbf{r}|\mathbf{s}_m)P(\mathbf{s}_m)} \\ &= \frac{f(\mathbf{r}|\mathbf{s}_m)}{\sum_{m=1}^M f(\mathbf{r}|\mathbf{s}_m)}. \end{aligned}$$

Consequently, the decision rule based on finding the signal that maximizes $P(\mathbf{s}_m|\mathbf{r})$ is equivalent to finding the signal that maximizes $f(\mathbf{r}|\mathbf{s}_m)$.

The conditional PDF $f(\mathbf{r}|\mathbf{s}_m)$ or any monotonic function of it is called the **likelihood function**.

The decision criterion based on the maximum of $f(\mathbf{r}|\mathbf{s}_m)$ over the M signals is called the **maximum-likelihood (ML) criterion**.

A detector that is based on the ML criterion makes the same decisions as a detector based on the MAP criterion when the a priori probabilities $P(\mathbf{s}_m)$ are all equal; that is, the signals $\{\mathbf{s}_m\}$ are equiprobable.

For an AWGN channel, the likelihood function $f(\mathbf{r}|\mathbf{s}_m)$ is given by

$$f(\mathbf{r}|\mathbf{s}_m) = \prod_{k=1}^N f(r_k|s_{mk}) \quad (7.5.11)$$

$$= \prod_{k=1}^N \frac{1}{\sqrt{\pi N_0}} e^{-\frac{(r_k - s_{mk})^2}{N_0}}, \quad m = 1, 2, \dots, M. \quad (7.5.12)$$

For simplicity of computation, take the natural logarithm of $f(\mathbf{r}|\mathbf{s}_m)$, which is a monotonic function:

$$\ln f(\mathbf{r}|\mathbf{s}_m) = -\frac{N}{2} \ln(\pi N_0) - \frac{1}{N_0} \sum_{k=1}^N (r_k - s_{mk})^2. \quad (7.5.40)$$

The maximization of $\ln f(\mathbf{r}|\mathbf{s}_m)$ over \mathbf{s}_m is equivalent to finding the signal \mathbf{s}_m that minimizes the Euclidean distance

$$D(\mathbf{r}, \mathbf{s}_m) = \sum_{k=1}^N (r_k - s_{mk})^2. \quad (7.5.41)$$

$D(\mathbf{r}, \mathbf{s}_m)$, $m = 1, 2, \dots, M$, are called the **distance metrics**.

Hence, for the AWGN channel, the decision rule based on the ML criterion reduces to finding the signal \mathbf{s}_m that is closest to the received signal vector \mathbf{r} which is called **minimum distance detection**.

By expanding the distance metrics in (7.5.41) , we obtain

$$\begin{aligned}
 D(\mathbf{r}, \mathbf{s}_m) &= \sum_{n=1}^N r_n^2 - 2 \sum_{n=1}^N r_n s_{mn} + \sum_{n=1}^N s_{mn}^2 \\
 &= \|\mathbf{r}\|^2 - 2\mathbf{r} \cdot \mathbf{s}_m + \|\mathbf{s}_m\|^2, \quad m = 1, 2, \dots, M,
 \end{aligned}
 \tag{7.5.42}$$

where $\|\mathbf{r}\|^2$ is common to all decision metrics and, hence, it can be ignored in the computations of the metrics.

Then, we have a set of modified distance metrics given by

$$D'(\mathbf{r}, \mathbf{s}_m) \triangleq -2\mathbf{r} \cdot \mathbf{s}_m + \|\mathbf{s}_m\|^2, \quad m = 1, 2, \dots, M.
 \tag{7.5.43}$$

Selecting the signal \mathbf{s}_m that minimizes $D'(\mathbf{r}, \mathbf{s}_m)$ is equivalent to selecting the signal that maximizes the metric which is given by

$$\begin{aligned}
 C(\mathbf{r}, \mathbf{s}_m) &\triangleq -D'(\mathbf{r}, \mathbf{s}_m) \\
 &= 2\mathbf{r} \cdot \mathbf{s}_m - \|\mathbf{s}_m\|^2.
 \end{aligned}
 \tag{7.5.44}$$

$C(\mathbf{r}, \mathbf{s}_m)$, $m = 1, 2, \dots, M$, are called the **correlation metrics** for deciding which of the M signals was transmitted.

The term $\mathbf{r} \cdot \mathbf{s}_m$ represents the projection of the received signal vector \mathbf{r} onto each of the M possible transmitted signal vectors \mathbf{s}_m , $m = 1, 2, \dots, M$, or, in other words, the correlation between the received vector \mathbf{r} and the signal \mathbf{s}_m .

The term $\|\mathbf{s}_m\|^2 = \mathcal{E}_m$, $m = 1, 2, \dots, M$, in (7.5.44) serves as compensation for a signal set which has unequal symbol energies, such as PAM.

If all signals have the same energy, $\|\mathbf{s}_m\|^2$ can be ignored in the computation of correlation metrics $C(\mathbf{r}, \mathbf{s}_m)$ as well as the distance metrics $D(\mathbf{r}, \mathbf{s}_m)$ or $D'(\mathbf{r}, \mathbf{s}_m)$.

In summary, the ML detector computes a set of M distances $D(\mathbf{r}, \mathbf{s}_m)$ or $D'(\mathbf{r}, \mathbf{s}_m)$ and selects the signal corresponding to the smallest (distance) metric.

Equivalently, the ML detector computes a set of M correlation metrics $C(\mathbf{r}, \mathbf{s}_m)$ and selects the signal corresponding to the largest correlation metric.

Note that the optimum detector becomes a ML detector when all signals are equi-probable.

That is, the MAP criterion is equivalent to the ML criterion when all signals are equi-probable.

However, when the signals are not equi-probable, the optimum MAP detector bases its decision on the probabilities $P(\mathbf{s}_m | \mathbf{r})$, $m = 1, 2, \dots, M$, given by (7.3.38) or, equivalently, on the **a posteriori probability metrics**,

$$PM(\mathbf{r}, \mathbf{s}_m) = f(\mathbf{r} | \mathbf{s}_m)P(\mathbf{s}_m). \quad (7.5.45)$$

Ex. 7.5.3 (Binary PAM)

Consider binary PAM signals in which the two possible signal points are $s_1 = -s_2 = \sqrt{\varepsilon_b}$,

where ε_b is the bit energy.

The a priori probabilities are $P(s_1) = p$ and $P(s_2) = 1 - p$.

Determine the metrics for the optimum MAP detector when the transmitted signal is corrupted with AWGN.

Solution

The received signal vector (one dimensional) for binary PAM is given by

$$r = \pm\sqrt{\varepsilon_b} + y_n(T) \quad (7.5.46)$$

where $y_n(T)$ is a zero-mean Gaussian random variable with variance $\sigma_n^2 = \frac{N_0}{2}$.

Consequently, the conditional PDFs for the two signals are given by

$$f(r | s_1) = \frac{1}{\sqrt{2\pi}\sigma_n} e^{-\frac{(r-\sqrt{\varepsilon_b})^2}{2\sigma_n^2}} \quad (7.5.47)$$

and

$$f(r | s_2) = \frac{1}{\sqrt{2\pi}\sigma_n} e^{-\frac{(r+\sqrt{\varepsilon_b})^2}{2\sigma_n^2}}. \quad (7.5.48)$$

Then, the metrics $\text{PM}(r, s_1)$ and $\text{PM}(r, s_2)$ defined by (7.5.45) are given by

$$\begin{aligned} \text{PM}(r, s_1) &= p f(r | s_1) \\ &= p \cdot \frac{1}{\sqrt{2\pi}\sigma_n} e^{-\frac{(r-\sqrt{\varepsilon_b})^2}{2\sigma_n^2}} \end{aligned} \quad (7.5.49)$$

$$\text{PM}(r, s_2) = (1 - p) \cdot \frac{1}{\sqrt{2\pi}\sigma_n} e^{-\frac{(r+\sqrt{\epsilon_b})^2}{2\sigma_n^2}}. \quad (7.5.50)$$

If $\text{PM}(r, s_1) > \text{PM}(r, s_2)$, then we select s_1 as the transmitted signal; otherwise, we select s_2 .

This decision rule may be expressed as

$$\frac{\text{PM}(r, s_1)}{\text{PM}(r, s_2)} > \frac{s_1}{s_2} 1. \quad (7.5.51)$$

Since

$$\frac{\text{PM}(r, s_1)}{\text{PM}(r, s_2)} = \frac{p}{1 - p} e^{\frac{(r+\sqrt{\epsilon_b})^2 - (r-\sqrt{\epsilon_b})^2}{2\sigma_n^2}}, \quad (7.5.52)$$

(7.5.51) may be expressed as

$$\frac{(r + \sqrt{\epsilon_b})^2 - (r - \sqrt{\epsilon_b})^2}{2\sigma_n^2} > \frac{s_1}{s_2} \ln \frac{1 - p}{p} \quad (7.5.53)$$

or, equivalently,

$$\begin{aligned}
 r\sqrt{\varepsilon_b} & \underset{s_2}{>} \frac{\sigma_n^2}{2} \ln \frac{1-p}{p} \\
 & \underset{s_1}{<} \\
 & = \frac{N_0}{4} \ln \frac{1-p}{p}
 \end{aligned} \tag{7.5.54}$$

for the optimum detector.

Note that in the case of unequal a priori probabilities, it is necessary to know not only the a priori probabilities but also the power spectral density N_0 , in order to compute the threshold in the RHS of (7.5.54).

When $p = \frac{1}{2}$, the threshold is zero, and knowledge of N_0 is not required by the detector.

Now we prove that the decision rule based on the maximum-likelihood criterion minimizes the probability of error when the M signals are equi-probable a priori.

Let R_m denote the **decision region** in the N -dimensional vector space for which we decide that signal $s_m(t)$ was transmitted when the vector $\mathbf{r} = (r_1, r_2, \dots, r_N)$ is received.

The probability of a decision error given that $s_m(t)$ was transmitted is given by

$$P(e | \mathbf{s}_m) = \int_{R_m^c} f(\mathbf{r} | \mathbf{s}_m) d\mathbf{r} \quad (7.5.55)$$

where R_m^c is the complement of R_m .

When the signals $\{\mathbf{s}_m\}$ are equiprobable, the average probability of error is given by

$$\begin{aligned} P(e) &= \sum_{m=1}^M \frac{1}{M} P(e | \mathbf{s}_m) \\ &= \sum_{m=1}^M \frac{1}{M} \int_{R_m^c} f(\mathbf{r} | \mathbf{s}_m) d\mathbf{r} \\ &= \sum_{m=1}^M \frac{1}{M} \left[1 - \int_{R_m} f(\mathbf{r} | \mathbf{s}_m) d\mathbf{r} \right]. \end{aligned} \quad (7.5.56)$$

Note that $P(e)$ is minimized by selecting the signal \mathbf{s}_m if $f(\mathbf{r} | \mathbf{s}_m)$ is larger than $f(\mathbf{r} | \mathbf{s}_k)$ for all $m \neq k$.

Similarly for the MAP criterion, when the M signals are not equi-probable, the average probability of error is given by

$$P(e) = 1 - \sum_{m=1}^M \int_{R_m} P(\mathbf{s}_m | \mathbf{r}) f(\mathbf{r}) d\mathbf{r}.$$

$P(e)$ is a minimum when the points that are to be included in each decision region R_m are those for which $P(\mathbf{s}_m | \mathbf{r})$ exceeds all other posterior probabilities.

7.5.4 Demodulation and Detection of Carrier-Amplitude Modulated Signals (ASK Signals)

The demodulation of a bandpass digital PAM signal may be accomplished by means of correlation or matched filtering.

The transmitted PAM signal in a signaling interval is given by

$$u_m(t) = A_m g_T(t) \cos 2\pi f_c t, \quad 0 \leq t \leq T. \quad (7.5.57)$$

The received signal is given by

$$r(t) = A_m g_T(t) \cos 2\pi f_c t + n(t), \quad 0 \leq t \leq T, \quad (7.5.58)$$

where $n(t)$ is a bandpass noise process which is given by

$$n(t) = n_c(t) \cos 2\pi f_c t - n_s(t) \sin 2\pi f_c t. \quad (7.5.59)$$

By crosscorrelating the received signal $r(t)$ with the basis function $\psi(t)$, we have

$$\int_0^T r(t) \psi(t) dt = A_m \sqrt{\frac{2}{\mathcal{E}_g}} \int_0^T g_T^2(t) \cos^2 2\pi f_c t dt + \int_0^T n(t) \psi(t) dt$$

$$= A_m \sqrt{\frac{\mathcal{E}_g}{2}} + n \quad (7.5.60)$$

where the random variable n represents the additive noise component at the output of the correlator.

An identical result is obtained if a matched filter is used instead of the correlator to demodulate the received signal.

Carrier-Phase Recovery.

We assumed that the function $\psi(t)$ is perfectly synchronized with the signal component of $r(t)$ in both time and carrier phase, as shown in Figure 7.38 for PAM.

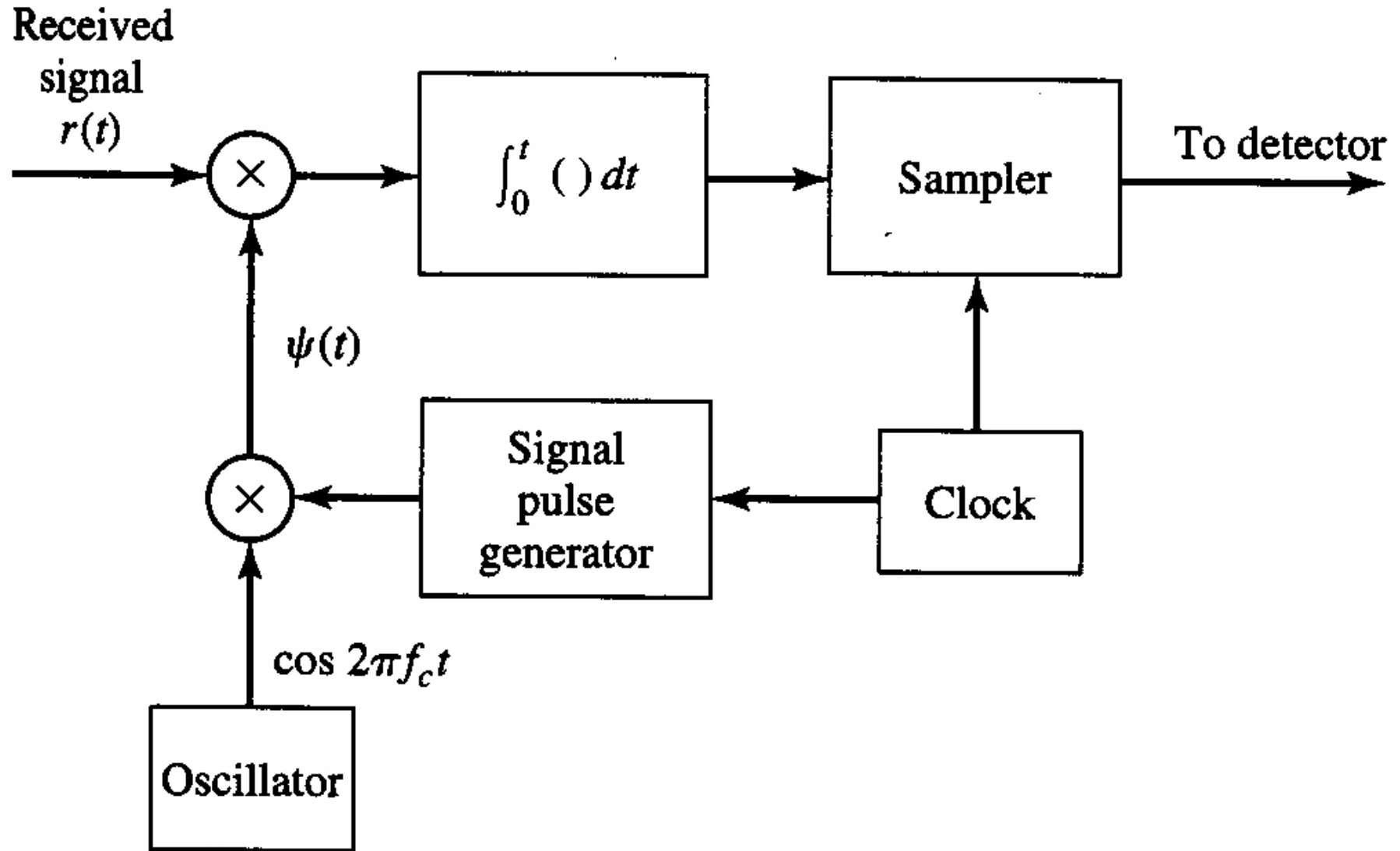


Figure 7.38 Demodulation of bandpass digital PAM signal.

However, these ideal conditions do not hold in practice.

First, the propagation delay encountered in the channel results in a carrier-phase offset in the received signal.

Second, the oscillator generating the carrier signal $\cos 2\pi f_c t$ at the receiver is not generally phase locked to the oscillator at the transmitter.

Also practical oscillators usually drift in frequency and phase.

Consequently, the demodulation of the bandpass PAM signal, as shown in Figure 7.38, is ideal not practical.

In general, the received signal has a carrier phase offset ϕ .

To estimate a carrier phase offset ϕ from the received signal $r(t)$, it is required to observe $r(t)$ over many signal intervals.

Because when the message signal is observed over many signal intervals it has zero mean due to the randomness in the signal amplitude values $\{A_m\}$, the transmitted DSB-SC amplitude-modulated signal has zero-average power at the carrier frequency f_c .

Consequently, it is not possible to estimate the carrier phase directly from $r(t)$.

Squaring $r(t)$, we can generate a frequency component at $f = 2f_c$, which has nonzero-average power.

The frequency component at $f = 2f_c$ can be filtered out by a narrowband filter tuned to $2f_c$, which can be used to drive a PLL (see Section 5.2).

A functional block diagram of the receiver that employ a PLL for estimating the carrier phase is shown in Figure 7.39.

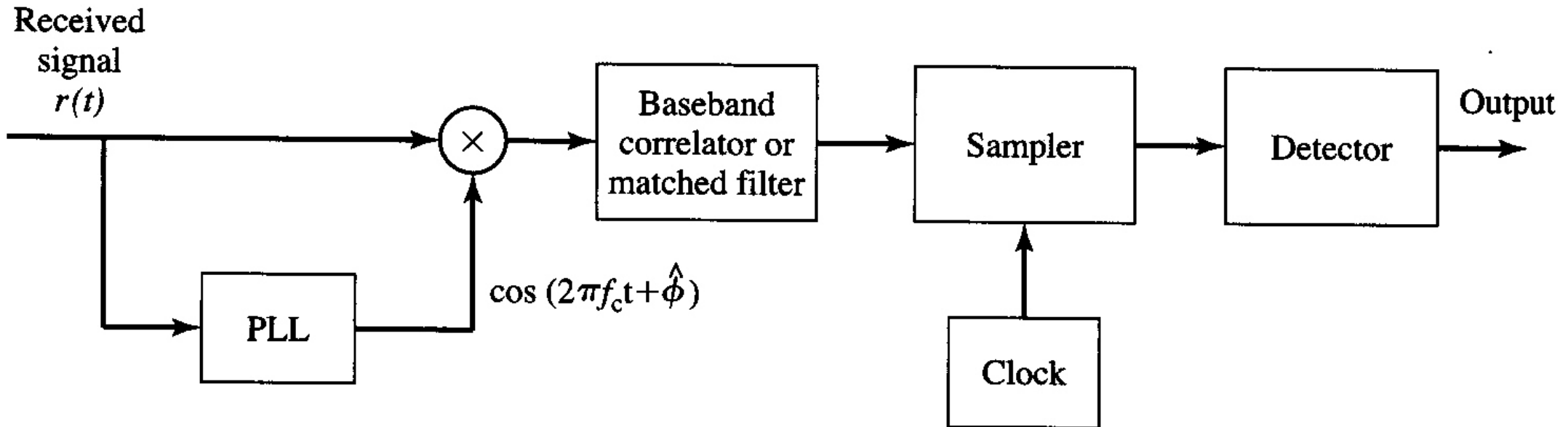


Figure 7.39 Demodulation of carrier-amplitude modulated signal.

The Costas loop (see Section 5.2) is an alternative method for estimating the carrier phase from the received signal $r(t)$.

The PLL and the Costas loop yield phase estimates that are comparable in quality in the presence of additive channel noise.

As an alternative to performing the correlation or matched filtering at baseband as shown in Figure 7.39, we may perform crosscorrelation or matched filtering either at bandpass or at some convenient intermediate frequency.

In particular, a bandpass correlator can be used to multiply the received signal $r(t)$ by the amplitude-modulated carrier $g_T(t)\cos(2\pi f_c t + \hat{\phi})$, where $\cos(2\pi f_c t + \hat{\phi})$ is the output of the PLL.

The product signal is integrated over the signaling interval T , the output of the integrator is sampled at $t = T$, and the sample is passed to the detector.

If a matched filter instead of a correlator is used, the filter impulse response is given by $g_T(T-t)\cos[2\pi f_c(T-t) - \hat{\phi}]$.

The functional block diagrams for these demodulators are shown in Figure 7.40.

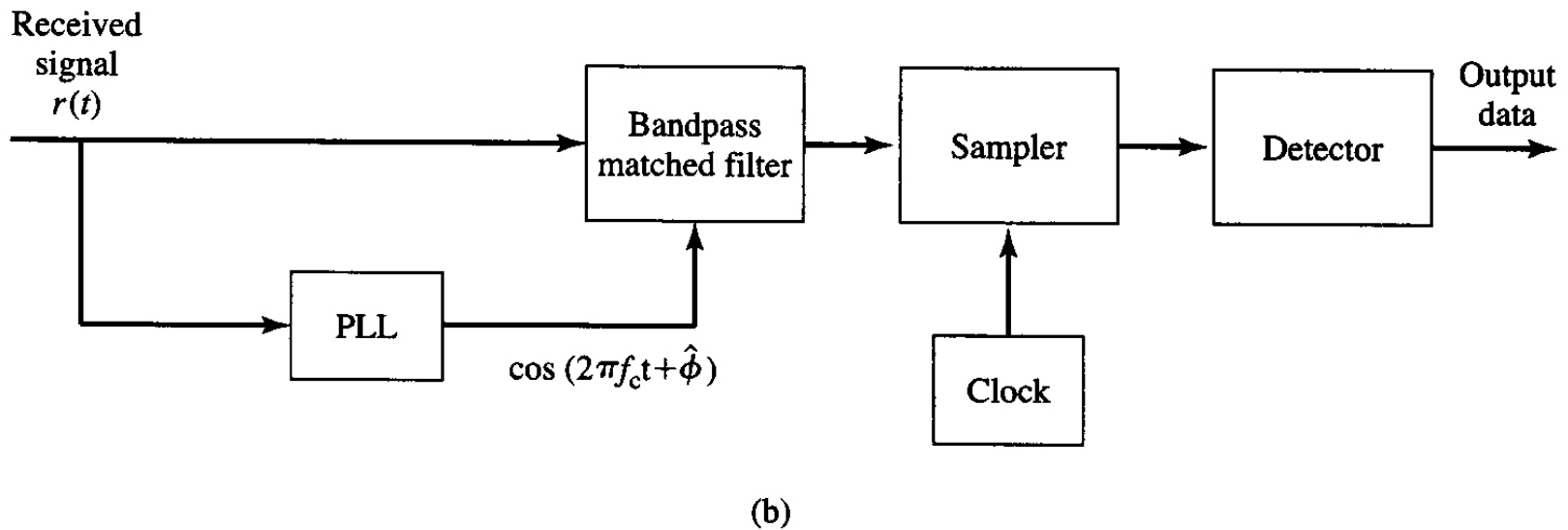
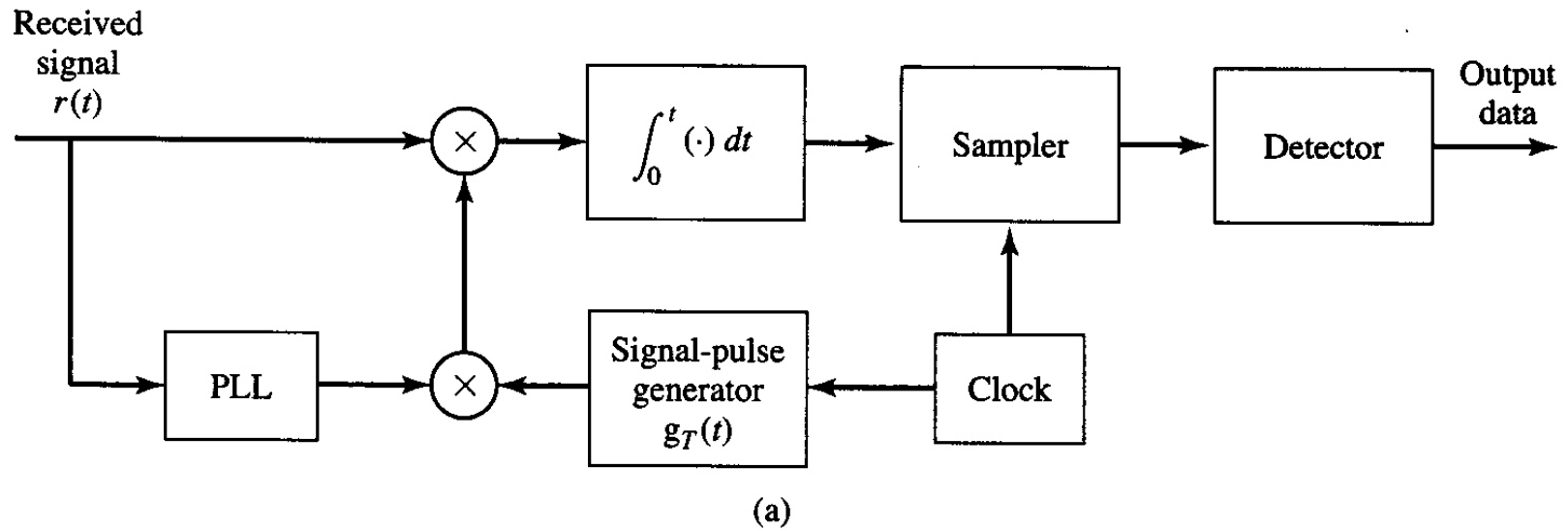


Figure 7.40 Bandpass demodulation of digital PAM signal via (a) bandpass correlation and (b) bandpass matched filtering.

Optimum Detector

In the case of a perfect (noise-free) carrier-phase estimate, $\phi = \hat{\phi}$, and the input to the detector is the signal plus noise term given by (7.5.60).

As in the case of baseband PAM, for equiprobable messages, the optimum detector bases its decision on the distance metrics

$$D(r, s_m) = (r - s_m)^2, \quad m = 1, 2, \dots, M, \quad (7.5.61)$$

or, equivalently, on the correlation metrics

$$C(r, s_m) = 2rs_m - s_m^2. \quad (7.5.62)$$

7.5.5 Demodulation and Detection of Carrier-Phase Modulated Signals

(PSK Signals. 2-dim. Signals)

The received bandpass signal from an AWGN channel in a signaling interval $0 \leq t \leq T$, is given by

$$\begin{aligned} r(t) &= u_m(t) + n(t) \\ &= [A_{mc}g_T(t) + n_c(t)]\cos 2\pi f_c t - [A_{ms}g_T(t) + n_s(t)]\sin 2\pi f_c t, \quad m = 1, 2, \dots, M, \end{aligned} \quad (7.5.63)$$

where $n(t)$ is the additive bandpass Gaussian noise and

A_{mc} and A_{ms} are the information bearing signal components that correspond to the transmitted carrier phase by (7.3.16).

The received signal are correlated with basis functions of the transmitted signal set given by

$$\psi_1(t) = \sqrt{\frac{2}{\mathcal{E}_s}} g_T(t) \cos 2\pi f_c t \quad \text{and}$$

$$\psi_2(t) = -\sqrt{\frac{2}{\mathcal{E}_s}} g_T(t) \sin 2\pi f_c t.$$

The outputs of the two correlators yield the two noise corrupted signal components, which is given by

$$\mathbf{r} = \mathbf{s}_m + \mathbf{n}$$
$$= \left(\sqrt{\varepsilon_s} \cos 2\pi \frac{m}{M} + n_c, \sqrt{\varepsilon_s} \sin 2\pi \frac{m}{M} + n_s \right) \quad (7.5.64)$$

where

$$n_c = \frac{1}{\sqrt{2\varepsilon_g}} \int_0^T g_T(t) n_c(t) dt$$

and

$$n_s = \frac{1}{\sqrt{2\varepsilon_g}} \int_0^T n_s(t) g_T(t) dt. \quad (7.5.65)$$

The quadrature noise components $n_c(t)$ and $n_s(t)$ are zero mean and uncorrelated [see the argument following (4.6.4)], that is,

$$E[n_c] = E[n_s]$$
$$= 0$$

and

$$E[n_c n_s] = 0.$$

The variance of the noise components is given by

$$\begin{aligned}
 E[n_c^2] &= E[n_s^2] \\
 &= \frac{1}{2\mathcal{E}_g} \int_0^T \int_0^T g_T(t)g_T(\tau)E[n_c(t)n_c(\tau)]dtd\tau \\
 &= \frac{N_0}{2\mathcal{E}_g} \int_0^T g_T^2(t)dt \\
 &= \frac{N_0}{2}.
 \end{aligned} \tag{7.5.66}$$

The optimum detector projects the received signal vector onto each of the M possible transmitted signal vectors $\{\mathbf{s}_m\}$ and selects the vector corresponding to the largest projection; that is, we compute the correlation metrics given by

$$C(\mathbf{r}, \mathbf{s}_m) = r \cdot s_m, \quad m = 1, 2, \dots, M, \tag{7.5.67}$$

and select the signal vector which results in the largest correlation.

Because all signals have equal energy, an equivalent optimum detector for digital-phase modulation computes the phase of the received signal vector $\mathbf{r} = (r_1, r_2)$ which is given by

$$\Theta = \tan^{-1} \frac{r_2}{r_1} \quad (7.5.68)$$

and selects the signal from the set $\{\mathbf{s}_m\}$ whose phase is closed to Θ_r .

Carrier-Phase Estimation.

In any carrier-modulation system, the oscillators at the transmitter and the receiver are not phase-locked.

The received signal is given by

$$r(t) = A_{mc} g_T(t) \cos(2\pi f_c t + \phi) - A_{ms} g_T(t) \sin(2\pi f_c t + \phi) + n(t) \quad (7.5.69)$$

where ϕ is the carrier-phase offset.

This phase offset must be estimated at the receiver, so that it could be used in the demodulation of the received signal.

Then, the received signal must be correlated with the two orthogonal basis functions:

$$\psi_1(t) = \sqrt{\frac{2}{\mathcal{E}_s}} g_T(t) \cos(2\pi f_c t + \hat{\phi})$$

and

$$\psi_2(t) = -\sqrt{\frac{2}{\mathcal{E}_s}} g_T(t) \sin(2\pi f_c t + \hat{\phi}) \tag{7.5.70}$$

where $\hat{\phi}$ is the estimate of the carrier phase, as shown in Figure 7.41 for the case in which $g_T(t)$ is a rectangular pulse.

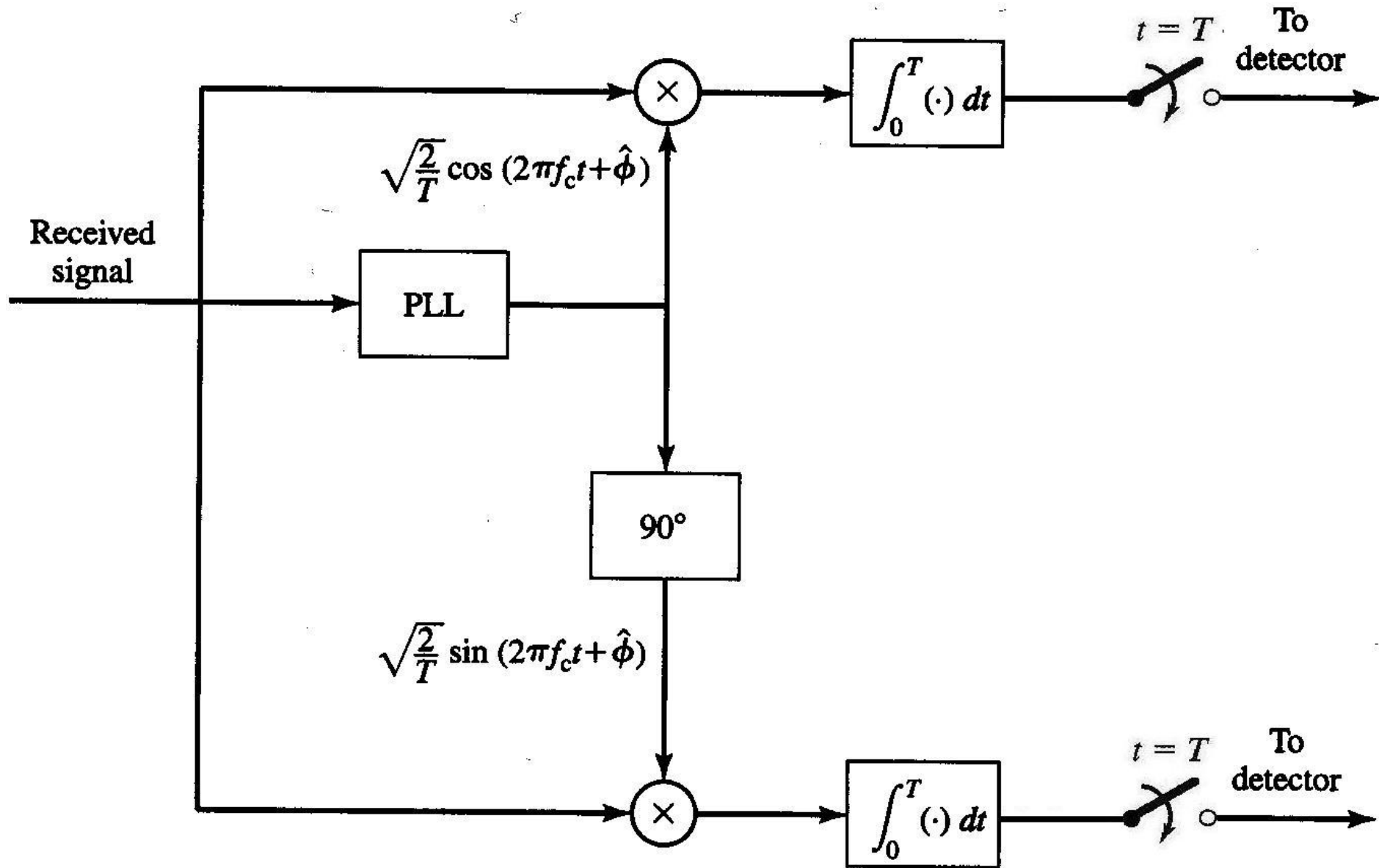


Figure 7.41 Demodulator for PSK signals.

For M -ary PSK, a PLL may be used in the receiver to estimate the carrier-phase offset.

For $M = 2$, the squaring PLL and the Costas loop described in Section 5.2 are directly applicable.

For $M > 2$, the received signal may first be raised to the M th power so that the phase which depends on the transmitted information could become 0 as shown in Figure 7.42.

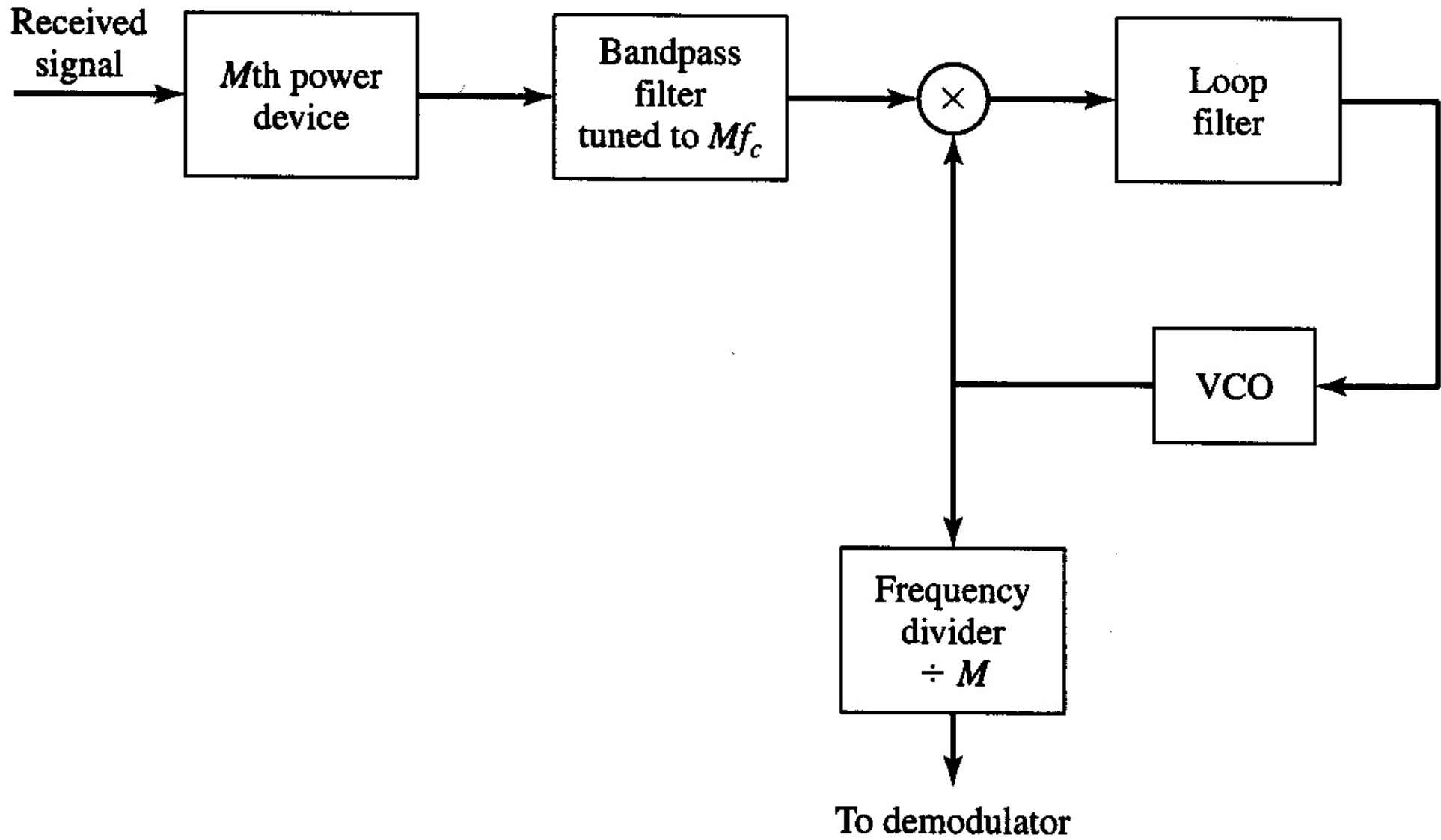


Figure 7.42 Carrier-phase estimation for M -ary PSK signals.

If the received signal is given by

$$\begin{aligned} r(t) &= s_m(t) + n(t) \\ &= g_T(t) \cos\left(2\pi f_c t + \phi + \frac{2\pi m}{M}\right) + n(t) \end{aligned} \quad (7.5.71)$$

and $r(t)$ is passed through an M th power device, then its output will contain harmonics of the carrier f_c .

The harmonic that we wish to select is $\cos(2\pi M f_c t + M \phi)$ for driving the PLL.

We note that

$$\begin{aligned} M \left(\frac{2\pi m}{M} \right) &= 2\pi m \\ &= 0 \pmod{2\pi}, \quad m = 1, 2, \dots, M. \end{aligned} \quad (7.5.72)$$

so that the information is removed from the M th harmonic.

The bandpass filter tuned to the frequency $M f_c$ produces the desired frequency component $\cos(2\pi M f_c t + M \phi)$ driving the PLL.

The output of the VCO is given by $\sin(2\pi Mf_c t + M\hat{\phi})$.

The frequency divider divides its frequency by M to yield $\sin(2\pi f_c t + \hat{\phi})$, and then it is phase-shifted by $\frac{\pi}{2}$ to yield $\cos(2\pi f_c t + \hat{\phi})$.

The two quadrature-carrier components are then passed to the demodulator.

We should note that the quadrature-phase carrier components generated as described above contain phase ambiguities of multiples of $\frac{2\pi}{M}$ that result from multiplying the carrier phase ϕ by M .

Because $M\phi \pmod{2\pi}$ is less than 2π , dividing the resulting angle by M yields a phase estimate of $|\hat{\phi}| < \frac{2\pi}{M}$, when the true carrier phase may exceed this estimate by multiples of $\frac{2\pi}{M}$, that is, by $2\pi \frac{k}{M}$, for $k = 1, 2, \dots, M - 1$.

Just as in the case of the squaring PLL, the M th power PLL operates in the presence of noise that has been enhanced by the M th power-law device.

The variance of the phase error in the PLL resulting from the additive noise is given in the simple form by

$$\sigma_{\hat{\phi}}^2 = \frac{1}{S_{ML}\rho_L} \quad (7.5.73)$$

where ρ_L is the loop SNR and S_{ML} is the M -**phase power loss**.

S_{ML} has been evaluated by Lindsey and Simon (1973) for $M = 4$ and $M = 8$.

Another method for extracting a carrier-phase estimate & from the received signal for M -ary phase modulation is the decision-feedback PLL (DFPLL), which is shown in Figure 7.43.

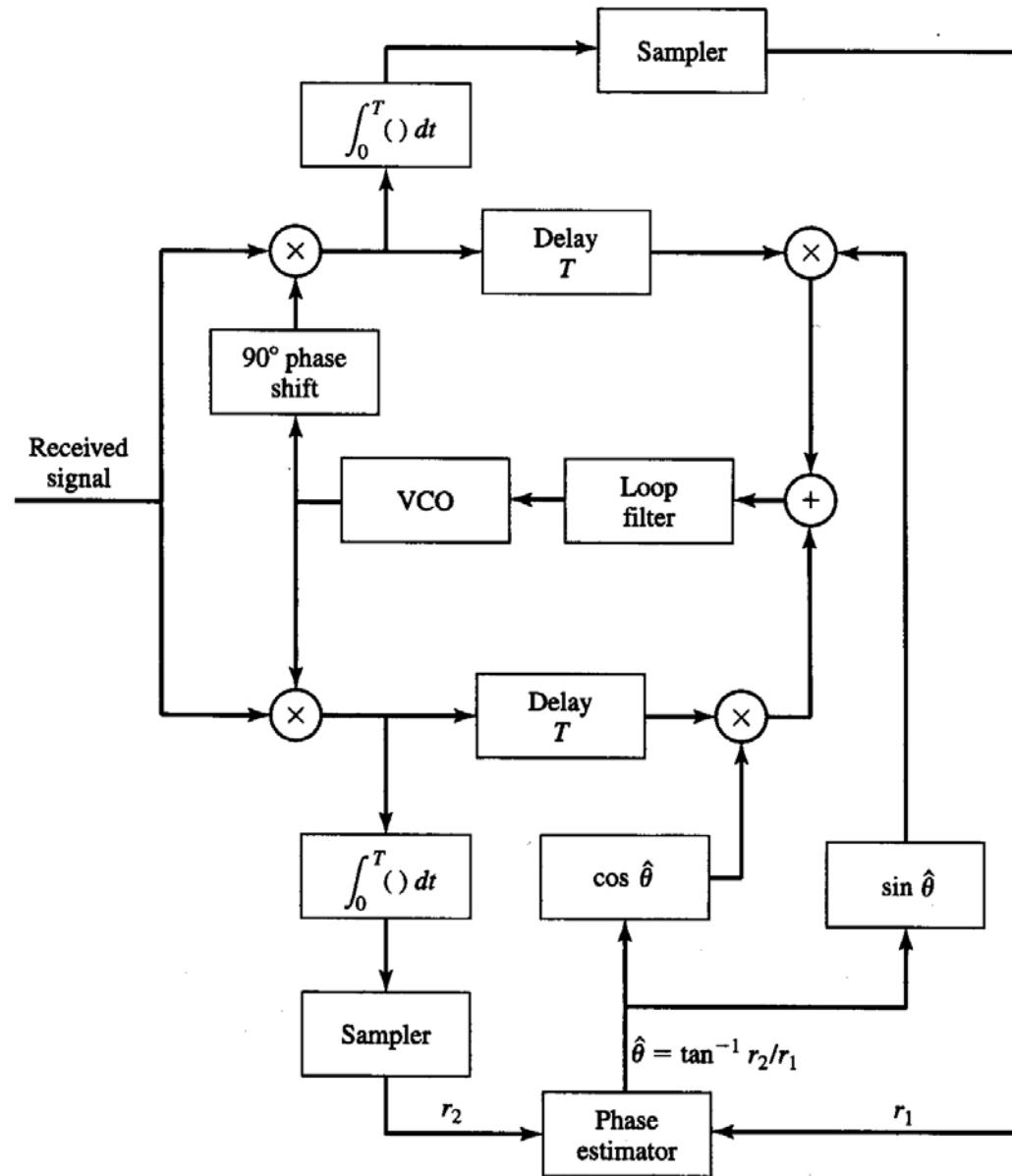


Figure 7.43 Carrier recovery for M -ary PSK using a DFPLL.

The received signal is demodulated by using two quadrature phase-locked carriers to yield $\mathbf{r} = (r_1, r_2)$ at the sampling instants.

The phase estimate $\hat{\Theta}_r = \tan^{-1} \frac{r_2}{r_1}$ is computed at the detector and quantized to the nearest of the M possible transmitted phases, which we denote as $\hat{\theta}_m$.

The two outputs of the quadrature multipliers are delayed by one symbol interval T and multiplied by $\cos \theta_m$ and $-\sin \theta_m$.

Thus, we obtain

$$-r(t) \cos(2\pi f_c t + \hat{\phi}) \sin \theta_m = -\frac{1}{2} [g_T(t) \cos \theta_m + n_c(t)] \sin \theta_m \cos(\phi - \hat{\phi}) + \frac{1}{2} [g_T(t) \sin \theta_m + n_s(t)] \sin \theta_m \sin(\phi - \hat{\phi})$$

+ double-frequency terms

$$-r(t) \sin(2\pi f_c t + \hat{\phi}) \cos \theta_m = -\frac{1}{2} [g_T(t) \cos \theta_m + n_c(t)] \cos \theta_m \sin(\phi - \hat{\phi}) + \frac{1}{2} [g_T(t) \sin \theta_m + n_s(t)] \cos \theta_m \cos(\phi - \hat{\phi})$$

+ double-frequency terms.

These two signals are added together to generate the error signal

$$e(t) = g_T(t)\sin(\phi - \hat{\phi}) + \frac{1}{2}n_c(t)\sin(\phi - \hat{\phi} - \theta_m) + \frac{1}{2}n_s(t)\cos(\phi - \hat{\phi} - \theta_m) + \text{double-frequency terms} \quad (7.5.74)$$

which is the input to the loop filter that provides the control signal for the VCO.

Observe that the two quadrature noise components in (7.5.74) appear as additive terms and no term involves a product of two noise components as in the output of the M th power-law device.

Consequently, there is no power loss resulting from nonlinear operations on the received signal in the DFPLL.

The M -phase decision-feedback tracking loop also has a phase ambiguities of $2\pi\frac{k}{M}$, necessitating the need for differentially encoding the information sequence prior to transmission and differentially decoding the received sequence at the detector to recover the information.

Differential-Phase Modulation and Demodulation (DPSK)

For ideal coherent phase demodulation, a carrier signal, called a pilot signal, must be transmitted along with the information signal.

In the receiver the carrier signal component in the received signal is filtered to be used for phase-coherent demodulation.

However, when no separate carrier signal is transmitted, the receiver must estimate the carrier phase from the received signal.

The phase at the output of a PLL has ambiguities of multiples of $\frac{2\pi}{M}$, which necessitate differential encoding of the data prior to modulation (see Section 7.5.5).

By using differential encoding it becomes possible to decode the received data in the presence of the phase ambiguities at the detector.

In differential encoding, the information is delivered by phase shifts between two successive signal intervals.

For example, in binary phase modulation

the information bit 1 is transmitted by shifting the carrier phase by 180° from the carrier phase in the preceding interval,

while the information bit 0 is transmitted by a zero phase shift relative to the carrier phase in the preceding interval.

Table 6.1 illustrates the generation of a DPSK signal for a sample sequence m_k which follows the relationship $d_k = \overline{m_k \oplus d_{k-1}}$ [T. Rappaport, Wireless Communications, 2/e. Prentice Hall, 2002].

Table 6.1 Illustration of the Differential Encoding Process

k	0	1	2	3	4	5	6	7	8
$\{m_k\}$		1	0	0	1	0	1	1	0
$\{d_{k-1}\}$		1	1	0	1	1	0	0	0
$\{d_k\}$	1	1	0	1	1	0	0	0	1

In four-phase modulation (such as QPSK), the relative phase shifts between successive intervals are 0° , 90° , 180° , and 270° corresponding to the information bits 00, 01, 11, and 10, respectively.

Differential encoding is generalized straightforward for $M > 4$.

This encoding process for phase modulation is called **differentially encoding**.

The differentially encoded phase-modulated signal can be demodulated and detected using the output of a PLL as described in the preceding section.

The received signal phase $\Theta_r = \tan^{-1} \frac{r_2}{r_1}$ at the detector is mapped into one of the M possible transmitted signal phases $\{\theta_m\}$ that is closest to Θ_r .

Following the detector, a relatively simple phase comparator compares the phases of the detected signals over two consecutive intervals to extract the transmitted information.

Thus, phase ambiguities of $\frac{2\pi}{M}$ becomes irrelevant.

A differentially encoded phase-modulated signal also makes another type of demodulation possible which does not require the estimation of the carrier phase. Instead, the phase of the received signal in any given signaling interval is compared with that of the preceding interval.

Suppose that we demodulate the differentially encoded signal by multiplying $r(t)$ with $\cos 2\pi f_c t$ and $\sin 2\pi f_c t$ and integrating the two products over the interval T .

At the k th interval, the demodulator output is given by

$$r_k = \sqrt{\varepsilon_s} e^{j(\theta_k - \phi)} + n_k \quad (7.5.75)$$

where θ_k is the phase angle of the transmitted signal at the k th signaling interval,

ϕ is the carrier phase, and

$n_k = n_{kc} + jn_{ks}$ is the noise vector.

Similarly, the demodulator output in the preceding interval is given by

$$r_{k-1} = \sqrt{\varepsilon_s} e^{j(\theta_{k-1} - \phi)} + n_{k-1}. \quad (7.5.76)$$

The decision variable for the phase detector is the phase difference between these two complex numbers.

Equivalently, the projection of r_k onto r_{k-1} can be used as decision variable:

$$r_k r_{k-1}^* = \varepsilon_s e^{j(\theta_k - \theta_{k-1})} + \sqrt{\varepsilon_s} e^{j(\theta_k - \phi)} n_{k-1} + \sqrt{\varepsilon_s} e^{-j(\theta_{k-1} - \phi)} n_k + n_k n_{k-1}^* \quad (7.5.77)$$

which yields the phase difference $\theta_k - \theta_{k-1}$ in the absence of noise.

Notice that the mean of $r_k r_{k-1}^*$ is independent of the carrier phase.

Differentially encoded PSK that is demodulated and detected as described above is called **differential PSK (DPSK)**.

The work 'DPSK' is used for a binary modulation.

Differentially encoded and detected as described above is called DQPSK (differential quadrature phase modulation).

A modified version of DQPSK, called $\pi/4$ DQPSK, is used in the US TDMA cellular system (IS-54).

The demodulation and detection of DSPK using matched filter is shown in Figure 7.44.

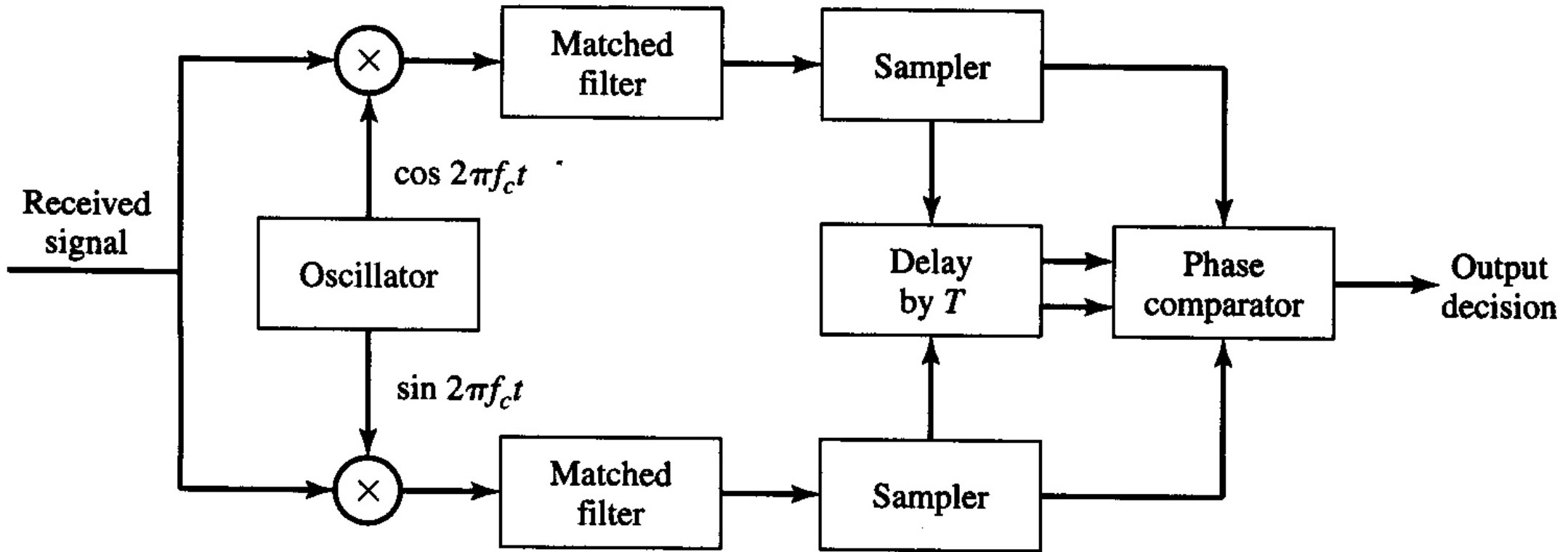


Figure 7.44 DPSK demodulator.

If the pulse $g_T(t)$ is rectangular, the matched filters may be replaced by integrators, which are also called **integrate-and-dump filters**. (In the text, 'integrate-and-dump' filters are distinguished from the correlator type demodulator as in this sentence. But they often mean the same)

7.5.6 Demodulation and Detection of Quadrature Amplitude Modulated (QAM) Signals

Assume that a carrier-phase offset is introduced in the signal from the channel.

Also assume that the received signal is corrupted by additive Gaussian noise.

Then, the received signal is given by

$$r(t) = A_{mc}g_T(t)\cos(2\pi f_c t + \phi) + A_{ms}g_T(t)\sin(2\pi f_c t + \phi) + n(t) \quad (7.5.78)$$

where ϕ is the carrier phase and $n(t)$ is the noise process.

Suppose that an estimate $\hat{\phi}$ of the carrier phase is available at the demodulator.

Then, the received signal is correlated with the two basis functions

$$\begin{aligned}\psi_1(t) &= \sqrt{\frac{2}{\mathcal{E}_s}} g_T(t) \cos(2\pi f_c t + \hat{\phi}) \\ \psi_2(t) &= \sqrt{\frac{2}{\mathcal{E}_s}} g_T(t) \sin(2\pi f_c t + \hat{\phi})\end{aligned}\tag{7.5.79}$$

as shown in Figure 7.45, and the outputs of the correlators are sampled and passed to the detector.

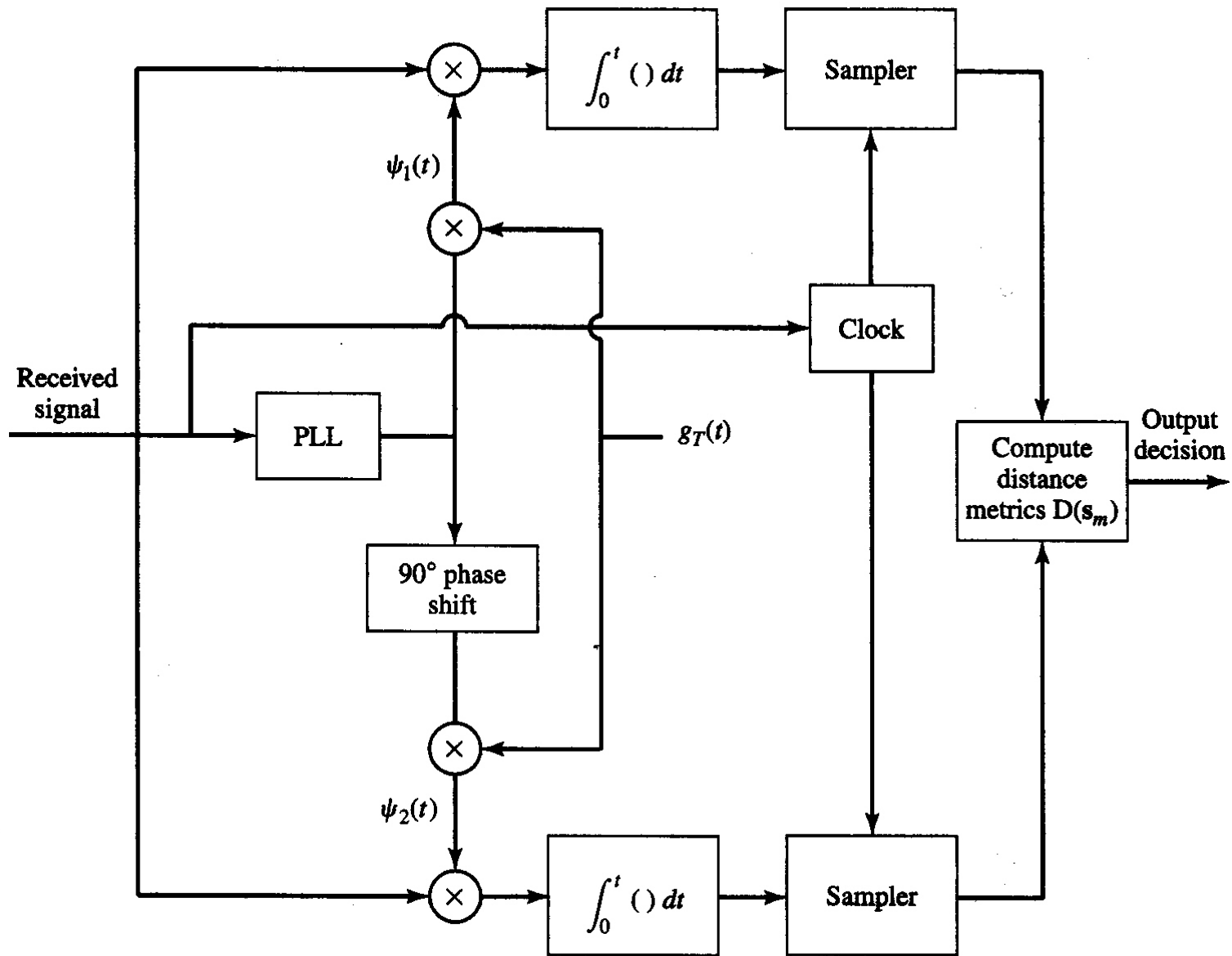


Figure 7.45 Demodulation and detection of QAM signals.

The input to the detector consists of the two sampled components r_1 and r_2 which are given by

$$\begin{aligned}r_1 &= A_{mc} \sqrt{\varepsilon_s} \cos(\phi - \hat{\phi}) + A_{ms} \sqrt{\varepsilon_s} \sin(\phi - \hat{\phi}) + n_c \sin(\hat{\phi}) - n_s \cos(\hat{\phi}) \\r_2 &= A_{mc} \sqrt{\varepsilon_s} \sin(\phi - \hat{\phi}) + A_{ms} \sqrt{\varepsilon_s} \cos(\phi - \hat{\phi}) + n_c \sin(\hat{\phi}) - n_s \cos(\hat{\phi})\end{aligned}\tag{7.5.80}$$

where $\varepsilon_s = \frac{\varepsilon_g}{2}$.

We observe that the effect of an imperfect phase estimate is two-fold: SNR reduction and component leakage.

First, the desired signal components in r_1 and r_2 are reduced in amplitude by the factor $\cos(\phi - \hat{\phi})$ which reduces the SNR by the factor $\cos^2(\phi - \hat{\phi})$.

Second, there is a leakage of the quadrature signal components into the desired signal.

This signal leakage, which is scaled by $\sin(\phi - \hat{\phi})$, causes a significant performance degradation unless $\phi - \hat{\phi}$ is very small.

This is why having an accurate carrier-phase estimate is important to demodulation of a QAM signal.

The optimum detector computes the distance metrics which are given by

$$D(\mathbf{r}, \mathbf{s}_m) = \|\mathbf{r} - \mathbf{s}_m\|^2, \quad m = 1, 2, \dots, M, \quad (7.5.81)$$

and selects the signal corresponding to the smallest value of $D(\mathbf{r}, \mathbf{s}_m)$.

If a correlation metric is used in place of a distance metric, correlation metrics must employ bias correction because the QAM signals are not equal energy signals.

Carrier-Phase Estimation

The demodulation of a QAM signal requires a carrier that is phase-locked to the phase of the received carrier signal.

Carrier-phase estimation for QAM is accomplished in various ways depending on the signal-point constellation and the phase relationships of the various signal points.

For example, consider the 8-point QAM signal constellation shown in Figure 7.17(b) where the signal

points in this constellation have one of two possible amplitude values and 8 possible phases and the phases are spaced 45° apart.

This phase symmetry allows us to use a PLL driven by the output of an 8th power-law device that generates a carrier component at $8f_c$, where f_c is the carrier frequency.

Thus, the method shown in Figure 7.42 can be used for any QAM signal constellation that contains signal points with phases that are multiples of some phase angle θ , where $L \cdot \theta = 360^\circ$ for some integer L .

Another method to estimate a carrier-phase from the received M -ary QAM signal is the DFPLL in Section 7.5.5 which estimates the phase of the QAM signal in each interval and removes the phase modulation from the carrier.

The DFPLL can be used with any QAM signal, irrespective of the phase relationships among the signal points.

The received QAM signal is given by

$$r(t) = A_m g_T(t) \cos(2\pi f_c t + \theta_n + \phi) + n(t), \quad (7.582)$$

where θ_n is the phase of the signal point and ϕ is the carrier phase.

This signal is demodulated by crosscorrelating $r(t)$ with $\psi_1(t)$ and $\psi_2(t)$, which are given by (7.5.79).

The sampled values at the output of the correlator are given by

$$r_1 = A_m \sqrt{\varepsilon_s} \cos(\theta_n + \phi - \hat{\phi}) + n_c \cos(\theta_n + \phi - \hat{\phi}) - n_s \sin(\theta_n + \phi - \hat{\phi}) \quad (7.5.83a)$$

$$r_2 = A_m \sqrt{\varepsilon_s} \sin(\theta_n + \phi - \hat{\phi}) + n_c \sin(\theta_n + \phi - \hat{\phi}) - n_s \sin(\theta_n + \phi - \hat{\phi}). \quad (7.5.83b)$$

Suppose that the detector, based on r_1 and r_2 , has made the correct decision on the transmitted signal point.

Then, by multiplying r_1 in (7.5.83a) by $-\sin \theta_n$ and r_2 in (7.5.83b) by $\cos \theta_n$, we obtain

$$\begin{aligned} -r_1 \sin \theta_n &= -A_m \sqrt{\varepsilon_s} \cos(\theta_n + \phi - \hat{\phi}) \sin \theta_n + \text{noise component} \\ &= A_m \sqrt{\varepsilon_s} \left[-\sin \theta_n \cos \theta_n \cos(\phi - \hat{\phi}) + \sin^2 \theta_n \sin(\phi - \hat{\phi}) \right] + \text{noise component} \end{aligned} \quad (7.5.84a)$$

and

$$\begin{aligned}
 r_2 \cos \theta_n &= A_m \sqrt{\varepsilon_s} \sin(\theta_n + \phi - \hat{\phi}) \cos \theta_n + \text{noise component} \\
 &= A_m \sqrt{\varepsilon_s} \left[\sin \theta_n \cos \theta_n \cos(\phi - \hat{\phi}) + \cos^2 \theta_n \sin(\phi - \hat{\phi}) \right] + \text{noise component.}
 \end{aligned} \tag{7.5.84b}$$

By adding (7.5.84a) and (7.5.84b), an error signal is obtained as

$$\begin{aligned}
 e(t) &= r_2 \cos \theta_n - r_1 \sin \theta_n \\
 &= A_m \varepsilon_s \sin(\phi - \hat{\phi}) + \text{noise components}
 \end{aligned} \tag{7.5.85}$$

which is to be passed to the loop filter that drives the VCO.

Thus, only the phase of the QAM signal (not the phase of the signal point θ_n) is used in obtaining an estimate of the carrier phase.

Consequently, the DFPLL in Figure 7.43 applies to carrier-phase estimation for an M -ary QAM signal.

As in the case of digitally phase-modulated signals, the method described above for carrier-phase recovery results in phase ambiguities.

7.5.7 Demodulation and Detection of Frequency-Modulated Signals (FSK signals)

Assume that the FSK signals are transmitted through an additive white Gaussian noise channel.

Furthermore, we assume that each signal is delayed in the transmission through the channel.

Consequently, the filtered received signal at the input to the demodulator is given by

$$r(t) = \sqrt{\frac{2\mathcal{E}_s}{T}} \cos(2\pi f_c t + 2\pi m \Delta f t + \phi_m) + n(t) \quad (7.5.86)$$

where ϕ_m is the phase shift of the m th signal (due to the transmission delay) and

$n(t)$ is the additive bandpass noise, which is given by

$$n(t) = n_c(t) \cos 2\pi f_c t - n_s(t) \sin 2\pi f_c t. \quad (7.5.87)$$

The demodulation and detection of the M FSK signals may be accomplished by one of two methods.

One approach is to estimate the M carrier-phase shifts $\{\phi_m\}$ and perform **phase-coherent demodulation and detection**.

In another approach the carrier phases may be ignored in the demodulation and detection of the FSK signals.

The latter is called **noncoherent demodulation and detection**.

In phase-coherent demodulation, the received signal $r(t)$ is correlated with each of the M possible received signals $\cos(2\pi f_c t + 2\pi m \Delta f t + \hat{\phi}_m)$, $m = 0, 1, \dots, M - 1$, where $\{\hat{\phi}_m\}$ are the carrier phase estimates.

A block diagram of coherent demodulation is shown in Figure 7.46.

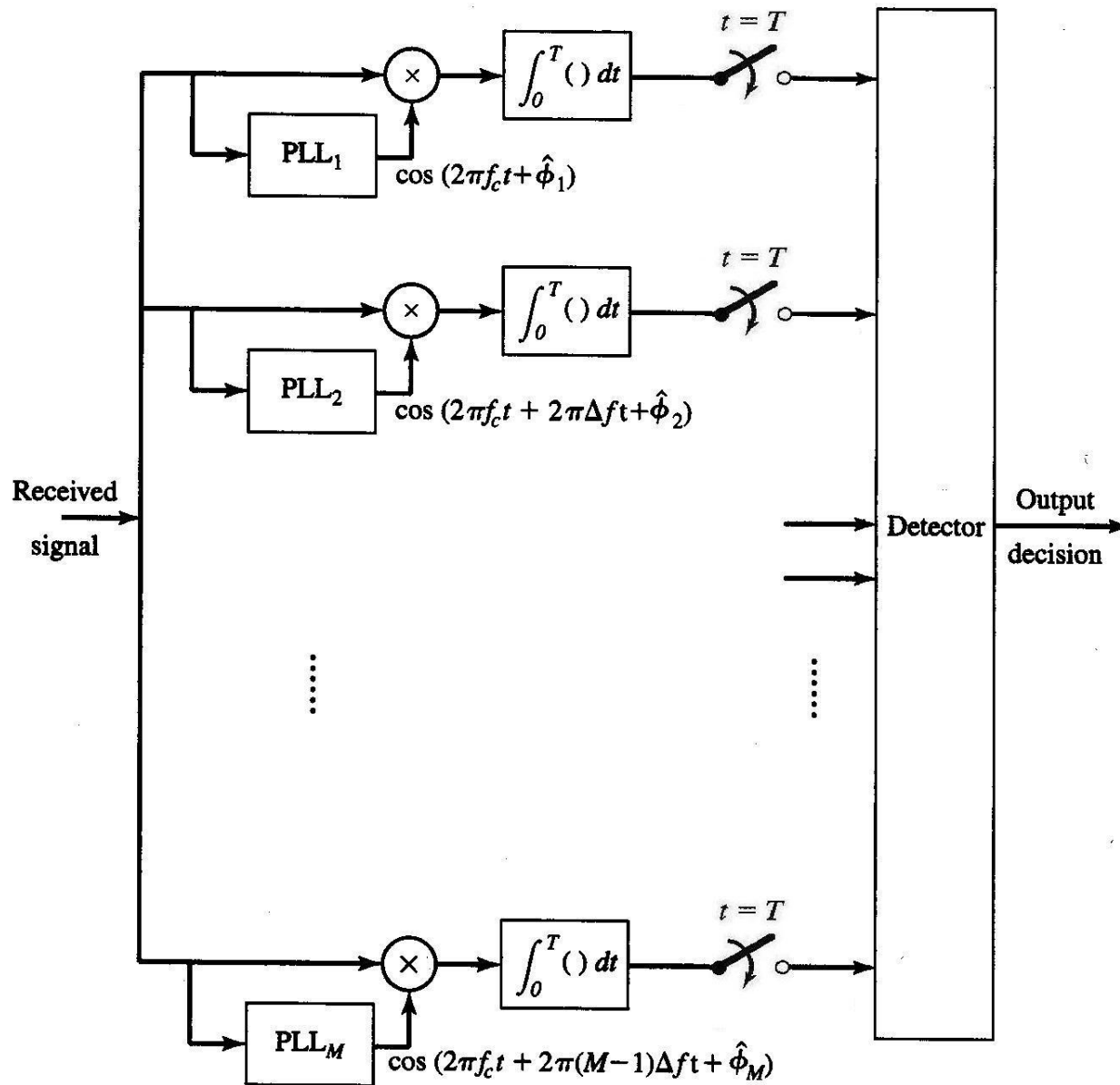


Figure 7.46 Phase-coherent demodulation of M -ary FSK signals.

Note that when $\hat{\phi}_m \neq \phi_m$, $m = 0, 1, \dots, M - 1$, (imperfect phase estimates), the frequency separation required for signal orthogonality at the demodulator is $\Delta f = \frac{1}{T}$ (see Problem 7.51), which is twice the minimum separation for orthogonality when $\phi \neq \hat{\phi}$.

The requirement for estimating M carrier phases makes coherent demodulation of FSK signals extremely complex and impractical, especially when the number of signal points is large.

Now we now consider a method for demodulation and detection that does not require knowledge of the carrier phases.

The block diagram of noncoherent demodulation is shown in Figure 7.47.

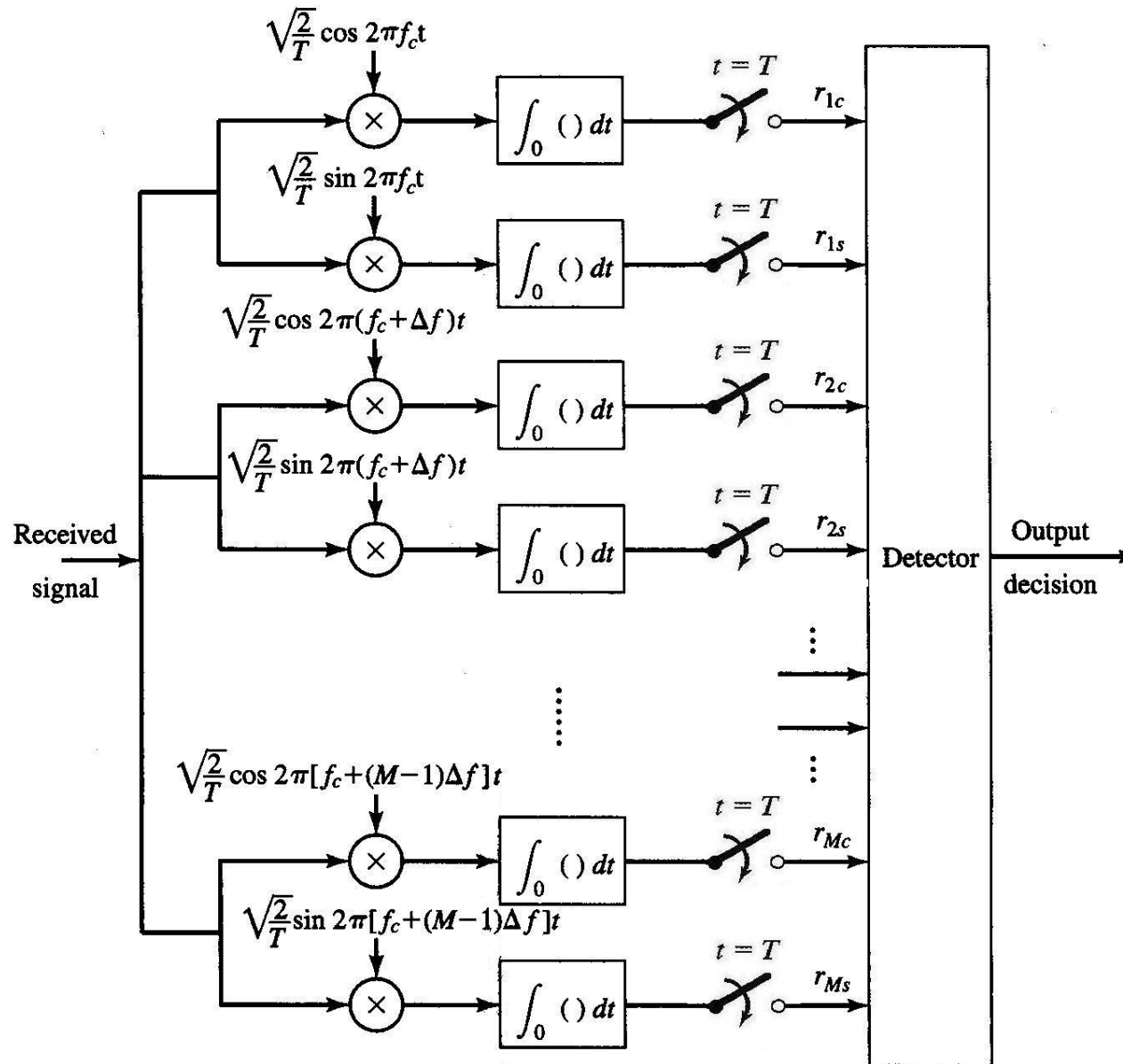


Figure 7.47 Noncoherent demodulation of M -ary FSK signals.

In noncoherent demodulation there are two correlators per signal, or a total of $2M$ correlators.

The received signal is correlated with the basis functions (quadrature carriers) $\sqrt{\frac{2}{T}} \cos(2\pi f_c t + 2\pi m \Delta f t)$

and $\sqrt{\frac{2}{T}} \sin(2\pi f_c t + 2\pi m \Delta f t)$ for $m = 0, 1, \dots, M - 1$.

The $2M$ outputs of the correlators are sampled at the end of the interval T and the $2M$ samples are passed to the detector.

Thus, if the m th signal is transmitted, the outputs from the k th pair of samplers are given by

$$r_{kc} = \sqrt{\varepsilon_s} \left[\frac{\sin 2\pi(k-m)\Delta f T}{2\pi(k-m)\Delta f T} \cos \phi_m + \frac{\cos 2\pi(k-m)\Delta f T - 1}{2\pi(k-m)\Delta f T} \sin \phi_m \right] + n_{kc}$$

and

$$r_{ks} = \sqrt{\varepsilon_s} \left[\frac{\cos 2\pi(k-m)\Delta f T - 1}{2\pi(k-m)\Delta f T} \cos \phi_m + \frac{\sin 2\pi(k-m)\Delta f T}{2\pi(k-m)\Delta f T} \sin \phi_m \right] + n_{ks}. \quad (7.5.88)$$

where n_{kc} and n_{ks} are the Gaussian noise components in the sampled outputs.

The outputs from the m th pair of samplers (that is, $k = m$) are given by

$$r_{mc} = \sqrt{\varepsilon_s} \cos \phi_m + n_{mc}$$

and

$$r_{ms} = \sqrt{\varepsilon_s} \sin \phi_m + n_{ms}. \quad (7.5.89)$$

Furthermore, we observe that when $k \neq m$,

the signal components in the samples r_{kc} and r_{ks} will vanish, independent of the values of the phase shift ϕ_k ,

provided that the frequency separation between successive frequencies is $\Delta f = \frac{1}{T}$.

In such a case, each of the $2(M - 1)$ correlator outputs consists of noise only; that is,

$$r_{kc} = n_{kc}$$

$$r_{ks} = n_{ks} \quad \text{for } k \neq m. \quad (7.5.90)$$

Assume that $\Delta f = \frac{1}{T}$, so that the signals are orthogonal.

Then, it is shown (see Problem 7.52) that the $2M$ noise samples $\{n_{kc}\}$ and $\{n_{ks}\}$ are zero-mean, mutually uncorrelated (thus, independent) Gaussian random variables with equal variance $\sigma^2 = \frac{N_0}{2}$.

Consequently, the joint PDF for r_{mc} and r_{ms} conditioned on ϕ_m is given by

$$f_{\mathbf{r}_m}(r_{mc}, r_{ms} | \phi_m) = \frac{1}{2\pi\sigma^2} e^{-\frac{(r_{mc} - \sqrt{\varepsilon_s} \cos \phi_m)^2 + (r_{ms} - \sqrt{\varepsilon_s} \sin \phi_m)^2}{2\sigma^2}} \quad (7.5.91)$$

and for $k \neq m$,

$$f_{\mathbf{r}_k}(r_{kc}, r_{ks}) = \frac{1}{2\pi\sigma^2} e^{-\frac{(r_{kc}^2 + r_{ks}^2)}{2\sigma^2}}. \quad (7.5.92)$$

Given the $2M$ observed random variables $r_{kc}, r_{ks}, k = 1, 2, \dots, M$, the optimum detector selects the signal that corresponds to the maximum of the a posteriori probabilities

$$P(s_m \text{ was transmitted} | \mathbf{r}) \equiv P(s_m | \mathbf{r}), \quad m = 1, 2, \dots, M, \quad (7.5.93)$$

where \mathbf{r} is the vector with $2M$ elements $r_{kc}, r_{ks}, k = 1, 2, \dots, M$.

Optimum Detector for Binary FSK

In binary orthogonal FSK, the two a posteriori probabilities are given by

$$P(s_1|\mathbf{r}) = \frac{f_{\mathbf{r}}(\mathbf{r}|s_1)P(s_1)}{f_{\mathbf{r}}(\mathbf{r})}$$

and

$$P(s_2|\mathbf{r}) = \frac{f_{\mathbf{r}}(\mathbf{r}|s_2)P(s_2)}{f_{\mathbf{r}}(\mathbf{r})} \tag{7.5.94}$$

and, hence, the optimum detection rule is expressed as

$$P(s_1|\mathbf{r}) \underset{s_2}{\overset{s_1}{>}} P(s_2|\mathbf{r}) \tag{7.5.95}$$

or, equivalently,

$$\frac{f_{\mathbf{r}}(\mathbf{r}|s_1)P(s_1)}{f_{\mathbf{r}}(\mathbf{r})} \underset{s_2}{\overset{s_1}{>}} \frac{f_{\mathbf{r}}(\mathbf{r}|s_2)P(s_2)}{f_{\mathbf{r}}(\mathbf{r})}. \tag{7.5.96}$$

where \mathbf{r} is the four-dimensional vector $\mathbf{r} = (r_{1c}, r_{1s}, r_{2c}, r_{2s})$.

(7.5.96) is simplified to the detection rule

$$\frac{f_{\mathbf{r}}(\mathbf{r}|s_1)}{f_{\mathbf{r}}(\mathbf{r}|s_2)} \underset{s_2}{\overset{s_1}{>}} \frac{P(s_2)}{P(s_1)}. \tag{7.5.97}$$

The ratio of PDFs in the left-hand side of (7.5.97) is the likelihood ratio which is denoted as

$$\Lambda(\mathbf{r}) = \frac{f_{\mathbf{r}}(\mathbf{r} | \mathbf{s}_1)}{f_{\mathbf{r}}(\mathbf{r} | \mathbf{s}_2)}. \quad (7.5.98)$$

Note that the right-hand side of (7.5.97) becomes 1 when the two signals are equi-probable.

The PDFs $f_{\mathbf{r}}(\mathbf{r} | \mathbf{s}_1)$ and $f_{\mathbf{r}}(\mathbf{r} | \mathbf{s}_2)$ in the likelihood ratio $\Lambda(\mathbf{r})$ are given by

$$f_{\mathbf{r}}(\mathbf{r} | \mathbf{s}_1) = \int_0^{2\pi} f_{\mathbf{r}_1}(r_{1c}, r_{1s} | \phi_1) f_{\phi_1}(\phi_1) d\phi_1 \cdot f_{\mathbf{r}_2}(r_{2c}, r_{2s}) \quad (7.5.99a)$$

and

$$f_{\mathbf{r}}(\mathbf{r} | \mathbf{s}_2) = f_{\mathbf{r}_1}(r_{1c}, r_{1s}) \int_0^{2\pi} f_{\mathbf{r}_2}(r_{2c}, r_{2s} | \phi_2) f_{\phi_2}(\phi_2) d\phi_2 \quad (7.5.99b)$$

where $f_{\mathbf{r}_m}(r_{mc}, r_{ms} | \phi_m)$ and $f_{\mathbf{r}_k}(r_{kc}, r_{ks})$, $m \neq k$, are given by (7.5.91) and (7.5.92), respectively.

$$f_{\mathbf{r}_m}(r_{mc}, r_{ms} | \phi_m) = \frac{1}{2\pi\sigma^2} e^{-\frac{(r_{mc} - \sqrt{\epsilon_s} \cos \phi_m)^2 + (r_{ms} - \sqrt{\epsilon_s} \sin \phi_m)^2}{2\sigma^2}} \quad (7.5.91)$$

and for $k \neq m$,

$$f_{\mathbf{r}_k}(r_{kc}, r_{ks}) = \frac{1}{2\pi\sigma^2} e^{-\frac{(r_{kc}^2 + r_{ks}^2)}{2\sigma^2}}. \quad (7.5.92)$$

When the carrier phase is not known at all by the receiver, it is assumed that ϕ_m has a uniform PDF which is called the **least favorable** PDF for ϕ_m .

By substituting $f_{\phi_m}(\phi_m) = \begin{cases} \frac{1}{2\pi}, & 0 \leq \phi_m \leq 2\pi, \\ 0, & \text{otherwise,} \end{cases}$ into the R.H.S. of (7.5.99a) and (7.5.99b), we obtain

$$\begin{aligned} \int_0^{2\pi} f_{\mathbf{r}_m}(r_{mc}, r_{ms} | \phi_m) f_{\phi_m}(\phi_m) d\phi_m &= \frac{1}{2\pi} \int_0^{2\pi} f_{\mathbf{r}_m}(r_{mc}, r_{ms} | \phi_m) d\phi_m \\ &= \frac{1}{2\pi\sigma^2} e^{-\frac{r_{mc}^2 + r_{ms}^2 + \mathcal{E}_s}{2\sigma^2}} \frac{1}{2\pi} \int_0^{2\pi} e^{\frac{\sqrt{\mathcal{E}_s} r_{mc} \cos \phi_m + r_{ms} \sin \phi_m}{\sigma^2}} d\phi_m \quad \text{for } m=1, 2. \end{aligned} \quad (7.5.100)$$

Note that

$$\frac{1}{2\pi} \int_0^{2\pi} e^{\frac{\sqrt{\mathcal{E}_s} r_{mc} \cos \phi_m + r_{ms} \sin \phi_m}{\sigma^2}} d\phi_m = I_0 \left(\frac{\sqrt{\mathcal{E}_s} (r_{mc}^2 + r_{ms}^2)}{\sigma^2} \right) \quad (7.5.101)$$

where $I_0(x)$ is the modified Bessel function of order zero.

The modified Bessel function of order zero $I_0(x)$ is a monotonically increasing function as shown in Figure 7.48.

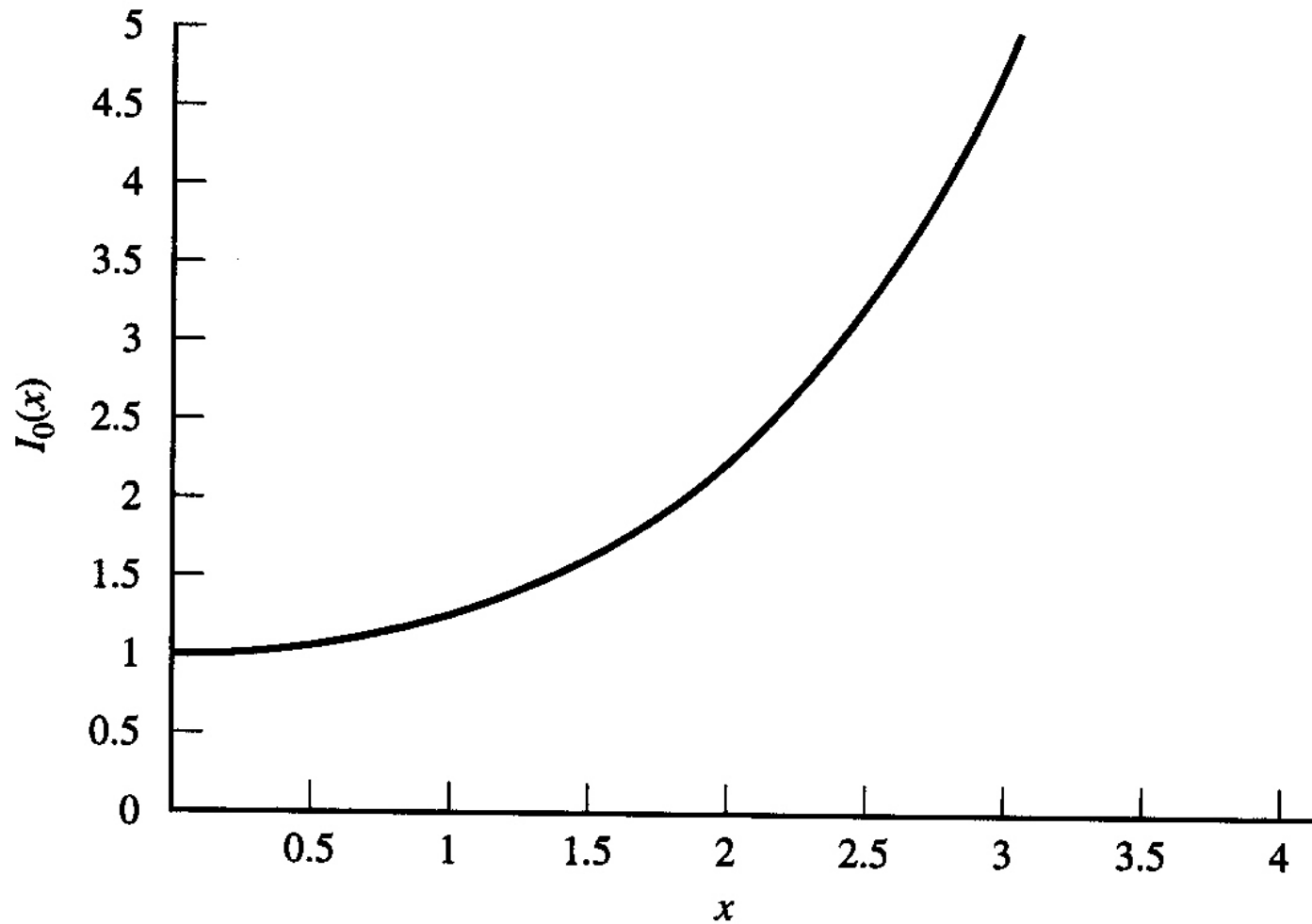


Figure 7.48 Bessel function of order zero $I_0(x)$.

The modified Bessel function of order zero $I_0(x)$ has the power series expansion

$$I_0(x) = \sum_{k=0}^{\infty} \frac{x^{2k}}{2^{2k} (k!)^2}. \quad (\text{This equation is not to appear again in the text.}) \quad (7.5.102)$$

From (7.5.101), (7.5.99a), (7.5.99b), it becomes

$$f_{\mathbf{r}}(\mathbf{r} | \mathbf{s}_1) = \frac{1}{2\pi\sigma^2} e^{-\frac{r_c^2 + r_s^2 + \varepsilon_s}{2\sigma^2}} I_0\left(\frac{\sqrt{\varepsilon_s}(r_{1c}^2 + r_{1s}^2)}{\sigma^2}\right) \cdot \frac{1}{2\pi\sigma^2} e^{-\frac{(r_{2c}^2 + r_{2s}^2)}{2\sigma^2}} \quad (7.5.102-1a)$$

and

$$f_{\mathbf{r}}(\mathbf{r} | \mathbf{s}_2) = \frac{1}{2\pi\sigma^2} e^{-\frac{(r_c^2 + r_s^2)}{2\sigma^2}} \cdot \frac{1}{2\pi\sigma^2} e^{-\frac{r_{2c}^2 + r_{2s}^2 + \varepsilon_s}{2\sigma^2}} I_0\left(\frac{\sqrt{\varepsilon_s}(r_{2c}^2 + r_{2s}^2)}{\sigma^2}\right). \quad (7.5.102-1b)$$

From (7.5.97), (7.5.98), (7.5.102-1a), and (7.5.102-1b), the likelihood ratio is given by

$$\Lambda(\mathbf{r}) = \frac{I_0\left(\frac{\sqrt{\varepsilon_s}(r_{1c}^2 + r_{1s}^2)}{\sigma^2}\right)}{I_0\left(\frac{\sqrt{\varepsilon_s}(r_{2c}^2 + r_{2s}^2)}{\sigma^2}\right)} \stackrel{s_1}{>} \frac{P(\mathbf{s}_2)}{P(\mathbf{s}_1)}. \quad (7.5.103)$$

Thus, the optimum detector computes the two envelopes $r_1 = \sqrt{r_{1c}^2 + r_{1s}^2}$ and $r_2 = \sqrt{r_{2c}^2 + r_{2s}^2}$ and the corresponding values of the Bessel function $I_0\left(\frac{\sqrt{\epsilon_s} r_1^2}{\sigma^2}\right)$ and $I_0\left(\frac{\sqrt{\epsilon_s} r_2^2}{\sigma^2}\right)$ to obtain the likelihood ratio.

Then, the likelihood ratio is compared with the threshold $\frac{P(\mathbf{s}_2)}{P(\mathbf{s}_1)}$ to determine which signal was transmitted.

When the two signals are equi-probable, the threshold becomes unity and, due to the monotonicity of the Bessel function, the optimum detector rule simplifies to

$$\sqrt{r_{1c}^2 + r_{1s}^2} \underset{s_2}{\overset{s_1}{>}} \sqrt{r_{2c}^2 + r_{2s}^2}. \quad (7.5.104)$$

That is, for an equi-probable signal set, the optimum detector makes a decision based on the two envelopes $r_1 = \sqrt{r_{1c}^2 + r_{1s}^2}$ and $r_2 = \sqrt{r_{2c}^2 + r_{2s}^2}$ and, hence, it is called an **envelope detector**.

Note that in this detector the carrier signal phases $\{\phi_m\}$ is irrelevant in the decision about which signal was transmitted.

Equivalently, the decision is based on the squared envelopes r_1^2 and r_2^2 , in which case the detector is called a **square-law-detector**.

Figure 7.49 shows the block diagram of the noncoherent demodulator and the square-law detector for equiprobable BFSK signals.

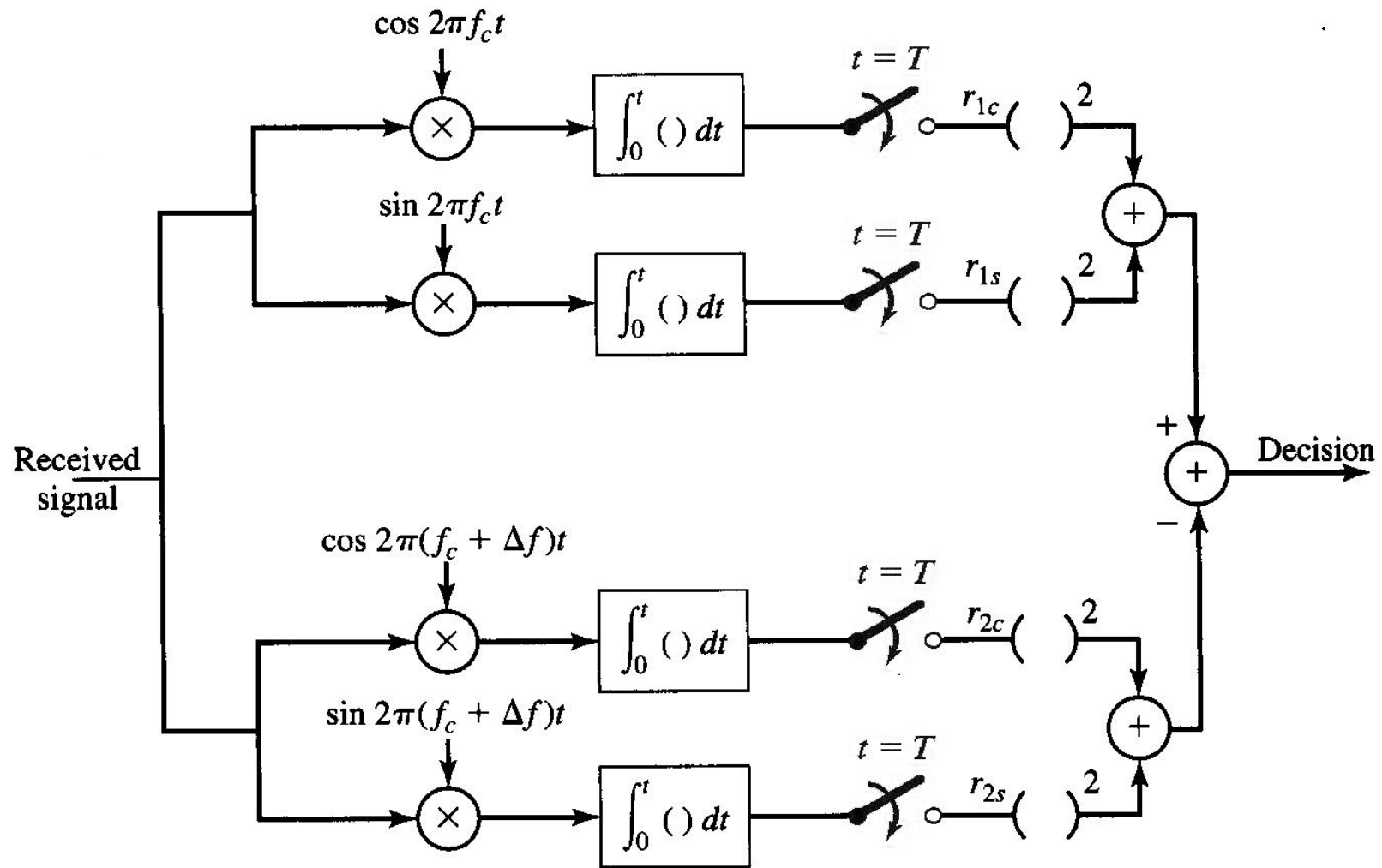


Figure 7.49 Noncoherent demodulation and square-law detection for equiprobable binary FSK signals.

The generalization of the optimum demodulator and detector to M -ary orthogonal FSK signals is straightforward.

As shown in Figure 7.47, the output of the optimum demodulator at the sampling instant consists of the $2M$ vector components $r_{1c}, r_{1s}, r_{2c}, r_{2s}, \dots, r_{Mc}, r_{Ms}$.

Then, the optimum noncoherent detector computes the M envelopes given by

$$r_m = \sqrt{r_{mc}^2 + r_{ms}^2}, \quad m = 1, 2, \dots, M. \quad (7.5.105)$$

Thus, the unknown carrier phases of the received signals are irrelevant to the decision as to which signal was transmitted.

When all the M signals are equi-probable, the optimum detector selects the signal corresponding to the largest envelope (or squared envelope).

In the case of non-equiprobable transmitted signals, the optimum detector must compute the M a posteriori probabilities in (7.5.93) and then select the signal corresponding to the largest posterior probability.

7.6 Probability of Error for Signal Detection in Additive White Gaussian Noise

Assume that the channel has additive white Gaussian noise.

7.6.1 Probability of Error for Binary Modulation

Consider binary PAM baseband signals, where the two **antipodal** signals are 1 and $s_2(t) = -g_T(t)$,

where $g_T(t)$ is an arbitrary pulse which is nonzero in the interval $0 \leq t \leq T_b$ and zero elsewhere and has the energy per bit ε_b .

PAM signals are represented geometrically as one-dimensional vectors.

For binary PAM, the signal points are $s_1 = \sqrt{\varepsilon_b}$ and $s_2 = -\sqrt{\varepsilon_b}$ as shown in Figure 7.50.

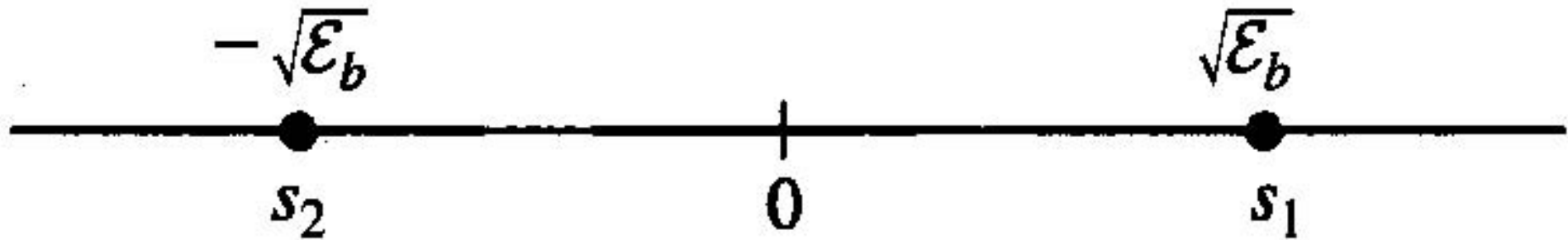


Figure 7.50 Signal points for antipodal signals (binary PAM).

Assume that the two signals are equi-probable .

Then, the received signal from the (matched filter or correlation-type) demodulator is given by

$$\begin{aligned} r &= s_1 + n \\ &= \sqrt{\epsilon_b} + n \end{aligned} \tag{7.6.1}$$

where n represents the additive Gaussian noise component which has zero mean and variance $\sigma_n^2 = \frac{N_0}{2}$.

The decision rule based on the correlation metric given by (7.5.44) compares r with the threshold 0 .

If $r > 0$ the decision is made that $s_1(t)$ was transmitted, and if $r < 0$ the decision is made that $s_2(t)$ was transmitted.

The conditional PDFs of r are given by

$$f(r | s_1) = \frac{1}{\sqrt{\pi N_0}} e^{-(r - \sqrt{E_b})^2 / N_0} \quad (7.6.2)$$

$$f(r | s_2) = \frac{1}{\sqrt{\pi N_0}} e^{-(r + \sqrt{E_b})^2 / N_0} . \quad (7.6.3)$$

These two conditional PDFs are shown in Figure 7.51.

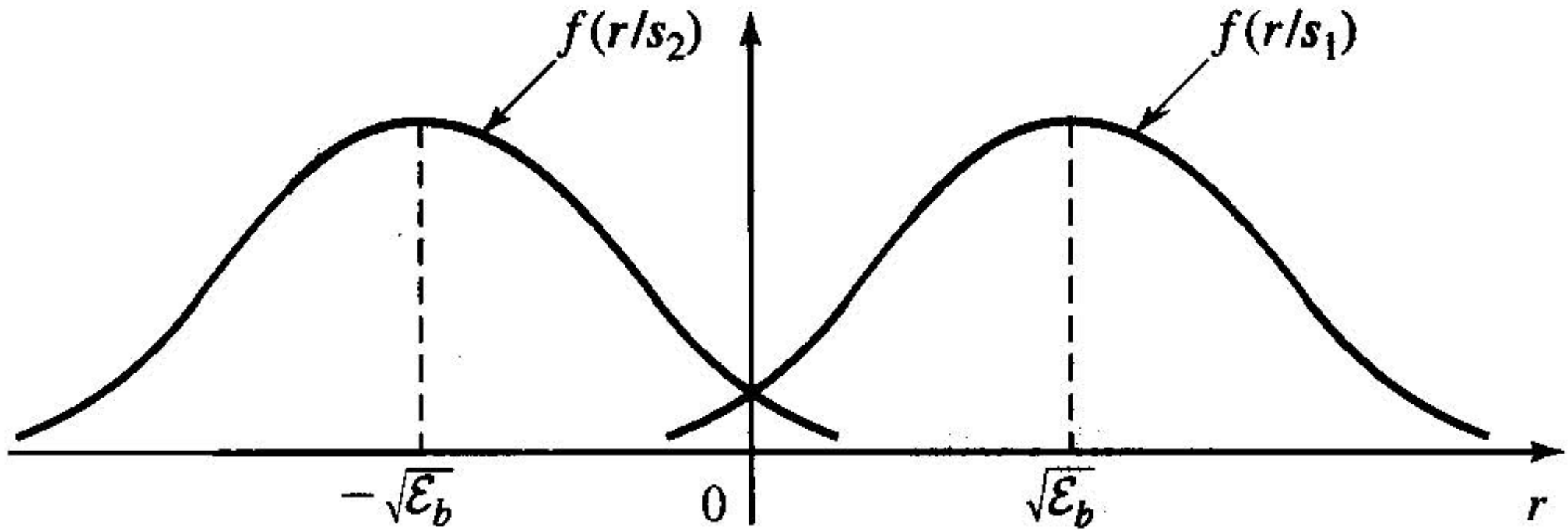


Figure 7.51 Conditional PDF's of two signals.

Given that $s_1(t)$ was transmitted, the probability of error is simply the probability that $r < 0$; that is,

$$P(e | s_1) = \int_{-\infty}^0 p(r | s_1) dr \quad (7.6.4)$$

$$= \frac{1}{\sqrt{\pi N_0}} \int_{-\infty}^0 e^{-(r - \sqrt{\mathcal{E}_b})^2 / N_0} dr \quad (7.6.5)$$

$$= \frac{1}{\sqrt{2\pi}} \int_{-\infty}^{-\sqrt{2\mathcal{E}_b / N_0}} e^{-x^2 / 2} dx \quad (7.6.6)$$

$$= \frac{1}{\sqrt{2\pi}} \int_{\sqrt{2\mathcal{E}_b / N_0}}^{\infty} e^{-x^2 / 2} dx \quad (7.6.7)$$

$$= Q\left(\sqrt{\frac{2\mathcal{E}_b}{N_0}}\right) \quad (7.6.8)$$

where $Q(x)$ is the Q -function.

Similarly, if we assume that $s_2(t)$ was transmitted,

then $r = -\sqrt{\mathcal{E}_b} + n$ and the probability that $r > 0$ is also given by

$$P(e | s_2) = Q\left(\sqrt{\frac{2\mathcal{E}_b}{N_0}}\right).$$

Since the signals $s_1(t)$ and $s_2(t)$ are equi-probable, the average probability of error is given by

$$\begin{aligned} P_b &= \frac{1}{2}P(e | s_1) + \frac{1}{2}P(e | s_2) \\ &= Q\left(\sqrt{\frac{2\varepsilon_b}{N_0}}\right). \end{aligned} \tag{7.6.9}$$

Note that the probability of error depends only on the ratio $\frac{\varepsilon_b}{N_0}$ and not on any other characteristics of the signals and noise.

Also note that $\frac{2\varepsilon_b}{N_0}$ is the output SNR from the matched filter (and correlation-type) demodulator.

The ratio $\frac{\varepsilon_b}{N_0}$ is usually called the **signal-to-noise ratio** (SNR), or SNR/bit.

From Figure 7.50, it is shown that the two signals are separated by the distance $d_{12} = 2\sqrt{\varepsilon_b}$.

By substituting $\varepsilon_b = \frac{d_{12}^2}{4}$ in (7.6.9), the average probability of error is obtained as

$$P_b = Q\left(\sqrt{\frac{d_{12}^2}{2N_0}}\right). \quad (7.6.10)$$

which implies that the probability of error is determined by the distance between the two signals s_1 and s_2 .

(7.6.10) is used for computing the error probability of any binary communication system with two equiprobable messages.

Next, evaluate the error probability for binary orthogonal signals.

Recall the binary PPM is an example of binary orthogonal signaling and the signal vectors s_1 and s_2 are two-dimensional, as shown in Figure 7.52, and are expressed, according to (7.3.8), as

$$\mathbf{s}_1 = (\sqrt{\varepsilon_b}, 0) \quad (7.6.11)$$

$$\mathbf{s}_2 = (0, \sqrt{\varepsilon_b}) \quad (7.6.12)$$

where ε_b denotes the energy for each of the waveforms.

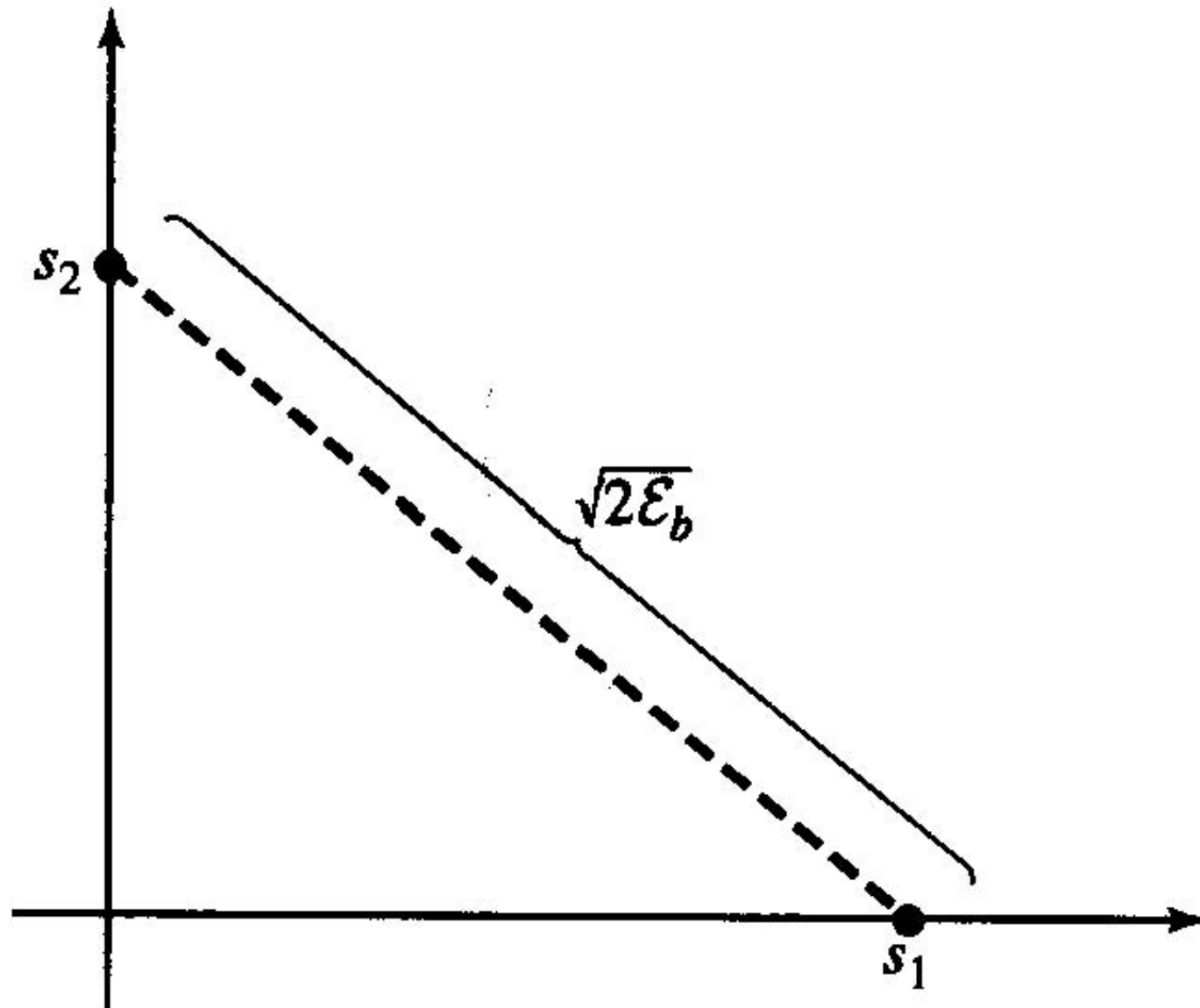


Figure 7.52 Signal points for orthogonal signals.

Note that the distance between the two signal points is $d_{12} = \sqrt{2\varepsilon_b}$.

Assume that \mathbf{s}_1 was transmitted.

Then, the received vector at the output of the demodulator is given by

$$\mathbf{r} = (\sqrt{\varepsilon_b} + n_1, n_2). \quad (7.6.13)$$

From (7.5.44) and (7.6.13), the probability of bit error is given by

$$\begin{aligned} P(e | \mathbf{s}_1) &= P\{C(\mathbf{r}, \mathbf{s}_2) > C(\mathbf{r}, \mathbf{s}_1)\} \\ &= P(2\mathbf{r} \cdot \mathbf{s}_2 - \|\mathbf{s}_2\|^2 > 2\mathbf{r} \cdot \mathbf{s}_1 - \|\mathbf{s}_1\|^2) \\ &= P\{n_2\sqrt{\varepsilon_b} > (\sqrt{\varepsilon_b} + n_1)\sqrt{\varepsilon_b}\} \\ &= P(n_2 - n_1 > \sqrt{\varepsilon_b}). \end{aligned} \quad (7.6.14)$$

Since n_1 and n_2 are zero-mean, statistically independent Gaussian random variables, each with variance

$\frac{N_0}{2}$, the random variable $x = n_2 - n_1$ is zero mean Gaussian with variance N_0 .

Hence, from (7.6.14)

$$\begin{aligned}
 P(e | \mathbf{s}_1) &= P(n_2 - n_1 > \sqrt{\varepsilon_b}) \\
 &= \frac{1}{\sqrt{2\pi N_0}} \int_{\sqrt{\varepsilon_b}}^{\infty} e^{-(n_2 - n_1)^2 / 2N_0} dx \\
 &= \frac{1}{\sqrt{2\pi N_0}} \int_{\sqrt{\varepsilon_b}}^{\infty} e^{-x^2 / 2N_0} dx \tag{7.6.15}
 \end{aligned}$$

$$= \frac{1}{2\pi} \int_{\sqrt{\varepsilon_b} / N_0}^{\infty} e^{-x^2 / 2} dx \tag{7.6.16}$$

$$= Q\left(\sqrt{\frac{\varepsilon_b}{N_0}}\right). \tag{7.6.17}$$

Due to symmetry, the same error probability is obtained when we assume that \mathbf{s}_2 is transmitted, that is,

$$P(e | \mathbf{s}_2) = P(e | \mathbf{s}_1).$$

Hence, the average error probability for binary orthogonal signals is given by

$$P_b = \frac{1}{2} P(e | \mathbf{s}_1) + \frac{1}{2} P(e | \mathbf{s}_2)$$

$$= Q\left(\sqrt{\frac{\varepsilon_b}{N_0}}\right). \quad (7.6.18)$$

Note that orthogonal signals require a factor of two more energy to achieve the same error probability as antipodal signals.

Since $10\log_{10}2 = 3$ dB, we say that antipodal signals are 3-dB better than orthogonal signals.

The difference of 3 dB is simply due to the distance between the two signal points, which is $d_{12}^2 = 2\varepsilon_b$ for orthogonal signals, whereas $d_{12}^2 = 4\varepsilon_b$ for antipodal signals.

The error probability versus $20\log_{10}\frac{\varepsilon_b}{N_0}$ for these two of signal set is shown in Figure 7.53.

In Figure 7.53 it is shown that at any given error probability, the $\frac{\varepsilon_b}{N_0}$ required for orthogonal signals is 3dB more than that for antipodal signals.

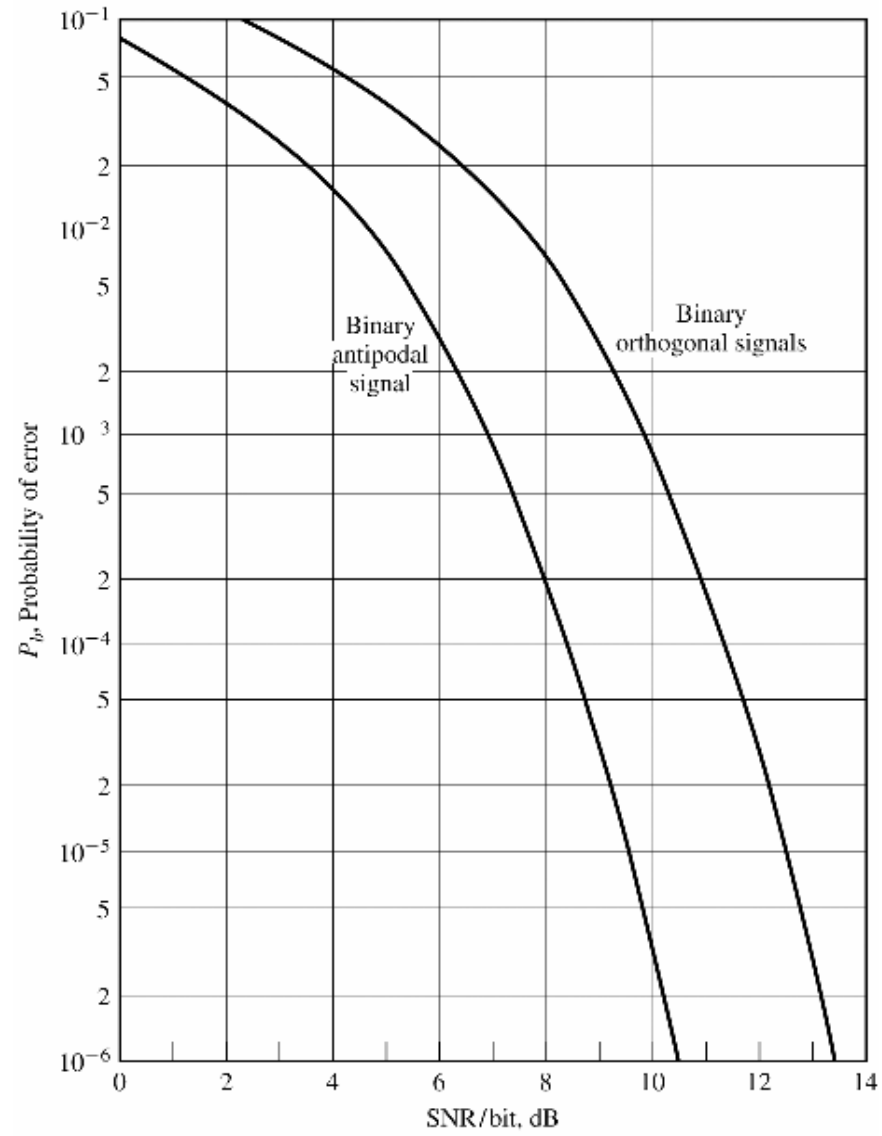


Figure 7.53

Probability of error for binary signals.

7.6.2 Probability of Error for M -ary PAM

Recall that baseband M -ary PAM signals are represented geometrically as M one-dimensional signal points:

$$s_m = \sqrt{\varepsilon_g} A_m, \quad m = 1, 2, \dots, M, \quad (7.6.19)$$

where ε_g is the energy of the basic signal pulse $g_T(t)$ and A_m is the amplitude of the signal given by

$$A_m = (2m - 1 - M), \quad m = 1, 2, \dots, M. \quad (7.6.20)$$

From (7.6.19) and (7.6.20), it is shown that the distance between two adjacent signal points is $2\sqrt{\varepsilon_g}$.

The energy of the m th PAM signal is given by

$$\begin{aligned} \varepsilon_m &= \varepsilon_g A_m^2 \\ &= \varepsilon_g (2m - 1 - M)^2. \end{aligned}$$

Assume that all M signals have equal a priori probability.

Then the average symbol energy is given by

$$\begin{aligned}\varepsilon_{av} &= \sum_{m=1}^M \varepsilon_m P(s_m) \\ &= \frac{1}{M} \sum_{m=1}^M \varepsilon_m\end{aligned}\tag{7.6.21}$$

$$= \frac{\varepsilon_g}{M} \sum_{m=1}^M (2m-1-M)^2\tag{7.6.22}$$

$$= \frac{\varepsilon_g}{M} \frac{M(M^2-1)}{3}\tag{7.6.23}$$

$$= \left(\frac{M^2-1}{3} \right) \varepsilon_g.\tag{7.6.24}$$

Equivalently, the average power is given by

$$\begin{aligned}P_{av} &= \frac{\varepsilon_{av}}{T} \\ &= \left(\frac{M^2-1}{3} \right) \frac{\varepsilon_g}{T}.\end{aligned}\tag{7.6.25}$$

The average probability of error for M -ary PAM is determined from the decision rule which maximizes the correlation metrics given by (7.5.44).

Equivalently, the detector compares the demodulator output r with a set of $M - 1$ thresholds, which are placed at the midpoints of successive two signal points (in the case of an equiprobable signal set), as shown in Figure 7.54.

That is, a decision is made in favor of the amplitude level that is closest to r .

The decision region of each signal point is obtained accordingly. DIY

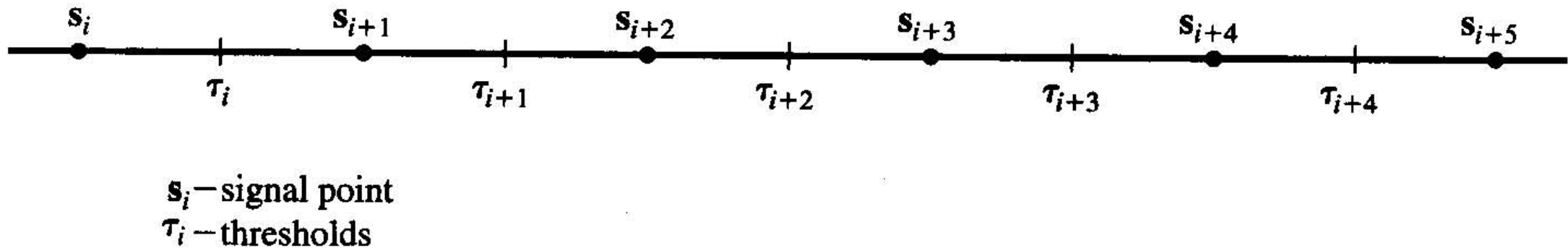


Figure 7.54 Placement of thresholds at midpoints of successive amplitude levels.

Note that if the m th signal is transmitted, the demodulator output is given by

$$\begin{aligned} r &= s_m + n \\ &= \sqrt{\mathcal{E}_g} A_m + n \end{aligned} \tag{7.6.26}$$

where the noise random variable n has zero mean and variance $\sigma_n^2 = \frac{N_0}{2}$.

For an equiprobable signal set, the average probability of symbol error (symbol error probability; ‘average’ can be omitted) is the probability that the noise random variable n exceeds one-half of the distance between levels.

When either of the two far outside levels $\pm(M-1)$ is transmitted, an error can occur in one direction only.

The probability of symbol error for M -ary PAM is given by

$$\begin{aligned} P_M &= P(s_1)P(r - s_1 > \sqrt{\mathcal{E}_g}) + \sum_{m=2}^{M-1} P(s_m)P(|r - s_m| > \sqrt{\mathcal{E}_g}) + P(s_M)P(r - s_M > -\sqrt{\mathcal{E}_g}) \\ &= \frac{1}{M}P(r - s_1 > \sqrt{\mathcal{E}_g}) + (M-2)\frac{1}{M}P(|r - s_m| > \sqrt{\mathcal{E}_g}) + \frac{1}{M}P(r - s_M > -\sqrt{\mathcal{E}_g}) \\ &= \frac{M-1}{M}P(|r - s_m| > \sqrt{\mathcal{E}_g}) \end{aligned} \tag{7.6.27}$$

$$= \frac{M-1}{M} \cdot \frac{2}{\sqrt{\pi N_0}} \int_{\sqrt{\varepsilon_g}}^{\infty} e^{-\frac{x^2}{N_0}} dx \quad (7.6.28)$$

$$= \frac{M-1}{M} \cdot \frac{2}{\sqrt{2\pi}} \int_{\sqrt{2\varepsilon_g/N_0}}^{\infty} e^{-\frac{x^2}{2}} dx \quad (7.6.29)$$

$$= \frac{2(M-1)}{M} Q\left(\sqrt{\frac{2\varepsilon_g}{N_0}}\right). \quad (7.6.30)$$

From (7.6.25), we have

$$\varepsilon_g = \frac{3}{M^2 - 1} P_{av} T. \quad (7.6.31)$$

From (7.6.30) and (7.6.31), the probability of symbol error for M -ary PAM is given by

$$P_M = \frac{2(M-1)}{M} Q\left(\sqrt{\frac{6P_{av} T}{(M^2 - 1)N_0}}\right) \quad (7.6.32)$$

or, equivalently,

$$P_M = \frac{2(M-1)}{M} Q\left(\sqrt{\frac{6\varepsilon_{av}}{(M^2 - 1)N_0}}\right) \quad (7.6.33)$$

where $\varepsilon_{av} = P_{av} T$ is the average energy.

Usually the probability of a symbol error for M -ary signals such as M -ary PAM is plotted with respect to the average SNR/bit.

From (7.6.33) with $T = kT_b$ and $k = \log_2 M$, the probability of symbol error for M -ary PAM is given by

$$P_M = \frac{2(M-1)}{M} Q\left(\sqrt{\frac{6(\log_2 M)\epsilon_{bav}}{(M^2-1)N_0}}\right) \quad (7.6.34)$$

where $\epsilon_{bav} = P_{av}T_b$ is the average bit energy and $\frac{\epsilon_{bav}}{N_0}$ is the average SNR/bit.

Figure 7.55 shows the probability of symbol error as a function of $10\log_{10}\frac{\epsilon_{bav}}{N_0}$ for various values of M .

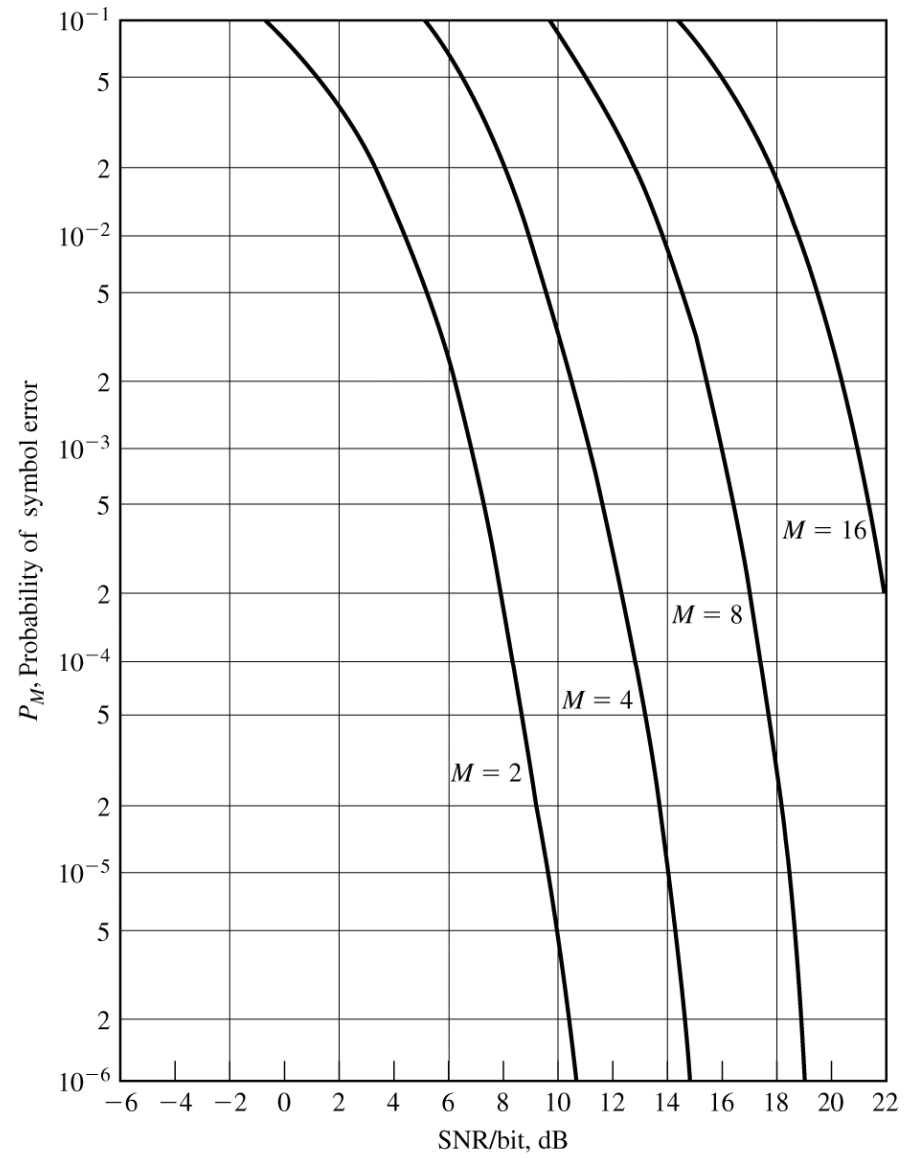


Figure 7.55

Probability of a symbol error for PAM.

Note that when $M = 2$, the probability of symbol error becomes the probability of bit error for binary antipodal signals.

In Figure 7.55 it is shown that the SNR/bit increases by more than 4 dB for every increase of factor of two in M .

It can be shown that the increase of SNR/bit approaches 6 dB as M increases by factor of two when M is large.

Bandpass PAM Signals

In (7.5.60), the input to the detector is given by

$$\begin{aligned} r &= A_m \sqrt{\frac{\mathcal{E}_g}{2}} + n \\ &= s_m + n \end{aligned}$$

where the Gaussian random variable n has mean $E[n] = 0$ and variance

$$\sigma_n^2 = E[n^2]$$

$$\begin{aligned}
 &= \int_0^T \int_0^T E[n(t)n(\tau)]\psi(t)\psi(\tau)dt d\tau \\
 &= \frac{N_0}{2} \int_0^T \psi^2(t)dt \\
 &= \frac{N_0}{2}.
 \end{aligned}$$

Following the derivation for baseband PAM signals, the probability of symbol error for M -ary bandpass PAM is given by

$$P_M = \frac{M-1}{M} P\left(|r - s_m| > \sqrt{\frac{\mathcal{E}_g}{2}}\right) \quad (7.6.35)$$

$$= \frac{2(M-1)}{M} Q\left(\sqrt{\frac{\mathcal{E}_g}{N_0}}\right). \quad (7.6.36)$$

The average symbol energy is given by

$$\mathcal{E}_{av} = P_{av}T \quad (7.6.37)$$

$$= \sum_{m=1}^M \mathcal{E}_m \quad (7.6.38)$$

$$= \frac{\mathcal{E}_g}{2} \sum_{m=1}^M (2m-1-M)^2 \quad (7.6.39)$$

$$= \frac{M^2 - 1}{6} \varepsilon_g. \quad (7.6.40)$$

Hence,

$$\varepsilon_g = \frac{6P_{av}T}{M^2 - 1}. \quad (7.6.41)$$

From (7.6.36) and (7.6.41), the probability of symbol error for M -ary bandpass PAM is obtained as

$$P_M = \frac{2(M-1)}{M} Q\left(\sqrt{\frac{6P_{av}T}{(M^2-1)N_0}}\right) \quad (7.6.42)$$

which is exactly the same result as the probability of symbol error for M -ary PAM over a baseband AWGN channel.

7.6.3 Probability of Error for Phase-Coherent PSK Modulation

Assume that the receiver for M -ary PSK has a perfect estimate of the received carrier phase .

Suppose that the carrier phase of the transmitted signal $u_0(t)$ is 0° and hence, the transmitted signal vector is given by

$$\mathbf{s}_0 = (\sqrt{\mathcal{E}_s}, 0) \quad (7.6.43)$$

and components of the received signal vector $\mathbf{r} = (r_1, r_2)$ are given by

$$\begin{aligned} r_1 &= \sqrt{\mathcal{E}_s} + n_c \\ r_2 &= n_s. \end{aligned} \quad (7.6.44)$$

Since n_c and n_s are jointly Gaussian random variables, r_1 and r_2 are jointly Gaussian random variables with

$$E[r_1] = \sqrt{\mathcal{E}_s}$$

$$E[r_2] = 0$$

and

$$\begin{aligned}\sigma_{r_1}^2 &= \sigma_{r_2}^2 \\ &= \frac{N_0}{2} \\ &= \sigma_r^2.\end{aligned}$$

Consequently, the joint PDF of the received signal vector is given by

$$f_{\mathbf{r}}(r_1, r_2) = \frac{1}{2\pi\sigma_r^2} e^{-\frac{(r_1 - \sqrt{\epsilon_s})^2 + r_2^2}{2\sigma_r^2}}. \quad (7.6.45)$$

We have the phase $\Theta_r = \tan^{-1} \frac{r_2}{r_1}$ as the decision metric.

Express the received vector in polar coordinates to have

$$\begin{aligned}V &= \sqrt{r_1^2 + r_2^2} \\ \Theta_r &= \tan^{-1} \frac{r_2}{r_1}.\end{aligned} \quad (7.6.46)$$

Then, the joint PDF of random variables V and Θ_r is given by

$$f_{V,\Theta_r}(v,\theta_r) = \frac{v}{2\pi\sigma_r^2} e^{-\frac{(v^2 + \varepsilon_s - 2\sqrt{\varepsilon_s} v \cos \theta_r)}{2\sigma_r^2}}. \quad (7.6.47)$$

The marginal probability of the random variable Θ_r is given by

$$\begin{aligned} f_{\Theta_r}(\theta_r) &= \int_0^\infty f_{V,\Theta_r}(v,\theta_r) dv \\ &= \frac{1}{2\pi\sigma_r^2} e^{-\frac{\varepsilon_s - \varepsilon_s \cos^2 \theta_r}{2\sigma_r^2}} \int_0^\infty v e^{-\frac{(v - \sqrt{\varepsilon_s} \cos \theta_r)^2}{2\sigma_r^2}} dv. \end{aligned} \quad (7.6.48)$$

Put $v' = \frac{v}{\sigma_r}$ and $dv' = \frac{1}{\sigma_r} dv$, then (7.6.48) becomes

$$\begin{aligned} f_{\Theta_r}(\theta_r) &= \frac{1}{2\pi\sigma_r^2} e^{-\frac{\varepsilon_s \sin^2 \theta_r}{2\sigma_r^2}} \int_0^\infty \sigma_r v' e^{-\frac{(v' - \frac{\sqrt{\varepsilon_s}}{\sigma_r} \cos \theta_r)^2}{2}} \sigma_r dv' \\ &= \frac{1}{2\pi} e^{-\rho_s \sin^2 \theta_r} \int_0^\infty v' e^{-\frac{(v' - \sqrt{4\rho_s} \cos \theta_r)^2}{2}} dv' \end{aligned} \quad (7.6.49)$$

where $\rho_s = \frac{\mathcal{E}_s}{2\sigma_r^2} = \frac{\mathcal{E}_s}{N_0}$ is the symbol SNR (or SNR/symbol).

Figure 7.56 shows $f_{\Theta_r}(\theta_r)$ for various values of the symbol SNR ρ_s when the transmitted phase is zero.

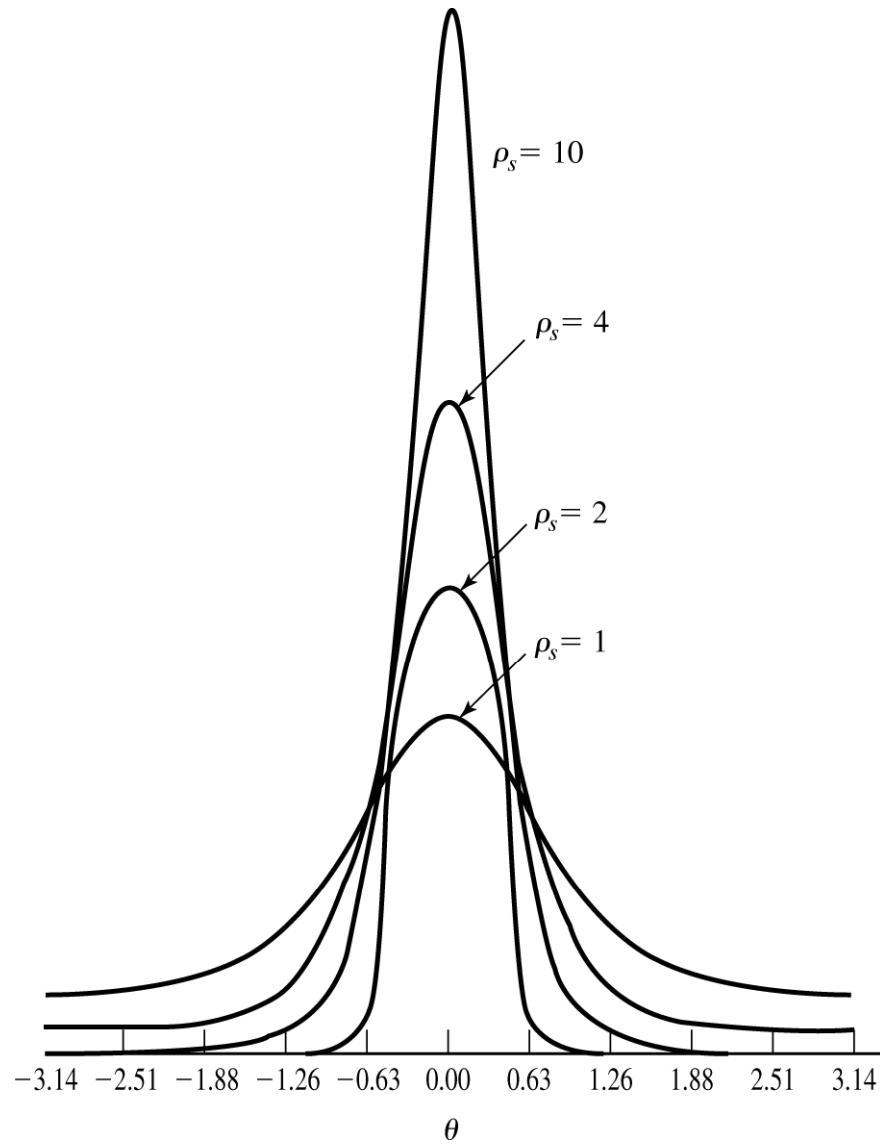


Figure 7.56

Probability density function $p(\theta)$ for $\rho_s = 1, 2, 4, 10$.

In Figure 7.56 it is shown that the curve shape of $f_{\Theta_r}(\theta_r)$ becomes narrower and more peaked about $\theta_r = 0$ as the symbol SNR ρ_s increases.

When the M -ary PSK signal $u_0(t)$ is transmitted, a decision error is made if the noise causes the phase to fall outside the range $-\frac{\pi}{M} \leq \theta_r < \frac{\pi}{M}$.

Hence, the probability of symbol error is given by

$$P_M = 1 - \int_{-\frac{\pi}{M}}^{\frac{\pi}{M}} f_{\Theta_r}(\theta_r) d\theta_r. \quad (7.6.50)$$

which can be evaluated numerically except for $M = 2$ (BPSK) and $M = 4$ (QPSK).

For binary PSK, the two signals $u_0(t)$ and $u_1(t)$ are antipodal.

Hence the bit error probability is given by

$$P_2 = Q\left(\sqrt{\frac{2\mathcal{E}_b}{N_0}}\right). \quad (7.6.51)$$

When $M = 4$ (QPSK), the signal set has two sets of binary PSK signals in phase quadrature.

Assume that the receiver has a perfect estimate of the carrier phase, then there is no crosstalk or interference between the two quadrature carriers.

Hence, the bit error probability for $M = 4$ is identical to that in (7.6.51).

Since two noise components in phase quadrature are independent, the probability of correct decision for a binary antipodal signal set (BPSK) is given by

$$\begin{aligned} P_c &= (1 - P_2)^2 \\ &= \left[1 - Q\left(\sqrt{\frac{2\mathcal{E}_b}{N_0}}\right) \right]^2. \end{aligned} \tag{7.6.52}$$

The symbol error probability for M -ary PSK with $M = 4$ is given by

$$P_4 = 1 - P_c \tag{7.6.53}$$

$$= 2Q\left(\sqrt{\frac{2\mathcal{E}_b}{N_0}}\right) \left[1 - \frac{1}{2}Q\left(\sqrt{\frac{2\mathcal{E}_b}{N_0}}\right) \right]. \tag{7.6.54}$$

For $M > 4$, the symbol error probability P_M is obtained from (7.6.50) by numerical method.

Figure 7.57 shows the symbol error probability for M -ary PSK with respect to the SNR/bit for various values of M .

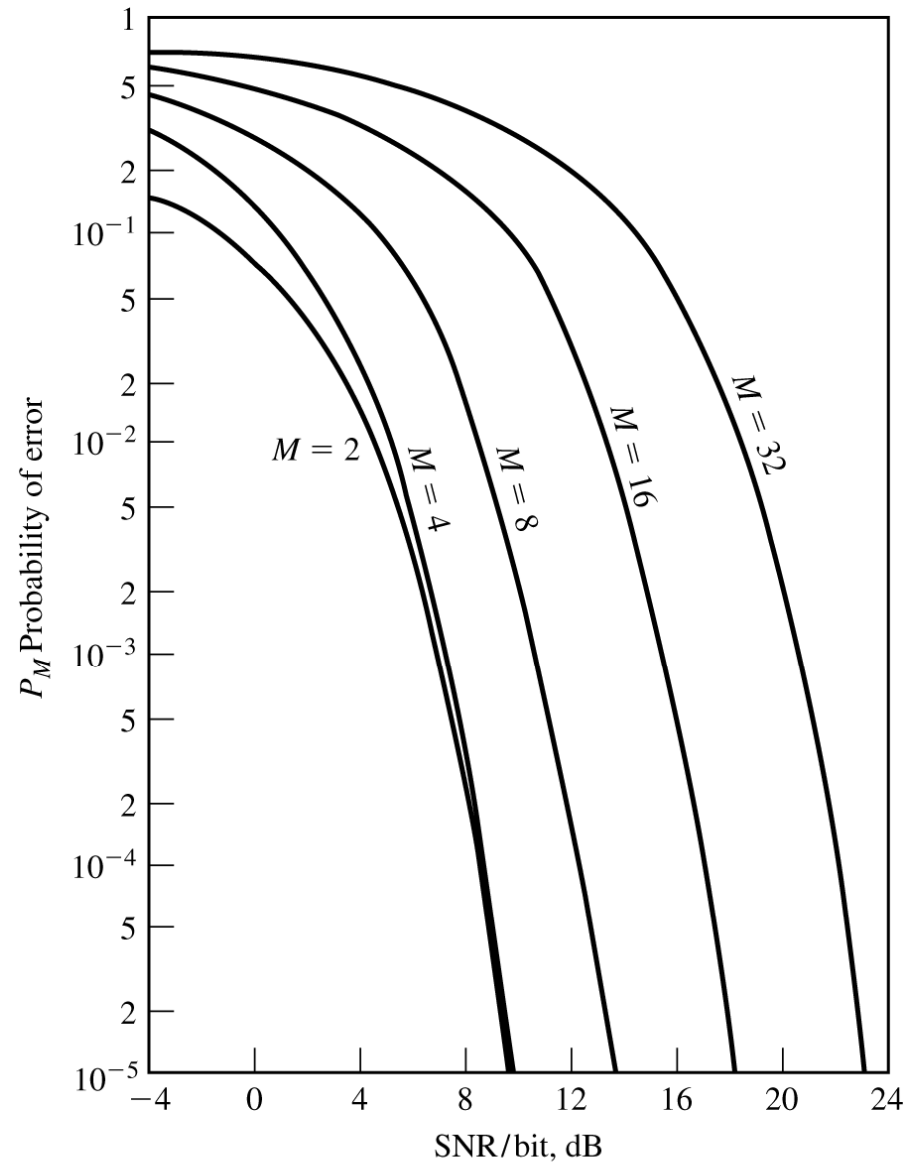


Figure 7.57

Probability of a symbol error for PSK signals.

Figure 7.57 shows that at $P_M = 10^{-5}$ the SNR/bit increases approximately 4 dB as M increase from 4 to 8, and increases approximately 5 dB as M increase from 8 to 16.

For large values of M , doubling M (that is, making phase gap between adjacent signals half) requires an additional 6 dB/bit to achieve the same SNR/bit.

For $\frac{\mathcal{E}_s}{N_0} \gg 1$ and $|\theta_r| \leq \frac{\pi}{2}$, $f_{\Theta_r}(\theta_r)$ of (7.6.49) is approximated as

$$f_{\Theta_r}(\theta_r) \approx \sqrt{\frac{\rho_s}{\pi}} \cos \theta_r e^{-\rho_s \sin^2 \theta_r}. \quad (7.6.55)$$

From (7.6.50) and (7.6.55), the symbol error probability (or symbol error rate) is given by

$$\begin{aligned} P_M &= 1 - \int_{-\frac{\pi}{M}}^{\frac{\pi}{M}} f_{\Theta_r}(\theta_r) d\theta_r \\ &\approx 1 - \int_{-\frac{\pi}{M}}^{\frac{\pi}{M}} \sqrt{\frac{\rho_s}{\pi}} \cos \theta_r e^{-\rho_s \sin^2 \theta_r} d\theta_r. \end{aligned} \quad (7.6.56)$$

Note that the integrand of the integral in R.H.S. is an even function of θ_r .

By putting $u = \sqrt{\rho_s} \sin \theta_r$, (7.6.56) becomes

$$P_M \approx \frac{2}{\sqrt{2\pi}} \int_{\sqrt{2\rho_s} \sin \frac{\pi}{M}}^{\infty} e^{-\frac{u^2}{2}} du \quad (7.6.57)$$

$$= 2Q\left(\sqrt{2\rho_s} \sin \frac{\pi}{M}\right) \quad (7.6.58)$$

$$= 2Q\left(\sqrt{2k\rho_b} \sin \frac{\pi}{M}\right) \quad (7.6.59)$$

where $k = \log_2 M$ and $\rho_s = k\rho_b$.

This approximation to the symbol error probability is valid for all values of M .

For example, the approximation in (7.6.59) gives $P_2 = P_4 = 2Q(\sqrt{2\rho_b})$ for $M = 2$ and $M = 4$

where $\rho_b = \frac{\mathcal{E}_b}{N_0}$, while the exact bit error probability in (7.6.51) gives $P_2 = Q\left(\sqrt{\frac{2\mathcal{E}_b}{N_0}}\right)$ for $M = 2$ (notice the

difference of factor 2) and the exact symbol error probability in (7.6.54) gives

$$P_4 = 2Q\left(\sqrt{\frac{2\mathcal{E}_b}{N_0}}\right) \left[1 - \frac{1}{2}Q\left(\sqrt{\frac{2\mathcal{E}_b}{N_0}}\right)\right] \text{ for } M = 4.$$

The bit error probability for M -ary PSK depends on mapping of each k -bit symbol into a signal phase.

When a Gray code is used in the mapping, two k -bit symbols corresponding to two adjacent signal phases differ in only one bit.

Because the most probable errors due to noise are resulted from the erroneous selection of an adjacent phase to the correct phase, most k -bit symbol errors contain only a single bit error.

Hence, when the noise variance is relatively small, the bit error probability for M -ary PSK is approximated as

$$P_b \approx \frac{1}{k} P_M. \quad (7.6.60)$$

The performance analysis given above applies to phase coherent demodulation (in which the receiver has exact phase estimate for synchronization) with absolute (nor differential) phase mapping of the information into signal phases.

Coherent demodulation of differentially encoded phase-modulated signals has a higher error probability than that for absolute phase encoding.

With differently encoded signals, an error in the detected phase due to noise will frequently cause decoding errors over two consecutive symbol intervals, especially when error probability is below 10^{-1} .

Table 6.1 Illustration of the Differential Encoding Process

k	0	1	2	3	4	5	6	7	8
$\{m_k\}$		1	0	0	1	0	1	1	0
$\{d_{k-1}\}$		1	1	0	1	1	0	0	0
$\{d_k\}$	1	1	0	1	1	0	0	0	1

Therefore, the error probability for differentially encoded M -ary phase modulation is approximately twice that for M -ary phase modulation with absolute phase encoding.

However, a factor-of-2 increase in the error probability corresponds to a relatively small loss in SNR, as can be seen in Figure 7.57.

7.6.4 Probability of Error for DPSK

Consider the evaluation of the error probability of a DPSK demodulator and detector.

The derivation of the exact probability of error for M -ary DPSK is extremely difficult except for $M = 2$, because it is difficult to determine the PDF for the phase of the random variable $r_k r_{k-1}^*$ given by (7.5.77).

$$r_k r_{k-1}^* = \varepsilon_s e^{j(\theta_k - \theta_{k-1})} + \sqrt{\varepsilon_s} e^{j(\theta_k - \phi)} n_{k-1} + \sqrt{\varepsilon_s} e^{-j(\theta_{k-1} - \phi)} n_k + n_k n_{k-1}^*. \quad (7.5.77)$$

However, an approximation to the performance of DPSK is easily obtained, as we now demonstrate.

Suppose the phase difference $\theta_k - \theta_{k-1} = 0$ without loss of generality,.

Furthermore, the exponential factors $e^{j(\theta_k - \phi)}$ and $e^{-j(\theta_{k-1} - \phi)}$ in (7.5.77) can be absorbed into the Gaussian noise components n_{k-1} and n_k , (see Problem 4.29), without changing their statistical properties.

Therefore, $r_k r_{k-1}^*$ in (7.5.77) can be rewritten as

$$r_k r_{k-1}^* = \mathcal{E}_s + \sqrt{\mathcal{E}_s} (n_k + n_{k-1}^*) + n_k n_{k-1}^* \quad (7.6.61)$$

in which the term $n_k n_{k-1}^*$ is small relative to the dominant noise term $\sqrt{\mathcal{E}_s} (n_k + n_{k-1}^*)$ at SNRs of practical interest.

If we neglect the term $n_k n_{k-1}^*$ and normalize $r_k r_{k-1}^*$ by dividing it by $\sqrt{\mathcal{E}_s}$, we obtain a new set of decision metrics given by

$$\begin{aligned} x &= \sqrt{\mathcal{E}_s} + \text{Re}(n_k + n_{k-1}^*) \\ y &= \text{Im}(n_k + n_{k-1}^*). \end{aligned} \quad (7.6.62)$$

The random variables x and y are uncorrelated Gaussian random variables with identical variances

$$\sigma_n^2 = N_0.$$

The phase is given by

$$\Theta_r = \tan^{-1} \frac{y}{x}. \quad (7.6.63)$$

At this stage we have a problem that is identical to the one we solved previously for phase-coherent demodulation and detection.

(The only difference is that the noise variance is now twice as large as in the case of BPSK.

Thus, we can conclude that the performance of binary DPSK is 3-dB poorer than that for BPSK.

However, this result is relatively valid for $M \geq 4$, but is pessimistic for $M = 2$ because the loss in binary DPSK in comparison with binary PSK is less than 3 dB at large SNR.)

In binary DPSK, the two possible transmitted phase differences are zero and π radians.

As a consequence, only the real part of $r_k r_{k-1}^*$ is needed for recovering the information which is given by

$$\text{Re}[r_k r_{k-1}^*] = \frac{1}{2}(r_k r_{k-1}^* + r_k^* r_{k-1}).$$

Because the phase difference between the two successive intervals is zero, an error is made if $\text{Re}[r_k r_{k-1}^*]$ is less than zero.

The probability that $r_k r_{k-1}^* + r_k^* r_{k-1} < 0$ is a special case of a derivation, given in Appendix A, concerned with the probability that a general quadratic form in complex-valued Gaussian random variables is less than zero.

The result for the error probability of binary DPSK is given by

$$P_2 = \frac{1}{2} e^{-\rho_b} \tag{7.6.64}$$

where $\rho_b = \frac{\mathcal{E}_b}{N_0}$ is the SNR/bit.

Figure 7.58 shows the bit error probability for binary DPSK with the bit error probability for binary PSK.

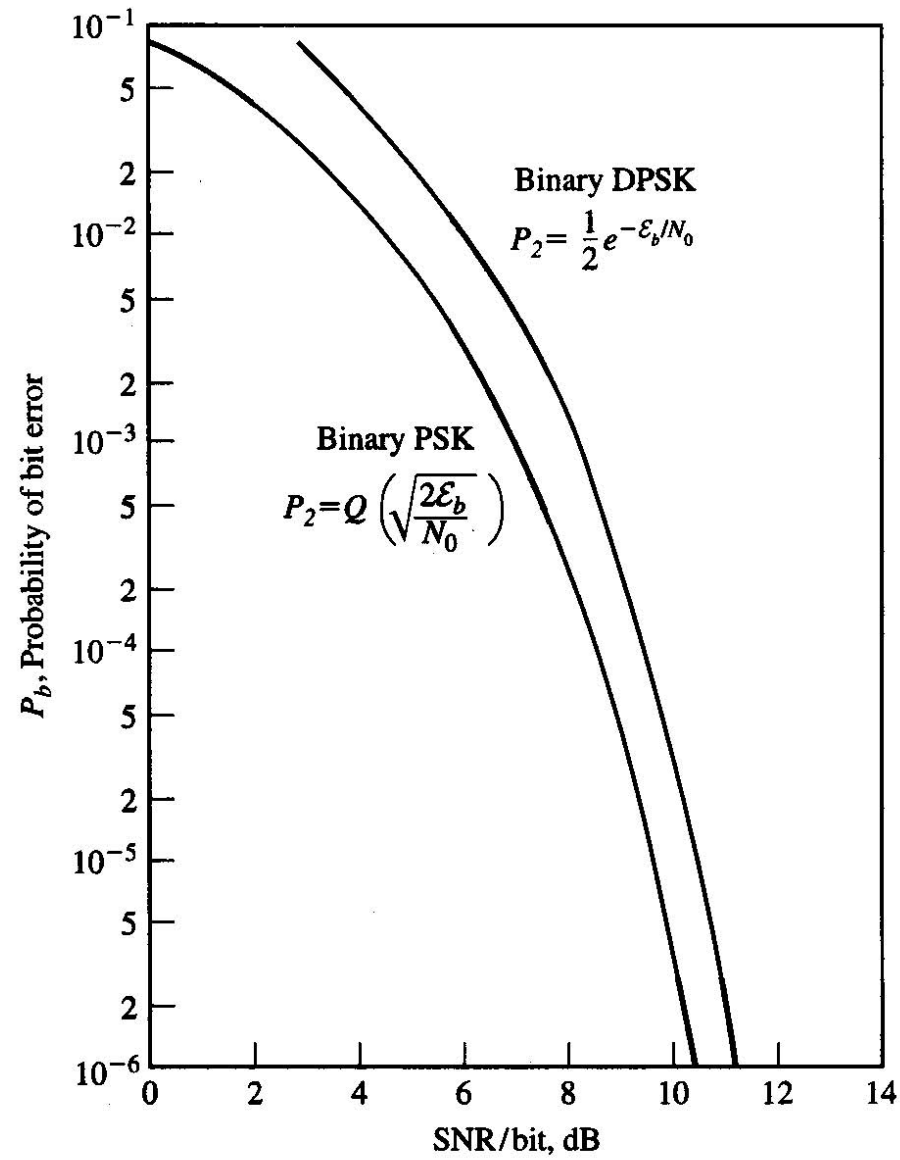


Figure 7.58 Probability of error for binary PSK and DPSK.

In Figure 7.58 it is shown that at bit error probabilities below 10^{-4} the difference in SNR between binary PSK and binary DPSK is less than 1 dB.

7.6.5 Probability of Error for QAM

To determine the probability of error for QAM, we begin with signal sets having $M = 4$ points.

Figure 7.59 shows two signal sets with 4 signals.

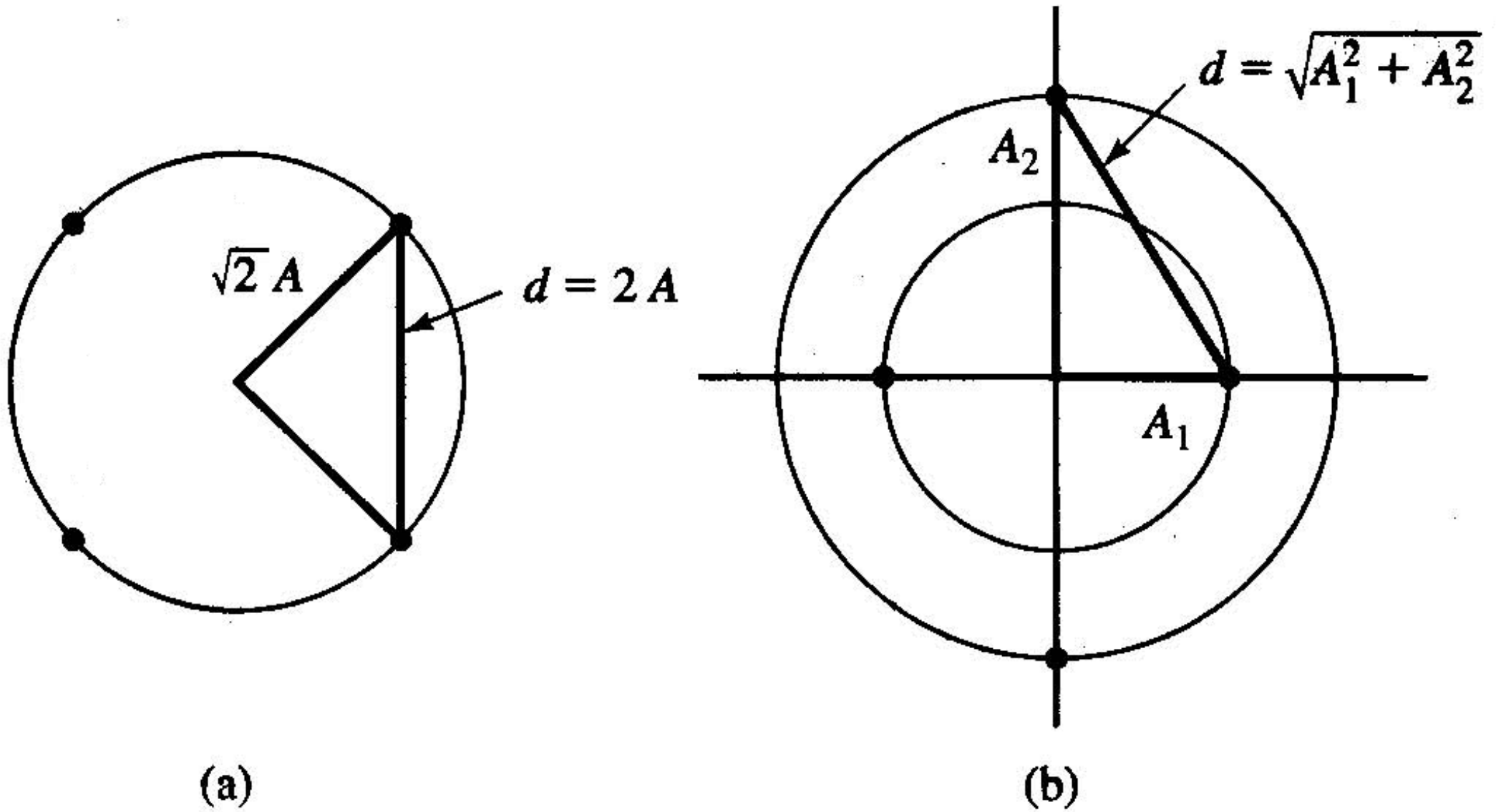


Figure 7.59 Two 4-point signal constellations.

Figure 7.59a) shows a 4-ary PSK (or QPSK) signal set and
Figure 7.59b) shows a QAM signal sets with two amplitude levels, labeled A_1 and A_2 , and four phase.

Assume that all signal points in both signal sets are equi-probable and suppose that the minimum distance $d_{\min} = 2A$ for both signal constellations.

For the 4-ary PSK in Figure 7.59a), the average energy per symbol is given by

$$\begin{aligned}\varepsilon_{av} &= \frac{1}{4} \cdot 4 \cdot (\sqrt{2}A)^2 \\ &= 2A^2.\end{aligned}\tag{7.6.65}$$

For the two-amplitude, four-phase QAM, suppose that we place the signal points on circles of radii A and $\sqrt{3}A$.

Then, $d_{\min} = 2A$, and the average energy per symbol is given by

$$\varepsilon_{av} = \frac{1}{4} \left\{ 2 \cdot A^2 + 2 \cdot (\sqrt{3}A)^2 \right\}$$

$$= 2A^2 \tag{7.6.66}$$

which is the same as for 4-ary PSK.

Since the average energy per symbol and the minimum distance are the same for the two signal sets, their symbol error rate performances are almost the same (the same for all practical applications in which SNR/bit is reasonably high).

In other words, there is no advantage of two-amplitude four-phase QAM over 4-ary PSK.

Consider the four signal constellations of $M = 8$ QAM (or simply 8-QAM) shown in Figure 7.60, each of which consists of two amplitudes and has the minimum distance (distance between two nearest signal points) of $2A$.

Figure 7.60 shows the coordinates (A_{mc}, A_{ms}) for each signal point normalized by A .

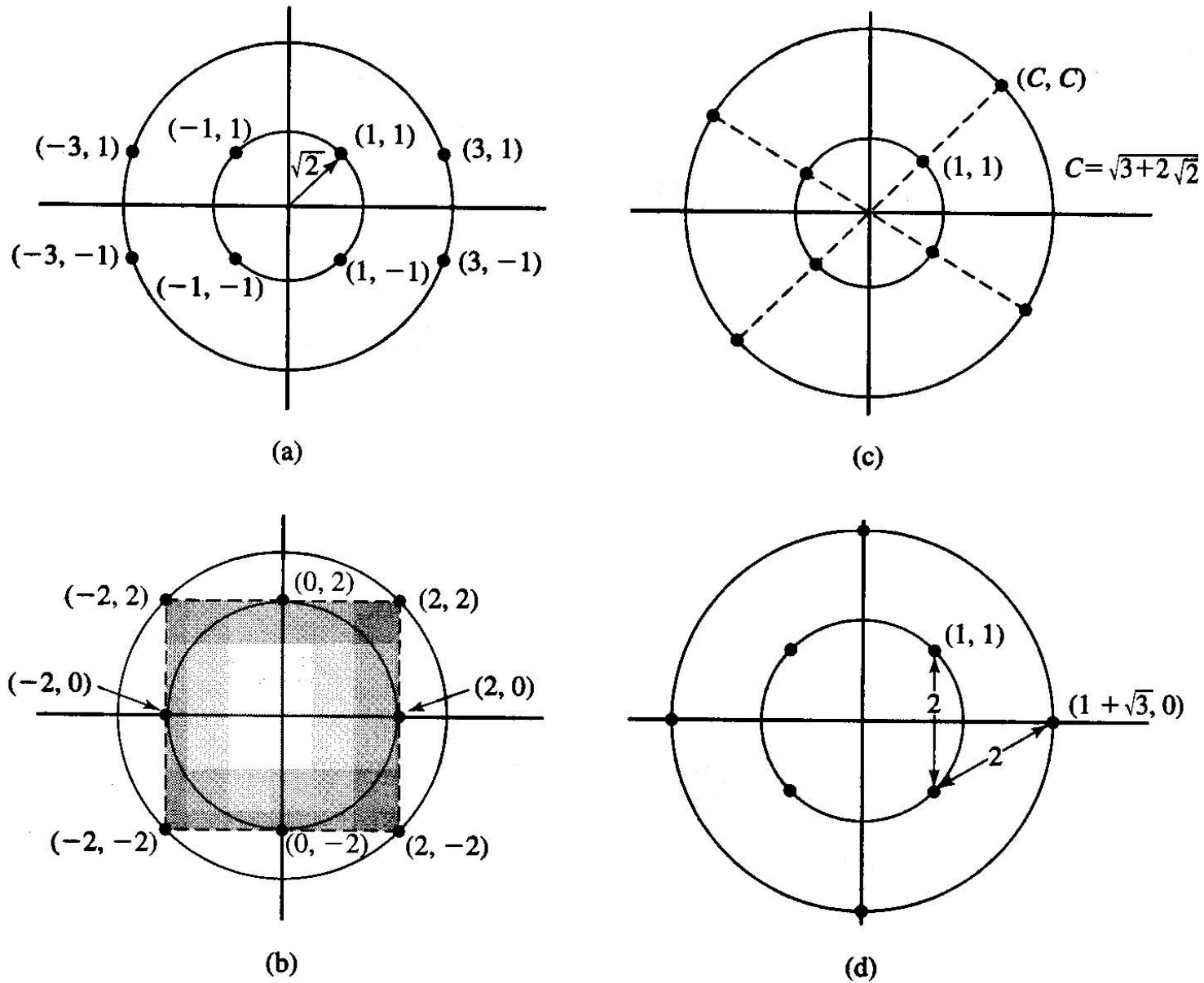


Figure 7.60 Four 8-point QAM signal constellations.

Assuming that the signal points are equi-probable, the average energy per symbol is given by

$$\begin{aligned}\varepsilon_{av} &= \frac{1}{M} \sum_{m=1}^M \frac{1}{2} (A_{mc}^2 + A_{ms}^2) \\ &= \frac{A^2}{2M} \sum_{m=1}^M (a_{mc}^2 + a_{ms}^2)\end{aligned}\tag{7.6.67}$$

where (a_{mc}, a_{ms}) are the coordinates of the signal points normalized by A as shown in Figure 7.60.

The signal sets in Figure 7.60a) and Figure 7.60b) contain signal points that fall on a rectangular grid and have the average energy per symbol $\varepsilon_{av} = 3A^2$.

The signal set in Figure 7.60 c) requires the average energy per symbol $\varepsilon_{av} = 3.41A^2$, and the signal set in Figure 7.60 d) requires $\varepsilon_{av} = 2.37A^2$.

Therefore, the signal set in Figure 7.60 d) requires approximately 1-dB less power (or power) than the signal sets in Figure 7.60 a) and Figure 7.60 b), and 1.6-dB less power than the signal set in Figure 7.60 c) to achieve the same probability of error (that is to have the same minimum distance).

This is why the signal constellation in Figure 7.60 d) is known to be the best 8-QAM constellation.

For $M \geq 16$, there are many more possibilities for selecting the QAM signal points in the two-dimensional space.

Figure 7.61 shows an example of 16-QAM with a circular multi-amplitude constellation where the signal points at a given amplitude level are phase rotated by $\frac{\pi}{4}$ relative to the signal points at adjacent amplitude levels.

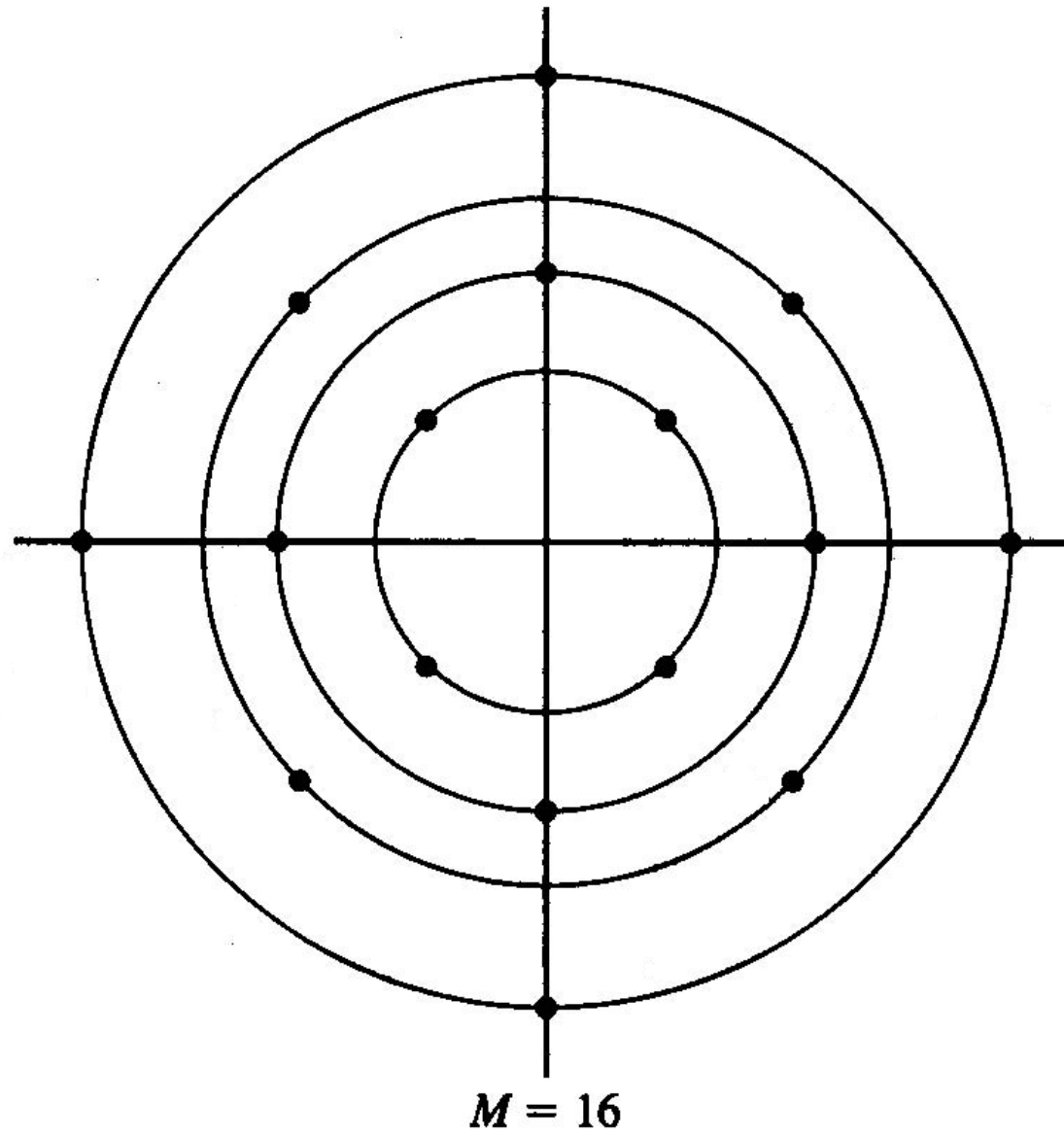


Figure 7.61 Circular 16-point QAM signal constellation.

Although this circular 16-QAM constellation is a generalization of the optimum 8-QAM constellation, it is not the best 16-QAM signal constellation for an AWGN channel.

Rectangular QAM signal constellations have the distinct advantages: 1) being easily generated as two PAM signals impressed on inphase and quadrature carriers, and 2) being easily demodulated as previously described.

Although rectangular QAM signal constellations are not the best M -ary QAM signal constellations for $M \geq 16$, the average symbol energy required to achieve a given minimum distance is only slightly greater than that for the best M -ary QAM signal constellation.

For these reasons, rectangular M -ary QAM constellations are most frequently used in practice.

For rectangular QAM signal constellations in which $M = 2^k$ where k is even, the constellation is equivalent to two PAM constellations on inphase and quadrature carriers, each having $\sqrt{M} = 2^{\frac{k}{2}}$ signal points.

Because the signals in the phase-quadrature components are perfectly separated by coherent detection when $\phi = \hat{\phi}$, the symbol error probability for QAM is easily determined from that for PAM.

The probability of correct decision for the M -ary QAM is given by

$$P_{c, M, \text{QAM}} = (1 - P_{\sqrt{M}, \text{PAM}})^2. \quad (7.6.68)$$

where $P_{\sqrt{M}, \text{PAM}}$ is the symbol error probability for \sqrt{M} -ary PAM with one-half the average power in each quadrature signal of the equivalent QAM.

By appropriately modifying the error probability for M -ary PAM, we obtain

$$P_{\sqrt{M}} = 2 \left(1 - \frac{1}{\sqrt{M}} \right) Q \left(\sqrt{\frac{3}{M-1} \frac{\mathcal{E}_{av}}{N_0}} \right) \quad (7.6.69)$$

where $\frac{\mathcal{E}_{av}}{N_0}$ is the average SNR/symbol.

Therefore, the symbol error probability for the M -ary QAM is given by

$$\begin{aligned} P_{M, \text{QAM}} &= 1 - (1 - P_{\sqrt{M}, \text{PAM}})^2 \\ &= 1 - \left\{ 1 - 2 \left(1 - \frac{1}{\sqrt{M}} \right) Q \left(\sqrt{\frac{3}{M-1} \frac{\mathcal{E}_{av}}{N_0}} \right) \right\}^2. \end{aligned} \quad (7.6.70)$$

(7.6.70) holds for M -ary QAM with $M = 2^k$ when k is even.

When k is odd, there is no equivalent \sqrt{M} -ary PAM system.

The symbol error probability for QAM with rectangular signal constellation is obtained rather easily by categorizing its signals and calculating the error probability for each category of signal, assuming that the optimum detector is employed makes its decisions on the optimum distance metrics given by (7.5.41)

If the optimum detector is employed, the symbol error probability is tightly upper-bounded as

$$\begin{aligned}
 P_M &\leq 1 - \left[1 - 2Q\left(\sqrt{\frac{3\mathcal{E}_{av}}{(M-1)N_0}}\right) \right]^2 \\
 &\leq 4Q\left(\sqrt{\frac{3k\mathcal{E}_{bav}}{(M-1)N_0}}\right)
 \end{aligned} \tag{7.6.71}$$

for any $k \geq 1$, where $\frac{\mathcal{E}_{bav}}{N_0}$ is the average SNR/bit.

Figure 7.62 shows the symbol error probability versus the average SNR/bit.

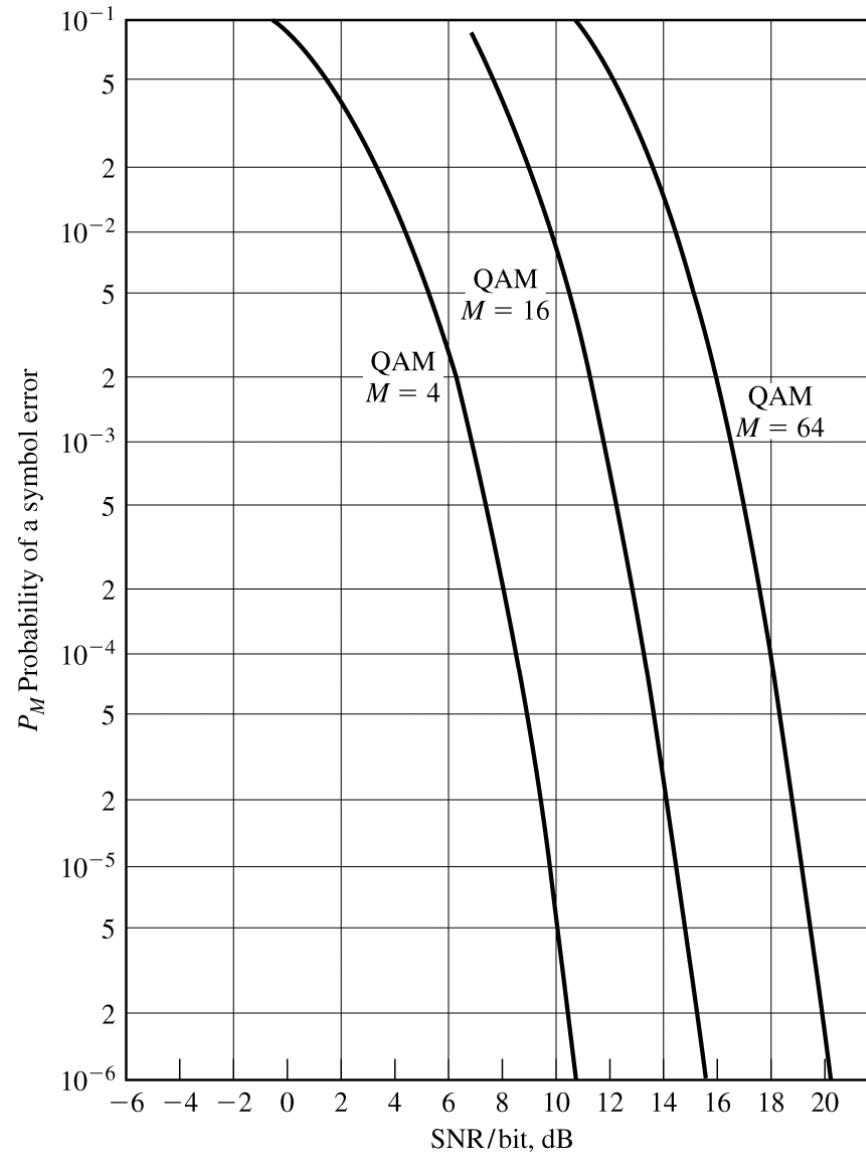


Figure 7.62

Probability of a symbol error for QAM.

Now we compare the symbol error probability of M -ary QAM with that of M -ary PAM, both of which are two-dimensional.

Recall that for M -ary PAM, the symbol error probability is approximated as

$$P_M \approx 2Q\left(\sqrt{2\rho_s} \sin\frac{\pi}{M}\right) \quad (7.6.72)$$

where $\rho_s = \frac{\mathcal{E}_{av}}{N_0}$ is the SNR/symbol.

For M -ary QAM, we may use the expression in (7.6.70).

Because the symbol error probability is dominated by the argument of the Q -function in (7.8.70) and (7.6.7.2), we may simply compare the arguments of Q for the two signal formats.

Thus, the ratio of these two arguments is given by

$$\mathfrak{R}_M = \sqrt{\frac{\frac{3}{M-1}}{2\sin^2 \frac{\pi}{M}}}. \quad (7.6.73)$$

For example, when $M = 4$, we have $\mathfrak{R}_M = 1$.

Hence, we can roughly say that 4-PSK and 4-QAM yield comparable symbol error rate performance for the same SNR/symbol.

On the other hand, when $M > 4$ we find that $\mathfrak{R}_M > 1$, so that M -ary QAM yields better performance than M -ary PSK.

Table 7.1 shows the SNR advantage of QAM over PSK for several values of M .

Table 7.1 SNR advantage of M -ary QAM over M -ary PSK.

M	$10 \log_{10} \mathcal{R}_M$
8	1.65
16	4.20
32	7.02
64	9.95

For example, we observe that 32-QAM has the advantage in SNR of 7-dB over 32-PSK.

7.6.6 Probability of Error for M -ary Orthogonal Signals (FSK with Coherent Detection and PPM)

In PPM, note that all signals have equal symbol energy ε_s .

For equal-energy orthogonal signals, the optimum detector selects the signal resulting in the largest crosscorrelation between the received vector \mathbf{r} and each of the M possible transmitted signal vectors $\{\mathbf{s}_m\}$, that is,

$$\begin{aligned} C(\mathbf{r}, \mathbf{s}_m) &= \mathbf{r} \cdot \mathbf{s}_m \\ &= \sum_{k=1}^M r_k s_{mk}, \quad m = 1, 2, \dots, M. \end{aligned} \tag{7.6.74}$$

Suppose that the signal \mathbf{s}_1 is transmitted.

Then, the received signal vector is given by

$$\mathbf{r} = (\sqrt{\varepsilon_S} + n_1, n_2, n_3, \dots, n_M) \quad (7.6.75)$$

where n_1, n_2, \dots, n_M are mutually independent Gaussian random variables with zero-mean and variance

$$\sigma_n^2 = \frac{N_0}{2}.$$

The outputs from the bank of M correlators are given by

$$C(\mathbf{r}, \mathbf{s}_1) = \sqrt{\varepsilon_S} (\sqrt{\varepsilon_S} + n_1)$$

$$C(\mathbf{r}, \mathbf{s}_2) = \sqrt{\varepsilon_S} n_2$$

⋮

$$C(\mathbf{r}, \mathbf{s}_M) = \sqrt{\varepsilon_S} n_M. \quad (7.6.76)$$

The scale factor $\sqrt{\varepsilon_S}$ can be eliminated from the correlator outputs by dividing each output by $\sqrt{\varepsilon_S}$.

Then, after this normalization, the PDF of the first correlator output ($r_1 = \sqrt{\varepsilon_S} + n_1$) is given by

$$f_{r_1}(x_1) = \frac{1}{\sqrt{\pi N_0}} e^{-\frac{(x_1 - \sqrt{\varepsilon_S})^2}{N_0}} \quad (7.6.77)$$

and the PDFs of the other $M - 1$ correlator outputs are given by

$$f_{r_m}(x_m) = \frac{1}{\sqrt{\pi N_0}} e^{-\frac{x_m^2}{N_0}}, \quad m = 2, 3, \dots, M. \quad (7.6.78)$$

The probability that the detector makes a correct decision is the probability that r_1 is larger than each of the other $M - 1$ correlator outputs n_2, n_3, \dots, n_M which is given by

$$P_c = \int_{-\infty}^{\infty} P(n_2 < r_1, n_3 < r_1, \dots, n_M < r_1) f_{r_1}(r_1) dr_1. \quad (7.6.79)$$

Since the $\{r_m\}$ are independent, the joint probability in (7.6.79) factors into a product of $M - 1$ marginal probabilities of the form

$$\begin{aligned} P(n_m < r_1) &= \int_{-\infty}^{r_1} f_{r_m}(x_m) dx_m, \quad m = 2, 3, \dots, M, \\ &= \frac{1}{\sqrt{2\pi}} \int_{-\infty}^{\sqrt{\frac{2r_1^2}{N_0}}} e^{-\frac{x^2}{2}} dx \\ &= 1 - Q\left(\sqrt{\frac{2r_1^2}{N_0}}\right) \end{aligned} \quad (7.6.80)$$

which are identical for $m = 2, 3, \dots, M$.

From (7.6.79) and (7.6.80), the probability of a correct decision is given by

$$P_c = \int_{-\infty}^{\infty} \left\{ 1 - Q \left(\sqrt{\frac{2r_1^2}{N_0}} \right) \right\}^{M-1} f_{r_1}(r_1) dr_1. \quad (7.6.81)$$

Therefore the symbol error probability is given by

$$P_M = 1 - P_c \quad (7.6.82)$$

$$= \frac{1}{\sqrt{2\pi}} \int_{-\infty}^{\infty} \left\{ 1 - [1 - Q(x)]^{M-1} \right\} e^{-\frac{\left(x - \sqrt{\frac{2\varepsilon_s}{N_0}}\right)^2}{2}} dx. \quad (7.6.83)$$

The same expression for the symbol error probability is obtained, when any of the $M - 1$ signals other than \mathbf{s}_1 is transmitted.

Since all the M signals are equally likely, the average symbol error probability is obtained as the expression for P_M in (7.6.83), which can be evaluated numerically.

In comparing the performance of various digital modulations, it is desirable to have the error probability expressed in terms of the SNR/bit $\frac{\varepsilon_b}{N_0}$, instead of the SNR/symbol $\frac{\varepsilon_s}{N_0}$.

With $M = 2^k$, each symbol conveys k bits of information and energy per symbol is given by $\varepsilon_s = k\varepsilon_b$, where ε_b is energy per bit.

For example, (7.6.83) can be expressed in terms of $\frac{\varepsilon_b}{N_0}$ by substituting $k\varepsilon_b$ for ε_s .

For equiprobable orthogonal signals, all symbol errors are equiprobable and occur with probability given by

$$\frac{P_M}{M-1} = \frac{P_M}{2^k-1}. \quad (7.6.84)$$

Furthermore, there are $\binom{k}{n}$ ways in which n bits out of k bits are in error.

Hence, the average number of bit errors per k -bit symbol is given by

$$\sum_{n=1}^k n \binom{k}{n} \frac{P_M}{2^k - 1} = k \frac{2^{k-1}}{2^k - 1} P_M \quad (7.6.85)$$

and the average bit error probability is just the result in (7.6.85) divided by k , the number of bits/symbol.

Thus,

$$\begin{aligned} P_b &= \frac{2^{k-1}}{2^k - 1} P_M \\ &\approx \frac{P_M}{2}, \quad k \gg 1. \end{aligned} \quad (7.6.86)$$

The probability of a binary digit error as a function of the SNR/bit, ε_b / N_0 , are shown in Figure 7.63 for $M = 2, 4, 8, 16, 32, 64$.

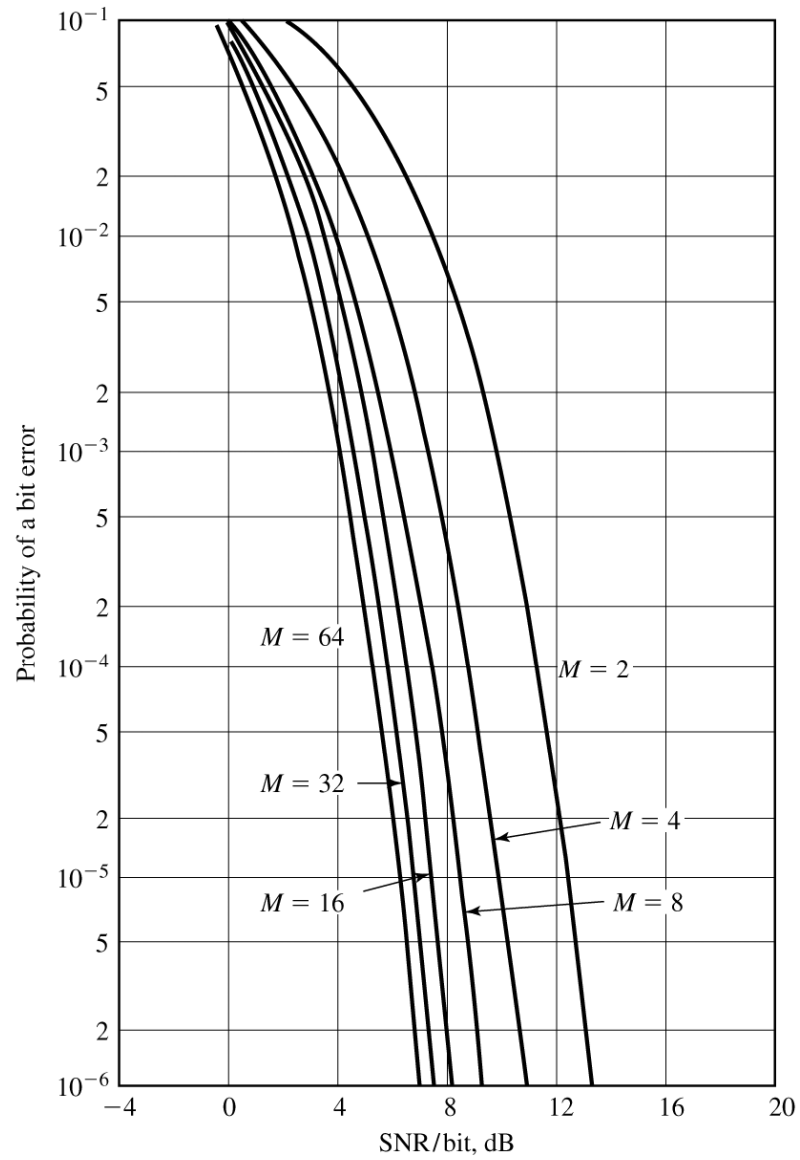


Figure 7.63

Probability of bit error for coherent detection of orthogonal signals.

In Figure 7.63 it is shown that by increasing the number signals M , the SNR/bit required to achieve a given bit error probability is reduced.

For example, to achieve the bit error probability of $P_b = 10^{-5}$, the required SNR/bit is a little more than 12 dB for $M = 2$, but it becomes approximately 6 dB when M is increased to 64 ($k = 6$ bits/symbol), which implies a savings of more than 6 dB (reduction of a factor of 4).

A Union Bound on the Probability of Error.

Since the detector for M orthogonal signals makes $M - 1$ binary decisions between the correlator output $C(\mathbf{r}, \mathbf{s}_1)$ that contains the signal component and the other $M - 1$ correlator outputs $C(\mathbf{r}, \mathbf{s}_m)$, $m = 2, 3, \dots, M$, the symbol error probability is upper-bounded by the **union bound** of the $M - 1$ events.

That is, let E_i denote the event that $C(\mathbf{r}, \mathbf{s}_m) > C(\mathbf{r}, \mathbf{s}_1)$ for $m \neq 1$, then the symbol error probability is bounded by the union bound as

$$P_M = P\left(\bigcup_{i=1}^n E_i\right) \\ \leq \sum_{i=1}^n P(E_i).$$

Hence,

$$P_M \leq (M - 1)P_2 \\ = (M - 1)Q\left(\sqrt{\frac{\mathcal{E}_s}{N_0}}\right) \\ < M Q\left(\sqrt{\frac{\mathcal{E}_s}{N_0}}\right). \tag{7.6.87}$$

This bound can be simplified further by upper-bounding $Q\left(\sqrt{\frac{\mathcal{E}_s}{N_0}}\right)$. From (4.1.7), we have

$$Q\left(\sqrt{\frac{\mathcal{E}_s}{N_0}}\right) < e^{-\frac{\mathcal{E}_s}{2N_0}}. \tag{7.6.88}$$

From (7.6.87) and (7.6.88), the symbol error probability is bounded as

$$\begin{aligned} P_M &< M e^{-\frac{\mathcal{E}_s}{2N_0}} \\ &= 2^k e^{-\frac{k\mathcal{E}_b}{2N_0}} \end{aligned}$$

where $k = \log_2 M$, or equivalently

$$P_M < e^{-\frac{k(\frac{\mathcal{E}_b}{N_0} - 2\ln 2)}{2}}. \quad (7.6.89)$$

As $k \rightarrow \infty$ (or equivalently, as $M \rightarrow \infty$), the symbol error probability approaches zero exponentially, provided that $\frac{\mathcal{E}_b}{N_0}$ is greater than $2\ln 2$, that is,

$$\begin{aligned} \frac{\mathcal{E}_b}{N_0} &> 2 \ln 2 \\ &= 1.39 \text{ (or } 1.42 \text{ dB)}. \end{aligned} \quad (7.6.90)$$

The upper-bound on the symbol error probability in (7.6.89) implies that as long as $\text{SNR} > 1.42$ dB, an arbitrarily small probability of symbol error P_M is achievable.

However, this union-bound is not a very tight upper-bound at a sufficiently small SNR because the upper-bound for the Q -function in (7.6.88) is loose.

By more elaborate bounding techniques, it is shown in Section 9.4 that the upper-bound in (7.6.89) is sufficiently tight for $\frac{\mathcal{E}_b}{N_0} < 4 \ln 2$.

For $\frac{\mathcal{E}_b}{N_0} < 4 \ln 2$, a tighter upper-bound on P_M is given by

$$P_M < 2e^{-k\left(\sqrt{\frac{\mathcal{E}_b}{N_0}} - \sqrt{\ln 2}\right)^2}. \quad (7.6.91)$$

Consequently, $P_M \rightarrow 0$ as $k \rightarrow \infty$, provided that

$$\begin{aligned} \frac{\mathcal{E}_b}{N_0} &> \ln 2 \\ &= 0.693 \text{ (or } -1.6 \text{ dB)}. \end{aligned} \quad (7.6.92)$$

Hence, -1.6 dB is the minimum required SNR/bit to achieve an arbitrarily small probability of error in the

limit as $k \rightarrow \infty$ ($M \rightarrow \infty$).

This is minimum SNR/bit (-1.6 dB) is called the **Shannon limit** for an additive white Gaussian noise channel.

7.6.7 Probability of Error for M -ary Biorthogonal Signals

A set of $M = 2^k$ biorthogonal signals are constructed from $\frac{M}{2}$ orthogonal signals by including the negatives of the orthogonal signals.

Since the demodulator for the M biorthogonal signals requires $\frac{M}{2}$ crosscorrelators or matched filters, whereas the demodulator for M orthogonal signals requires M matched filters or crosscorrelators, the former has a reduced complexity relative to the latter.

Assume that the signal $s_1(t)$ corresponding to the vector $\mathbf{s}_1 = (\sqrt{\varepsilon_s}, 0, 0, \dots, 0)$ was transmitted.

Then, the received signal vector is given by

$$\mathbf{r} = (\sqrt{\varepsilon_s} + n_1, n_2, \dots, n_{\frac{M}{2}}) \quad (7.6.93)$$

where the $\{n_m\}$ are zero-mean, independent and identically distributed (i.i.d.) Gaussian random variables

with variance $\sigma_n^2 = \frac{N_0}{2}$.

The optimum detector decides in favor of the signal corresponding to the largest in magnitude of output from the cross-correlators

$$\begin{aligned}
 C(\mathbf{r}, \mathbf{s}_m) &= \mathbf{r} \cdot \mathbf{s}_m \\
 &= \sum_{k=1}^{M/2} r_k s_{mk}, \quad m = 1, 2, \dots, \frac{M}{2},
 \end{aligned} \tag{7.6.94}$$

while the sign of this largest term is used to decide whether $s_m(t)$ or $-s_m(t)$ was transmitted.

According to this decision rule, the probability of correct decision is equal to the probability that $r_1 = \sqrt{\varepsilon_s} + n_1 > 0$ and r_1 is larger than $|r_m|$ (which is equal to $|n_m|$), $m = 2, 3, \dots, \frac{M}{2}$.

But,

$$\begin{aligned}
 P(r_1 > |n_m| \mid r_1 > 0) &= \frac{1}{\sqrt{\pi N_0}} \int_{-r_1}^{r_1} e^{-\frac{x^2}{N_0}} dx \\
 &= \frac{1}{\sqrt{2\pi}} \int_{-\frac{r_1}{\sqrt{N_0}}}{\frac{r_1}{\sqrt{N_0}}} e^{-\frac{x^2}{2}} dx.
 \end{aligned} \tag{7.6.95}$$

Then, the probability of correct decision is given by

$$\begin{aligned}
 P_c &= \int_0^\infty \left[P(r_1 > |n_m| \mid r_1 > 0) \right]^{\frac{M}{2}-1} f(r_1) dr_1 \\
 &= \int_0^\infty \left[\frac{1}{\sqrt{2\pi}} \int_{-\frac{r_1}{\sqrt{N_0/2}}}^{\frac{r_1}{\sqrt{N_0/2}}} e^{-\frac{x^2}{2}} dx \right]^{\frac{M}{2}-1} f(r_1) dr_1
 \end{aligned} \tag{7.6.95-1}$$

where

$$f_{r_1}(x_1) = \frac{1}{\sqrt{\pi N_0}} e^{-\frac{(x_1 - \sqrt{\varepsilon_s})^2}{N_0}} . \tag{7.6.77}$$

From (7.6.77) and (7.6.95-1), the probability of correct decision is given by

$$P_c = \int_{-\sqrt{\frac{2\varepsilon_s}{N_0}}}^\infty \left[\frac{1}{\sqrt{2\pi}} \int_{-v+\sqrt{\frac{2\varepsilon_s}{N_0}}}^{v+\sqrt{\frac{2\varepsilon_s}{N_0}}} e^{-\frac{x^2}{2}} dx \right]^{\frac{M}{2}-1} e^{-\frac{v^2}{2}} dv \tag{7.6.96}$$

which can be evaluated numerically for various values of M .

Finally, the symbol error probability is obtained as $P_M = 1 - P_c$.

Figure 7.64 shows P_M as a function of $\frac{\mathcal{E}_b}{N_0}$, where $\mathcal{E}_s = k\mathcal{E}_b$, for $M = 2, 4, 8, 16$, and 32 .

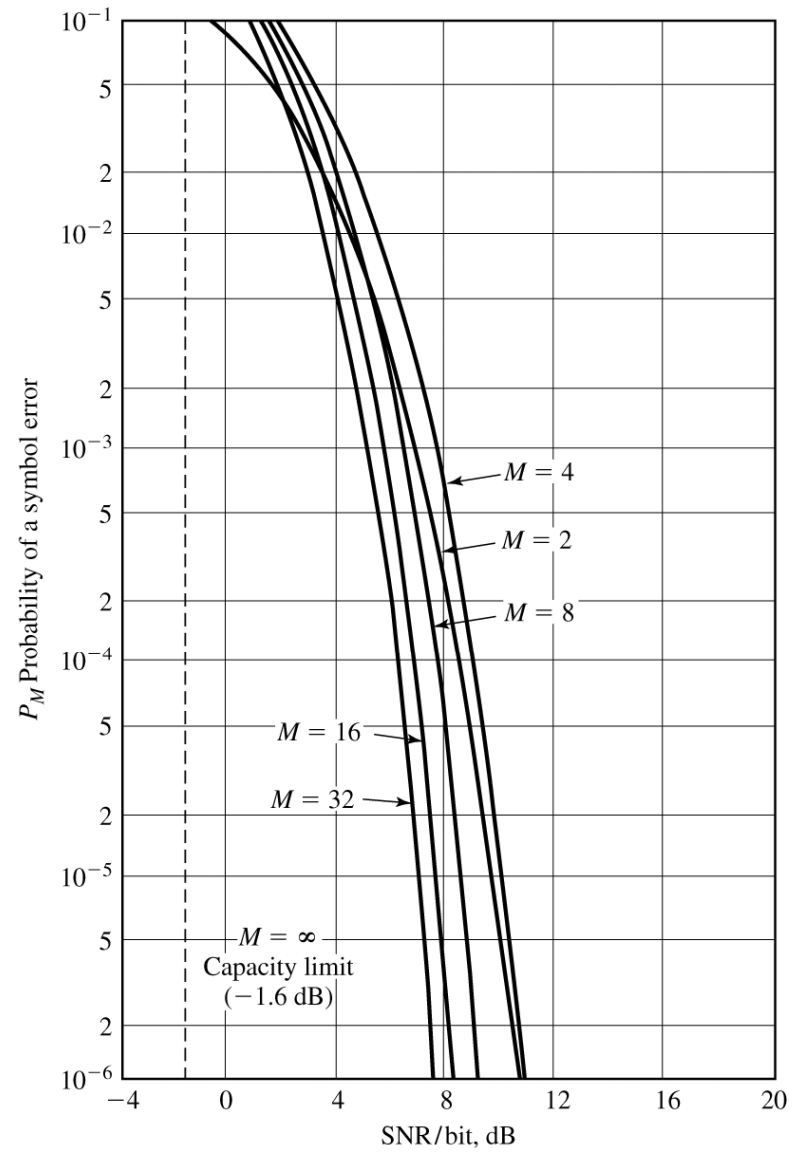


Figure 7.64

Probability of symbol error for biorthogonal signals.

Note that the symbol error probability of biorthogonal signals for $M = 4$ is larger than that for $M = 2$ in Figure 7.64, while the bit error probability of orthogonal signals for $M = 4$ is smaller than that for $M = 2$ in Figure 7.63.

Note that the bit error probability of biorthogonal signals for $M = 4$ is the same as that for $M = 2$. (DIY.)

As in the case of orthogonal signals, as $M \rightarrow \infty$ (or $k \rightarrow \infty$), the minimum required $\frac{\mathcal{E}_b}{N_0}$ to achieve an arbitrarily small probability of error is -1.6 dB, the Shannon limit.

7.6.8 Probability of Error for M -ary Simplex Signals

Simplex signals are a set of M equally correlated signals with mutual crosscorrelation coefficient

$$\gamma_{mn} = -\frac{1}{M-1}.$$

The simplex signal set have the same minimum distance of $\sqrt{2\varepsilon_s}$ between adjacent signal points as the orthogonal signal set having signal energy ε_s in the M -dimensional space, as the former is obtained by translating the latter.

The simplex signal set has the same minimum distance of $\sqrt{2\varepsilon_s}$ with signal energy of $\varepsilon_s \frac{M-1}{M}$, which is less than that of the orthogonal signal set by a factor of $\frac{M-1}{M}$.

Consequently, simplex signals achieve the same error probability as orthogonal signals at a lower SNR of

$$10\log(1 - \gamma_{mn}) = 10\log\frac{M}{M-1} \text{ (in dB)}. \quad (7.6.97)$$

7.6.9 Probability of Error for Noncoherent Detection of FSK

Assume that the M signals are equi-probable. Suppose that $s_1(t)$ was transmitted in the interval $0 \leq t \leq T$.

The M decision metrics at the detector are the M envelopes given by

$$r_m = \sqrt{r_{mc}^2 + r_{ms}^2} \quad m = 1, 2, \dots, M, \quad (7.6.98)$$

where

$$\begin{aligned} r_{1c} &= \sqrt{\mathcal{E}_s} \cos \phi_1 + n_{1c} \\ r_{1s} &= \sqrt{\mathcal{E}_s} \sin \phi_1 + n_{1s} \end{aligned} \quad (7.6.99)$$

and

$$\begin{aligned} r_{mc} &= n_{mc}, \quad m = 2, 3, \dots, M, \\ r_{ms} &= n_{ms}, \quad m = 2, 3, \dots, M. \end{aligned} \quad (7.6.100)$$

The additive noise components $\{n_{mc}\}$ and $\{n_{ms}\}$ are mutually independent zero-mean Gaussian random variables with equal variance $\sigma^2 = \frac{N_0}{2}$.

The PDFs of the random variables at the input to the detector are given by

$$f_{r_1}(r_{1c}, r_{1s}) = \frac{1}{2\pi\sigma^2} e^{-\frac{r_{1c}^2 + r_{1s}^2 + \varepsilon_s}{2\sigma^2}} I_0 \left(\sqrt{\frac{\varepsilon_s (r_{1c}^2 + r_{1s}^2)}{\sigma^2}} \right) \quad (7.6.101)$$

$$f_{r_m}(r_{mc}, r_{ms}) = \frac{1}{2\pi\sigma^2} e^{-\frac{r_{mc}^2 + r_{ms}^2}{2\sigma^2}}, \quad m = 2, 3, \dots, M. \quad (7.6.102)$$

Change variables in (7.6.101) and (7.6.102) by defining the two normalized variables:

$$R_m = \frac{\sqrt{r_{mc}^2 + r_{ms}^2}}{\sigma}$$

$$\Theta_m = \tan^{-1} \frac{r_{ms}}{r_{mc}}. \quad (7.6.103)$$

Then,

$$r_{mc} = \sigma R_m \cos \Theta_m$$

and

$$r_{ms} = \sigma R_m \sin \Theta_m.$$

The Jacobian of this transformation is given by

$$\begin{aligned}
 |\mathbf{J}| &= \begin{vmatrix} \sigma \cos \Theta_m & \sigma \sin \Theta_m \\ -\sigma R_m \sin \Theta_m & \sigma R_m \cos \Theta_m \end{vmatrix} \\
 &= \sigma^2 R_m .
 \end{aligned} \tag{7.6.104}$$

Consequently,

$$f_{R_1, \Theta_1}(R_1, \Theta_1) = \frac{R_1}{2\pi} e^{-\frac{R_1^2 + 2\frac{\mathcal{E}_s}{N_0}}{2}} I_0 \left(\sqrt{\frac{2\mathcal{E}_s}{N_0}} R_1 \right) \tag{7.6.105}$$

$$f_{R_m, \Theta_m}(R_m, \Theta_m) = \frac{R_m}{2\pi} e^{-\frac{R_m^2}{2}}, \quad m = 2, 3, \dots, M . \tag{7.6.106}$$

Finally, by averaging $f_{R_m, \Theta_m}(R_m, \Theta_m)$ over Θ_m , the factor of 2π is (see Problem 4.31) eliminated from (7.6.105) and (7.6.106).

Thus, we find that R_1 has Rician distribution and R_m , $m = 2, 3, \dots, M$, has Rayleigh distribution.

The probability of a correct decision is simply the probability that $R_1 > R_2$ and $R_1 > R_3, \dots$ and $R_1 > R_M$.

That is,

$$\begin{aligned}
 P_c &= P(R_2 < R_1, R_3 < R_1, \dots, R_M < R_1) \\
 &= \int_0^\infty P(R_2 < R_1, R_3 < R_1, \dots, R_M < R_1 | R_1 = x) f_{R_1}(x) dx.
 \end{aligned} \tag{7.6.107}$$

Because the random variables $R_m, m = 2, 3, \dots, M$, are i.i.d., the joint probability in (7.6.107) conditioned on R_1 factors into a product of $M - 1$ identical terms.

That is,

$$P_c = \int_0^\infty [P(R_2 < R_1 | R_1 = x)]^{M-1} f_{R_1}(x) dx \tag{7.6.108}$$

where

$$\begin{aligned}
 P(R_2 < R_1 | R_1 = x) &= \int_0^x f_{R_2}(r_2) dr_2 \\
 &= 1 - e^{-\frac{x^2}{2}}.
 \end{aligned} \tag{7.6.109}$$

The $(M - 1)$ st power of (7.6.109) is given by

$$\left(1 - e^{-\frac{x^2}{2}}\right)^{M-1} = \sum_{n=0}^{M-1} (-1)^n \binom{M-1}{n} e^{-\frac{nx^2}{2}}.$$

From (7.6.108) and (7.6.110), after integration over x the probability of correct decision is obtained as

$$P_c = \sum_{n=0}^{M-1} (-1)^n \binom{M-1}{n} \frac{1}{n+1} e^{-\frac{n}{n+1}\rho_s} \quad (7.6.111)$$

where $\rho_s = \frac{\mathcal{E}_s}{N_0}$ is the SNR/symbol.

Then, the symbol error probability becomes

$$\begin{aligned} P_M &= 1 - P_c \\ &= \sum_{n=1}^{M-1} (-1)^{n+1} \binom{M-1}{n} \frac{1}{n+1} e^{-\frac{nk\rho_b}{n+1}} \end{aligned} \quad (7.6.112)$$

where $\rho_b = \frac{\mathcal{E}_b}{N_0}$ is the SNR/bit.

For binary FSK ($M = 2$), (7.6.112) reduces to

$$P_2 = \frac{1}{2} e^{-\frac{\rho_b}{2}}. \quad (7.6.113)$$

Note that the performance of noncoherent FSK is 3-dB worse than binary DPSK.

$$\left(\text{Note that } P_2 = \frac{1}{2} e^{-\rho_b} \quad \text{for DPSK.} \right) \quad (7.6.64)$$

For $M > 2$, the bit error probability is given by

$$P_b = \frac{2^{k-1}}{2^k - 1} P_M \quad (7.6.114)$$

which was established in Section 7.6.6.

Figure 7.65 shows the bit error probability for noncoherent detection of orthogonal FSK as function of the SNR/bit ρ_b for $M = 2, 4, 8, 16,$ and 32 .

It is shown that for any given bit error probability the SNR/bit for noncoherent detection of orthogonal FSK decreases as M increases, as for coherent detection of M -ary orthogonal signals (see Section 7.6.6),

It will be shown in Chapter 9 that, in the limit as $M \rightarrow \infty$ (or $k = \log_2 M \rightarrow \infty$), the probability of a bit error P_b can be made arbitrarily small provided that the SNR/bit is larger than the Shannon limit of -1.6 dB.

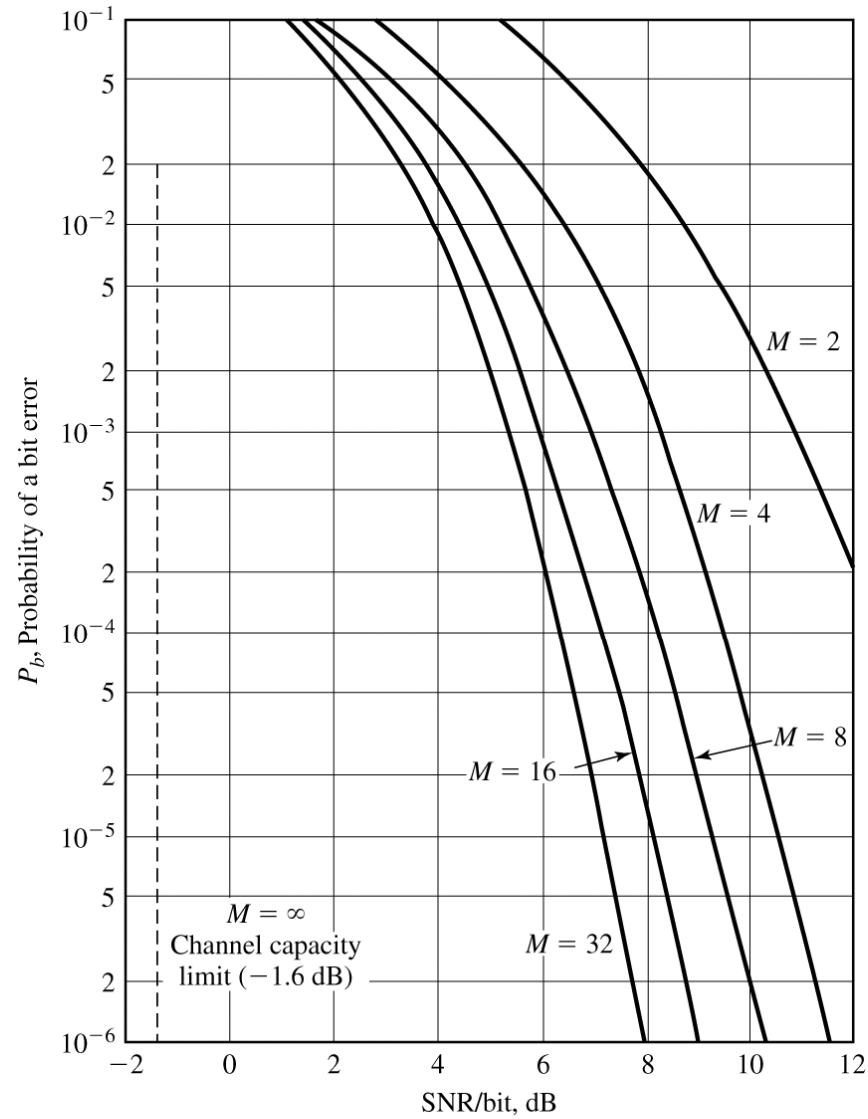


Figure 7.65

Probability of a bit error for noncoherent detection of orthogonal FSK signals.

7.6.10 Comparison of Modulation Methods

Suppose that the bit rate R_b is fixed.

Now we consider the channel bandwidth required to transmit various signals.

For (baseband) M -ary PAM with $M = 2^k$, the channel bandwidth required to transmit the signal is simply the bandwidth of the signal pulse $g_T(t)$, which depends on its waveform and duration.

Assume that a baseband pulse of duration T is $g_T(t)$, the symbol interval is T .

Then, its (half-power) bandwidth W is approximately $\frac{1}{2T}$ (that is, $W_{3dB} \approx \frac{1}{2T}$).

As k information bits are transmitted during one symbol interval, the bit rate is given by

$$R_b = k \cdot \frac{1}{T}.$$

Hence, the (half-power) channel bandwidth required to transmit the M -ary (baseband) PAM signal is given by

$$\begin{aligned} W &= \frac{1}{2T} \\ &= \frac{R_b}{2k} \\ &= \frac{R_b}{2 \log_2 M} \text{ Hz.} \end{aligned} \tag{7.6.115}$$

If the bandpass PAM (or ASK) signal is transmitted as a double-sideband suppressed carrier signal, the required channel bandwidth is twice that for the baseband PAM.

However, the bandwidth of the bandpass PAM (or ASK) signal can be reduced by a factor of two by transmitting only one of the sidebands, either the upper or the lower sideband of the bandpass signal.

Thus, the required channel bandwidth of the single-sideband bandpass PAM signal is exactly the same as the bandwidth of the baseband PAM signal. (However, this is not quite practical, as very sharp filter is required to extract the desired signal.)

For M -ary QAM, the (half-power) channel bandwidth is (approximately) $W = \frac{1}{T}$, but since the information is carried on two quadrature carriers, $R_b = \frac{2k}{T}$, where k is the number of information bits/carrier.

Hence, the (half-power) channel bandwidth required to transmit the M -ary QAM signal is given by

$$\begin{aligned} W &= \frac{1}{T} \\ &= \frac{R_b}{2k} \\ &= \frac{R_b}{2 \log_2 M_{\text{PAM}}} \\ &= \frac{R_b}{\log_2 M_{\text{QAM}}} \end{aligned} \tag{7.6.116}$$

where M_{QAM} is the number of signal points for M -ary QAM which is the square of the number of PAM signals, M_{PAM} .

For M -ary phase modulation (or PSK), the (half-power) channel bandwidth required to transmit the multiphase signals is given by

$$W = \frac{1}{T}$$

where $T = \frac{k}{R_b}$.

Hence, the (half-power) channel bandwidth required to transmit the M -ary PSK signal is given by

$$\begin{aligned} W &= \frac{R_b}{k} \\ &= \frac{R_b}{\log_2 M}. \end{aligned} \tag{7.6.117}$$

Note that PAM, QAM, and PSK signals have the characteristic that, for a fixed bit rate R_b , the channel bandwidth decreases as the number of signal points M increases.

This implies that the system becomes more bandwidth efficient as the number of signal points M increases

In Figures 7.55, 7.57, and 7.62, it is shown that in PAM, QAM, and PSK systems at a given $\frac{\mathcal{E}_b}{N_0}$, the error probability increases as the number of signal points M increases.

It is summarized that the bandwidth efficiency increases as the number of signal points M increases in ASK, QAM, and PSK systems, while their power efficiency decreases.

This is a direct consequence of the fact that the dimensionality of the signal space N is one (for ASK) or two (for PSK and QAM) and is independent of M in PAM, QAM, and PSK systems.

Orthogonal signals have totally different bandwidth requirements.

For (baseband) M -ary PPM signals, the symbol interval T is divided into M subintervals of duration $\frac{T}{M}$ and pulses of width $\frac{T}{M}$ are transmitted in the corresponding subintervals. (Sometimes bit duration is denoted by T_b ($=\frac{T_s}{M}$) where T_s is symbol duration.)

Hence, the (half-power) channel bandwidth required to transmit the (baseband) PPM signal is given by

$$\begin{aligned} W &= \frac{1}{2} \cdot \frac{M}{T} \\ &= \frac{M}{2 \frac{k}{R_b}} \\ &= \frac{M R_b}{2 \log_2 M} \text{ Hz.} \end{aligned}$$

If the bandpass PPM signal is transmitted as a double-sideband suppressed carrier signal, the required channel bandwidth is twice that for the baseband PPM.

For M -ary FSK signals with minimum frequency separation $\Delta f = \frac{1}{2T}$ for orthogonality, the required (half-power) channel bandwidth is given by

$$\begin{aligned} W &= \frac{1}{2T} + \frac{1}{2T}(M-1) + \frac{1}{2T} \\ &= \frac{(M+1)}{2T} \\ &= \frac{(M+1)R_b}{2\log_2 M} \text{ Hz.} \end{aligned}$$

For M -ary FSK signals with minimum frequency separation $\Delta f = \frac{1}{T}$ for orthogonality, the required (half-power) channel bandwidth is given by

$$\begin{aligned} W &= \frac{1}{2T} + \frac{1}{T}(M-1) + \frac{1}{2T} \\ &= \frac{M}{T} \\ &= \frac{M R_b}{\log_2 M} \text{ Hz.} \end{aligned}$$

In the case of biorthogonal signals, the required bandwidth is approximately one-half of that for orthogonal signals. (DIY.)

For orthogonal signals with a fixed R_b , it is shown that the bandwidth increase proportional to $\frac{M}{2\log_2 M}$ as M increases, which implies that the system becomes less bandwidth efficient as the number of signal points M increases

In Figures 7.63 and 7.64 it is shown that, for a fixed $\frac{\mathcal{E}_b}{N_0}$ in orthogonal and biorthogonal signal systems, as the number of signal points M increases, the error probability decreases to improve the power efficiency of the system.

Note that in orthogonal, biorthogonal, and simplex signal systems, the dimensionality of the signal space is not fixed but increases as the number of signal points M increases.

The comparison of the modulation schemes is usually based on the normalized bit rate $\frac{R_b}{W}$ (bps/Hz) versus the SNR/bit $\left(\frac{\mathcal{E}_b}{N_0}\right)$ required to achieve a given error probability.

In summary, we have the normalized bit rates (with half-power bandwidth) as follows

$$\text{(baseband) PAM: } \frac{R_b}{W} = 2\log_2 M_{\text{PAM}} \quad (7.6.118)$$

$$\text{ASK: } \frac{R_b}{W} = \log_2 M_{\text{ASK}} \quad (7.6.118)$$

$$\text{QAM: } \frac{R_b}{W} = \log_2 M_{\text{QAM}} \quad (7.6.119)$$

$$\text{PSK: } \frac{R_b}{W} = \log_2 M_{\text{PSK}} \quad , \quad (7.6.120)$$

Orthogonal signal sets

$$\text{(baseband) PPM: } \frac{R_b}{W} = \frac{2\log_2 M_{\text{PPM}}}{M_{\text{PPM}}} \quad (7.6.121-1)$$

$$\text{FSK (with } \Delta f = \frac{1}{2T} \text{): } \frac{R_b}{W} = \frac{2\log_2 M_{\text{FSK}, \frac{1}{2T}}}{M_{\text{FSK}, \frac{1}{2T}} + 1} \quad (7.6.121-2)$$

$$\text{FSK (with } \Delta f = \frac{1}{T} \text{): } \frac{R_b}{W} = \frac{\log_2 M_{\text{FSK}, \frac{1}{T}}}{M_{\text{FSK}, \frac{1}{T}}} \quad (7.6.121-3)$$

Figure 7.66 shows the normalized bit rate $\frac{R_b}{W}$ (measure of bandwidth efficiency) versus $\left(\frac{\mathcal{E}_b}{N_0}\right)$ (measure of power efficiency) required to achieve $P_M = 10^{-5}$ for (baseband) PAM, QAM, PSK, and orthogonal signals (PPM and FSK with $\Delta f = \frac{1}{2T}$).

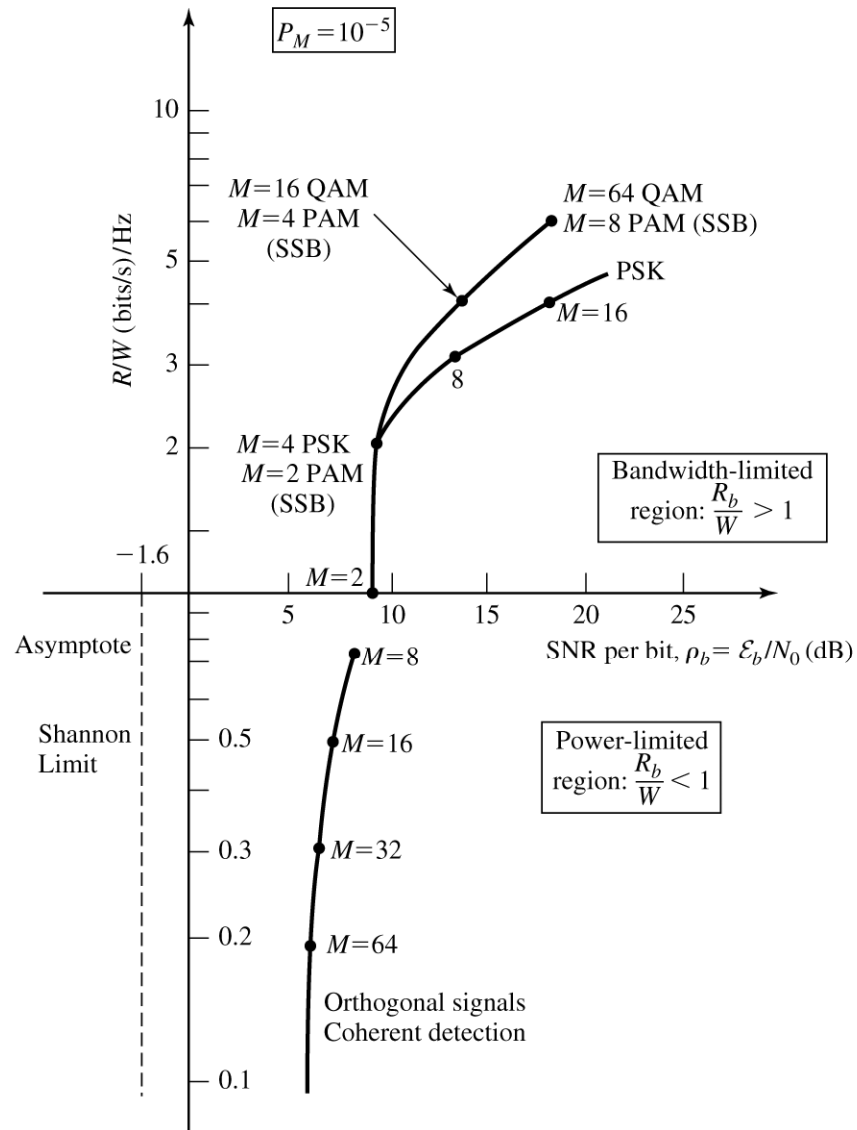


Figure 7.66

Comparison of several modulation methods at 10^{-5} symbol error probability.

In Figure 7.66 it is shown that for (baseband) PAM, QAM, and PSK, increasing the number of signal points M results in a higher bit rate to bandwidth ratio $\frac{R_b}{W}$ at the cost of a increase in the SNR/bit.

Hence, PAM, QAM, and PSK are appropriate for a communication system with the desired bit rate-to-bandwidth ratio $\frac{R_b}{W} > 1$ having a bandwidth-limited channel which has sufficiently high SNR to support multiple amplitudes and phases of the signals.

Be reminded that for PSK the cost of doubling the number of phases (increasing the number of bits per symbol by one bit) is approximately 6 dB (a factor of 4) more transmitted power for large M .

Also be reminded that for QAM the cost of doubling the number of signal points (increasing the number of bits per symbol by one bit) is approximately 3 dB (a factor of 2) more transmitted power.

Hence, QAM (and PAM) is preferable to PSK for a large signal set. (See Table 7.1)

Table 7.2 shows the increase in average power required to maintain a given level of performance for QAM with rectangular constellation, $10\log_2 \frac{M-1}{3}$.

Table 7.2 Relative average power of QAM signal sets.

Number of signal points M	Increase in average power (dB) relative to $M = 2$
4	3
8	6.7
16	10.0
32	13.2
64	16.2
128	19.2

In Figure 7.66, it is shown that an orthogonal signal set yields a normalized bit rate of $\frac{R_b}{W} < 1$, while PAM, QAM, and PSK achieves a normalized bit rate of $\frac{R_b}{W} > 1$

In Figure 7.66, it is shown that, for an orthogonal signal set (baseband PPM), the normalized bit rate $\frac{R_b}{W}$ decreases due to an increase in the required channel bandwidth as the number of signal points M increases, while the SNR/bit required to achieve a given error probability (for example, @ $P_M = 10^{-5}$) decreases.

Hence, an orthogonal signal set, as well as biorthogonal and simplex signal sets, are appropriate for a communication system with a power-limited channel that has sufficiently large bandwidth to accommodate a large number of signals.

In this case, as $M \rightarrow \infty$, the error probability can be made as small as desired, provided that $\frac{\mathcal{E}_b}{N_0} > 0.693$

(or -1.6 dB).

This is the minimum SNR/bit required to achieve reliable transmission in the limit as the channel bandwidth $W \rightarrow \infty$ and the corresponding bit rate-to-bandwidth ratio $\frac{R_b}{W} \rightarrow 0$.

7.7 Performance Analysis for Wireline and Radio Communication Channels

In the transmission of digital signals through an AWGN channel, the performance of the communication system is measured in terms of the probability of error which depends on the received SNR, $\frac{\varepsilon_b}{N_0}$, where

ε_b is the transmitted energy/bit and $\frac{N_0}{2}$ is the power-spectral density of the additive white Gaussian noise.

Hence, the additive noise limits the performance of the communication system.

In addition to the additive noise, another factor that affects the performance of a communication system is channel attenuation.

As all physical channels are lossy, the signal is attenuated as it travels through the channel.

If the transmitted signal is $s(t)$, the received signal is given by

$$r(t) = \alpha s(t) + n(t) \tag{7.7.1}$$

where α is the attenuation factor of the channel.

Then, if the energy in the transmitted signal is ε_b , then the energy of the transmitted signal component in the received signal is given $\alpha^2 \varepsilon_b$ and the received signal has an SNR $\frac{\alpha^2 \varepsilon_b}{N_0}$.

As in an analog communication system, the effect of signal attenuation in a digital communication system is to reduce the energy in the received signal to make the communication system more vulnerable to additive noise.

In analog communication systems, amplifiers called repeaters are used periodically to boost the signal strength in transmission through the channel, which also boost the noise.

In digital communication systems it is possible to detect and regenerate a clean (noise-free) signal

Such devices, called **regenerative repeaters**, are used in wireline and fiber optic communication channels frequently.

7.7.1 Regenerative Repeaters

In the front end of each regenerative repeater, a demodulator/detector that demodulates and detects the transmitted digital information sequence sent by the preceding repeater or the original transmitter.

Once detected, the sequence is passed to the transmitter of the repeater which maps the sequence into a signal that is to be transmitted to the next repeater or the destination.

Since a noise-free signal is regenerated at each repeater, the additive noise does not accumulate.

However, when errors occur in the detector of a repeater, the errors are propagated to the following repeaters in the channel.

Suppose that binary PAM is adopted as a modulation scheme. Then the bit error probability for one hop (signal transmission from one repeater to the next repeater in the chain) is given by

$$P_2 = Q\left(\sqrt{\frac{2\mathcal{E}_b}{N_0}}\right).$$

Assuming that errors occur with low probability in detection, we may ignore the probability that any one bit is detected incorrectly more than once in transmission through a channel with K repeaters.

Then the number of errors will increase linearly with the number of regenerative repeaters K in the channel. Hence, the overall probability of error is approximated as

$$P_b \approx (K + 1)Q\left(\sqrt{\frac{2\mathcal{E}_b}{N_0}}\right). \quad (7.7.2)$$

In contrast, the use of K analog repeaters in the channel reduces the received SNR by $K + 1$.

Hence, the bit error probability is given by

$$P_b = Q\left(\sqrt{\frac{2\mathcal{E}_b}{(K + 1)N_0}}\right). \quad (7.7.3)$$

Since the Q function decreases very fast as its variable increase, the use of regenerative repeaters saves its transmitter power significantly compared with analog repeaters for the same error probability.

Hence, in digital communication systems, regenerative repeaters are preferred.

Ex. 7.7.1

A binary digital communication system transmits data over a wireline channel of length 1000 km.

Repeaters are used every 10 km to offset the effect of channel attenuation.

Determine the $\frac{\mathcal{E}_b}{N_0}$ that is required to achieve a probability of a bit error of 10^{-5} if (1) analog repeaters are employed, and (2) regenerative repeaters are employed.

Solution

The number of repeaters used in the system is $K = 99$.

If regenerative repeaters are used, the $\frac{\mathcal{E}_b}{N_0}$ obtained from (7.7.2) is given by

$$10^{-5} = 100 Q\left(\sqrt{\frac{2\mathcal{E}_b}{N_0}}\right)$$

$$10^{-7} = Q\left(\sqrt{\frac{2\mathcal{E}_b}{N_0}}\right)$$

which yields an $\frac{\mathcal{E}_b}{N_0}$ of approximately 11.3 dB.

If analog repeaters are used, the $\frac{\mathcal{E}_b}{N_0}$ obtained from (7.7.3) is given by

$$10^{-5} = Q\left(\sqrt{\frac{2\mathcal{E}_b}{100N_0}}\right)$$

which yields an $\frac{\mathcal{E}_b}{N_0}$ of 29.6 dB.

Hence, the system with analog repeaters requires $(29.6 - 11.3 =)$ 18.3 dB more transmitted power than the system with regenerative repeaters.

7.7.2 **Link Budget Analysis for Radio Channels** (skipped. To be dealt in a graduate level course titled Wireless and Satellite communications.)

Suppose that a transmitting antenna radiates isotropically in free space at a power level P_T watts, as shown in Figure 7.67.

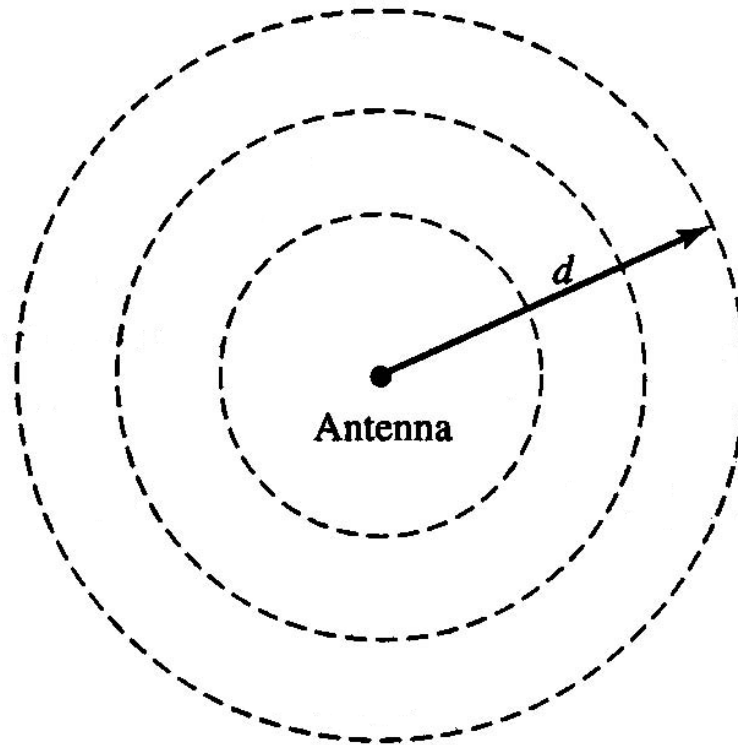


Figure 7.67 Antenna that radiates isotropically in free space.

The power density at a distance d from the antenna is $\frac{P_T}{4\pi d^2}$ W/m².

If the transmitting antenna has directivity in a particular direction, the power density in that direction is increased by a factor called the transmitter **antenna gain** G_T .

Then, the power density at a distance d is $\frac{P_T G_T}{4\pi d^2}$ W/m².

The product $P_T G_T$ is usually called the **effective isotropically radiated power** (EIRP), which is basically the radiated power relative to an isotropic antenna for which $G_T = 1$.

A receiving antenna pointed in the direction of the radiated power gathers a portion of the power that is proportional to its cross-sectional area.

Hence, the received power extracted by the receiving antenna is given by

$$P_R = \frac{P_T G_T A_R}{4\pi d^2} \tag{7.7.4}$$

where A_R is the **effective area of the antenna**.

The basic relationship between the antenna gain and its effective area is given by

$$A_R = \frac{G_R \lambda^2}{4\pi} \text{ m}^2 \quad (7.7.5)$$

where G_R is the receiver antenna gain and λ is the wavelength of the transmitted signal.

From (7.7.45) and (7.7.5) the received power is given by

$$\begin{aligned} P_R &= \frac{P_T G_T G_R}{\left(\frac{4\pi d}{\lambda}\right)^2} \\ &= \frac{P_T G_T G_R}{\mathcal{L}_s} \end{aligned} \quad (7.7.6)$$

where $\mathcal{L}_s = \left(\frac{4\pi d}{\lambda}\right)^2$ is the free-space path loss.

Other losses such as atmospheric losses, which are encountered in the transmission of the signal, are accounted for an additional loss factor \mathcal{L}_a .

Then, the received power is given by

$$P_R = \frac{P_T G_T G_R}{\mathcal{L}_s \mathcal{L}_a} \quad (7.7.7)$$

or, equivalently,

$$P_R |_{\text{dBW}} = P_T |_{\text{dBW}} + G_T |_{\text{dB}} + G_R |_{\text{dB}} - \mathcal{L}_s |_{\text{dB}} - \mathcal{L}_a |_{\text{dB}}. \quad (7.7.8)$$

The effective area for an antenna generally depends on the wavelength λ of the transmitted signal and the physical dimension of the antenna.

For example, a parabolic (dish) antenna of diameter D has an effective area

$$A_R = \frac{\pi D^2}{4} \eta \quad (7.7.9)$$

where $\frac{\pi D^2}{4}$ is the physical area and η is the **illumination efficiency factor**, which is typically in the range

$$0.5 \leq \eta \leq 0.6.$$

From (7.7.5) and (7.7.9) the receiver antenna gain for a parabolic antenna of diameter D is given by

$$\begin{aligned} G_R &= \frac{4\pi}{\lambda^2} A_R \\ &= \eta \left(\frac{\pi D}{\lambda} \right)^2, \quad \text{parabolic antenna.} \end{aligned} \tag{7.7.10}$$

As a second example, a horn antenna of physical area A has an efficiency factor of 0.8, an effective area of $A_R = 0.8A$, and a gain of

$$G_R = \frac{10A}{\lambda^2}, \quad \text{horn antenna.} \tag{7.7.11}$$

Another parameter that is related to the gain (or directivity) of an antenna is its beamwidth Θ_B which is shown in Figure 7.68.

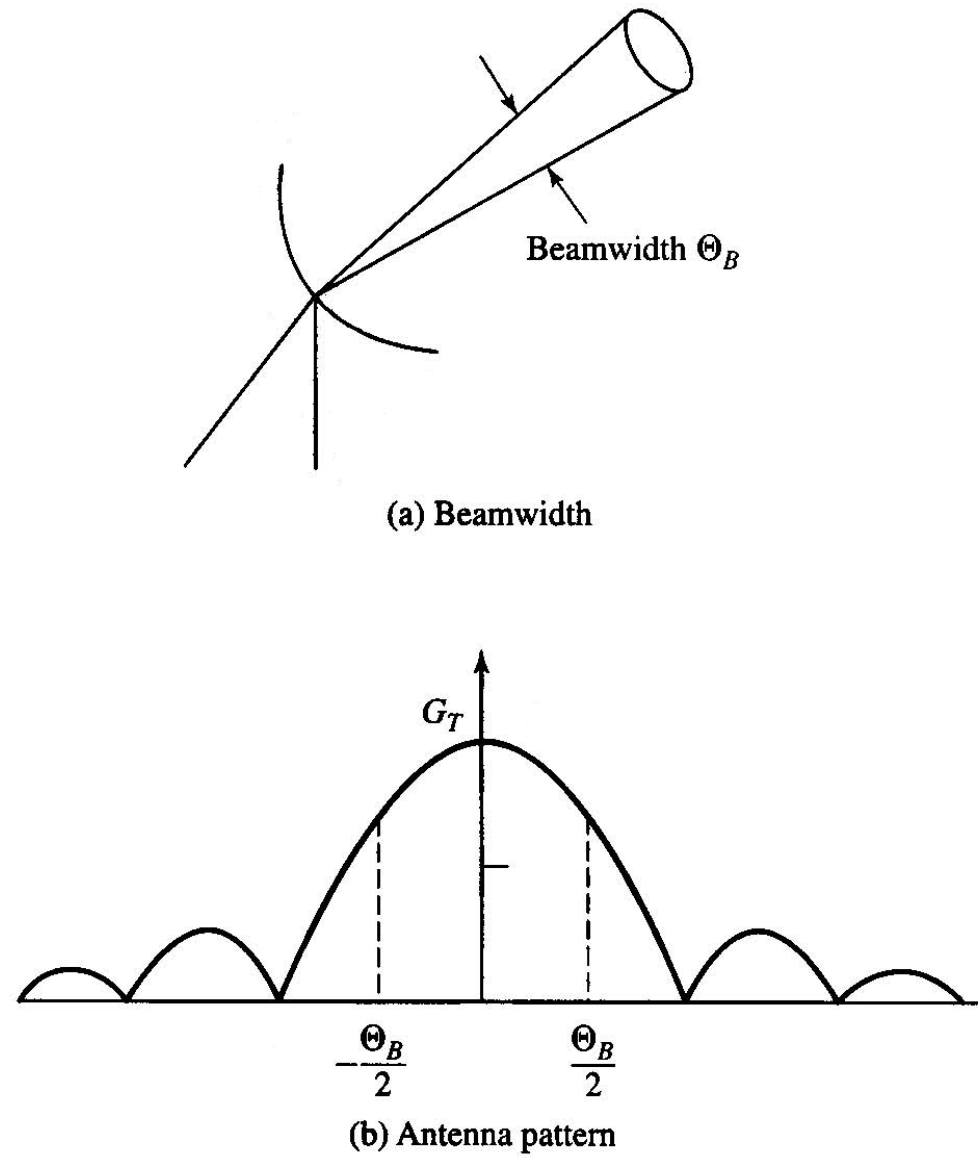


Figure 7.68 A narrow beam antenna and its radiation pattern.

Usually, the beamwidth is measured as the -3 dB width of the antenna pattern.

For example, the -3 dB beamwidth of a parabolic antenna is approximately given by

$$\Theta_B \approx 70 \frac{\lambda}{D} \text{ deg}$$

so that G_T is inversely proportional to Θ_B^2 .

Hence, if the beamwidth is increased by a factor of two which is obtained by doubling the diameter, the antenna gain increases by a factor of four (i.e., 6 dB).

Ex. 7.7.2

A satellite in geosynchronous orbit (36,000 km above the earth's surface) radiates power of 100 W (20 dBW).

The transmitting antenna in the satellite has a gain of 18 dB, so that the EIRP = 38 dBW.

In the downlink (from the satellite to earth station), a signal is transmitted at a frequency of 4 GHz.

The earth station has a 3-meter parabolic antenna with and the **illumination efficiency factor** $\eta = 0.5$.

Determine the received power.

Solution

The wavelength $\lambda = 0.075$ m and distance $d = 36,000$ km.

From (7.7.6), the free-space path loss is given by

$$\begin{aligned}\mathcal{L}_s |_{\text{dB}} &= 20 \log \left(\frac{4\pi d}{\lambda} \right) \\ &= 195.6 \text{ dB}.\end{aligned}$$

From (7.7.10), the receiver antenna gain is given by

$$\begin{aligned}G_R &= \eta \left(\frac{\pi D}{\lambda} \right)^2 \\ &= 0.5 \left(\frac{\pi \cdot 3}{0.075} \right)^2 \\ &= 39 \text{ dB}.\end{aligned}$$

Since no other losses are assumed,

$$\begin{aligned} P_R |_{\text{dB}} &= 20 + 18 + 39 - 195.6 \\ &= -118.6 \text{ dBW}, \end{aligned}$$

or equivalently,

$$P_R = 2.5 \times 10^{-11} \text{ W}.$$

Since,

$$\begin{aligned} \frac{\mathcal{E}_b}{N_0} &= \frac{T_b P_R}{N_0} \\ &= \frac{1}{R_b} \frac{P_R}{N_0}, \end{aligned} \tag{7.7.12}$$

it follows that

$$\frac{P_R}{N_0} = R_b \left(\frac{\mathcal{E}_b}{N_0} \right)_{\text{req}} \tag{7.7.13}$$

where $\left(\frac{\mathcal{E}_b}{N_0} \right)_{\text{req}}$ is the required SNR/bit to achieve the desired performance.

We have

$$10\log_{10} R_b = \left(\frac{P_R}{N_0} \right)_{\text{dB}} - 10\log_{10} \left(\frac{\mathcal{E}_b}{N_0} \right)_{\text{req}} . \quad (7.7.14)$$

Ex. 7.7.3

Suppose that $\left(\frac{\mathcal{E}_b}{N_0} \right)_{\text{req}} = 10 \text{ dB}$.

Determine the bit rate for the satellite communication system in Example 7.7.2.

Assume that the receiver front-end has a noise temperature of 300 K, which is typical for a receiver in the 4 GHz range.

Solution

Since $T_0 = 290 \text{ K}$ and $T_e = 10 \text{ K}$, it follows that

$$\begin{aligned} N_0 &= kT \\ &= 4.1 \times 10^{-21} \text{ W/Hz} \end{aligned}$$

or, equivalently, -203.9 dBW/Hz.

Then,

$$\begin{aligned}\left(\frac{P_R}{N_0}\right)_{\text{dB}} &= -118.6 + 203.9 \\ &= 85.3 \text{ dB/Hz}.\end{aligned}$$

Therefore, from (7.7.14) we obtain

$$\begin{aligned}10\log_{10} R_b &= 85.3 - 10 \\ &= 75.3,\end{aligned}$$

or equivalently,

$$R_b = 33.9 \times 10^6 \text{ bps}$$

which implies that this satellite channel can support a bit rate of 33.9 Mbps.

7.8 Symbol Synchronization

Phase synchronization for both analog and digital communications is obtained in a various way such as PLL.

In a digital communication system, the output of the receiving filter $y(t)$ must be sampled periodically at the symbol rate, at the precise sampling time instants $t_m = mT + \tau_0$, where T is the symbol interval and τ_0 is a time delay that accounts for the propagation time of the signal from the transmitter to the receiver.

To perform this periodic sampling, a clock signal is required at the receiver.

The process of extracting a clock signal at the receiver is called **symbol synchronization** or **timing recovery**.

Note that the receiver must know not only the frequency $\left(\frac{1}{T}\right)$ at which the outputs of the matched filters or correlators are sampled, but also where to take the samples within each symbol interval.

The choice of sampling instant within the symbol interval of duration T is called the **timing phase**.

The best timing phase corresponds to the time instant when the signal output of the receiver filter is a maximum.

In a practical communication system, the receiver clock must be continuously adjusted in frequency $\left(\frac{1}{T}\right)$ and in timing phase τ_0 to compensate for frequency drifts between the oscillators used in the transmitter and receiver clocks so that the sampling time instants of the matched filter or correlator outputs are optimized.

Symbol synchronization is accomplished in various ways.

One method to achieve symbol synchronization is use a master clock signal from a master radio station so that the transmitter and receiver clocks are synchronized to a master clock, which provides a very precise timing signal.

This method is adopted in radio communication systems that operate in the very low frequency (VLF) band (below 30 kHz).

Another method to achieve symbol synchronization is for the transmitter to simultaneously transmit the

pilot signal of clock frequency $\frac{1}{T}$ or a multiple of $\frac{1}{T}$ along with the information signal.

Then the receiver may simply employ a narrowband filter tuned to the pilot signal of clock frequency and, thus, extract the clock signal for sampling.

This method has the advantage of being simple to implement, while it has several disadvantages such as

- 1) the transmitter must allocate some of its available power to the transmission of the pilot signal,
- 2) some small fraction of the available channel bandwidth must be allocated for the transmission of the pilot signal.

Despite of these disadvantages, this method is frequently used in telephone transmission systems which employ large bandwidths to transmit the signals of many users, because the transmitted pilot signal is shared by many users in the demodulation.

Also a clock signal can be extracted from the received data signal so that the receiver could achieve self-synchronization.

Now we consider four approaches to achieve symbol synchronization from the received signal (Sections

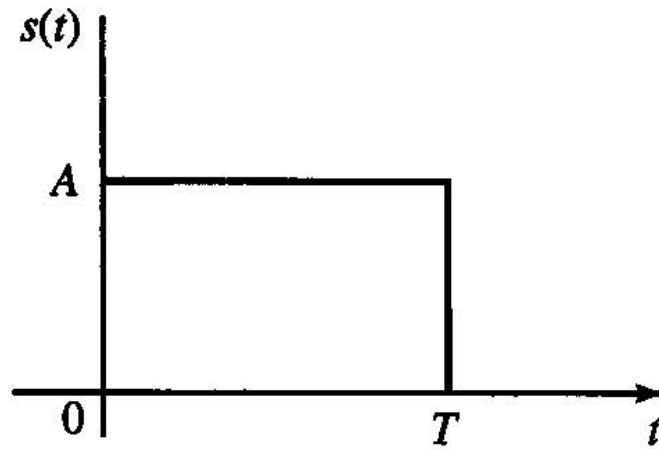
7.8.1-7.8.4).

7.8.1 Early-Late Gate Synchronizers

Consider the rectangular pulse $s(t), 0 \leq t \leq T$, shown in Figure 7.69(a).

The output of the matched filter is the time autocorrelation function of the pulse $s(t)$.

The output of the filter matched to $s(t)$ has its maximum value at time $t = T$ as shown in Figure 7.69(b).



(a)

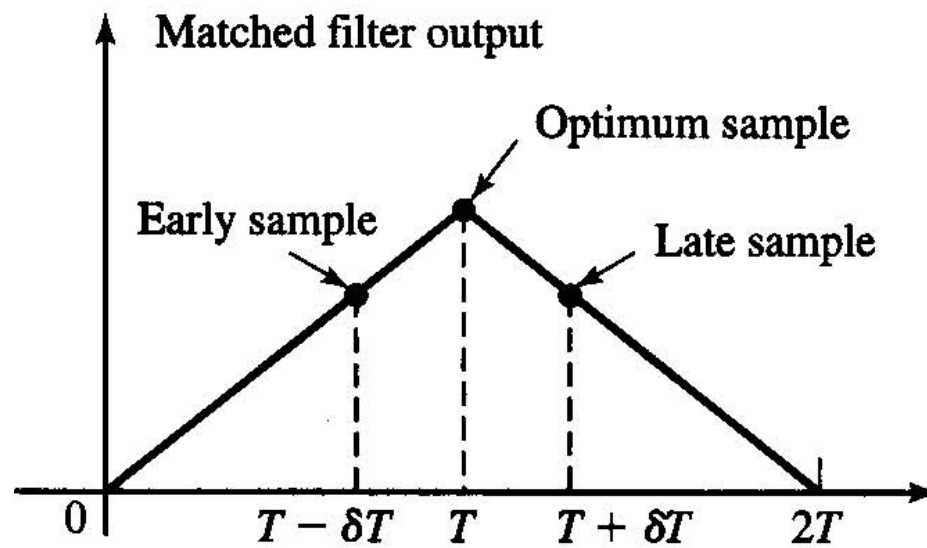


Figure 7.69 (a) Rectangular signal pulse, (b) its matched filter output.

As this statement holds for pulse with any shape, the approach described above is applicable to any signal pulse.

Although the proper time to sample the output of the matched filter for a maximum output is $t = T$, that is, at the peak of the correlation function, it is difficult to identify the peak value of the signal in the presence of noise.

Suppose that the receiver samples early, at $t = T - \delta T$ and late at $t = T + \delta T$ instead the peak.

The absolute values of the early samples $|y[m(T - \delta T)]|$ and the late samples $|y[m(T + \delta T)]|$ is smaller (on the average in the presence of noise) than the samples of the peak value $|y(mT)|$.

Since the auto-correlation function is even with respect to $t = T$, the absolute values of the correlation function at $t = T - \delta T$ and $t = T + \delta T$ are equal.

Hence, the proper sampling time is the midpoint between $T - \delta T$ and $T + \delta T$.

This is the basis for the early-late gate symbol synchronizer.

Figure 7.70 shows the block diagram of an early-late gate synchronizer.

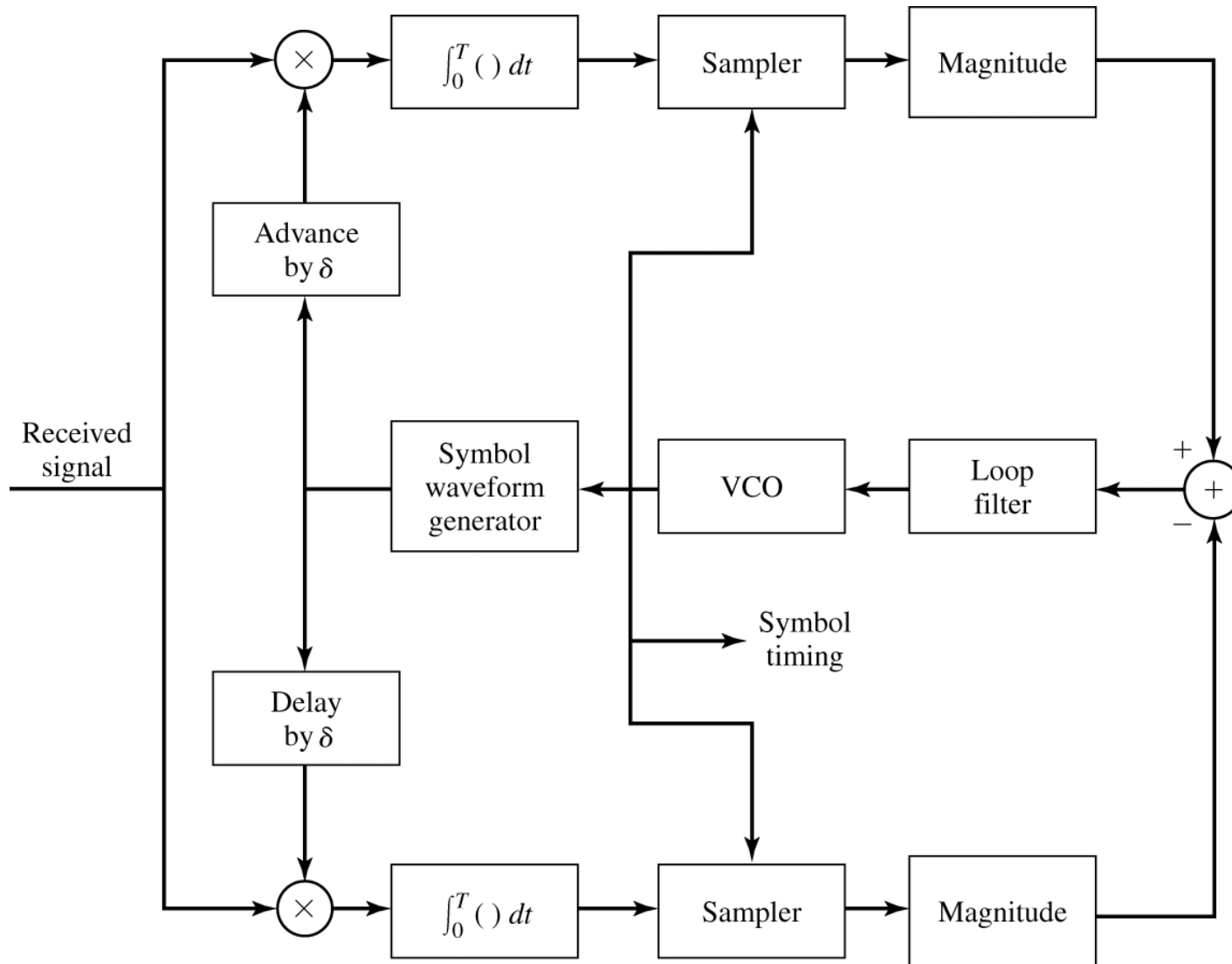


Figure 7.70

Block diagram of early-late gate synchronizer.

In this figure, correlators are used in place of the equivalent matched filters.

The two correlators integrate over the symbol interval T , but one correlator starts integrating δT early relative to the estimated optimum sampling time and the other integrator starts integrating δT late relative to the estimated optimum sampling time.

An error signal is formed by taking the difference between the absolute values of the two correlator outputs.

To smooth the noise corrupting the signal samples, the error signal is passed through a lowpass filter.

If the timing is off relative to the optimum sampling time, the average error signal at the output of the lowpass filter is nonzero, and the clock signal is either retarded or advanced, depending on the sign of the error.

Thus, the smoothed error signal is used to drive a voltage-controlled oscillator (VCO), whose output is the desired clock signal to be used for sampling.

The output of the VCO is also used as a clock signal for a symbol waveform generator which produces the same basic pulse waveform (of any form) as used the transmitter. Note that if the signal pulses are rectangular,

there is no need for a signal pulse generator within the tracking loop.

This pulse waveform is advanced and delayed and then fed to the two correlators, as shown in Figure 7.70.

The early-late gate synchronizer is basically a closed-loop control system whose bandwidth is relatively narrow compared to the symbol rate $\frac{1}{T}$.

The bandwidth of the loop determines the quality of the timing estimate.

A narrowband loop provides more averaging over the additive noise to improve the quality of the estimated sampling instants, provided that the channel propagation delay is constant and the clock oscillator at the transmitter is not drifting with time (drifting very slowly with time).

If the channel propagation delay is changing with time and/or the transmitter clock is also drifting with time, then the bandwidth of the loop must be increased to provide faster tracking of time variations in symbol timing.

However, the wider bandwidth of the loop increases the noise in the loop to degrade the quality of the timing estimate.

In the tracking mode, the two correlators are affected by adjacent symbols.

However, if the sequence of information symbols has zero mean as in PAM with the equiprobable source, the contribution from adjacent symbols to the output of the correlators averages out to zero in the lowpass filter.

An equivalent realization of the early-late gate synchronizer that is easier to implement is shown in Figure 7.71.

In this case, the clock from the VCO is advanced and delayed by δT to be used to sample the outputs of the two correlators.

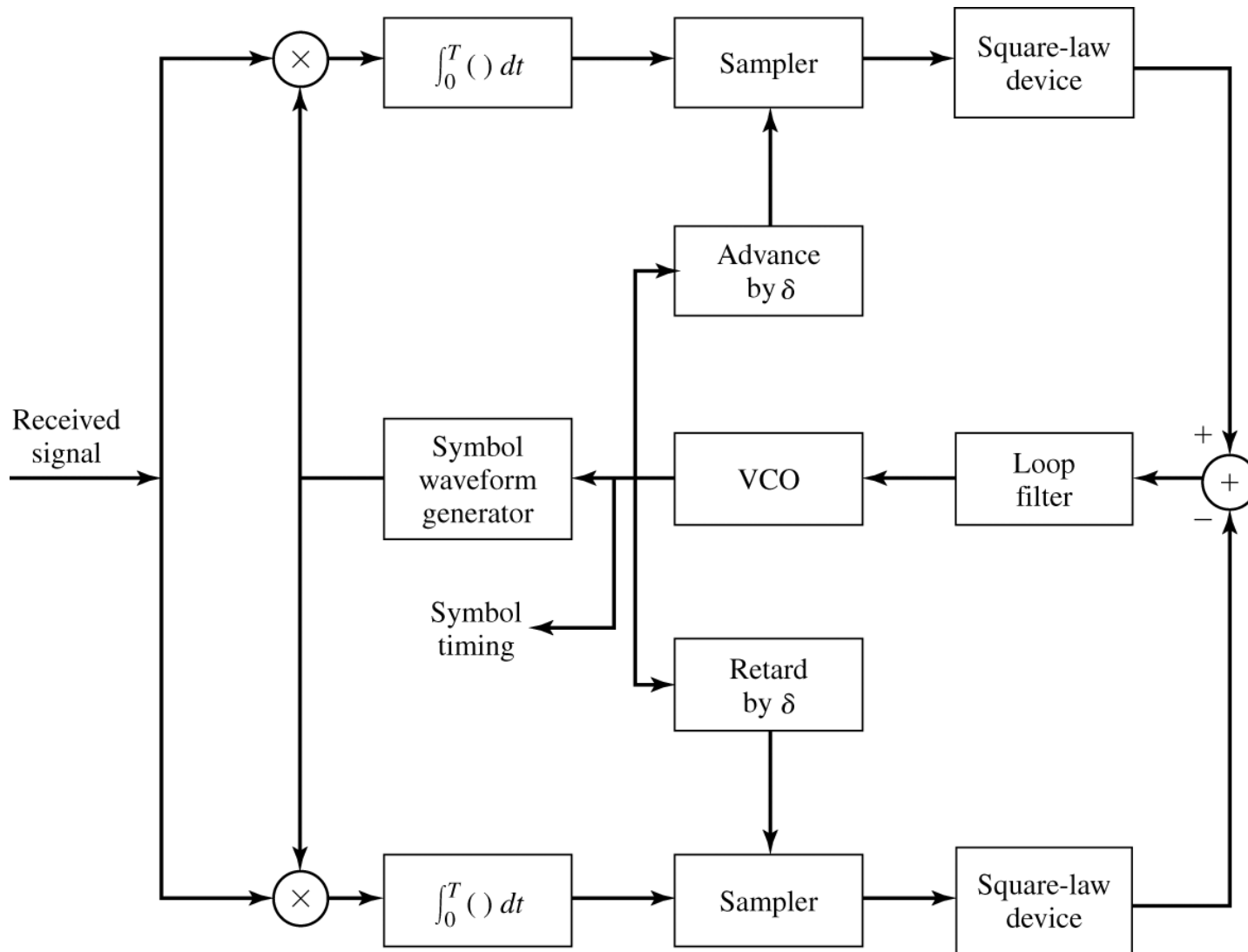


Figure 7.71

Block diagram of early-late gate synchronizer—an alternative form.

7.8.2 Minimum Mean-Square-Error Method (skipped)

Another approach to the problem of timing recovery from the received signal is based on the minimization of the mean-square-error (MSE) between the samples at the output of the receiver filter and the desired symbols.

Assume that the baseband signal at the transmitter is of the form

$$v(t) = \sum_{n=-\infty}^{\infty} a_n g_T(t - nT) \quad (7.8.1)$$

where $\{a_n\}$ is the data sequence and T is the symbol interval.

To be specific, assume that $v(t)$ is a PAM baseband signal and the data sequence $\{a_n\}$ is a zero-mean, stationary sequence with statistically i.i.d. elements.

Therefore, the signal $v(t)$ has zero mean; i.e., $E[v(t)] = 0$.

Furthermore, assume that the autocorrelation function of $v(t)$ is periodic in T and, hence, $v(t)$ is a cyclostationary process.

The received signal at the output of the matched filter at the receiver is given by

$$y(t) = \sum_{n=-\infty}^{\infty} a_n x(t - nT - \tau_0) + v(t) \quad (7.8.2)$$

where $x(t) = g_T(t) * g_R(t)$, $g_R(t)$ is the impulse response of the receiver filter,

$v(t)$ is the noise at the output of the receiver filter and τ_0 ($\tau_0 < T$) is the timing phase.

The MSE between the output of the receiver filter and desired symbol at the m th symbol interval is defined as

$$\text{MSE} = E \left[\{y_m(\tau_0) - a_m\}^2 \right] \quad (7.8.3)$$

where

$$y_m(\tau_0) = \sum_{n=-\infty}^{\infty} a_n x(mT - nT - \tau_0) + v(mT). \quad (7.8.4)$$

Since the desired symbol a_m is not known a priori at the receiver, we may use the output of the detector

\hat{a}_m for the m th symbol; that is, we substitute \hat{a}_m for a_m in the MSE expression.

Hence, the MSE is redefined as

$$\text{MSE} = E \left[\{y_m(\tau_0) - \hat{a}_m\}^2 \right]. \quad (7.8.5)$$

The minimum of (MSE) with respect to the timing phase τ_0 is founded by differentiating (7.8.5) with respect to τ_0 .

Thus, we obtain the necessary condition

$$\sum_m [y_m(\tau_0) - \hat{a}_m] \frac{dy_m(\tau_0)}{d\tau_0} = 0. \quad (7.8.6)$$

which implies that the optimum sampling time corresponds to the condition that error signal $[y_m(\tau_0) - \hat{a}_m]$ is uncorrelated with the derivative $\frac{dy_m(\tau_0)}{d\tau_0}$.

Since the detector output is used in the formation of the error signal $y_m(\tau_0) - \hat{a}_m$, this timing phase-estimation method is said to be **decision-directed**.

Figure 7.72 shows an implementation of the system that is based on the condition given in (7.8.6).

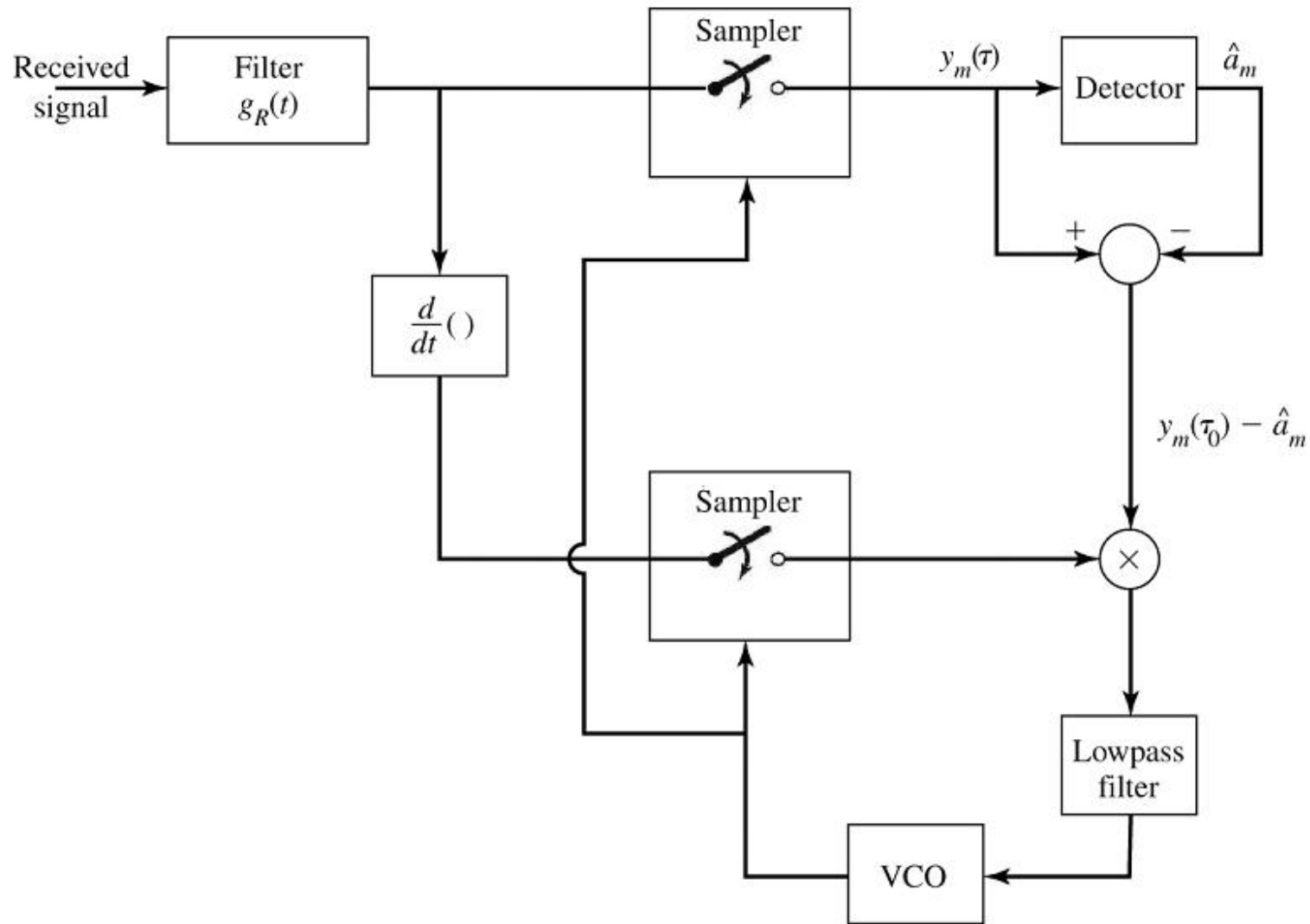


Figure 7.72

Timing recovery based on minimization of MSE.

Note that the summation operation is implemented as a lowpass filter, which averages a number of symbols.

The averaging time is roughly equal to the reciprocal of the bandwidth of the filter.

The filter output drives the voltage-controlled oscillator (VCO), which provides the best MSE estimate of the timing phase τ_0 .

7.8.3 Maximum-Likelihood Methods (skipped)

In the ML criterion, the optimum symbol timing is obtained by maximizing the **likelihood function**.

$$\Lambda(\tau_0) = \sum_m a_m y_m(\tau_0) \quad (7.8.7)$$

where $y_m(\tau_0)$ is the sampled output of the receiving filter given by (7.8.4).

From a mathematical viewpoint, the likelihood function can be shown to be proportional to the probability of the received signal (vector) conditioned on a known transmitted signal.

Physically, $\Lambda(\tau_0)$ is simply the output of the matched filter or correlator at the receiver averaged over a number of symbols.

A necessary condition for τ_0 to be the ML estimate is that

$$\begin{aligned} \frac{d\Lambda(\tau_0)}{d\tau_0} &= \sum_m a_m \frac{dy_m(\tau_0)}{d\tau_0} \\ &= 0. \end{aligned} \quad (7.8.8)$$

This result suggests the implementation of the tracking loop shown in Figure 7.73.

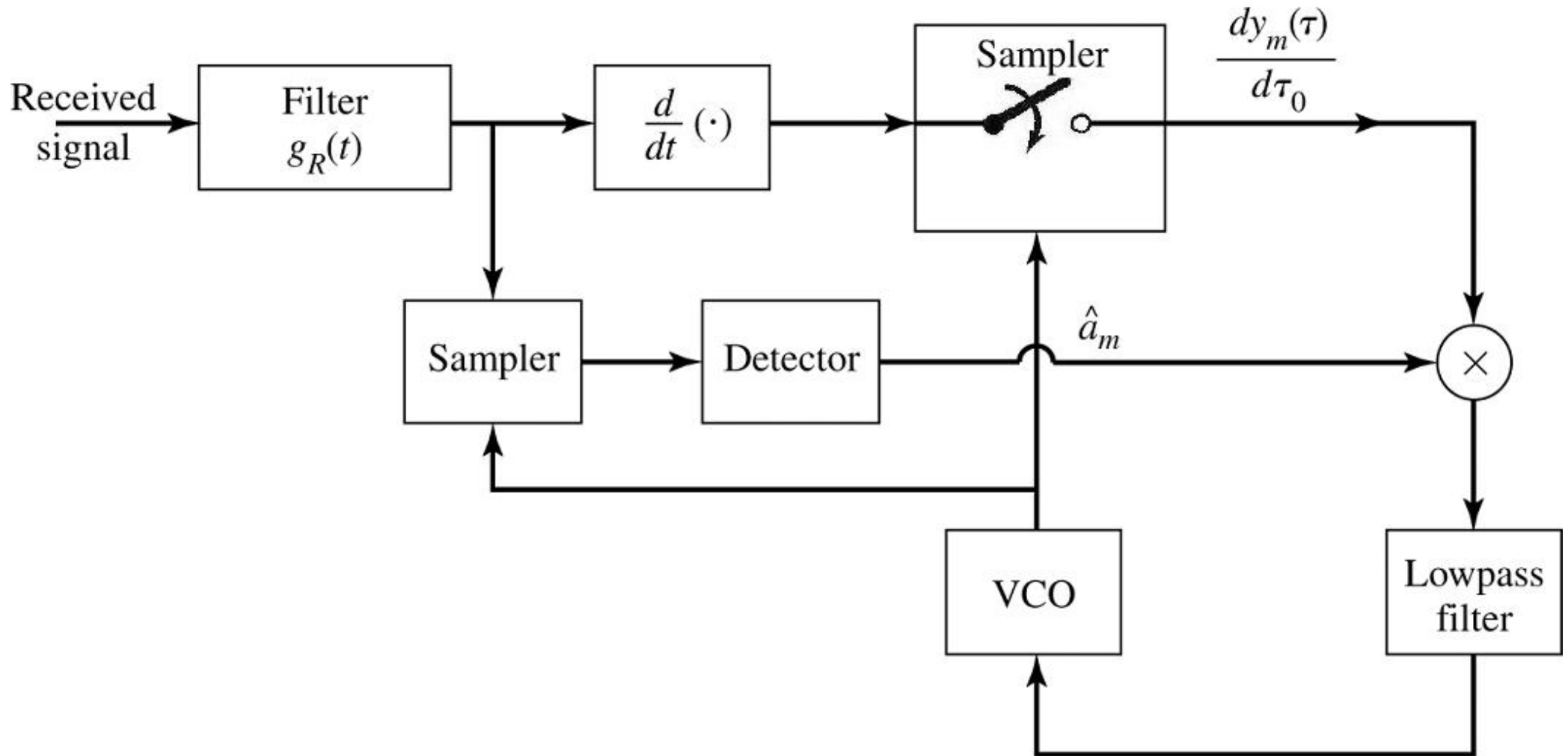


Figure 7.73

Decision-directed ML timing recovery method for baseband PAM.

We observe that the product of the detector output \hat{a}_m with $\frac{dy_m(\tau_0)}{d\tau_0}$ is averaged by a lowpass filter that drives the VCO.

Since the detector output is used in the estimation method, the estimate $\hat{\tau}$ is decision-directed.

As an alternative to the use of the output symbols from the detector, we may use **a nondecision-directed method** that does not require knowledge of the information symbols.

This method is based on averaging over the statistics of the symbols.

For example, we may square the output of the receiving filter and maximize the function with respect to τ_0 .

Thus, we obtain

$$\begin{aligned} \frac{d\Lambda_2(\tau_0)}{d\tau_0} &= 2 \sum_m y_m(\tau_0) \frac{dy_m(\tau_0)}{d\tau_0} \\ &= 0. \end{aligned} \tag{7.8.10}$$

The condition for the optimum τ_0 given by (7.8.10) may be satisfied by the implementation shown in Figure 7.74.

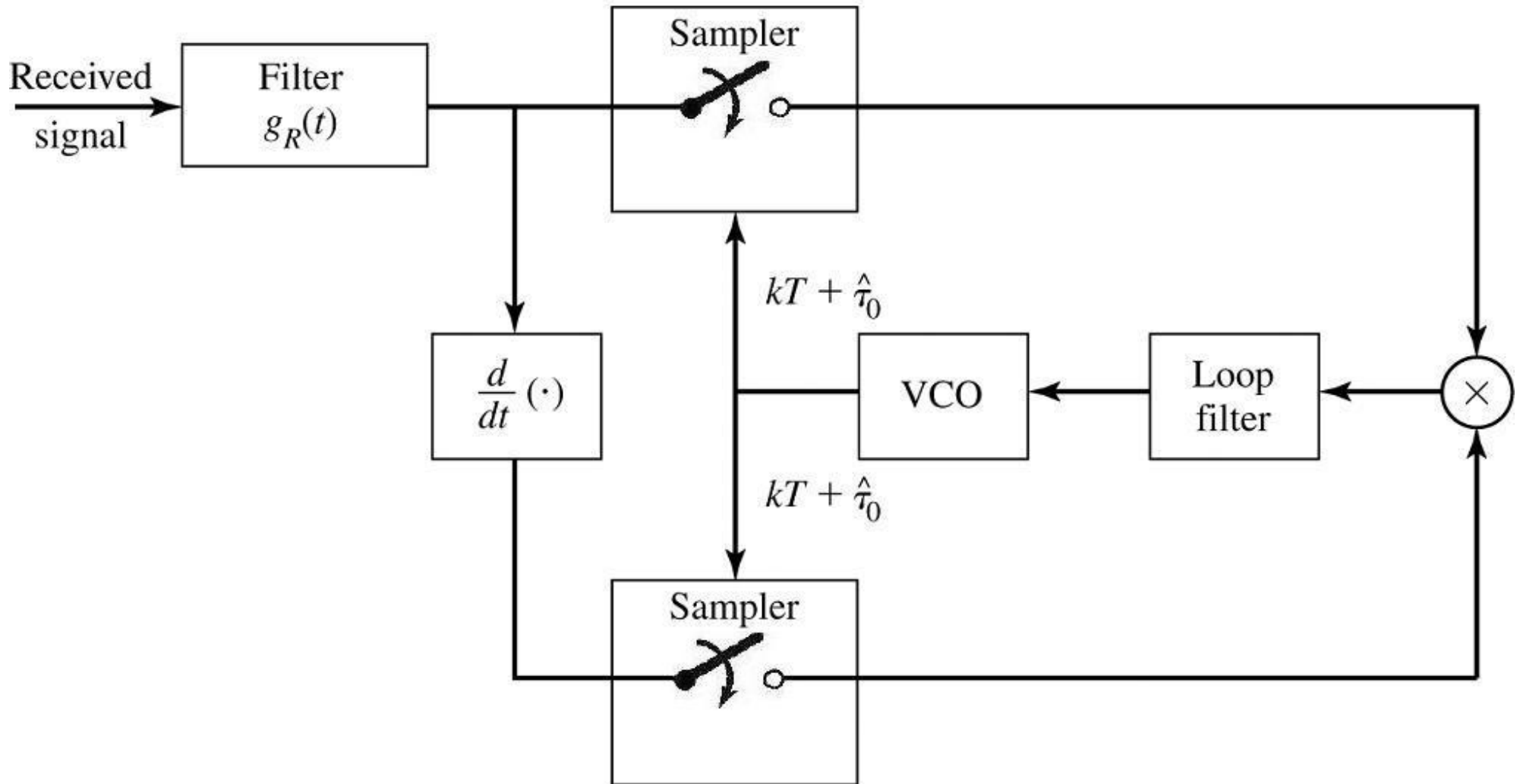


Figure 7.74

Nondecision-directed estimation of timing for baseband PAM.

In this case, there is no need to know the data sequence $\{a_m\}$.

Hence, the method is nondecision-directed.

7.8.4 Spectral-Line Methods (skipped)

Since the signal component at the output of the receiver filter is periodic with period T , we can recover a clock signal with frequency $\frac{1}{T}$ by filtering out a signal component at $f = \frac{1}{T}$.

However, $E[y(t)] = 0$ because $E(a_n) = 0$.

Therefore, $y(t)$ cannot be used directly to generate a frequency component at $f = \frac{1}{T}$.

On the other hand, a nonlinear operation on $y(t)$ can be performed to generate power at $f = \frac{1}{T}$ and its harmonics.

Consider a square-law nonlinearity. Squaring the signal $y(t)$ given by (7.8.2) and taking the expected value with respect to the data sequence $\{a_n\}$, we obtain

$$E[y^2(t)] = E\left[\sum_n \sum_m a_n a_m x(t - mT - \tau_0)x(t - nT - \tau_0)\right] + \text{noise component}$$

$$= \sigma_a^2 \sum_{n=-\infty}^{\infty} x^2(t - nT - \tau_0) + \text{noise component} \quad (7.8.11)$$

where $\sigma_a^2 = E[a_n^2]$.

Since $E[y^2(t)] > 0$, we may use $y^2(t)$ to generate the desired frequency component.

Apply the Poisson Sum Formula on the signal component (see Problem 2.23) to express (7.8.11) in the form of a Fourier series.

Then,

$$\sigma_a^2 \sum_n x^2(t - nT - \tau_0) = \frac{\sigma_a^2}{T} \sum_m c_m e^{j2\pi m(t-\tau_0)/T} \quad (7.8.12)$$

where

$$c_m = \int_{-\infty}^{\infty} X(f) X\left(\frac{m}{T} - f\right) df. \quad (7.8.13)$$

By design, assume that the transmitted signal spectrum is confined to frequencies below $\frac{1}{T}$.

Hence, $X(f) = 0$ for $|f| > \frac{1}{T}$ and, consequently, there are only three nonzero terms ($m = 0, \pm 1$) in (7.8.12).

Therefore, the square of the signal component contains a dc component and a component at the frequency $\frac{1}{T}$.

The above development suggests that we square the signal $y(t)$ at the output of the receiving filter and filter $y^2(t)$ with a narrowband filter $B(f)$ tuned to the symbol rate $\frac{1}{T}$.

If we set the filter response $B\left(\frac{1}{T}\right) = 1$, then

$$\frac{\sigma_a^2}{T} \operatorname{Re} \left[c_1 e^{j2\pi(t-\tau_0)/T} \right] = \frac{\sigma_a^2}{T} c_1 \cos \frac{2\pi}{T} (t - \tau_0) \quad (7.8.14)$$

so that the timing signal is a sinusoid with a phase of $-\frac{2\pi\tau_0}{T}$, assuming that $X(f)$ is real.

We may use alternate zero crossings of the timing signal as an indication of the correct sampling times.

However, the alternate zero crossings of the signal given by (7.8.14) occur at

$$\frac{2\pi}{T}(t - \tau_0) = (4k + 1)\frac{\pi}{2} \quad (7.8.15)$$

or, equivalently, at

$$t = kT + \tau_0 + \frac{T}{4} \quad (7.8.16)$$

which is offset in time by $\frac{T}{4}$ relative to the desired zero crossings.

In a practical system the timing offset can be easily compensated either by relatively simple clock circuitry or by designing the bandpass filter $B(f)$ to have a $\frac{\pi}{2}$ phase shift at $f = \frac{1}{T}$.

Figure 7.75 shows this method for generating a timing signal at the receiver.

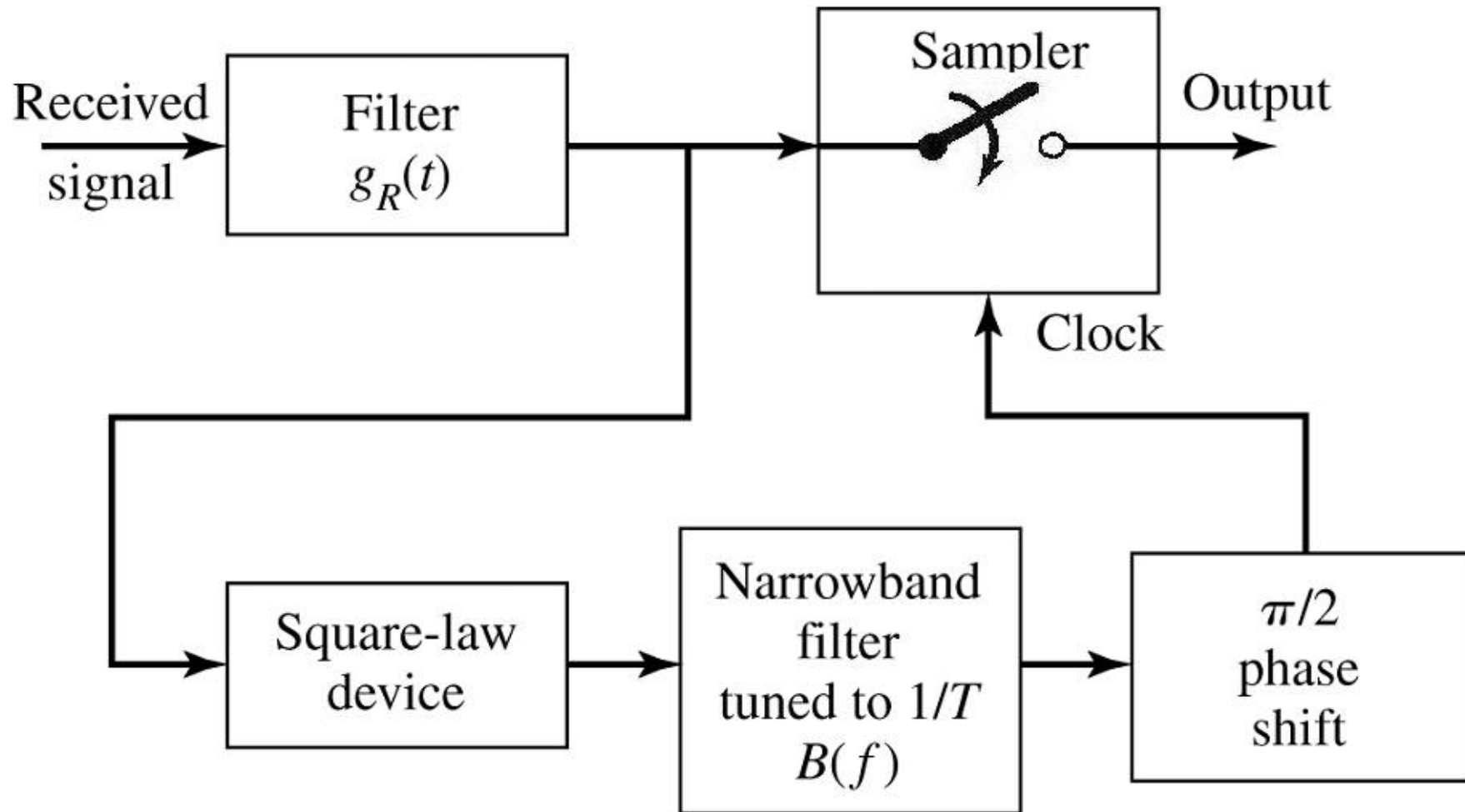


Figure 7.75

Symbol timing based on spectral-line method.

The additive noise that corrupts the signal will generally cause fluctuations in the zero crossings of the desired signal.

The effect of the fluctuations will depend on the amplitude c_1 of the mean timing sinusoidal signal given by (7.8.14).

Note that the signal amplitude c_1 is proportional to the slope of the timing signal in the vicinity of the zero crossing as shown in Figure 7.76.

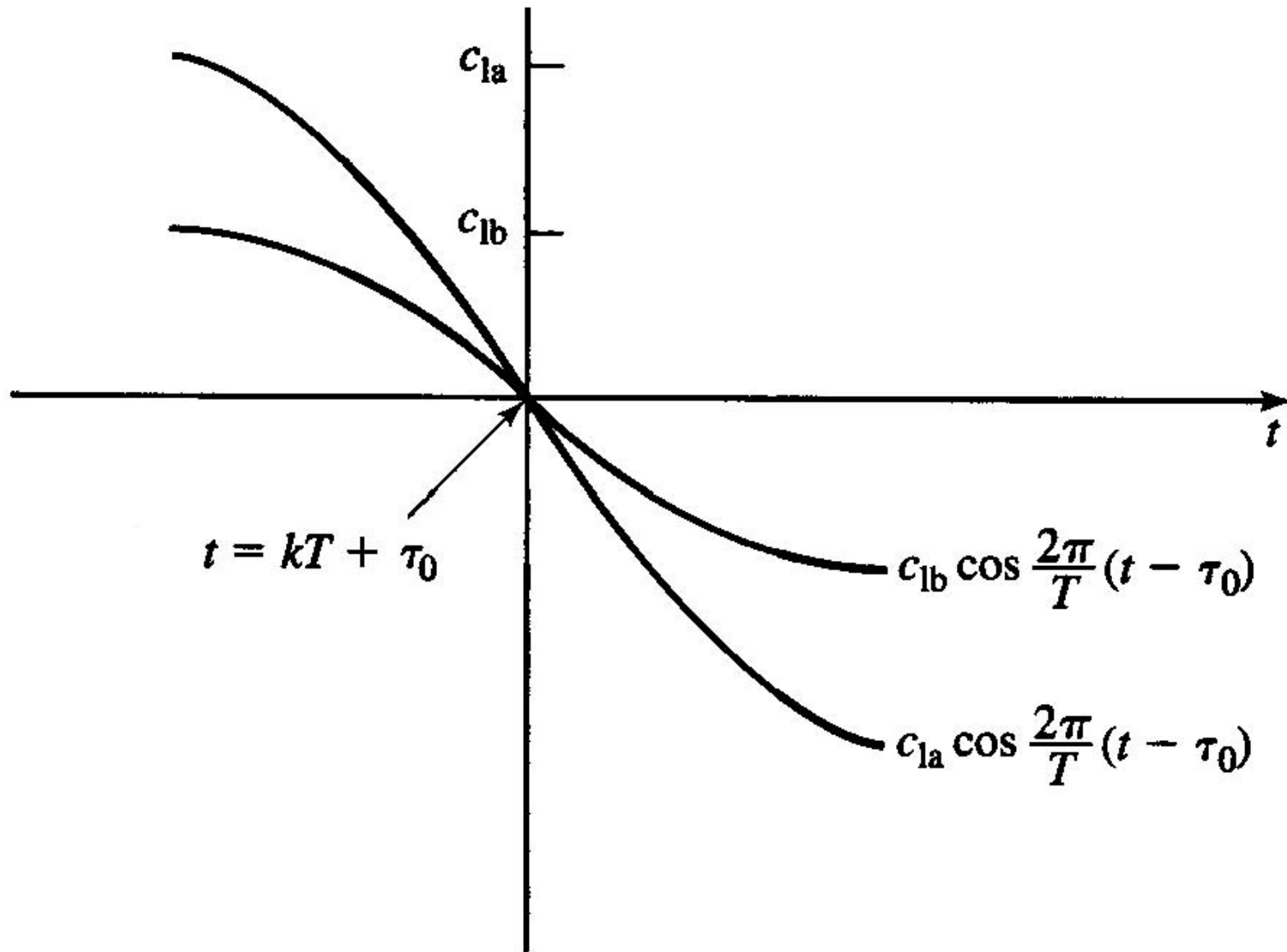


Figure 7.76 Slope of the sinusoid at the zero crossing as a function of the amplitude.

Therefore, the larger the amplitude c_1 , the larger will be the slope and, consequently, the timing errors due to the noise will be smaller.

From (7.8.13) we observe that c_1 depends on the amount of spectral overlap of $X(f)$ and $X\left(\frac{1}{T} - f\right)$.

Thus, c_1 depends on the amount by which the bandwidth of $X(f)$ exceeds the Nyquist bandwidth $\frac{1}{2T}$; i.e., $X(f) = 0$, for $|f| > \frac{1}{2T}$, then $c_1 = 0$, and this method fails to provide a timing signal.

If the excess bandwidth is large, say $\frac{\alpha}{2T}$ where $\alpha = \frac{1}{2}$ or 1, the timing signal amplitude will be sufficiently large to yield relatively accurate symbol timing estimates.

7.8.5 Symbol Synchronization for Carrier-Modulated Signals (skipped)

The Symbol-timing synchronization methods described in Section 7.8.4 for baseband signals apply as well to bandpass signals.

Because any carrier-modulated signal can be converted to a baseband signal by a simple frequency translation, symbol timing can be recovered from the received signal after frequency conversion to baseband.

For QAM signals the spectral-line methods described in Section 7.8.4 have proved to be particularly suitable for timing recovery.

Figure 7.77 shows a spectral-line method which is based on filtering out a signal component at the frequency $\frac{1}{2T}$ and squaring the filter output to generate a sinusoidal signal at the desired symbol rate $\frac{1}{T}$.

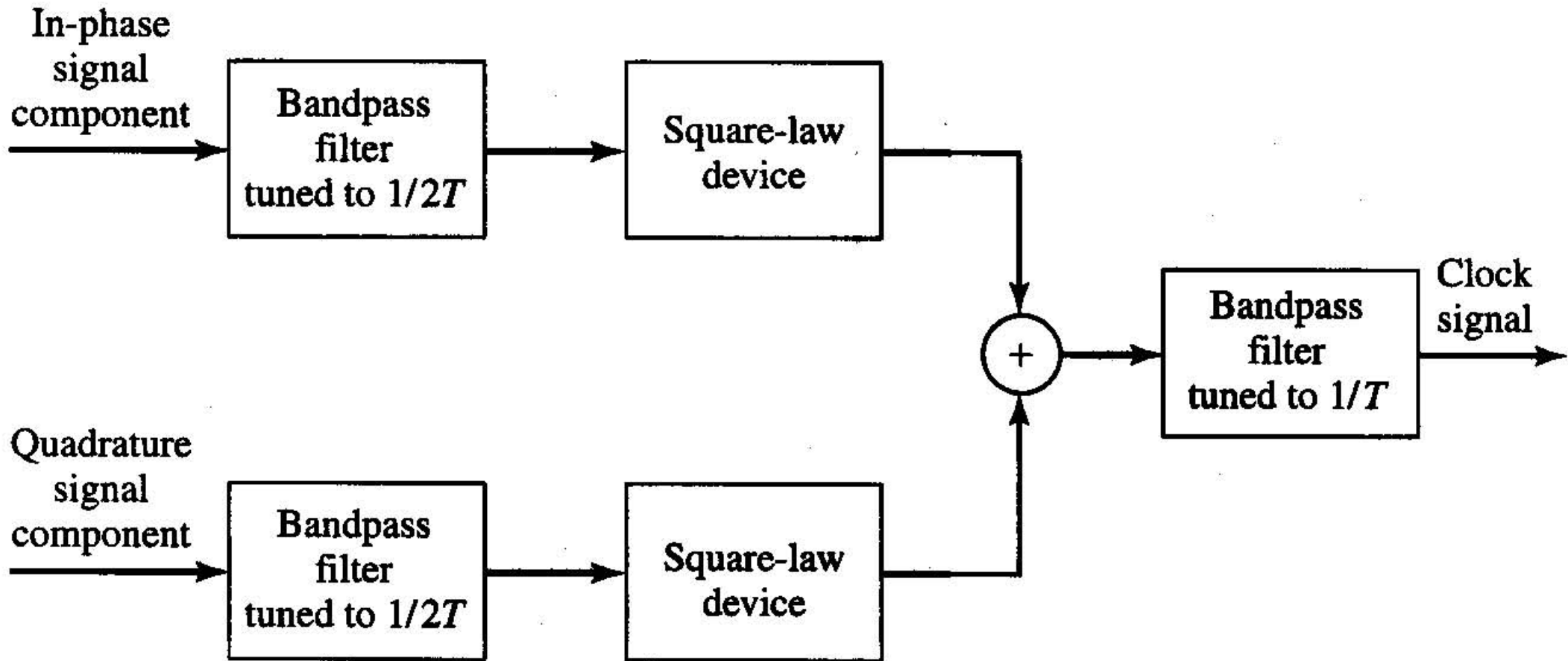


Figure 7.77 Block diagram of timing recovery method for QAM.

Because the demodulation of the QAM signal is accomplished as described above, by multiplication of the input signal with the two quadrature-carrier signals $\psi_1(t)$ and $\psi_2(t)$, the in-phase and quadrature signal

components at the outputs of the two correlators are used as the inputs to the two bandpass filters tuned to $\frac{1}{2T}$.

The two filter output are squared (rectified), summed, and then filtered by a narrowband filter tuned to the clock frequency $\frac{1}{T}$.

Thus, we generate a sinusoidal signal that is the appropriate clock signal for sampling the outputs of the correlators to recover the information.

In many modern communication systems, the received signal is processed (demodulated) digitally after it has been sampled at the Nyquist rate or faster.

In such a case, symbol timing and carrier phase are recovered by signal-processing operations performed on the signal samples.

Thus, a PLL for carrier recovery is implemented as a digital PLL and the clock recovery loop of a type described in this section is also implemented as a digital loop.